Site-Specific Chemical Modification of Antibodies for the Modulation of Function

A thesis submitted to the Board of the Faculty of Physical Sciences in partial fulfilment of the requirements for the degree of Doctor of Philosophy at the University of Oxford

Smita B. Gunnoo

St. Cross College, Oxford

Trinity Term 2013

Author's declaration

The work presented in this thesis was conducted at the Chemistry Research Laboratory at the University of Oxford under the supervision of Professor Ben Davis. All the work is my own, except where otherwise stated, and has not been submitted for any other degree at this or any other university.

Smita B. Gunnoo

October 2013

This thesis is dedicated to the memory of Chandrawatee Gunnoo

Short Abstract for Bodleian Library Indexing

Site-Specific Chemical Modification of Antibodies for the Modulation of Function

Smita B. Gunnoo

St. Cross College

University of Oxford

Submitted for the degree of Doctor of Philosophy in Organic Chemistry

Trinity Term 2013

Chemical modification of antibodies is critical for many research areas including therapeutic and biotechnological applications. In particular, strategies for site-specific chemical modification via non-natural amino acids forming homogenous immunoconjugates are of interest. The use of fully functional single-domain antibodies derived from naturally occurring heavy chain antibodies in *Camelidae* species is attractive due to their enhanced properties, which are discussed in this piece of work. In terms of chemical antibody modification, much of the existing research is focused on modification away from binding regions, thus minimising disturbance to antibody function. In this thesis however, modifications within the binding region of the single-domain antibody cAb-Lys3 are described in a site-specific fashion with the aim of modulating binding affinities. An efficient and high yielding method for the expression and purification of cAb-Lys3 is described, followed by the site-specific installation of dehydroalanine, an electrophilic non-natural amino acid, able to react with nucleophiles that are inert to reaction with other proteinogenic amino acids. Then, the use of dehydroalanine as a unique reaction handle is explored. Firstly, the addition of short alkyl chains to dehydroalanine within the binding region of cAb-Lys3 is described with the aim of increasing hydrophobic interactions when binding to antigen. This has been attempted in two ways – via the addition of thiols, and by zinc-mediated radical additions. Secondly, the development of an antibody-based AND logic gate, converting cAb-Lys3 to a multi input protein requiring more than antigen for its binding is described. Site-specific chemical methods via dehydroalanine are utilised, and the application of the antibody-based AND logic gate *in vitro* and in mammalian tissue are discussed, as well as the prospects of the research.

Full Abstract

Site-Specific Chemical Modification of Antibodies for the Modulation of Function

Smita B. Gunnoo

St. Cross College

University of Oxford

Submitted for the degree of Doctor of Philosophy in Organic Chemistry

Trinity Term 2013

The chemical modification of antibodies forming immunoconjugates has long been recognised as an important area of research for a multitude of applications, particularly in the field of therapeutics. For instance, the attachment of certain moieties can enhance the pharmacokinetic properties of an antibody therapeutic, or the attachment of an antibody to a cytotoxin can aid specificity and minimise side effects. Much of the research carried out on modifying antibodies focuses on modifications away from the binding region, with minimum disturbance to function. However, the work described in this thesis focuses on site-specific modifications within the binding region of the single-domain antibody cAb-Lys3, with the aim of altering binding affinities. Single-domain antibodies derived from heavy chain antibodies naturally occurring in the *Camelidae* species are widely used in research, and they possess enhanced properties in comparison to intact antibodies and other fragments.

A challenge faced when chemically modifying antibodies, and proteins in general, is the heterogeneity encountered when targeting proteinogenic amino acid side chains, which can be alleviated by the use of non-natural functionalities, possessing reactivities differing from those of natural groups. Another challenge faced is the need to perform modifications in ambient conditions such that protein structure and function are not compromised. The site-specific chemical modification of antibodies using the non-natural amino acid dehydroalanine as an electrophilic precursor is described for the installation of a range of non-natural functionalities and post-translational modification (PTM) mimics.

cAb-Lys3 Expression and Purification

A high yielding and efficient method for the expression of cAb-Lys3 in mammalian cells was carried out. This followed multiple attempts to express in *E. coli*, which lead to the formation

of inclusion bodies only. cAb-Lys3 is a single-domain antibody binding to the active site of lysozyme. The crystal structure of the cAb-Lys3-lysozyme complex reveals hydrophobic interactions mediated by an alanine residue at position 104, contributing to the high binding affinity. In addition to the wild type antibody, a mutant containing cysteine at position 104, pivotal to binding was expressed and purified for the purpose of carrying out chemical modifications. Both the wild type antibody and the cysteine-containing mutant (cAb-Lys3-Cys104) were found to be active in binding to lysozyme. Additionally, chemical tests revealed the cysteine at position 104 to be uniquely reactive in the presence of native disulfide bonds.

Towards 'Chemical Affinity Maturation'

The installation of dehydroalanine within the binding region of cAb-Lys3 was optimised using the uniquely reactive cysteine as a precursor. cAb-Lys3-Dha104 was found to be an efficient electrophilic precursor for the addition of a range of short chain alkyl thiol nucleophiles. Investigations into whether an increase in hydrophobicity within the binding region could increase affinity, thereby creating a more potent antibody, were carried out. Following this, a zinc-mediated radical addition with short chain alkyl groups to dehydroalanine forming carbon-carbon bonds was attempted. Unfortunately, antibody was found to be unstable to the required reaction conditions.

Building Conditionally Functional Synthetic Proteins – Creation of an AND Antibody

In the final chapter, the conversion of an antibody from a single input protein (requiring one input, antigen for function) to a multi input protein is described. Here, the installation of PTM mimics via dehydroalanine within the binding region of cAb-Lys3 was performed, with the aim of inhibiting binding, followed by a subsequent 'lift' in inhibition on treatment with the relevant PTM-processing enzymes. Initially, *S*-linked glycosyl groups were introduced into cAb-Lys3, and the glycosylated forms were found to inhibit binding activity. Unfortunately, the glycosylated antibodies were impervious to treatment with glycosidases. Instead, a thiophosphate group was installed into cAb-Lys3, inhibiting binding function. This inhibition was found to be temporary, as the thiophosphate could be processed by a range of phosphatases, regenerating the original and active cysteine mutant. Phosphorylated cAb-Lys3 could therefore be considered a multi input protein requiring both antigen and phosphatase for function, following Boolean AND logic. The AND-gated antibody concept was demonstrated by the specific targeting of cell surfaces *in vitro*, and in more complex

mammalian tissue. This concept may be applicable in a therapeutic context, where antibody therapeutic could be targeted to tumour environments overexpressing an increased level of a certain processing enzyme, minimising binding to cell surface receptors in healthy tissues.

Acknowledgements

Thank you to Professor Ben Davis for guidance, putting me on a project I have thoroughly enjoyed, and showing enthusiasm. Thank you also to Dr. Daniel Anthony for his valuable input on the *in vivo* parts of the antibody switch project, and carrying out animal experiments.

I'd like to thank the NMR facility, in particular Dr. Tim Claridge for help with carrying out NMR on proteins. I am indebted to the staff of the mass spectrometry facility for all their help over the 4 years, James Wickens, Lingzhi Gong, Colin Sparrow and James McCullagh. A special thanks to James Wickens for always being supportive and helpful in times of need. My PhD required me spending probably an unhealthy amount of time in the first floor LCT room, and James Wickens made it much easier. Also, thanks to all the support staff in the building, especially in stores, and Karen on reception. Outside of Chemistry, thank you to Nigel Emptage for letting me work in his lab and use his equipment, as well as Lindsey McGuinness and Zahid Padamsey for taking the time to show me shooting techniques.

Thank you to UCB for providing funding over 4 years. As well as financial aid, I have been lucky enough to use facilities in Slough, so thank you to Laura Griffin, Hanna Hailu, and Terry Baker for making this possible. Thanks to Rachel Garlish for running my samples on their precious HDX machine and Helene Finney for providing me with lysozyme DNA. Further thanks to Alastair Lawson, Terry Baker, John Porter and Helene Finney for their scientific input and insight into my projects over the course of the DPhil.

When I first came to Oxford, my molecular biology knowledge was approximately zero, and I owe a lot to Craig McKibbin for teaching me with the utmost patience. We got protein eventually! Thanks to Alison Parry for teaching me chemistry and the many many laughs shared. My development into protein modification would not have been possible without Justin Chalker. Thank you for the practical and less practical lessons taught. Thank you to David Vocadlo (Simon Fraser University) and Serge Muyldermans (VIB) for taking the time out of their busy schedules to reply to my emails, it is very much appreciated.

Thank you to everyone who has proof read this thesis for me – Tom Parsons, Balakumar Vijayakrishnan, Mahima Sharma, Sylvain Rover, Hua Wang and Kimberly Marsh. Thanks to Jessica Liley and Laura Jennings for their careful checking.

The BGD group is enormous, and many people special to me have come and gone over the 4 years. There are way too many people to thank individually! Amy, thank you for all your help in the lab, and being patient with me in 'sad times'. A special thanks to Jo for going out of her way

to help me organise my trip to Boston, and continued encouragement. Chris, Regis and Bala I think have had to hear the majority of my whining, so thank you. As well as listening to my whining, Bala has helped me consistently with absolutely everything over the four years, it is so appreciated, and I probably couldn't have done it without you! Regis, you have always dropped whatever you're doing to help me, in both a work and friend sense. Thank you for this, and providing me with a LOT of laughs over the 4 years. Hua, you're someone unlike anyone I have ever met, truly unique and pretty marvellous actually! Thank you also to Therese, so glad to have met you, and even happier that it's just the same every time I see you. Thank you to Anaelle, Conor, m@ and other post-docs past and present for being great advisers. Thanks to Arghya aka Argos for kindly giving me his sugar, and all the valuable advice on the sugar aspect of my work. Thank you to Phin for all the phospho talk and giving me some TEV in my desperate last few days! And of course, 'Hi Seb!' Thanks to all LG10 workers past and present for providing a fun atmosphere to work in.

Outside of the lab, thanks to my girls (Jess, Becky, Charley, Laura and Cat) and Ruby for their ongoing support and non-BGD time. Jess, as well as being a wonderful friend, your accents have me in fits and have always brightened things up. Thank you to ALL of you for always being there for me, I will miss Pizza Express, rosé and dough balls (and garlic butter!) ☺ xx Thanks to my oldest friend ever Rajvir for just understanding everything without me having to explain anything, and my Bristol girls too for continued support.

Thank you to Pieter for your graphics (AND gate), ridding me of my fear of dogs, always wanting to go to tea and absolutely all of the good times shared in Oxford and beyond.

Kim, you have been my ROCK, as two wise girls once said 'why can't all friendships be this easy?!' You are undoubtedly one of the best things I could have found in Oxford, and I am never letting go! ;P I would have struggled to do this without you looking after me right until the end.

Lastly, I could not have done any of this without the support of my wonderful family – Mum, Dad, Sabrina and Vikesh. Thank you for encouraging me, listening to me whine and keeping me grounded (I hope). I'm sorry for all the times I've been moody and feeling sorry for myself – which mum has had to be the key witness to in my final weeks! I hope with all my heart that I have made my parents proud of me; this is most certainly for them. And yes mum, I will get a 'proper' job now, and sort out the stuff in the loft.

Finally, thank you to my thesis examiners – Dr. Martin Smith and Dr. Sander van Kasteren for a thoroughly stimulating, challenging yet enjoyable viva.

Publications

1. Chalker, J. M., Gunnoo, S. B., Boutureira, O., Gerstberger, S. C., Fernandez-Gonzalez, M., Bernades, G. J. L., Griffin, L., Hailu. H., Schofield, C. J., Davis, B. G., Methods for converting cysteine to dehydroalanine on peptides and proteins. *Chem. Sci.* **2,** 1666-1676 (2011).

2. Gunnoo, S. B., Finney, H. M., Baker, T. S., Lawson, A. D., Anthony, D. C., Davis, B. G., A Conditionally Functional Synthetic Protein - Creation of an AND Antibody. *Manuscript Submitted*

Table of Contents

Abbreviations

2-Pr	Isopropyl
Ab	Antibody
acp	acid phosphatase
ADC	antibody-drug conjugate
aq.	aqueous
bIMP	alkaline phosphatase from bovine intestinal mucosa
cAb-Lys3	camel antibody binding to lysozyme
CD	circular dichroism
CDR	complementarity determining region
CHO	Chinese hamster ovary
Cu	copper
Dha	dehydroalanine
DNA	deoxyribonucleic acid
DTT	dithiothreitol
E. coli	*Escherichia coli*
EDTA	ethylenediaminetetraacetic acid
ELISA	enzyme-linked immunosorbent assay
EPL	expressed protein ligation
Et	ethyl
Fab	fragment antigen binding
FACS	fluorescence activated cell sorting
Fc	fragment crystallisable
Gal	galactose
GlcNAc	*N*-acetyl-D-glucosamine
Glu	glucose
HcAb	heavy-chain antibody
HEK	human embryonic kidney
HEPES	4-(2-hydroxyethyl)-1-piperazineethanesulfonic acid
His-tag	hexahistidine tag

IgG	immunoglobulin G
In	indium
IPTG	isopropyl-β-D-1-thiogalactopyranoside
K_2CO_3	potassium carbonate
LB	luria bertani
LC-MS	liquid chromatography mass spectrometry
LRMS	low resolution mass spectrometry
mAb	monoclonal antibody
Me	methyl
MeOH	methanol
MES	2-(*N*-morpholino)ethanesulfonic acid
MS	mass spectrum/ mass spectrometry
MSH	*O*-mesitylenesulfonylhydroxylamine
MWCO	molecular weight cut off
Na_3SPO_3	sodium thiophosphate
NaCl	sodium chloride
$NaHCO_3$	sodium hydrogen carbonate
NCL	native chemical ligation
NH_4Cl	ammonium chloride
NH_4OAc	ammonium acetate
OD	optical density
OGA	*O*-GlcNAcase
PBS	phosphate buffered saline
PCR	polymerase chain reaction
pCys	phosphocysteine
PLAP	placental alkaline phosphatase
Ppase	phosphatase
Pr	propyl
PTM	post-translational modification
QL	quick ligase
sat.	saturated
SBL	subtilisin from *Bacillus lentus*
scFv	single-chain variable fragment

sdAb	single-domain antibody
SDS-PAGE	sodium dodecyl sulfate-polyacrylamide gel electrophoresis
SEAP	secreted embryonic alkaline phosphatase
TNF	tumour necrosis factor
Tris	trisaminomethane
V_HH	heavy chain of the variable domain of the HcAb
WT	wild type
Zn	zinc

Chapter 1: Introduction to Antibodies, Antibody Fragments and Chemical Modification of Antibodies

'Sometimes it's better to do basic research and be opportunistic… That's often the beauty of fundamental research.'

Sir Greg Winter, 2013.

1.1 Antibody Structure

Antibodies are immune proteins (or immunoglobulins) responsible for recognising and binding to foreign material as part of the body's defence system. Antibodies recognise antigenic determinants on the surfaces of foreign material. These antigenic determinants may be proteins or carbohydrates on a bacterial cell surface, or envelope spikes on the surface of a virus. Importantly, the antigenic determinants differ from molecular structures made by the cells of the host. Although antibodies show great structural diversity, enabling recognition of a large repertoire of antigens, they also require common features. It would not be practical for Nature to devise a different molecular solution for the elimination of each antigen the body had to encounter. The general structure of antibodies has evolved to account for the diverse requirements.

Immunoglobulin G (IgG) is the major antibody in serum. It is a distorted Y shape, made up of four polypeptide chains, comprising two identical heavy chains and two identical light chains (**Figure 1.1**).

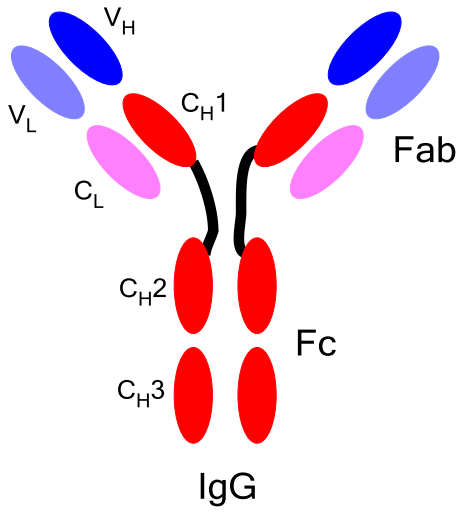

Figure 1.1. Immunoglobulin G (IgG) structure. Domains within the Fab fragments are separated from those within the Fc by the flexible hinge region (in black).

The structure can be divided into three overall units, one fragment crystallisable (Fc) containing the C_H2 and C_H3 domains (C_H – constant-heavy) at the C-terminus, and two fragment antigen-binding (Fab) arms containing the V_H, C_H1, V_L and C_L domains (V_H – variable-heavy, V_L – variable-light, C_L – constant-light) at the N-termini. There are twelve domains in total, each stabilised by an internal disulfide bond. As the name suggests, the Fab arms are responsible for antigen binding, with the presence of two arms giving enhanced binding when multiple copies of antigen are present. The Fc portion is responsible for effector functions, and binds to effector molecules to trigger antigen elimination and mediate certain immune functions. Amino acid sequences amongst the Fc are largely conserved, and differences can lead to the triggering of different effector functions. At the amino terminal end where antibody binds antigen, there can be extreme variation in the amino acid sequence from one antibody to another, which gives rise to different specificities for different antigens. These areas are referred to as hypervariable regions, or complementarity determining regions (CDRs). In IgG, antigen binding is a combined property of the V_H and V_L. The Fc and Fab arms are linked by the flexible hinge region. This region is susceptible to proteolysis which aids detailed analysis of antibodies in a laboratory environment. The presence of interchain

disulfide bonds means that an antibody is readily reducible into smaller components. With the exception of the two C_H2 domains, there is close lateral association between other pairs of domains (V_H and V_L, C_H1 and C_L, C_H3 and C_H3), a phenomenon termed domain pairing. The C_H2 domains have two carbohydrate chains interposed between them. Each antibody contains a common pattern of peptide chain folding, termed the immunoglobulin (Ig) fold. This refers to the two twisted, stacked β-sheets enclosing internal tightly packed hydrophobic residues, an arrangement which improves the solubility of the protein. Internal disulfide bonds link the two β-sheets, stabilising the structure. Each β-sheet is made up of three or four anti-parallel β-strands, where the amino acid sequences are largely conserved. In the loops connecting each strand however, amino acid sequence is known to vary. As well as IgG, there are four other structural isotypes of immunoglobulins in humans: IgM, IgA, IgD and IgE. Each form has the same basic structure with 4 polypeptide chains, but they differ in their heavy chains, termed γ, μ, α, δ and ε respectively. Light chains exist in two forms, κ and λ. The structural differences of each immunoglobulin type lead to varying polymerisation states of the monomer unit. IgG can further be divided into four subclasses, each containing different heavy chains. These are γ1, γ2, γ3, and γ4, forming IgG1, IgG2, IgG3 and IgG4. Although sequences for these subclasses are similar, they vary at the hinge region, which leads to the triggering of different effector functions.[1,2]

1.2 Antibody Fragments

Both monoclonal antibodies and antibody fragments are important in the biotechnology market. Research into the development of antibody fragments and potential applications of these has received, and continues to receive, much attention in the literature.[3,4] The generation of antibody fragments involves the removal of domains deemed non-essential for function, but with the retention of antigen-binding ability. This is done by the dissection of

intact antibodies into minimal binding fragments, as well as by engineering variants (**Figure 1.2**).

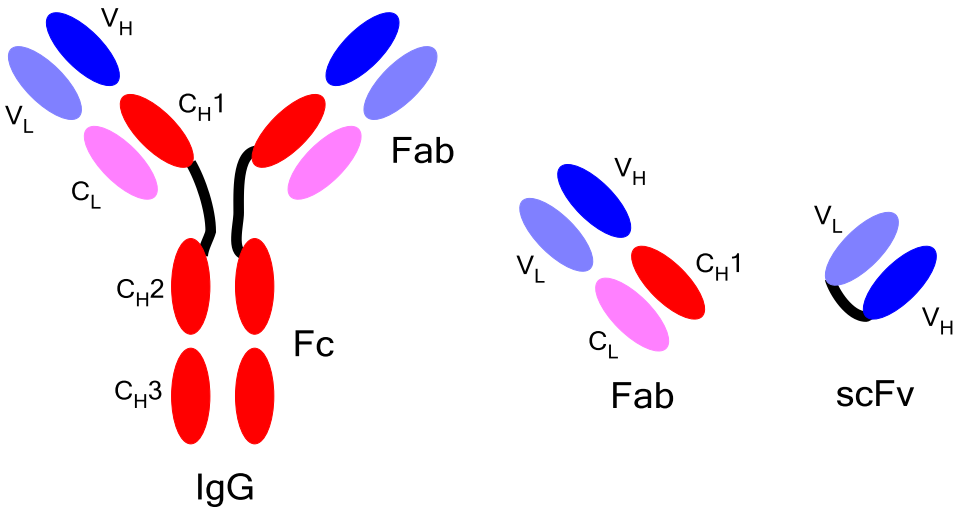

Figure 1.2. IgG (left) can be dissected into the smaller Fab fragment (middle) by proteolysis. scFvs (right) can be recombinantly expressed.

Also, the discovery of heavy-chain antibodies (HcAbs) completely devoid of light chains in camels[5] and sharks[6] has further expanded the repertoire of antibody fragments (**Figure 1.3**). The continuous development and improvement of methods for the generation of antibody fragments as well as advances in the use of novel and impressive conjugation strategies has meant that such fragments have attracted attention for a range of biotechnological applications. Some of these are as therapeutic agents,[7,8] as diagnostic reagents as biosensors,[9] as conjugation partners in enzyme prodrug strategies,[10,11] and in tumour imaging strategies[12,13] amongst others.[14,15]

For therapeutic purposes, antibody fragments possess an advantage over full-sized monoclonal antibodies in that their smaller size may permit more efficient penetration into tissues. Furthermore, they may be easier and hence less costly to manufacture as glycosylation may not be essential to antibody function, and so prokaryotic expression systems can be used. There are associated disadvantages in losing the Fc portion, in that it is

responsible for stabilising antibody structure, and the Fc allows FcR-mediated recycling, meaning that antibody fragments may be rapidly degraded in the body, and are associated with short circulating half lives.

1.2.1 Fab fragments

Fragment antigen-binding (Fab) fragments were the earliest class of antibody fragments to be isolated and studied in depth.[16] The various Fab forms can be obtained by the proteolytic digestion of intact IgG, and comprise the V_H, V_L, C_H1 and C_L domains (**Figure 1.2**). The expression and secretion of an isolated Fab protein binding to the human carcinoma cell line C3347 was demonstrated in *E. coli*.[17] In general, the retention of specific monovalent antigen-binding affinity is observed, but with improved pharmacokinetics for tissue penetration due to the smaller size of the protein. In therapeutics, Fab fragments have been developed for the treatment of cancer, infectious disease and inflammatory disease.[4] As well as the monovalent Fab fragment, advances in gene technology allow for the formation of bispecific Fabs (Fab_2), and also bivalent Fabs (Fab bivalent).[4] In 2010, it was reported that Fab fragments make up 49% of antibody fragments in the commercial clinical pipeline for therapeutics.[3] In 2008, the FDA approved the PEGylated anti-TNF-α Fab Cimzia® (UCB) for the treatment of Crohn's disease and rheumatoid arthritis.[18]

1.2.2 Single-chain variable fragments

Single chain variable fragments (scFvs) were the first class of engineered antibody fragment.[19] They are recombinant proteins encoding the antigen-binding domains (V_H and V_L) engineered into a single polypeptide chain (**Figure 1.2**). The two domains are joined by a flexible polypeptide linker sequence, and libraries of variants with different linker lengths are routinely made for optimising binding affinities and stabilities.[19] In a therapeutic context,

scFv forms have reached Phase 3 testing.[16] There is a growing diversity in the morphology of scFvs, such as paired scFvs, which bind to each other through complementarity regions forming bivalent (diabodies[20]), trivalent (triabodies[21,22]) and tetravalent (tetrabodies[23]) molecules. Multivalent antibody fragments have particular potential in a therapeutic context. Within tissue, monovalent antibodies and fragments tend to exhibit fast dissociation rates despite high affinity interactions. In contrast the use of engineered multivalent antibodies leads to slower dissociation rates and an increase in functional affinities (avidity).[4] As multivalent antibody fragments are still smaller than intact antibodies,[4] improved tumour penetration and faster blood clearance is still observed. In fact, multivalent diabodies have been reported to outperform monovalent Fab and scFv fragments in terms of efficacy *in vivo*.[24] Multimeric scFv fragments are engineered by reducing the domain linker length to between zero and five residues. A short linker length does not allow domains of the same chain to pair with each other, driving self-assembly of multimeric antibody fragments by the pairing to complementary domains of other chains, producing two or more antigen-binding sites in a single protein.[25]

1.2.3 Heavy-chain antibodies

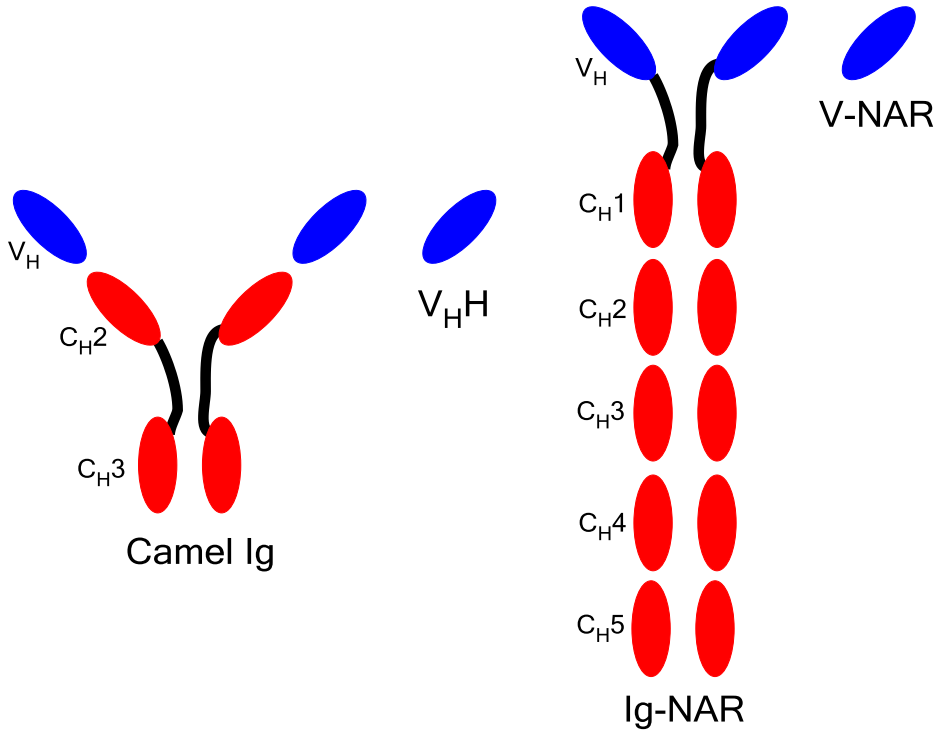

Figure 1.3. Heavy-chain antibodies (HcAbs) completely devoid of light chains are naturally occurring in camel (left) and some shark (right) species. In both cases, the single variable domain can be expressed in the absence of constant domains and retain function.

In addition to conventional antibodies, mammals of the *Camelidae* family and some cartilaginous fish (nurse sharks, wobbegong sharks) have evolved heavy-chain antibodies (HcAbs), so called because they are completely devoid of light chains.[5,6] Shark HcAbs contain one variable and five constant domains, and exist as a dimer in solution (**Figure 1.3**). The single variable domain responsible for antigen binding is referred to as the variable domain of the shark new antigen receptor (V-NAR).[6,26] In *Camelidae* HcAbs, the antigen-binding site is also confined to a single-domain, and the overall structure is a dimer of the V_HH (variable domain of heavy chain of HcAb), C_H2 and C_H3 domains (**Figure 1.3**). The single variable domains can be expressed recombinantly in the absence of constant domains, giving rise to single-domain antibodies (sdAbs), the smallest known intact antigen-binding fragments with high binding affinities.[27] The reasons why two distantly related species have

evolved these antibodies are currently unknown, but of great interest.[28] *Camelidae* sdAbs have received extensive attention in the literature, for use in a broad range of biophysical and pharmaceutical applications. These sdAbs are of particular interest due to their small size (~ 15 kDa), single-domain nature and attractive properties (high stability, the ability to withstand high pressures and low pHs,[29] retention of binding activity in the presence of proteases and detergents,[30] and high solubility[31]).[32,33] Further structural details of sdAbs will be discussed in Chapter 2, whilst selected applications of camelid sdAbs in therapy, diagnostics and immunoanalytical methods will be discussed here.

The small size of sdAbs enhances their potential as therapeutics as they can penetrate tissues and intercellular spaces inaccessible to larger antibodies and some fragments. It has been found that sdAbs have potential uses in diagnostics and for the treatment of neurodegenerative diseases as they are small enough for transmigration across the blood-brain barrier, a major obstacle for larger antibody fragments and intact antibodies.[34,35] However, their small size is also a limitation as it results in a rapid clearance from the blood by renal filtration. Conjugation to other sdAbs which bind to serum albumins and immunoglobulins can prolong half life, and has been demonstrated in pigs using genetic fusion technology.[36] Effective tissue penetration and fast blood clearance are positive features when constructing sdAbs as imaging probes for the *in vivo* monitoring of tumours and metastatic lesions. Following the administration of a ^{99m}Tc-labelled sdAb, antigen targeting is rapid, a contrast-enhanced imaging signal can be obtained, and a reduced accumulation of labelled antibody is observed compared to intact antibodies.[37] As well as their size, sdAbs have a number of unique physicochemical and pharmacological properties making them attractive therapeutic agents, with several sdAbs in phase I and II of clinical testing.[33] The binding site of sdAbs differs from conventional antibodies in that binding is normally

mediated by a protruding CDR3 loop. This means many sdAbs preferentially bind into clefts and cavities on protein surfaces, potentially making them ideal agents for enzyme inhibition[38] and for the neutralisation of proteolytic toxins[39] in cancer and inflammatory diseases. Vercruysse and co-workers showed that intracellular antigens (for example anti-apoptotic proteins, oncogenes and viral proteins) could be targeted by the direct intracellular expression of sdAbs ('intrabodies').[40] The intracellular expression of sdAbs fused to fluorescent moieties ('chromobodies') in living cells has application in tracing these intracellular antigens, and perhaps even modifying protein function.[41] The high structural stability of sdAbs in conditions considered too harsh for other antibodies means they may be ideally suited for the treatment of gastrointestinal disorders in an oral fashion.[42] As with scFvs, sdAbs may be engineered into elaborate multivalent formats for increased therapeutic potency.[43,44] Cortez-Retamozo and co-workers investigated the potential of sdAbs in antibody-directed prodrug strategies.[10] They identified a sdAb binding to human tumour-associated carcinoembryonic antigen, conjugated it to *Enterobacter clocae* β-lactamase, and found the conjugate did have the capacity to activate drug release in desired cells only.[11] As well as their therapeutic potential, sdAbs have been developed for a number of other applications. For example, when used in immunoassays and in biosensors their small size and lower aggregation propensity enables the immobilisation of large amounts of desired sdAb on the surface of wells, resulting in an increase in sensitivity of the immunodetection system. Some of these systems are for the quantitative analysis of contaminants and toxins in food and environmental samples.[45,46] Impressively, sdAbs are also suitable crystallography chaperones, stabilising certain protein conformations during crystallisation trials. In 2011, Rasmussen and co-workers obtained the crystal structure of a usually unstable G protein-coupled receptor (GPCR) in an agonist-bound active state by complexing it to a sdAb raised against the human β_2 adregernic receptor.[47] Lastly, sdAbs are useful agents for immunoaffinity chromatography.

Their ability to bind partners with high affinity, as well as resistance to organic solvents used for the elution of captured ligands and in the regeneration of columns makes them suitable for affinity-based separations.[48]

Single-domain antibodies are constantly being developed further in the therapeutic and biotechnological fields mentioned above, and more. For this reason, there is a wealth of literature available, as well as many up to date reviews.[32,33,49]

1.3 Chemical Modification of Antibodies

Intact antibodies and associated fragments are valuable for biotechnological applications in their own right. However, chemical conjugation to various entities – forming so called immunoconjugates – allows access to species with multiple desired properties. The field of immunoconjugation, including the development of conjugation strategies and the use of different antibody conjugation partners is vast, with many academic groups as well as industrial companies involved in research.[8] The reasons for conjugating antibodies to molecules are numerous, with the main applications being in therapeutics and diagnostics.[15,50,51] For example, the conjugation of an antibody to a small cytotoxic drug results in an antibody-drug conjugate (ADC) where one part recognises a target (an antibody specific for a tumour-associated antigen (TAA) perhaps), and the other is responsible for therapeutic action.[14,52] The antibody provides specificity such that there is an accumulation of the drug in targeted areas, minimising cross-reactivity in healthy tissues. There is evidence that the conjugation of antibody and drug results in increased therapeutic efficiency and potency, meaning that ADCs are a step towards Paul Ehrlich's vision of 'magic bullets' – the historical concept of having agents that target only disease-causing organisms.[53] Antibodies may also be decorated with radiolabels, for diagnostic applications and the delivery of radioisotopes,[13,54] and also non-immunogenic, non-toxic and hydrophilic polymers such as

polyethylene glycol (PEG), which serve to sterically shield the antibody thereby increasing retention times and reducing dosage requirements.[7,18]

1.3.1 Non-site specific chemical strategies for immunoconjugate formation

Non-site specific conjugation to groups of interest (radiolabels, cytotoxic drugs, hydrophilic polymers) can be carried out using functional groups of side chains of amino acids exposed on the surface of a protein. The ε-amino group of lysine residues, the phenol of tyrosine residues and the carboxylate group of aspartate and glutamate residues have all been utilised in non-site specific conjugations.[17,21,24–57] Although modifications via these residues can be useful in antibodies and proteins in general,[58] and have led to therapeutics which have reached various stages of clinical trials, this technique has several disadvantages .[15,50,59–61] For example, in the synthesis of ADCs, non-specific conjugation strategies leads to a complex mixture of species with different molar ratios of drug to antibody and with heterogeneous binding properties. Each ADC form is likely to exhibit distinct *in vivo* pharmacokinetic, efficacy and safety profiles.[62] In a more general sense, non-site specific conjugations can result in lower affinity antibodies;[13] if conjugation occurs close to the CDR then the conjugate may sterically block binding between the antibody and antigen. For the purposes of conjugation mentioned thus far, antibody binding ability needs not to be perturbed by modification, and it is impossible to truly control this when targeting common residues which are present throughout the protein structure. For these reasons, the modification of antibodies in a site-specific fashion is an area of considerable current interest.

1.3.2 Site-specific chemical strategies for immunoconjugate formation at native sites

Glycosylation sites

In 1986, Rodwell and co-workers described the site-specific conjugation of radiolabels to oligosaccharide moieties at Asn-297 of the C_H2 domain within the Fc. Site-specific conjugation was achieved by oxidation of the oligosaccharide terminus with sodium periodate, then reaction of the resulting aldehyde with a compound of interest containing an amine group (**Figure 1.4**).[13] They found that these conjugates were homogeneous and retained binding affinity to a greater extent than heterogeneous conjugate forms obtained by non-specific reactions. Furthermore, *in vivo* studies indicated that homogeneous conjugates localised into target tumours more efficiently than heterogeneous conjugates.[13,63] The disadvantages of the methodology were that it could not be applied to Fab arms (and other antibody fragments), as glycosylation was located in the Fc, and that the conjugation partner would perhaps be limited by size, as the site of reaction is in an internal space, and therefore sterically hindered. The issue of a lack of glycosylation sites in Fabs was circumvented by Qu and co-workers in 1998, by mutating glycosylation acceptor sequences (AST) into the Cκ or C_H1 domains of humanised anti-CD22 mAb hLL2.[54]

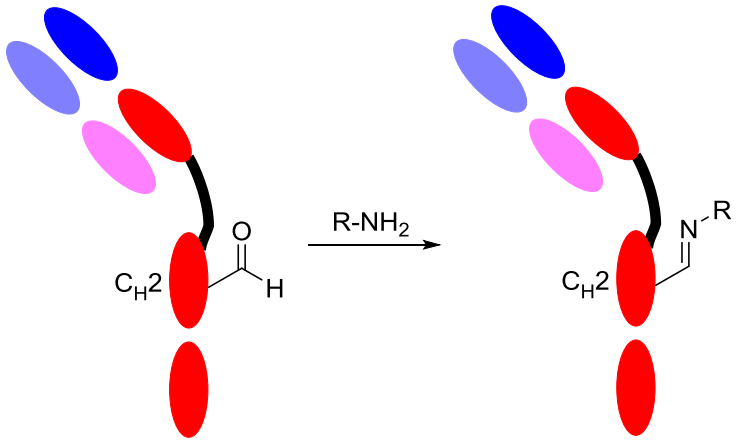

Figure 1.4. Site-specific imine formation at Asn-297 within the C_H2 of IgG. For clarity, only one half of the intact IgG structure is shown.[13]

Cysteine residues

The cysteine moieties which are usually involved in interchain disulfide bonds have been used to site-specifically attach groups of interest to antibodies.[64] This may be achieved by mild reduction of the antibody (so as not to disturb intrachain disulfides holding framework regions together), then reaction with an electrophilic group of interest. Cysteine residues are an attractive precursor for site-specific modifications as they are relatively rare and are readily introduced using standard mutagenesis techniques.[65] However, the method does not always result in singly-modified homogeneous immunoconjugates as a number of interchain disulfides are present, and are equally susceptible to mild reduction. This issue has been addressed by using mutagenesis to replace one of the cysteines of an interchain disulfide pair with the chemically similar serine residue, so as to have one reactive thiol only for single modification.[66] This may disrupt the quaternary structure of the antibody, thus potentially perturbing antibody activity. Junutula and co-workers have described a phage-display method for predicting suitable conjugation sites on antibody surfaces.[67] They have used this method to install cysteine residues at these sites in the Fab of trastuzumab (a clinically approved monoclonal antibody (mAb) for the treatment of breast cancer) and in anti-MUC16 3A5. These modified proteins were able to react with maleimides only at the engineered cysteines, and without disrupting native intra- and inter- chain disulfides (**Figure 1.5**). In these examples the antibody did not lose any affinity for antigen.[62] Alternatively, Schumacher and co-workers have very recently described an approach for functionalising disulfide bonds in an scFv with bis-reactive maleimide bridging reagents.[68] Targeting both cysteines following reduction of the disulfide bond circumvents stability issues that are encountered when opening up a disulfide bond and targeting a single cysteine and leaving one unpaired.[69] Furthermore, the nitrogen of the maleimide may be functionalised with a range of groups of

interest, such as PEG and fluorescence labels.[68] Casi and co-workers have also used cysteine as a ligation partner for forming ADCs. In their 2012 study, they did not use existing disulfide bonds, instead engineering cysteine residues at the N-terminus of the clinical stage human mAb F8. These residues were used to carry out site-specific modification with an aldehyde-bearing potent drug, forming a thiazolidine linkage via condensation (**Figure 1.5**).[70]

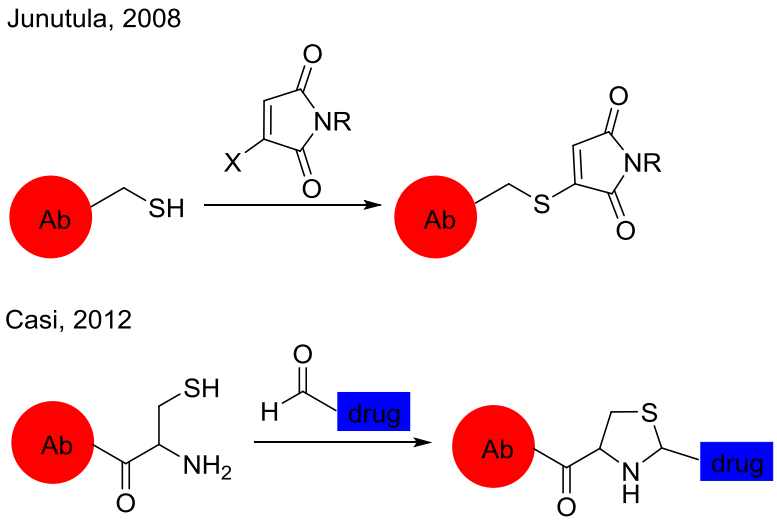

Figure 1.5. Selected examples of site-specific antibody modification via cysteine.[67,70]

The field of covalent antibody conjugation is constantly expanding, and very recently, Baran's group have also described antibody-drug conjugation using cysteines on the surface of the mAb MOR1 to react with a maleimide-DBCO moiety (DBCO – dibenzylazacyclooctyne).[71] Interestingly, the focus of their study was not the site of conjugation on the antibody, but expanding the repertoire of compounds that can be conjugated to the antibody. They were successful in equipping a range of complex natural products and non-natural biologically active agents lacking in conventional functional groups for activation (i.e. heteroatom-H, π-bonds) with a chemical handle for conjugation purposes. This was achieved by reacting the seemingly inert substrate with the reagent sodium (difluoroalkylazide) sulfinate, which on reacting, forms radicals *in situ* via an oxidative process resulting in C-H activation. The product of such reactions is an azide which enables

subsequent bioconjugation by strain-promoted cycloaddition with the cyclooctyne functionality[72,73] linked to the mAb. Although the antibody conjugation methodology used here is not novel, and arguably perhaps not the most exciting method for site-specific conjugation, the study provides an interesting insight into expanding the repertoire of conjugation partners to antibodies.

Nucleotide binding site

Earlier this year, Alves and co-workers identified the nucleotide binding site (NBS) found in Fab variable domains as an attractive target for site-specific covalent functionalisation. The NBS is rich in the aromatic residues tyrosine, phenylalanine and tryptophan, and the region has thus far received relatively little attention in terms of functionalisation. Indole-3-butyric acid (IBA) was found to bind to the NBS with micromolar affinities. Furthermore it can be covalently attached to the aromatic residues within the NBS only via photocrosslinking upon exposure to UV irradiation (**Figure 1.6**). Determination of the covalent linkage formed was carried out by in-depth mass spectrometry analysis and detailed docking minimisation. IBA derivatives were conjugated to a range of reporter groups, allowing access to a range of immunoconjugates.[74] This technique is particularly impressive as site-specificity can be achieved without having to incorporate non-natural amino acids.

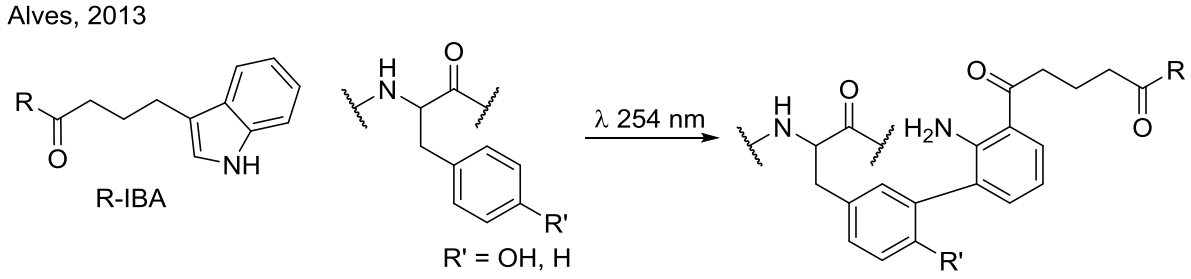

Figure 1.6. Proposed photocrosslinking mechanism between Tyr or Phe within the NBS with IBA.[74]

1.3.3 Site-specific chemical strategies for immunoconjugate formation using non-natural amino acids

The issue of modification having detrimental or unpredictable effects on the structure and function of an antibody may be alleviated by the use of non-natural amino acids. Non-natural amino acids are commonly engineered genetically or post-translationally into proteins as orthogonal handles for further transformation.[75,76] As well as the orthogonality allowing control of the stoichiometry of conjugation, the site of introduction can be chosen.

Ketone introduction at the N-terminus

Scheck and Francis have demonstrated the introduction of a ketone moiety at the N-terminus of antibodies using a biomimetic transamination reaction in the presence of PLP (pyridoxal 5'-phosphate). The ketone could undergo further site-specific functionalisation with alkoxyamine compounds (**Figure 1.7**).[77] The methodology was demonstrated on mouse anti-flag IgG, mouse α-actin and mouse α-biotin-peroxidase, although the authors indicate that the use of elevated temperatures and prolonged incubation times in their procedures decreases the potential generality of the method. It may be considered a disadvantage that the reaction is restricted to the N-terminus of an antibody, but its selectivity is impressive, showing no cross reaction with lysine residues. This methodology has been developed further by the decoration of Fc domains. A ketone was introduced as described earlier using the biomimetic transamination reaction,[77] followed by further reaction with an alkoxyamine compound containing an aniline group. This second chemical handle could then be selectively ligated with an amino phenol reagent containing a DNA aptamer. The resulting antibody-DNA aptamer conjugates were found to be functional, the antibody portion retaining binding activity, and the DNA aptamer portion retaining specificity for its cellular target.[78]

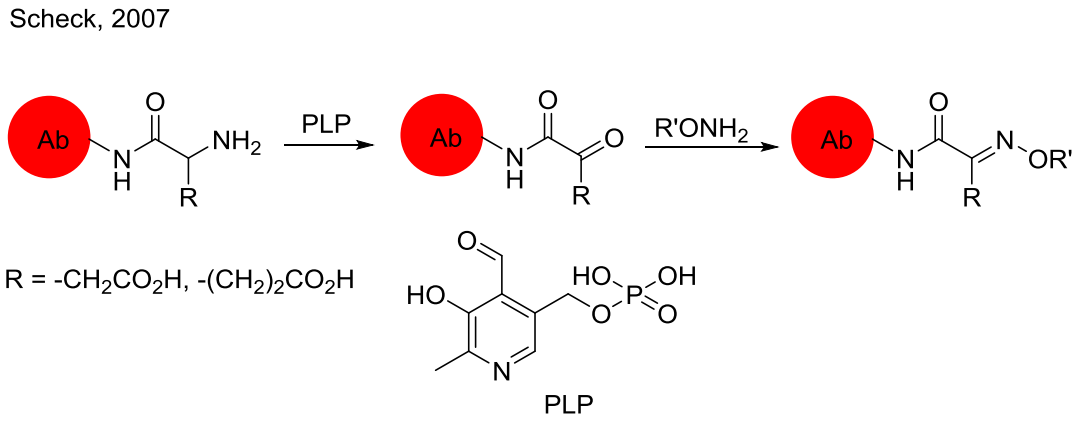

Figure 1.7. N-terminal introduction of ketone moiety by a biomimetic transamination reaction using PLP (pyridoxal 5'-phosphate), and subsequent functionalisation with an alkoxyamine compound.[77]

p-Acetylphenylalanine

The non-natural amino acid *p*-acetylphenylalanine (pAcPhe) can react with alkoxyamine-derivatised compounds to give oxime-linked conjugates (**Figure 1.8**).[79,80] None of the 20 proteinogenic amino acids exhibit this reactivity, making pAcPhe a useful orthogonal handle for chemical conjugation.

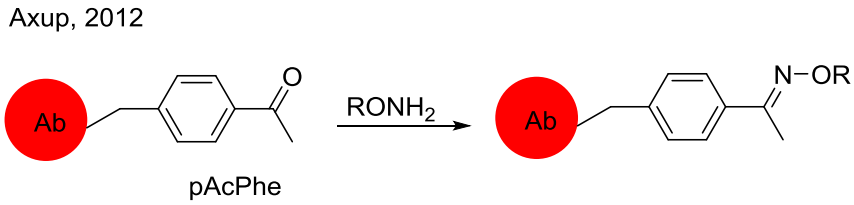

Figure 1.8. Oxime formation via pAcPhe reaction with an alkoxyamine.[79]

pAcPhe can be site-specifically installed genetically using an orthogonal amber suppressor tRNA/aminoacyl-tRNA synthetase (aaRS) pair in response to an amber nonsense codon.[81] Such methodology has been used by the groups of Schultz and Smider to form an array of antibody conjugates.[79,80,82–85] pAcPhe was installed at various sites distant from the binding region of the anti-HER2 Fab fragment (HER2 – human epidermal growth receptor 2). Conjugation to an alkoxyamine-derivatised auristatin molecule was then carried out, and the resulting oxime-linked conjugate exhibited similar pharmacokinetic and cytotoxic properties

to the wild type.[79] One disadvantage of this method is the long reaction times; in some cases conjugation took up to 2 days to reach completion. This orthogonal reaction handle was also used to functionalise anti-HER2 with hydroxylamine biotin, which was further assembled into multimers in the presence of tetrameric biotin-binding NeutrAvidin. These multimers were retained specificity and were functional in $HER2^+$ cells.[82] Furthermore, the same methodology was used to form antibody-oligonucleotide conjugates which were able to self assemble into a number of multimers, driven by the oligonucleotides forming diverse chemical structures.[85] Two Fab fragments, specific for HER2 and CD20 were used, resulting in a bispecific conjugate. An elegant alternative approach to a bispecific antibody involves encoding pAcPhe into both anti-HER2 and anti-CD3, then reaction with a bifunctional ethylene glycol linker with alkoxyamine at one end and either an azide or cyclooctyne at the other for subsequent copper-free (Cu-free) cycloaddition ligations.[73,83] Conjugation of anti-HER2 to a bifunctional linker containing an alkoxyamine at one end and a maleimide at the other allowed further reaction with thiol-functionalised singly-stranded DNA (ssDNA) to form oligobodies. These were then observed in immuno-PCR assays, allowing detection of $HER2^+$ cells in complex environments with increased sensitivity and specificity as compared to non-specifically coupled fragments.[86] Finally, orthogonal reactions with pAcPhe has also been used to synthesise antibody-polymer conjugates (with anti-HER2 and full length IgG) for the specific delivery of small interference RNAs (siRNAs) to $HER2^+$ cells.[84]

It is clear from the examples described above that the use of non-natural amino acids and orthogonal reactivity allows the formation of a wide range of homogeneous immunoconjugates with enhanced properties.

Formylglycine

The group of Bertozzi have developed a method for the incorporation of an aldehyde tag in the form of the non-natural amino acid formylglycine (fGly) at the N-terminus of a protein.[87] This is achieved by engineering the amino acid sequence CxPxR into the antibody at the N-terminus. This sequence is recognised by formylglycine-generating enzyme (FGE), which oxidises the cysteine to fGly during expression, resulting in a protein containing an orthogonal aldehyde tag which may subsequently be modified by hydrazone or oxime formation (**Figure 1.9**).[87]

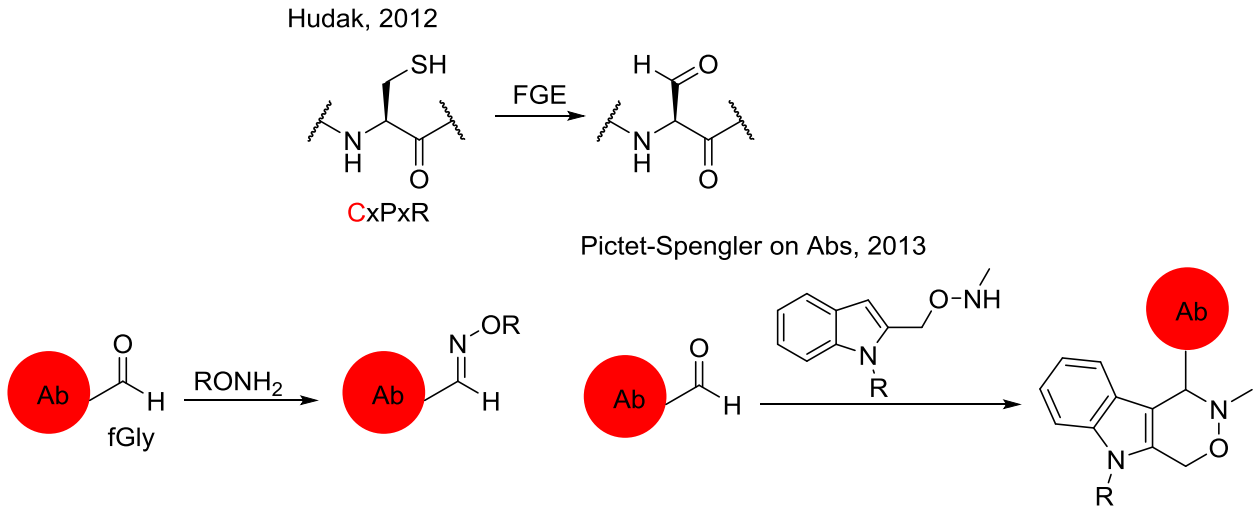

Figure 1.9. Formylglycine-generating enzyme (FGE) converts cysteine to fGly, and can be functionalised further with alkoxyamine compounds.[87]

fGly was incorporated into human IgG and used to form a conjugate with a bifunctional linker bearing an alkoxyamine group at one end and a cyclooctyne at the other for subsequent conjugation via Cu-free click ligation to an azide-bearing group of interest.[73] The same group have recently described the incorporation of an aldehyde tag into trastuzumab with subsequent conjugation via a Pictet-Spengler ligation with alkoxyamine-functionalised indoles (**Figure 1.9**).[88]

Expressed protein ligation

Proteins can be synthesised by fusing multiple peptide fragments together using Native Chemical Ligation (NCL).[89] Furthermore, Expressed Protein Ligation (EPL), where a recombinant α-thioester is installed at the C-terminus of a protein using intein-mediated protein splicing can be used to carry out ligations to N-terminal cysteine-containing peptides (**Figure 1.10**).

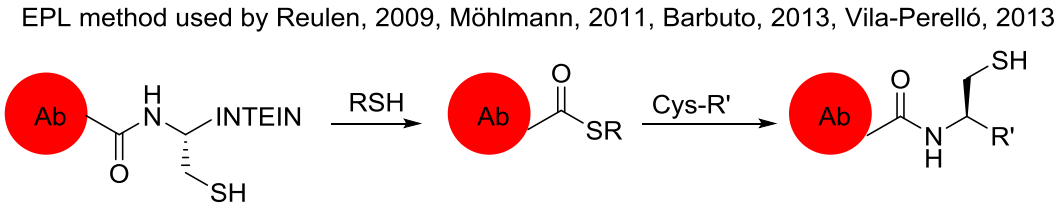

Figure 1.10. Expressed Protein Ligation (EPL).[90–93]

Mölhmann and co-workers applied this methodology to a full length IgG specific for fibronectin extra domain-B (ED-B),[94] which was expressed as a fusion protein bearing inteins at the C-terminus heavy chains which were subsequently ligated to biotin.[91] The group of Tom Muir used EPL to site-specifically ligate a mAb against the C-type lectin DEC205 to a fluorescent peptide using a newly developed streamlined procedure for purification and generation of protein α-thioesters from cell lysates.[93] The methodology need not be restricted to conjugations between proteins. A homogenous DEC205-dsDNA (ds – double-stranded) conjugate was prepared by the expression of DEC205 bearing inteins at the C-terminal heavy chains. The inteins were cleaved with MESNA (2-mercaptoethane sulfonate) to give the required α-thioester moieties, which were subsequently ligated to cysteine-dsDNA, and elongated with the immune stimulant, poly dA:dT. The targeted delivery of poly dA:dT to human monocyte-derived dendritic cells (MoDCs, DCs – dendritic cells) led to the production of type 1 interferon (IFN), and *in vivo*, the secretion of type 1 IFN.[92] The

formation of immunomicelles was described by Reulen and co-workers.[90] They expressed a correctly folded sdAb-intein fusion by exporting antibody to the oxidising periplasmic space in *E. coli*. MESNA-induced intein cleavage yielded the C-terminal α-thioester, which could be functionalised with cysteine-functionalised PEGylated phospholipids for the generation of immunomicelles. This approach of exporting the protein to the periplasm offers an attractive alternative to the more commonly used method of expressing intein fusion proteins for EPL purposes in the reducing cytoplasm of *E. coli*.[95] In the reducing environment the proper formation of disulfide bonds, essential for correct antibody folding, is prevented.

Post-translational modification using sortases

Ploegh has described the synthesis of a range of bispecific antibodies (including camelid sdAbs[5]) using ready-folded antibodies at the N- or C- termini to form unusual N-to-N or C-to-C linked fusion proteins.[96–98] An antibody bearing the recognition sequence for sortase A (LPXTG) at one of the termini is treated with enzyme, which cleaves between T and G forming a thioester linkage between the protein of interest and sortase A (**Figure 1.11**). The resulting conjugate is further treated with a peptide in which one amino acid bears a ligation partner for the Cu-free cycloaddition (azide or cyclooctyne).[73] The peptide displaces the enzyme portion, yielding the antibody bearing a terminal peptide with an orthogonal tag (**Figure 1.11**). Two antibodies with different specificities tagged with orthogonal ligation partners can then be reacted, forming a bispecific antibody.[99] Ploegh has also used sortase A to mediate the site-specific modification of αDEC205.[100]

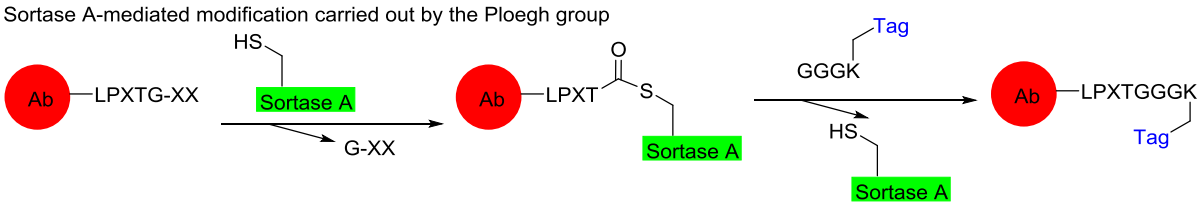

Figure 1.11. Sortase A-mediated modification of antibodies, incorporating orthogonal reaction tags for forming bispecific antibodies.[96]

1.3.4 Chemical modifications within binding regions using photoaffinity labelling

Much of the focus of forming immunoconjugates in the recent literature is focused on modifications away from the binding regions of antibodies and antibody fragments. This is understandable considering the vast potential of immunoconjugates for therapeutic and diagnostic applications.[8,50,52] However, the aim of the work described in this thesis was to investigate the effect of site-specific covalent modifications within the binding region of an antibody. The chemical modification of antibodies within binding regions is a relatively unstudied area, although in the 1970s several groups were involved in so-called photoaffinity labelling – that is, the non-site specific covalent attachment of photolysable groups with the aim of understanding the binding regions of an individual antibody on the structural level. Similar experiments were carried out in enzyme active sites in an analogous fashion.[101,102] In summary, antibodies could be raised against haptenic groups bearing photolysable functionality (e.g. 4-azido-2-nitrophenyl group) by immunisation, and then antibodies against the haptenic determinant could be isolated. Addition of the haptenic group to the isolated antibodies resulted in non-covalent antibody-hapten complexes. These complexes would undergo formation of covalent linkages upon photolysis.[103–108] Although the hapten groups reacted in a non-site specific manner, an original specificity between raised antibody and hapten implied that the hapten was focused predominantly in the binding region.

Although previous work on the photoaffinity labelling of antibodies in binding regions was seminal in reaching an understanding of the structure and location of epitope recognition sites, alternative methods for the site-specific covalent modification of the binding regions of antibodies have not since been developed for other purposes. This is despite an increasing interest in 'masking' antibodies for therapeutic targeting,[109,110] which will be discussed further in Chapter 4. It is thought that the application of site-specific methodology using non-natural amino acids which has been developed and utilised on other proteins should be applicable to the antibody binding region. Applications of site-specific conjugation in regions distant from the complementarity determining domains of antibodies have already been described and found to have various uses. The introduction of non-natural amino acids post-translationally and site-specifically into the binding region of an antibody fragment (namely within the CDR3 loop of the sdAb cAb-Lys3[111]) with the aim of modulating binding affinities will be the focus of the following chapters of this thesis.

1.4 Chapter 1 References

1. Delves, P., Martin, S., Burton, D., Roitt, I. *Roitt's Essential Immunology*. (Wiley-Blackwell, 2006).

2. Davies, D., Chacko, S. Antibody structure. *Acc. Chem. Res.* **26,** 421–427 (1993).

3. Nelson, A. L. Hope and hype. *MAbs* **2,** 77–83 (2010).

4. Holliger, P., Hudson, P. J. Engineered antibody fragments and the rise of single domains. *Nat. Biotechnol.* **23,** 1126–1136 (2005).

5. Hamers-Casterman, C., Atarhouch, T., Muyldermans, S., Robinson, G., Hamers, C., Songa, E. B., Bendahman, N., Hamers, R. Naturally occurring antibodies devoid of light chains. *Nature* **363,** 446–448 (1993).

6. Greenberg, A., Avila, D., Hughes, M. A new antigen receptor gene family that undergoes rearrangement and extensive somatic diversification in sharks. *Nature* **374,** 168–173 (1995).

7. Duncan, R. Polymer conjugates as anticancer nanomedicines. *Nat. Rev. Cancer* **6,** 688–701 (2006).

8. Webb, S. Pharma interest surges in antibody drug conjugates. *Nat. Biotechnol.* **29,** 297–298 (2011).

9. Pleschberger, M., Saerens, D., Weigert, S., Sleytr, U. B., Muyldermans, S., Sara, M., Egelseer, E. M. An S-layer heavy chain camel antibody fusion protein for generation of a nanopatterned sensing layer to detect the prostate-specific antigen by surface plasmon resonance technology. *Bioconjugate Chem.* **15,** 664–671 (2004).

10. Springer, C., Niculescu-Duvaz, I. Antibody-directed enzyme prodrug therapy (ADEPT): a review. *Adv. Drug Deliv. Rev.* **26,** 151–172 (1997).

11. Cortez-Retamozo, V., Backmann, N., Senter, P. D., Wernery, U., De Baetselier, P., Muyldermans, S., Revets, H. Efficient cancer therapy with a nanobody-based conjugate. *Cancer Res.* **64,** 2853–2857 (2004).

12. Scheinberg, D. A., Strand, M., Gansow, O. A. Tumor imaging with radioactive metal chelates conjugated to monoclonal antibodies. *Science* **215,** 1511–1513 (1982).

13. Rodwell, J. D., Alvarez, V. L., Lee, C., Lopes, A. D., Goers, J. W. F., King, H. D., Powsner, H. J., McKearn, T. J. Site-specific covalent modification of monoclonal antibodies: *in vitro* and *in vivo* evaluations. *Proc. Natl. Acad. Sci. U. S. A.* **83,** 2632–2636 (1986).

14. Wu, A. M., Senter, P. D. Arming antibodies: prospects and challenges for immunoconjugates. *Nat. Biotechnol.* **23,** 1137–1146 (2005).

15. Koshkaryev, A., Sawant, R., Deshpande, M., Torchilin, V. Immunoconjugates and long circulating systems: origins, current state of the art and future directions. *Adv. Drug Deliv. Rev.* **65,** 24–35 (2013).

16. Nelson, A. L., Reichert, J. M. Development trends for therapeutic antibody fragments. *Nat. Biotechnol.* **27,** 331–337 (2009).

17. Better, M., Chang, C. P., Robinson, R. R., Horwitz, A. H. *Escherichia coli* secretion of an active chimeric antibody fragment. *Science* **240,** 1041–1043 (1988).

18. Goel, N., Stephens, S. Certolizumab pegol. *MAbs* **2,** 137–147 (2010).

19. Bird, R. E., Hardman, K. D., Jacobson, J. W., Johnson, S., Kaufman, B. M., Lee, S. M., Lee, T., Pope, S. H., Riordan, G. S., Whitlow, M. Single-chain antigen-binding proteins. *Science* **242 ,** 423–426 (1988).

20. Holliger, P., Prospero, T., Winter, G. "Diabodies": small bivalent and bispecific antibody fragments. *Proc. Natl. Acad. Sci. U. S. A.* **90,** 6444–6448 (1993).

21. Pei, X. Y., Holliger, P., Murzin, A. G., Williams, R. L. The 2.0-A resolution crystal structure of a trimeric antibody fragment with noncognate V_H-V_L domain pairs shows a rearrangement of V_H CDR3. *Proc. Natl. Acad. Sci. U. S. A.* **94,** 9637–9642 (1997).

22. Iliades, P., Kortt, A. A., Hudson, P. J. Triabodies: single chain Fv fragments without a linker form trivalent trimers. *FEBS Lett.* **409,** 437–441 (1997).

23. Dolezal, O., De Gori, R., Walter, M., Doughty, L., Hattarki, M., Hudson, P. J., Kortt, A. A. Single-chain Fv multimers of the anti-neuraminidase antibody NC10: the residue at position 15 in the V_L domain of the scFv-0 (V_L-V_H) molecule is primarily responsible for formation of a tetramer-trimer equilibrium. *Protein Eng. Des. Sel.* **16,** 47–56 (2003).

24. Griffiths, G. L., Chang, C-H., McBride, W. J., Rossi, E. A., Sheerin, A., Tejada., G. R., Karacay, H., Sharkey, R. M., Horak, I. D., Hansen, H. J., Goldenberg, D. M. Reagents and methods for PET using bispecific antibody pretargeting and ^{68}Ga-radiolabeled bivalent hapten-peptide-chelate conjugates. *J. Nucl. Med.* **45,** 30–39 (2004).

25. Todorovska, A., Roovers, R. C., Dolezal, O., Kortt, A. A., Hoogenboom, H. R., Hudson, P. J. Design and application of diabodies, triabodies and tetrabodies for cancer targeting. *J. Immunol. Methods* **248,** 47–66 (2001).

26. Roux, K. H., Greenberg, A. S., Greene, L., Strelets, L., Avila, D., McKinney, E. C., Flajnik, M. F. Structural analysis of the nurse shark (new) antigen receptor (NAR): molecular convergence of NAR and unusual mammalian immunoglobulins. *Proc. Natl. Acad. Sci. U. S. A.* **95,** 11804–11809 (1998).

27. Harmsen, M. M., De Haard, H. J. Properties, production, and applications of camelid single-domain antibody fragments. *Appl. Microbiol. Biotechnol.* **77,** 13–22 (2007).

28. Flajnik, M. F., Deschacht, N., Muyldermans, S. A case of convergence: why did a simple alternative to canonical antibodies arise in sharks and camels? *PLoS Biol.* **9,** e1001120 (2011).

29. Dumoulin, M., Conrath, K., van Meirhaeghe, A., Meersman, F., Heremans, K., Frenken, L. G. J., Muyldermans, S., Wyns, L., Matagne, A. Single-domain antibody fragments with high conformational stability. *Protein Sci.* **11,** 500–515 (2002).

30. Dolk, E., van der Vaart, M., Hulsik, D. L., Vriend, G., de Haard, H., Spinelli, S., Cambillau, C., Frenken, L., Varrips, T. Isolation of Llama Antibody Fragments for Prevention of Dandruff by Phage Display in Shampoo Isolation of Llama Antibody Fragments for Prevention of Dandruff by Phage Display in Shampoo. *Appl. Environ. Microbiol.* **71,** 442–450 (2005).

31. Saerens, D., Pellis, M., Loris, R., Pardon, E., Dumoulin, M., Matagne, A., Wyns, L., Muyldermans, S., Conrath, K. Identification of a universal V_HH framework to graft non-canonical antigen-binding loops of camel single-domain antibodies. *J. Mol. Biol.* **352,** 597–607 (2005).

32. De Marco, A. Biotechnological applications of recombinant single-domain antibody fragments. *Microb. Cell Fact.* **10** (2011).

33. Eyer, L., Hruska, K. Single-domain antibody fragments derived from heavy-chain antibodies: a review. *Vet. Med. (Praha).* **57,** 439–513 (2012).

34. De Genst, E. J., Guilliams, T., Wellens, J., O'Day, E. M., Waudby, C. A., Meehan, S., Dumoulin, M., Hsu, S.-T. D., Cremades, N., Verschueren, K. H. G., Pardon, E., Wyns, L., Steyaert, J., Christodoulu, J., Dobson, C. M. Structure and properties of a complex of α-synuclein and a single-domain camelid antibody. *J. Mol. Biol.* **402,** 326–343 (2010).

35. Nabuurs, R. J. A., Rutgers, K. S., Wellings, M. M., Metaxas, A., de Backer, M. E., Rotman, M., Bacskai, B. J., van Buchem, M. A., van der Maarel, S. M., van der Weerd, L. *In vivo* detection of amyloid-β deposits using heavy chain antibody fragments in a transgenic mouse model for Alzheimer's disease. *PLoS One* **7,** e38284 (2012).

36. Harmsen, M. M., Van Solt, C. B., Fijten, H. P. D., Van Setten, M. C. Prolonged *in vivo* residence times of llama single-domain antibody fragments in pigs by binding to porcine immunoglobulins. *Vaccine* **23,** 4926–4934 (2005).

37. Gainkam, L. O. T., Keyaerts, M., Caveliers, V., Devoogdt, N., Vanhove, C., van Grunsven, L., Muyldermans, S., Lahoutte, T. Correlation between epidermal growth factor receptor-specific nanobody uptake and tumor burden: a tool for noninvasive monitoring of tumor response to therapy. *Mol. Imaging Biol.* **13,** 940–948 (2011).

38. Paalanen, M. M. I., Ekokoski, E., el Khattabi, M., Tuominen, R. K., Verrips, C. T., Boonstra, J., Blanchetot, C. The development of activating and inhibiting camelid V_HH

domains against human protein kinase C epsilon. *Eur. J. Pharm. Sci.* **42,** 332–339 (2011).

39. Hussack, G., Ghahroudi, M. A., van Faassen, H., Songer, J. G., Ng, K. K.-S. MacKenzie, R., Tanha, J. Neutralization of Clostridium difficile toxin A with single-domain antibodies targeting the cell receptor binding domain. *J. Biol. Chem.* **286,** 8961–8976 (2011).

40. Vercruysse, T., Pardon, E., Vanstreels, E., Steyaert, J., Daelemans, D. An intrabody based on a llama single-domain antibody targeting the N-terminal alpha-helical multimerization domain of HIV-1 rev prevents viral production. *J. Biol. Chem.* **285,** 21768–21780 (2010).

41. Schmidthals, K., Helma, J., Zolghadr, K., Rothbauer, U., Leonhardt, H. Novel antibody derivatives for proteome and high-content analysis. *Anal. Bioanal. Chem.* **397,** 3203–3208 (2010).

42. Vandenbroucke, K., de Haard, H., Beirnaert, E., Dreier, T., Lauwereys, M., Huyck, L., van Huysse, J., Demetter, P., Steidler, L., Remaut, E., Cuvelier, C., Rottiers, P. Orally administered *L. lactis* secreting an anti-TNF nanobody demonstrate efficacy in chronic colitis. *Mucosal Immunol.* **3,** 49–56 (2010).

43. Stone, E., Hirama, T., Tanha, J., Tong-Sevinc, H., Li, S., MacKenzie, C. R., Zhang, J. The assembly of single domain antibodies into bispecific decavalent molecules. *J. Immunol. Methods* **318,** 88–94 (2007).

44. Tijink, B. M., Laeremans, T., Budde, M., Stigter-van Walsum, M., Dreier, T., de Haard H. J., Leemans, C. R., van Dongen, G. A. M. S. Improved tumor targeting of anti-epidermal growth factor receptor nanobodies through albumin binding: taking advantage of modular nanobody technology. *Mol. Cancer Ther.* **7,** 2288–2297 (2008).

45. Conway, J. O., Sherwood, L. J., Collazo, M. T., Garza, J. A., Hayhurst, A. Llama single domain antibodies specific for the 7 botulinum neurotoxin serotypes as heptaplex immunoreagents. *PLoS One* **5,** e8818 (2010).

46. Doña, V., Urrutia, M., Bayardo, M., Alzogaray, V., Goldbaum, F. A., Chirdo, F. G. Single domain antibodies are specially suited for quantitative determination of gliadins under denaturing conditions. *J. Agric. Food Chem.* **58,** 918–926 (2010).

47. Rasmussen, S. G. F., Choi, H.-J. and co-workers, Structure of a nanobody-stabilized active state of the β(2) adrenoceptor. *Nature* **469,** 175–180 (2011).

48. Franco, E. J., Sonneson, G. J., DeLegge, T. J., Hofstetter, H., Horn, J. R., Hofstetter, O. Production and characterization of a genetically engineered anti-caffeine camelid antibody and its use in immunoaffinity chromatography. *J. Chromatogr. B. Analyt. Technol. Biomed. Life Sci.* **878,** 177–186 (2010).

49. Muyldermans, S. Nanobodies: natural single-domain antibodies. *Annu. Rev. Biochem.* **82,** 775–797 (2013).

50. Goldenberg, D. M., Sharkey, R. M. Novel radiolabeled antibody conjugates. *Oncogene* **26,** 3734–3744 (2007).

51. Wakankar, A., Chen, Y., Gokarn, Y., Jacobson, F. S. Analytical methods for physicochemical characterization of antibody drug conjugates. *MAbs* **3,** 161–172 (2011).

52. Alley, S. C., Okeley, N. M., Senter, P. D. Antibody-drug conjugates: targeted drug delivery for cancer. *Curr. Opin. Chem. Biol.* **14,** 529–537 (2010).

53. Stern, F. Paul Ehrlich: the founder of chemotherapy. *Angew. Chem. Int. Ed. Engl.* **43,** 4254–4261 (2004).

54. Qu, Z., Sharkey, R. M., Hansen, H. J., Shih, L. B., Govindson, S. V., Shen, J., Goldenberg, D. M., Leung, S. Carbohydrates engineered at antibody constant domains can be used for site-specific conjugation of drugs and chelates. *J. Immunol. Methods* **213,** 131–144 (1998).

55. Goldenberg, D., DeLand, F. Use of radio-labeled antibodies to carcinoembryonic antigen for the detection and localization of diverse cancers by external photoscanning. *N. Engl. J. Med.* **298,** 1384–1388 (1978).

56. Hammond, N., Moldofsky, P., Beardsley, M., Mulhern, C. J. External imaging techniques for quantitation of distribution of I-131 Fab′ fragments of monoclonal antibody in humans. *Med. Phys.* **11,** 778–783 (1984).

57. Kumaresan, P., Luo, J., Song, A. Evaluation of ketone-oxime method for developing therapeutic on-demand cleavable immunoconjugates. *Bioconjugate Chem.* **19,** 1313–1318 (2008).

58. Baslé, E., Joubert, N., Pucheault, M. Protein chemical modification on endogenous amino acids. *Chem. Biol.* **17,** 213–227 (2010).

59. Theuer, C. P., Kreitman, R. J., Fitzgerald, D. J. Immunotoxins made with a recombinant form of Pseudomonas exotoxin A that do not require proteolysis for activity. *Cancer Res.* **53,** 340–347 (1993).

60. Kreitman, R., Hansen, H., Jones, A. Pseudomonas exotoxin-based immunotoxins containing the antibody LL2 or LL2-Fab′ induce regression of subcutaneous human B-cell lymphoma in mice. *Cancer Res.* **53,** 819–825 (1993).

61. Trail, P. A., Willner, D., Lasch, S. J., Henderson, A. J., Hofstead, S., Casazza, A. M., Firestone, R. A., Hellstrom, I., Hellstrom, K. E. Cure of xenografted human carcinomas by BR96-doxorubicin immunoconjugates. *Science* **261,** 212–215 (1993).

62. Junutula, J. R., Raab, H. and co-workers, Site-specific conjugation of a cytotoxic drug to an antibody improves the therapeutic index. *Nat. Biotechnol.* **26,** 925–932 (2008).

63. Shih, L. B., Sharkey, R. M., Primus, F. J., Goldenberg, D. M. Site-specific linkage of methotrexate to monoclonal antibodies using an intermediate carrier. *Int. J. Cancer* **41,** 832–839 (1988).

64. Hamblett, K., Senter, P., Chace, D. Effects of drug loading on the antitumor activity of a monoclonal antibody drug conjugate. *Clin. Cancer Res.* **10,** 7063–7070 (2004).

65. Chalker, J. M., Bernardes, G. J. L., Lin, Y. A., Davis, B. G. Chemical modification of proteins at cysteine: opportunities in chemistry and biology. *Chem. Asian J.* **4,** 630–640 (2009).

66. Roberge, M., Estabrook, M., Basler, J., Chin, R., Gualfetti, P., Liu, A., Wong, S. B., Rashid, M. H., Graycar, T., Babé, L., Schellenberger, V. Construction and optimization of a CC49-based scFv-beta-lactamase fusion protein for ADEPT. *Protein Eng. Des. Sel.* **19,** 141–145 (2006).

67. Junutula, J. R., Bhakta, S., Raab, H., Ervin, K. E., Eigenbrot, C., Vandlen, R., Scheller, R. H., Lowman, H. B. Rapid identification of reactive cysteine residues for site-specific labeling of antibody-Fabs. *J. Immunol. Methods* **332,** 41–52 (2008).

68. Schumacher, F. F., Sanchania, V. A., Tolner, B., Wright, Z. V. F., Ryan, C. P., Smith, M. E. B., Ward, J. M., Caddick, S., Kay, C. W. M., Aeppli, G., Chester, K. A., Baker, J. R. Homogeneous antibody fragment conjugation by disulfide bridging introduces "spinostics". *Sci. Rep.* **3,** 1525 (2013) DOI: 10.1038/srep01525.

69. Liu, H., Chumsae, C., Gaza-Bulseco, G., Hurkmans, K., Radziejewski, C. H. Ranking the susceptibility of disulfide bonds in human IgG1 antibodies by reduction, differential alkylation, and LC-MS analysis. *Anal. Chem.* **82,** 5219–5226 (2010).

70. Casi, G., Huguenin-Dezot, N., Zuberbühler, K., Scheuermann, J., Neri, D. Site-specific traceless coupling of potent cytotoxic drugs to recombinant antibodies for pharmacodelivery. *J. Am. Chem. Soc.* **134,** 5887–5892 (2012).

71. Zhou, Q., Gui, J., Pan, C.-M., Albone, E., Cheng, X., Suh, E. M., Grasso, L., Ishihara, Y., Baran, P. S. Bioconjugation by native chemical tagging of C-H bonds. *J. Am. Chem. Soc.* **135,** 12994–12997 (2013).

72. Ning, X., Guo, J., Wolfert, M. A., Boons, G.-J. Visualizing metabolically labeled glycoconjugates of living cells by copper-free and fast huisgen cycloadditions. *Angew. Chem. Int. Ed. Engl.* **47,** 2253–2255 (2008).

73. Jewett, J. C., Bertozzi, C. R. Cu-free click cycloaddition reactions in chemical biology. *Chem. Soc. Rev.* **39,** 1272-1279 (2010).

74. Alves, N. J., Champion, M. M., Stefanick, J. F., Handlogten, M. W., Moustakas, D. T., Shi, Y., Shaw, B. F., Navari, R. M., Kiziltepe, T., Bilgicer, B. Selective photocrosslinking of functional ligands to antibodies via the conserved nucleotide binding site. *Biomaterials* **34,** 5700–5710 (2013).

75. De Graaf, A. J., Kooijman, M., Hennink, W. E., Mastrobattista, E. Nonnatural amino acids for site-specific protein conjugation. *Bioconjugate Chem.* **20,** 1281–1295 (2009).

76. Chalker, J. M., Bernardes, G. J. L., Davis, B. G. A "Tag-and-Modify" Approach to Site-Selective Protein Modification. *Acc. Chem. Res.* **44,** 730–741 (2011).

77. Scheck, R. A., Francis, M. B. Regioselective labeling of antibodies through N-terminal transamination. *ACS Chem. Biol.* **2,** 247–251 (2007).

78. Netirojjanakul, C., Witus, L. S., Behrens, C. R., Weng, C.-H., Iavarone, A. T., Francis, M. B. Synthetically modified Fc domains as building blocks for immunotherapy applications. *Chem. Sci.* **4,** 266-272 (2013).

79. Axup, J. Y. and co-workers, Synthesis of site-specific antibody-drug conjugates using unnatural amino acids. *Proc. Natl. Acad. Sci. U. S. A.* **109,** 16101–16106 (2012).

80. Kim, C. H., Axup, J. Y., Schultz, P. G. Protein conjugation with genetically encoded unnatural amino acids. *Curr. Opin. Chem. Biol.* **17,** 412–419 (2013).

81. Liu, D. R., Magliery, T. J., Pastrnak, M., Schultz, P. G. Engineering a tRNA and aminoacyl-tRNA synthetase for the site-specific incorporation of unnatural amino acids into proteins in vivo. *Proc. Natl. Acad. Sci. U. S. A.* **94,** 10092–10097 (1997).

82. Hutchins, B. M., Kazane, S. A., Staflin, K., Forsyth, J. S., Felding-Habermann, B., Schultz, P. G., Smider, V. V. Site-specific coupling and sterically controlled formation of multimeric antibody Fab fragments with unnatural amino acids. *J. Mol. Biol.* **406,** 595–603 (2011).

83. Kim, C. H., Axup, J. Y., Dubrovska, A., Kazane, S. A., Hutchins, B. A., Wold, E. D., Smider, V. V., Schultz, P. G. Synthesis of bispecific antibodies using genetically encoded unnatural amino acids. *J. Am. Chem. Soc.* **134,** 9918–9921 (2012).

84. Lu, H., Wang, D., Kazane, S., Javahishvili, T., Tian, F., Song, F., Sellers, A., Barnett, B., Schultz, P. G. Site-specific antibody-polymer conjugates for siRNA delivery. *J. Am. Chem. Soc.* Just Accepted, (2013). doi:10.1021/ja4059525

85. Kazane, S. A., Axup, J. Y., Kim, C. H., Ciobanu, M., Wold, E. D., Barluenga, S., Hutchins, B. A., Schutz, P. G., Winssinger, N., Smider, V. V. Self-assembled antibody multimers through peptide nucleic acid conjugation. *J. Am. Chem. Soc.* **135,** 340–346 (2013).

86. Kazane, S. A, Sok, D., Cho, E. H., Uson, M. L., Kuhn, P., Schultz, P. G., Smider, V. V. Site-specific DNA-antibody conjugates for specific and sensitive immuno-PCR. *Proc. Natl. Acad. Sci. U. S. A.* **109,** 3731–3736 (2012).

87. Hudak, J. E., Barfield, R. M., de Hart, G. W., Grob, P., Nogales, E. Bertozzi, C. R., Rabuka, D. Synthesis of heterobifunctional protein fusions using copper-free click chemistry and the aldehyde tag. *Angew. Chem. Int. Ed. Engl.* **51,** 4161–4165 (2012).

88. Agarwal, P., van der Weijden, J., Sletten, E. M., Rabuka, D. & Bertozzi, C. R. A Pictet-Spengler ligation for protein chemical modification. *Proc. Natl. Acad. Sci. U. S. A.* **110,** 46–51 (2013).

89. Dawson, P. E., Kent, S. B. Synthesis of native proteins by chemical ligation. *Annu. Rev. Biochem.* **69,** 923–960 (2000).

90. Reulen, S. W. A., van Baal, I., Raats, J. M. H., Merkx, M. Efficient, chemoselective synthesis of immunomicelles using single-domain antibodies with a C-terminal thioester. *BMC Biotechnol.* **9,** 66 (2009).

91. Möhlmann, S., Bringmann, P., Greven, S. & Harrenga, A. Site-specific modification of ED-B-targeting antibody using intein-fusion technology. *BMC Biotechnol.* **11,** 76 (2011).

92. Barbuto, S., Idoyaga, J., Vila-Perelló, M., Longhi, M. P., Breton, G., Steinman, R. M., Muir, T. W. Induction of innate and adaptive immunity by delivery of poly dA:dT to dendritic cells. *Nat. Chem. Biol.* **9,** 250–256 (2013).

93. Vila-Perelló, M., Liu, Z., Shah, N. H., Willis, J. A., Idoyaga, J., Muir. T. W. Streamlined expressed protein ligation using split inteins. *J. Am. Chem. Soc.* **135,** 286–292 (2013).

94. Menrad, A., Menssen, H. D. ED-B fibronectin as a target for antibody-based cancer treatments. *Expert Opin. Ther. Targets* **9,** 491–500 (2005).

95. Skerra, A., Pluckthun, A. Assembly of a functional immunoglobulin Fv fragment in *Escherichia coli. Science* **240,** 1038–1041 (1988).

96. Witte, M. D., Cragnolini, J. J., Dougan, S. K., Yoder, N. C., Popp, M. W., Ploegh, H. L. Preparation of unnatural N-to-N and C-to-C protein fusions. *Proc. Natl. Acad. Sci. U. S. A.* **109,** 11993–11998 (2012).

97. Theile, C. S., Witte, M. D., Blom, A. E. M., Kundrat, L., Ploegh, H. L., Guimaraes, C. P. Site-specific N-terminal labeling of proteins using sortase-mediated reactions. *Nat. Protoc.* **8,** 1800–1807 (2013).

98. Guimaraes, C. P., Theile, C. S., Bozkurt, G., Kundrat, L., Blom, A. E. M., Ploegh, H. L. Site-specific C-terminal and internal loop labeling of proteins using sortase-mediated reactions. *Nat. Protoc.* **8,** 1787–1799 (2013).

99. Witte, M. D., Theile, C. S., Wu, T., Guimaraes, C. P., Blom, A. E. M., Ploegh, H. L. Production of unnaturally linked chimeric proteins using a combination of sortase-catalyzed transpeptidation and click chemistry. *Nat. Protoc.* **8,** 1808–1819 (2013).

100. Swee, L. K., Guimaraes, C. P., Sehrawat, S., Spooner, E., Barrase, M. I., Ploegh, H. L. Sortase-mediated modification of αDEC205 affords optimization of antigen presentation and immunization against a set of viral epitopes. *Proc. Natl. Acad. Sci. U. S. A.* **110,** 1428-1433 (2013).

101. Winter, AB, Goldstein, A. A photochemical affinity-labelling reagent for the opiate receptor(s). *Mol. Pharmacol.* **6,** 601–611 (1972).

102. Ruoho, A. E., Kiefer, H., Roeder, P. E., Singer, S. J. The mechanism of photoaffinity labeling. *Proc. Natl. Acad. Sci. U. S. A.* **70,** 2567–2571 (1973).

103. Wofsy, L., Metzger, H., Singer, S. Affinity labeling- a general method for labeling the active sites of antibody and enzyme molecules. *Biochemistry* **1,** 1031–1039 (1962).

104. Fleet, G., Porter, R., Knowles, J. Affinity labelling of antibodies with aryl nitrene as reactive group. *Nature* **224,** 511–512 (1969).

105. Fleet, G., Knowles, J., Porter, R. The antibody binding site. Labelling of a specific antibody against the photo-precursor of an aryl nitrene. *Biochem. J.* **128,** 499–508 (1972).

106. Fisher, C., Press, E. Affinity labelling of the binding site of rabbit antibody. Evidence for the involvement of the hypervariable regions of the heavy chain. *Biochem. J.* **139,** 135–149 (1974).

107. Taylor, R., Tite, J., Manzo, C. Immunoregulatory effects of a covalent antigen–antibody complex. *Nature* **281,** 488–490 (1979).

108. Richards, F. F., Lifter, J. Photoaffinity probes in the antibody combining region. *Ann. N. Y. Acad. Sci.* **346,** 78–89 (1980).

109. Donaldson, J. M., Kari, C., Fragoso, R. C., Rodeck, U., Williams, J. C. Design and development of masked therapeutic antibodies to limit off-target effects: application to anti-EGFR antibodies. *Cancer Biol. Ther.* **8,** 2147–2152 (2009).

110. Janssen, B. M. G., Lempens, E. H. M., Olijve, L. L. C., Voets, I. K., van Dongen, J. L. J., de Greef, T. F. A., Merkx, M. Reversible blocking of antibodies using bivalent peptide–DNA conjugates allows protease-activatable targeting. *Chem. Sci.* **4,** 1442–1450 (2013).

111. Desmyter, A., Transue, T. R., Ghahroudi, M. A., Ti, M-H, D., Poortmans, F., Hamers, R., Muyldermans, S., Wyns, L. Crystal structure of a camel single-domain V_H antibody fragment in complex with lysozyme. *Nat. Struct. Biol.* **3,** 803–811 (1996).

Chapter 2: Expression and Purification of cAb-Lys3

'Heavy-chain antibodies fail to incorporate light chains.'

Serge Muyldermans, 2013.

2.1 Introduction

2.1.1 Heavy-chain antibodies

Heavy-chain antibodies (HcAbs) evolved in *Camelidae*[1] and some cartilaginous fish[2] differ from conventional antibodies in that they are completely devoid of light chains. HcAbs comprising a dimer of the C_H2, C_H3 and V_HH of the variable domains accounts for around 75% of the antibodies found in camels, and 45% in llamas.[3] Despite their smaller size, HcAbs are able to bind to a large repertoire of antigens with comparable affinities to conventional antibodies. This can be attributed to an extended CDR3 loop (around 20 – 24 amino acids), able to bind into clefts and cavities on protein surfaces inaccessible to conventional antibodies.[4] Since their discovery by Muyldermans and co-workers in 1993,[1] HcAbs have been developed extensively for a large range of therapeutic and biotechnological applications due to their numerous advantages over conventional intact antibodies and other antibody fragments (**Section 1.2.3, Chapter 1**).[3,5] Indeed, the publication outlining the original findings has received over 1,000 citations to date.[3] An important breakthrough in the field was the finding that it was possible to dissect the dimeric HcAb structure, cloning just the single variable domain of the heavy chain (V_HH) and retain antigen binding, giving rise to an active single-domain antibody (sdAb), the lowest molecular weight antibody fragment known (~ 15 kDa).[3,6] The use of antibodies of a single-domain nature alleviates the problem of having to refold to other domains to gain function, which may be useful for site-specific chemical modification. In addition to this, sdAbs show high stability (they can withstand

higher temperatures for prolonged periods of time and or refold efficiently after chemical or thermal denaturation) and higher solubilities due to hydrophilic residues replacing hydrophobic residues previously interacting with the V_L (light chain of variable domain).[6–10] When considering therapeutic applications of sdAbs, a further advantage is that the sequence homology between camelid HcAbs and human antibodies is greater than between mouse antibodies and human antibodies, thus providing a reduced potential for immunogenicity.[11]

2.1.2 Methods for the expression of single-domain antibodies

Methods for the generation and expression of sdAbs have received much attention in the literature.[6,12,13] Many groups have focused their attention on preparing antibodies *in vitro* by mimicking the selection strategies of the immune system.[14–17] Here, antibody fragments can be generated by phage display – in which antibody fragments of predetermined specificity are constructed from repertoires of variable (V) genes (or by immunisation with antigen). From here, they are harvested from populations of lymphocytes, and cloned for display of heavy and light chains on the surface of filamentous bacteriophage. Binding to antigen is used to detect rare phage, and then soluble antibody fragments can be expressed in bacteria. In this process, the V genes can undergo random mutations, which give rise to the possibility of mutants with higher binding affinities.

Following the successful generation of antibodies by phage display (and therefore an increased library of antibodies with chosen antigens available), it became apparent that there was a need for methods to express known antibody fragments using recombinant technology – namely by conventional transformation (bacterial systems) and transfection (yeast, eukaryotic systems) of plasmid DNA into cells.

In general, the expression of sdAbs in microbial systems (bacterial and yeast) is favoured over eukaryotic systems due to lower costs and shorter production times. Their single gene

nature and simple modular structure should make expression uncomplicated. In addition, as they are lacking in an Fc (effector function), glycosylation is not required. In established bacterial systems, antibody is commonly targeted to the secretory pathway into the oxidising periplasmic space resulting in soluble, correctly folded protein with efficient disulfide bond formation.[6] Efficient, high yielding expression systems in *Escherichia coli* (*E. coli*) have been described where antibody is expressed in the cytosol or periplasm.[12,13,18–20] Yeast expression systems, although less common, can also produce high levels of sdAbs utilising secretory pathways.[21–24] It is reported however that the addition of yeast-specific high mannose oligosaccharides may complicate the application of sdAbs in therapeutics due to binding to specific mannose receptors on the cell surfaces of the reticulo-endothelial system.[25] This may result in higher immunogenicities and a decreased serum half-life. Although a longer and more expensive process, the recombinant production of antibodies in eukaryotic cells is attractive due to the possibility of creating stable cell lines. Also, high yields and obtaining the correct post-translational modifications (PTMs) make this process more advantageous. Bazl and co-workers have described the construction of GFP-sdAb (GFP - Green Fluorescent Protein) fusion constructs in two different expression vectors for both the intra- and extracellular expression of sdAbs in Chinese Hamster Ovary (CHO) cells.[13] As well as expression in bacterial, yeast and mammalian cells, sdAbs have also been expressed in fungal expression systems,[26], transgenic tobacco plants,[27,28] on the surface of bacterial biogenic magnetic nanoparticles,[29] and even in transgenic mice.[30]

2.1.3 cAb-Lys3 structure and previous work

cAb-Lys3 was the first sdAb to have its crystal structure in complex with its antigen lysozyme solved.[31] It was initially generated by the immunisation of camels with lysozyme using standard immunisation protocols, and then its sequence, binding activities and stability tested and verified.[18] cAb-Lys3 is 15 kDa and formed of four framework regions (core of

immunoglobulin domain) and three Complementarity Determining Regions (CDRs) responsible for antigen binding. sdAbs are able to bind to their antigens with exceptionally high affinities, and a long, protruding CDR3 loop able to access hindered sites within the antigen is believed to contribute to this.[1,3,6] cAb-Lys3 is no exception, with the crystal structure revealing that the protruding CDR3 loop accounts for 70 % of antibody-antigen interaction.[31] The N-terminal section of the CDR3 loop containing ten residues inserts deeply into the active site of lysozyme. There is a high level of complementarity at the complex interface, and the CDR3 loop is stabilised by a proximate cysteine disulfide bond. cAb-Lys3 was chosen as the target to explore the effects of chemical modification at a single position within the CDR3 loop on binding affinities since a wealth of detailed structural information is known about it and its antigen lysozyme.[31,32] Previously, the expression of cAb-Lys3 has been described by the cloning of the cAb-Lys3 gene into a derivative of the pHEN1 vector[18,33] usually used for phage display, and then transformation and expression in *E. coli*, with the protein being exported to the periplasm under the control of the *pelB* leader sequence.[18,31,34] At first, the expression of cAb-Lys3 was attempted using this method. Teh and Kavanagh have also described the transient expression of cAb-Lys3 in *Nicotiana benthamiana*.[35] cAb-Lys3, and its binding activity in various contexts has been explored previously. As mentioned before, sdAbs exhibit binding through extended CDR3 loops, enabling access to clefts in protein antigens inaccessible to conventional and bulkier antibodies. cAb-Lys3 was found to bind in the active site of lysozyme, in a fashion mimicking certain carbohydrate substrates, thus making it an effective enzyme inhibitor.[36] The active site epitope is not recognised by other anti-lysozyme antibodies where complexes with lysozyme are structurally solved. The ability of cAb-Lys3 to specifically target transgenic tumours expressing lysozyme on their membrane was tested by Cortez-Retamozo and co-workers by subcutaneously inoculating mice with lysozyme-transfected tumour cells.

Specific targeting of the tumour cells displaying lysozyme *in vivo* was achieved, demonstrating the potential of sdAbs as therapeutics, with excess non-binding cAb-Lys3 being rapidly eliminated from the blood circulation. In addition, no immunogenicity as a result of cAb-Lys3 administration was observed in the mice.[37] The binding affinities of cAb-Lys3 under various conditions (pH, salt concentration and temperature) have also been investigated,[38] as well as by mutations to other canonical amino acids within and away from the CDR3 loop,[39] and by detailed analysis of the affinity maturation process for cAb-Lys3.[40]

In this chapter, the expression and purification of WT-cAb-Lys3 (WT – wild type) and cAb-Lys3-Cys104 (for chemical modifications[41]) is described. Initially, expression in *E. coli* was attempted. The expression of sdAbs in *E. coli* is described by others, however protocols followed were found to yield antibody in inclusion bodies, and refolding attempts were problematic. It was therefore decided to try and express WT-cAb-Lys3 and cAb-Lys3-Cys104 in a eukaryotic system – namely in Chinese Hamster Ovary (CHO) cells, where extracellular expression alleviates the possibility of inclusion bodies. Here, pure antibody was obtained in high yields. Extensive characterisation of both WT-cAb-Lys3 and cAb-Lys3-Cys104 revealed that the antibodies were active towards cognate antigen lysozyme and folded correctly. Furthermore, the antibodies exhibited expected reactivities, allowing cAb-Lys3-Cys104 to be used further as a model for site-specific chemical modifications.

2.2 Results

2.2.1 cAb-Lys3-Cys104 mutation

Site-directed mutagenesis was carried out on WT-cAb-Lys3 in pHEN1 vector (pHEN1:WT-cAb-Lys3) (**Figure 2.1**) in order to introduce cysteine at position 104 (A104C) as a site for chemical modification.[41] Primers for mutagenesis were designed manually with the aims of minimising mismatch and having a melting temperature higher than 70 °C (**Table 2.1**).

Figure 2.1. pHEN1:cAb-Lys3.

Primer	Sequence	T_m/ °C
A104C_F	CTACCATCTACTGCAGCTACTATG	70.2
A104C_R	CATAGTAGCTGCAGTAGATGGTAG	70.2

Table 2.1. Primers for site-directed mutagenesis. Underlined base pairs are new.

Mutagenesis was carried out with a site-directed mutagenesis kit whereby template DNA, forward and reverse primers, reaction buffer, dNTP mix and *PfuUltra* DNA polymerase were mixed and then subjected to polymerase chain reaction (PCR) amplification conditions. Following digestion of parental methylated and hemimethylated DNA with *Dpn I*, the reaction mixture was transformed into XL-1 Blue Supercompetent Cells for nick repair and plated onto agar plates for colony growth. Selected colonies were picked, grown in Luria Bertani (LB) medium, and then plasmid DNA was extracted and purified by Miniprep. Purified plasmid DNA was sequenced to confirm successful mutagenesis (**Figure 2.2**).

```
GCAGCGGACTCTACCATCTACGCCAGCTACTATGAATGCGGTCACGGTCTGTCTACTGGT
|||||||||||||||||||||  ||||||||||||||||||||||||||||||||||||
GCAGCGGACTCTACCATCTACTGCAGCTACTATGAATGCGGTCACGGTCTGTCTACTGGT
```

Figure 2.2. NCBI Blast: Nucleotide Sequence alignment for cAb-Lys3-A104C mutation. Highlighted base pairs are GCC (alanine) and TGC (cysteine).

2.2.2 Expression of pHEN1:WT-cAb-Lys3 in *E. coli*

pHEN1 is a phagemid expression vector reported to permit the display of antibody fragments on the surface of phage or the soluble expression of antibody fragments where the host is a suppressor of *E. coli*.[15,34] The *pelB* leader sequence directs expressed protein to the periplasmic space, and the C-terminal hexahistidine tag (His-tag) can be used for purification by affinity chromatography (**Figure 2.1**).

pHEN1:WT-cAb-Lys3 was transformed into *E. coli* BL21(DE3) competent cells by heat shock and then grown in LB followed by plating onto agar plates to allow overnight colony growth. Single colonies were used to inoculate small starter cultures before addition to larger cultures. Large cultures were grown to an OD_{600} of 0.6, and then protein expression was induced with the addition of 1 mM IPTG (isopropyl-β-D-1-thiogalactopyranoside). After overnight induction, cultures were harvested by centrifugation to isolate the cell pellets.

Cell lysis was carried out using an osmotic shock approach where the cell pellet (from 1 L culture) was incubated in TES buffer (20 mM Tris-HCl, 0.1 mM EDTA, 0.1 M sucrose) on ice for 30 minutes. Unfortunately, in most attempts, any expressed protein appeared to remain in inclusion bodies. This may be because secretory pathways are overloaded. In addition, ammonium sulfate precipitation did not help with the cell lysis process. In one case, purification by affinity chromatography yielded His-tagged protein around 15 kDa (as tested by Western blot) in poor yields (0.3 mg, 0.16 mg/mL, **Figure 2.3**).

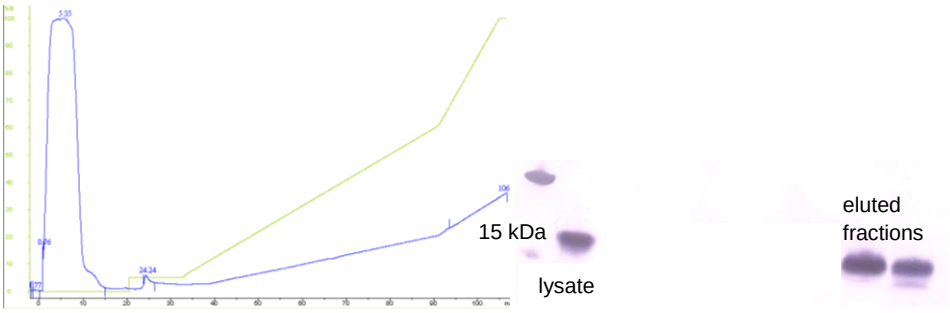

Figure 2.3. Left: FPLC trace for affinity chromatography purification of pHEN1:WT-cAb-Lys3. Blue: UV absorbance at 280 nm, green: concentration of elution buffer, right: corresponding Western blot for purification.

In a final attempt to establish a reliable and high yielding method for the expression of cAb-Lys3 in the pHEN1 phagemid system, a series of small scale expression trials were carried out. Here, different parameters (cell lysis method, induction time, temperature and addition of glucose as a carbon source) were varied in order to increase the yield of protein purified (**Table 2.2**).[18] It was found that His-tagged protein was present in most cases after extraction with the exception of extraction via osmotic shock (**Figure 2.4**). Although the successful extraction of protein was obtained on a small scale in pHEN1, it was not known whether this would be transferrable on a larger scale. Due to the unreliability of expression in the pHEN1 vector, and also the poor yields obtained, another expression vector was considered and it was decided to subclone the cAb-Lys3 gene into the expression vector pET-22b(+).

Entry	Variable	Glucose	IPTG/ mM	Induction temp/ °C	Induction time/ h	Extraction method
1	Extraction method	No	1 mM	30	16	BugBuster
2	Extraction method	No	1 mM	30	16	Osmotic
3	Extraction method	No	1 mM	30	16	Sonication
4	Induction time	No	1 mM	30	3	BugBuster
5	Induction temp	No	1 mM	16	16	BugBuster
6	Induction temp	No	1 mM	37	16	BugBuster
7	Glucose	0.1%	1 mM	30	16	BugBuster
8	Glucose	1%	1 mM	30	16	BugBuster

Table 2.2. Conditions for small scale expression trials of pHEN1:WT-cAb-Lys3. In all entries, antibody was expressed in BL21(DE3) cells.

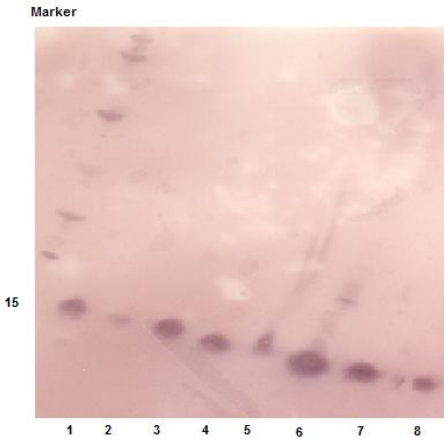

Figure 2.4. Western blot for small scale expression trials of pHEN1:WT-cAb-Lys3. Lanes 1 – 8 correspond to entries 1 – 8 in **Table 2.2**.

2.2.3 Expression of pET-22b(+):WT-cAb-Lys3 in *E. coli*

Subcloning of WT-cAb-Lys3 into pET-22b(+)

The expression of pHEN1:WT-cAb-Lys3 was found to be unreliable and produce too low an amount of protein for modification studies. It was therefore decided to subclone WT-cAb-

Lys3 into pET-22b(+), which contains the T7 promoter and is suitable for expression in *E. coli*. It also has a *pelB* leader sequence for exporting expressed protein to the periplasm (Appendix). Soluble sdAbs have previously been expressed in this system.[12] Primers were manually designed to introduce MscI and HindIII restriction sites flanking WT-cAb-Lys3 in pHEN1, whilst also cutting the C-terminal sequence after the His-tag (**Table 2.3**).

Primer	Sequence	T_m/ °C
MscI_F	5′-CATCATTGGCCATGGATGTGCAGCTGCAGGCGTCTGGTGGCGGTTCTGTACAGGC-3′	77
HindIII_R	3′-ATGATGAAGCTTGGCGGCCGCGCTCGAGACAG-5′	70

Table 2.3. Primers for introducing MscI and HindIII restriction sites at N- and C-termini of WT-cAb-Lys3 in pHEN1 (restriction sites highlighted).

PCR was set up with pHEN1:WT-cAb-Lys3 to incorporate primer sequences (**Table 2.4**) and then both the pET-22b(+) template and WT-cAb-Lys3 insert were sequentially digested with MscI then HindIII (**Table 2.5**).

Component	Volume/ μL
pHEN1:WT-cAb-Lys3 (20 ng, 107 ng/μL)	5.4
10 μM forward primer	2.5
10 μM reverse primer	2.5
10 mM dNTP mix	5
10x reaction buffer	5
Pfu ultra	1
MQ H_2O	28.6
Total	50

Table 2.4. PCR amplification conditions for WT-cAb-Lys3.

	pET-22b(+) template/μL (187 ng/μL)	WT-cAb-Lys3 insert/μL (39.5 ng/μL)
Template	10.7	50
NEBuffer 2	5	7
BSA (100x)	0.5	0.7
MscI 40 U	8	8
HindIII 40 U	2	2
MQ H_2O	23.8	23
Total	50	90.7

Table 2.5. Restriction digests. The digests were incubated for 3 hours at 37 °C.

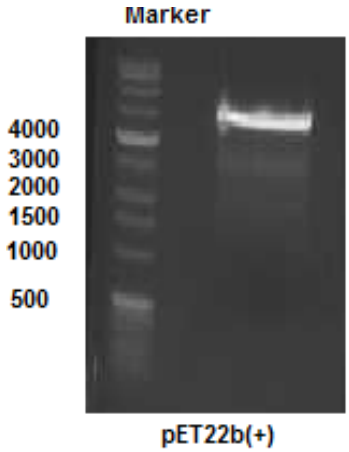

Figure 2.5. DNA agarose gel of pET-22b(+) after restriction digest.

The doubly digested vector was run on a DNA agarose gel and the band at 6,000 bp corresponding to cut DNA was excised and purified with a Gel Extraction kit to give 9.7 ng/μL DNA (**Figure 2.5**). The fainter band at 3,000 bp corresponds to supercoiled uncut DNA. The doubly digested PCR product (WT-cAb-Lys3 insert) was purified with a PCR purification kit to give 33 ng/μL DNA. Ligation reactions were set up according to the conditions shown in **Table 2.6**. After ligation, reactions were transformed into MaxEfficiency DH10Bac competent cells and then plated. Colonies obtained after overnight incubation were grown in LB, and plasmid DNA was extracted by Miniprep. Successful ligation forming pET-22b(+):WT-cAb-Lys3 was confirmed by DNA sequencing (**Figures 2.6** and **2.7**).

Template 9.7 ng/μL	10 μL (97 ng)
Insert 33 ng/μL	1.5 μL (50 ng)
T4 DNA ligase	5 μL
5x buffer	4 μL
Total	20.5 μL

Table 2.6. Ligation conditions. The reaction was incubated overnight at 16 °C.

ATTTTGTTTAACTTTAAGAAGGAGATATACATATGAAATACCTGCTGCCGACCGCTGCTGCTGGTCTG
CTGCTCCTCGCTGCCCAGCCGGCGATGGCCATGGATGTGCAGCTGCAGGCGTCTGGTGGCGGTTCTGT
ACAGGCAGGTGGTTCTCTGCGTCTGTCTTGCGCAGCTTCTGGCTACACCATCGGTCCATACTGCATGG
GTTGGTTTCGTCAGGCTCCGGGTAAAGAGCGTGAAGGTGTTGCTGCGATCAACATGGGTGGTGGTATC
ACCTATTACGCGGACTCTGTGAAAGGTCGTTTCACGATCAGCCAGGATAACGCGAAAAACACGGTTTA
CCTGCTCATGAACTCTCTGGAACCGGAAGATACCGCGATCTACTACTGTGCAGCGGACTCTACCATCT
ACGCCAGCTACTATGAATGCGGTCACGGTCTGTCTACTGGTGGTTACGGCTACGACTCTTGGGGTCAG
GGTACCCAGGTTACTGTCTCGAGCGCGGCCGCCAAGCTTGCGGCCGCACTCGAGCACCACCACCACCA
CCACTGAGATCCGG

Figure 2.6. DNA sequence obtained for WT-cAb-Lys3 in pET-22b(+). Highlighted: red: *pelB* signal sequence, pink: WT-cAb-Lys3 sequence, green: C-terminal His-tag, blue: stop codon.

MDVQLQASGGGSVQAGGSLRLSCAASGYTIGPYCMGWFRQAPGKEREGVAAINMGGGITYYADSVKGRFTISQDN
AKNTVYLLMNSLEPEDTAIYYCAADSTIYASYYECGHGLSTGGYGYDSWGQGTQVTVSSAAAKLAAALEHHHHHH

Figure 2.7. Corresponding translated sequence of WT-cAb-Lys3 in pET-22b(+).

Expression of pET-22b(+):WT-cAb-Lys3 in *E. coli*

As pET-22b(+) contains the *pelB* leader sequence for the exporting of antibody to the periplasm, it was decided to try and express using the same osmotic shock protocol[34] that had been used for pHEN1:WT-cAb-Lys3. The plasmid DNA was transformed into *E. coli* BL21(DE3) cells, colonies grown as small starter cultures, then larger cultures before induction with IPTG. After overnight induction, cells were harvested and then varying lysis protocols carried out on each cell pellet (per litre of culture).

Initially Skerra and Pluckthun's method commonly used with antibody fragments,[34] and in particular sdAbs[18,31] was followed. One cell pellet was resuspended in ice cold TES buffer, diluted 5 fold and stirred on ice for 30 minutes. The resulting cell suspension was very turbid, and so insoluble debris was removed by centrifugation. SDS-PAGE of supernatant and pellet samples showed that a protein around 15 kDa was present, and the more specific Western blot showed that the lysate and pellet samples contained His-tagged protein (lanes 1, 3 and 5, **Figure 2.8**). This implied that the protein may have aggregated as inclusion bodies (perhaps if secretory pathways were overloaded), or that the osmotic shock protocol was insufficient in extracting protein from cells.

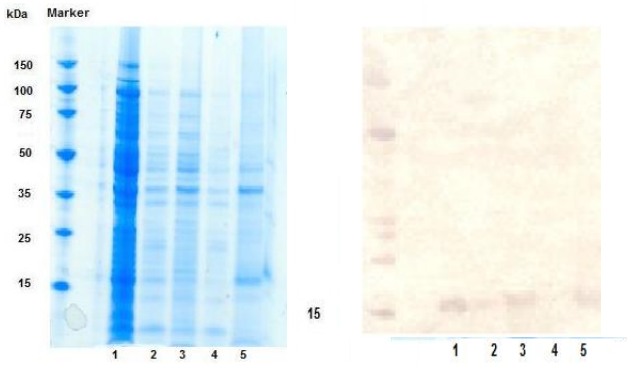

Figure 2.8. SDS-PAGE (left) and Western blot (right) for expression of pET-22b(+):WT-cAb-Lys3 and the osmotic shock protocol. 1: Lysate post osmotic shock, 2: supernatant after first centrifugation, 3: pellet after first centrifugation, 4: supernatant after second centrifugation, 5: pellet after second centrifugation.

Next, it was decided to introduce an additional shock step using magnesium chloride ($MgCl_2$), as demonstrated by Ahmadvand and co-workers when expressing sdAb-HRP (HRP – horseradish peroxidase) conjugates.[12] As expected, His-tagged protein remained in the pellet after the initial sucrose shock (lane 3, **Figure 2.9**), and unfortunately the additional $MgCl_2$ step did not lead to successful protein extraction (lane 5, **Figure 2.9**).

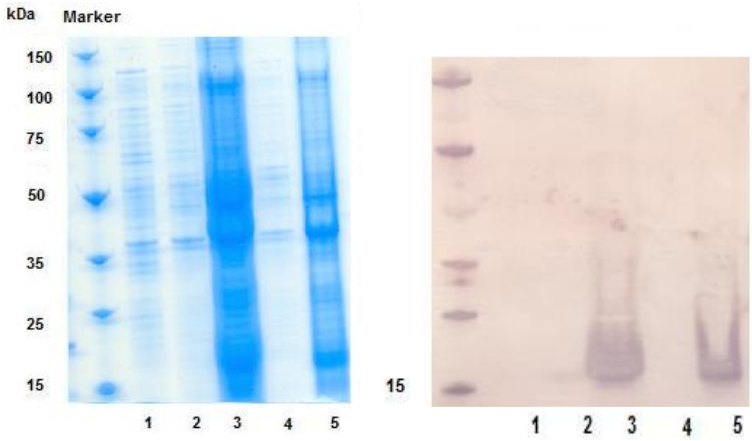

Figure 2.9. SDS-PAGE (left) and Western blot (right) for expression of pET-22b(+):WT-cAb-Lys3 and Ahmadvand's extraction method.[12] 1: Supernatant after first centrifugation, 2: supernatant after sucrose shock, 3: pellet after sucrose shock, 4: supernatant after $MgCl_2$ shock, 5: pellet after $MgCl_2$ shock.

Finally, cell lysis by sonication on ice was attempted (4 bursts of 30 seconds with a wait time of 1 minute in between). This was also unsuccessful (lane 2, **Figure 2.10**).

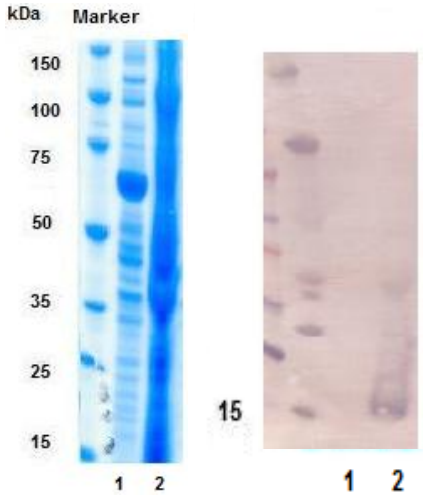

Figure 2.10. SDS-PAGE (left) and Western blot (right) for expression of pET-22b(+):WT-cAb-Lys3 and sonication. 1: Supernatant after sonication, 2: pellet after sonication.

Purification of WT-cAb-Lys3 in inclusion bodies and refolding

Inclusion bodies form as a result of the build up of inactive aggregates in the cell,[42] and a cause of insolubility is overproduction during expression.[43] It is for this reason that attempting to reduce the rate of protein expression may result in a higher level of soluble protein in its native form. Protein expression may be controlled by inducing at a lower temperature or by using a lower concentration of IPTG. However, based on previous observations that inclusion bodies of cAb-Lys3 are still obtained at lower temperatures,[44] it was decided to try to purify WT-cAb-Lys3 under denaturing conditions and then refold the protein.

Cell pellets were resuspended and lysed using BugBuster Protein Extraction Reagent (BBPER) and protein extracted by the solubilisation of inclusion bodies in denaturing buffer at pH 8 (**Experimental Section**). The resulting lysate was incubated with Ni-functionalised resin (for affinity chromatography) for 2 hours, before carrying out the purification. After the collection of the flow through, the resin was washed and eluted with denaturing buffer at decreasing pH. The decrease in pH should cause the histidine residues to protonate and

therefore the protein to elute. **Figure 2.11** shows that pure protein at around 15 kDa was obtained (lane 6).

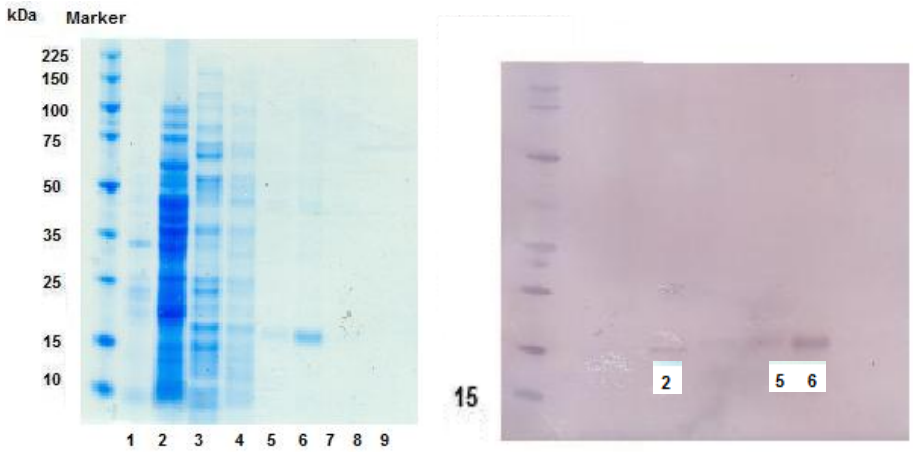

Figure 2.11. SDS-PAGE and Western blot of WT-cAb-Lys3 purified as inclusion bodies using denaturing buffer at a decreasing pH to elute protein. 1: Supernatant after osmotic shock, 2: supernatant after BBPER treatment, 3: flow through, 4: wash with denaturing buffer pH 6.3, 5: wash with denaturing buffer pH 5.9, 6 - 9: elution with denaturing buffer pH 4.5.

Fractions containing His-tagged protein were combined to a volume of 10 mL containing protein at 0.87 mg/mL in denaturing buffer (from 12 L culture). Liquid Chromatography-Mass Spectrometry (LC-MS) analysis confirmed successful expression and purification of denatured WT-cAb-Lys3 (**Figure 2.12**).

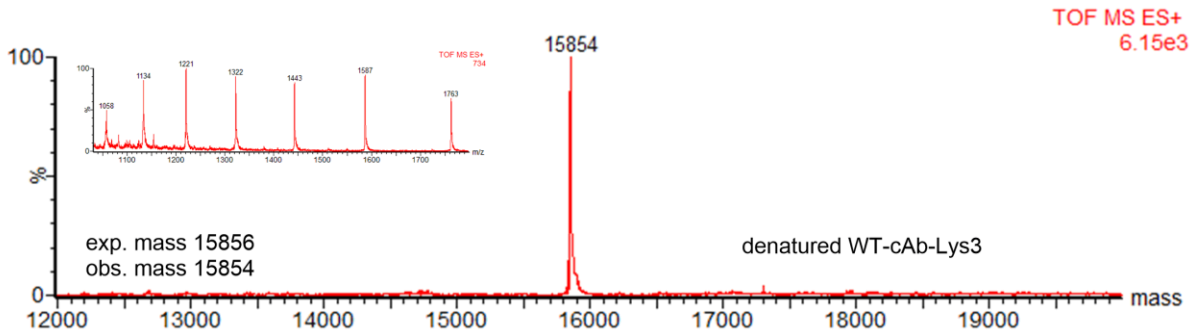

Figure 2.12. WT-cAb-Lys3 obtained from purifying from inclusion bodies under denaturing conditions.

Initially, protein refolding by dialysis using a 7 kDa MWCO dialysis cassette was used. The use of various components in phosphate-buffered saline (PBS) buffer was explored, as well as a HEPES-based refolding buffer containing oxidised and reduced glutathione for disulfide

shuffling. Glycerol was added in some conditions to help prevent protein aggregation,[45] as well as arginine. Although arginine is a common additive in protein refolding, its mechanism of action is not well understood.[46] In all cases, precipitate was observed after overnight dialysis (**Table 2.7**).

Entry	Conditions
1	PBS, pH 7.1
2	PBS + 10 % glycerol
3	PBS + 10 % glycerol + 0.4 M arginine
4	PBS + 0.4 M arginine
5	Refolding buffer

Table 2.7. Dialysis conditions for cAb-Lys3. Refolding buffer is 20 mM HEPES, 150 mM NaCl, 3 mM GSH (reduced glutathione), 0.3 mM GSSG (oxidised glutathione), 1 mM EDTA, pH 7.

Refolding by dilution was also attempted. Here, a small amount of protein in denaturing buffer was added dropwise to a stirring solution of desired buffer, then concentrated down. In all cases no precipitate could be observed during addition to the large volume of buffer, but on concentrating down, precipitate was seen (**Table 2.8**) and no protein could be detected in the buffer.

Entry	Conditions
1	PBS, pH 7.1
2	PBS + 10 % glycerol
3	PBS + 10 % glycerol + 0.4 M arginine
4	Refolding buffer

Table 2.8. Dilution refolding conditions for WT-cAb-Lys3.

Insufficient yields of WT-cAb-Lys3 were obtained from expression in *E. coli*, as well as the repeated occurrence of protein in inclusion bodies. For this reason, expression in eukaryotic systems was explored.

2.2.4 Expression of WT-cAb-Lys3 and cAb-Lys3-Cys104 in eukaryotic cells

Unfortunately, it was found that expression in *E. coli* is a poor and unreliable system for producing high yields of folded WT-cAb-Lys3, even when using an expression vector designed for overexpression. Refolding was problematic, and investigation into finding a

suitable method can use a lot of valuable antibody stock. It was decided to try and express both WT-cAb-Lys3 and cAb-Lys3-Cys104 in mammalian cells, as carried out regularly on other sdAbs by collaborators at UCB. High yields are reported, and the lack of N-X-S and N-X-T motifs in the amino acid sequence of cAb-Lys3 means that glycosylation should not occur. Others have also reported the generation of genetically engineered stable cell lines where transfection with expression vectors permitting the cytoplasmic and extracellular expression of single-domain antibodies was possible.[13] This alleviates the problem of obtaining inclusion bodies, thus eliminating the need for denaturation and refolding. Expression in mammalian cells was carried out only after attempts with *E. coli* were exhausted. This was due to higher costs associated with expression in eukaryotic systems, and different facilities required.

Subcloning of WT-cAb-Lys3 into mammalian expression vector

A gene encoding for WT-cAb-Lys3 flanked by restriction sites for HindIII and XhoI was digested alongside a proprietary mammalian expression vector (UCB) for the extracellular expression of protein (**Table 2.9**).

	UCB vector		**WT-cAb-Lys3 gene**	
	Concentration	Volume/ μL	Concentration	Volume/ μL
Vector	0.1 μg/μL, 100 μg	10	5800 μg/mL, 60 μg	1
HindIII	20 U/μL, 100 Y	5	20 U/μL, 100 U	5
XhoI	20 U/μL, 100 U	5	20 U/μL, 100 U	5
NEBuffer 2 (10x)		5		5
BSA (100x)		0.5		0.5
MQ H_2O		24.5		33.5
Total		50		50

Table 2.9. Double digest conditions for UCB vector and WT-cAb-Lys3. Each reaction was incubated at 37 °C overnight.

The digest reactions were run on a DNA agarose gel, where tight bands corresponding to cut DNA were observed (**Figure 2.13**). The relevant bands were excised and DNA was extracted

using a Gel Extraction kit. Ligation between the cut portions of DNA was carried out using Quick Ligase (**Table 2.10**).

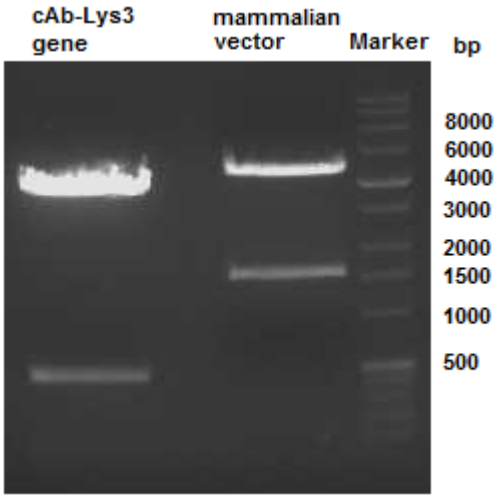

Figure 2.13. Restriction digest of WT-cAb-Lys3 gene and UCB vector. For the WT-cAb-Lys3 gene, a band at 450 bp corresponds to the cut gene encoding for protein. For the UCB vector, the cut backbone is at 4,500 bp.

	Volume/ µL
Vector 12.9 ng/µL	3.9 (50 ng)
Insert 17.4 ng/µL	0.6 (10 ng)
QL	1
2x buffer	10
MQ H_2O	4.5
Total	20

Table 2.10. Ligation reaction conditions. QL is Quick Ligase. The reaction was incubated at 25 °C for 1.5 hours.

Immediately after ligation, reactions were transformed into XL-1 Blue Supercompetent cells, and plated onto agar plates. 14 colonies were selected and grown individually in LB, and then the plasmid DNA was purified by Miniprep. To test for ligation success, purified DNA was subjected to a double digest with HindIII and XhoI (**Table 2.11**), and the reaction samples were run on a DNA agarose gel (**Figure 2.14**). In all cases, two bands were seen, corresponding to the UCB vector backbone (4,500 bp), and WT-cAb-Lys3 (450 bp), implying the successful construction of UCB vector:WT-cAb-Lys3.

	Concentration	Volume/ µL
Vector	~ 500 ng/µL, 1 µg	2
HindIII	20 U/µL, 20 U	1
XhoI	20 U/µL, 20 U	1
NEBuffer 2 (10x)		5
BSA (100x)		0.5
MQ H_2O		40.5
Total		50

Table 2.11. Double digest conditions for testing ligations. Each reaction was incubated at 37 °C for 5 hours.

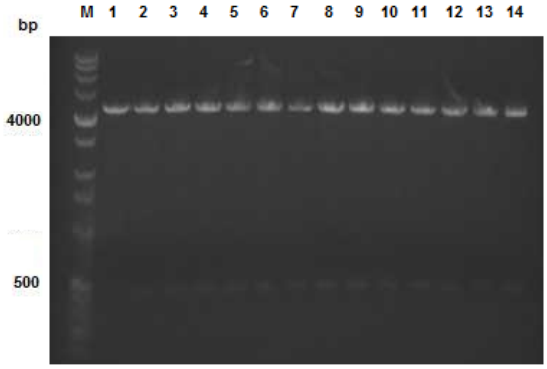

Figure 2.14. Restriction digests of ligation reaction.

Additionally, purified plasmid DNA was submitted for DNA sequencing. Gratifyingly, successful subcloning of WT-cAb-Lys3 into the UCB vector was confirmed (**Figures 2.15** and **2.16**).

ATGGATGTGCAGCTGCAGGCGTCTGGTGGCGGTTCTGTACAGGCAGGTGGTTCTCTGCGTCTGTCTTGCGCAGCT
TCTGGCTACACCATCGGTCCATACTGCATGGGTTGGTTTCGTCAGGCTCCGGGTAAAGAGCGTGAAGGTGTTGCT
GCGATCAACATGGGTGGTGGTATCACCTATTACGCGGACTCTGTGAAAGGTCGTTTCACGATCAGCCAGGATAAC
GCGAAAAACACGGTTTACCGCCTCATGAACTCTCTGGAACCGGAAGATACCGCGATCTACTACTGTGCAGCGGAC
TCTACCATCTACTGCAGCTACTATGAATGCGGTCACGGTCTGTCTACTGGTGGTTACGGCTACGACTCTTGGGGT
CAGGGTACCCAGGTTACTGTCTCGAGCGCGGCCGCCAAGCTTGCGGCCGCACTCGAGCACCACCACCACCACCAC

Figure 2.15. DNA sequence of WT-cAb-Lys3 (Ala104) in mammalian vector. Green: code for alanine at position 104.

DVQLVESGGGSVQAGGSLRLSCAASGYTIGPYCMGWFRQAPGKEREGVAAINMGGGITYYADSVKGRFTISQDNA
KNTVYLLMNSLEPEDTAIYYCAADSTIYASYYECGHGLSTGGYGYDSWGQGTQVTVSRENLYFQGHHHHHH

Figure 2.16. The corresponding protein sequence for WT-cAb-Lys3 in the UCB vector.

The A104C mutation required for selective modification was carried out using the same primers and method as described in **Section 2.2.1**. Again, the expected sequence was confirmed by DNA sequencing (**Figures 2.17** and **2.18**).

ATGGATGTGCAGCTGCAGGCGTCTGGTGGCGGTTCTGTACAGGCAGGTGGTTCTCTGCGTCTGTCTTGCGCAGCT
TCTGGCTACACCATCGGTCCATACTGCATGGGTTGGTTTCGTCAGGCTCCGGGTAAAGAGCGTGAAGGTGTTGCT
GCGATCAACATGGGTGGTGGTATCACCTATTACGCGGACTCTGTGAAAGGTCGTTTCACGATCAGCCAGGATAAC
GCGAAAAACACGGTTTACCTGCTCATGAACTCTCTGGAACCGGAAGATACCGCGATCTACTACTGTGCAGCGGAC
TCTACCATCTACTGCAGCTACTATGAATGCGGTCACGGTCTGTCTACTGGTGGTTACGGCTACGACTCTTGGGGT
CAGGGTACCCAGGTTACTGTCTCGAGCGCGGCCGCCAAGCTTGCGGCCGCACTCGAGCACCACCACCACCACCAC

Figure 2.17. DNA sequence of cAb-Lys3-Cys104 (A104C) in mammalian vector. Green: code for cysteine at position 104.

DVQLVESGGGSVQAGGSLRLSCAASGYTIGPYCMGWFRQAPGKEREGVAAINMGGGITYYADSVKGRFTISQDNA
KNTVYLLMNSLEPEDTAIYYCAADSTIYCSYYECGHGLSTGGYGYDSWGQGTQVTVSRENLYFQGHHHHHH

Figure 2.18. Corresponding protein sequence for cAb-Lys3-Cys104 in mammalian vector. Green: cysteine at position 104.

A large amount of plasmid DNA is required for expression in mammalian cells (4 mg per litre of culture). 11 mg of UCB vector:WT-cAb-Lys3 and UCB vector:cAb-Lys3-Cys104 was produced by growing colonies in large volumes of LB and isolating plasmid DNA by Gigaprep. Following isolation of plasmid DNA, it was washed by ethanol precipitation and dissolved in sterile filtered water ready for transfection.

Transfection and expression of WT-cAb-Lys3 and cAb-Lys3-Cys104 in eukaryotic cells[47]

Transfection and expression were carried out in the protein expression facility in UCB, Slough. CHO cells grown in the absence of antibiotic for one week were tested to ensure viability. Cells were then harvested and washed with Earle's balanced salt solution (EBSS). Transfection was carried out by electroporation of cells in EBSS with plasmid DNA. Immediately after electroporation, the cell-DNA solution was resuspended in CHO chemically defined medium, and shaken at 37 °C for 1 day, then 32 °C for 13 days. The decrease in temperature is to prevent the cells from getting exhausted. Cells were harvested,

and successful extracellular expression of protein in the supernatants was confirmed by SDS-PAGE (~ 15 kDa, **Figure 2.19**).

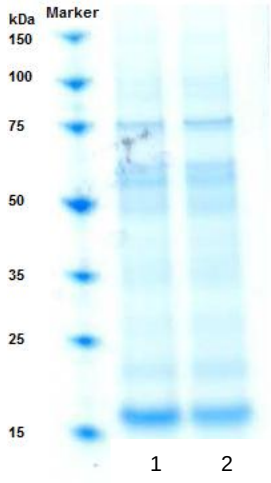

Figure 2.19. SDS-PAGE of supernatants after expression. 1: WT-cAb-Lys3, 2: cAb-Lys3-Cys104.

For both WT-cAb-Lys3 and cAb-Lys3-Cys104, the supernatant was purified by affinity chromatography. 1 L of supernatant was sequentially loaded in 200 mL portions onto a 5 mL HisTrap HP column. A simple step elution to 250 mM imidazole eluted both proteins (**Figures 2.20** and **2.21**). Fractions containing protein were combined and buffer exchanged (and desalted) into PBS, pH 8. 90 mg each of WT-cAb-Lys3 and cAb-Lys3-Cys104 were obtained.[47]

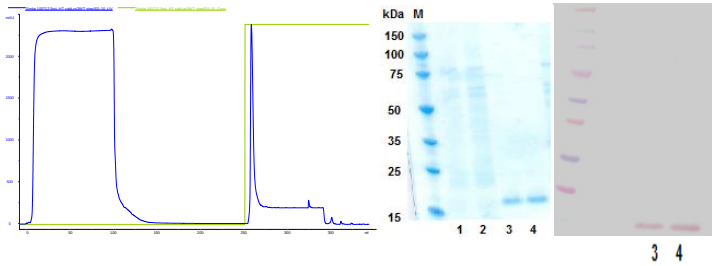

Figure 2.20. Purification of WT-cAb-Lys3. Left: FPLC trace, blue – UV absorbance (280 nm), green – concentration of elution buffer. Right: SDS-PAGE and Western blot, 1, 2 – flow through, 3, 4 – eluted fractions.

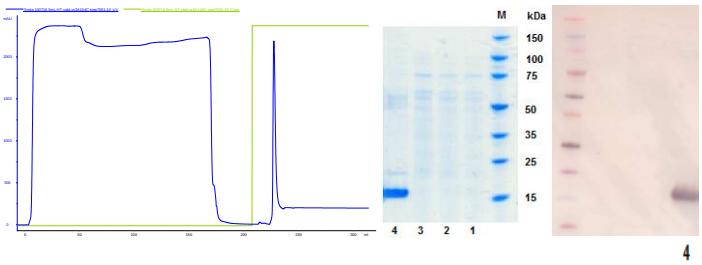

Figure 2.21. Purification of cAb-Lys3-Cys104. Left: FPLC trace, blue – UV absorbance (280 nm), green – concentration of elution buffer. Right: SDS-PAGE and Western blot, 1, 2, 3 – flow through, 4 – eluted fractions.

2.2.5 Characterisation of WT-cAb-Lys3 and cAb-Lys3-Cys104

In addition to SDS-PAGE and Western blot, cAb-Lys3 samples were characterised by LC-MS, ELISA (Enzyme-linked Immunosorbent Assay), Circular Dichroism (CD), proteolytic digests and by testing their reactivities.

WT-cAb-Lys3

WT-cAb-Lys3 was found to be the expected mass (**Figure 2.22**). It did not show any reactivity when reduced with dithiothreitol (DTT) and then treated with Ellman's reagent (as in Scheme 1), indicating that the two native disulfide bonds are inert to reaction (**Figure 2.23**). This lack of reactivity is essential in determining if cAb-Lys3-Cys104 would be a suitable substrate for site-specific chemical modification. Although there is a cysteine residue at the periphery of the CDR3 loop, it appeared to remain inert during reduction by DTT. Further tests described in Chapters 3 and 4 also support this observation. WT-cAb-Lys3 was found to exhibit binding to antigen lysozyme in the nanomolar range (**Figure 2.24**), in accordance with the literature,[31] and also showed predominant β-sheet structure, shown by a dip at 215 nm by CD (**Figure 2.25**).

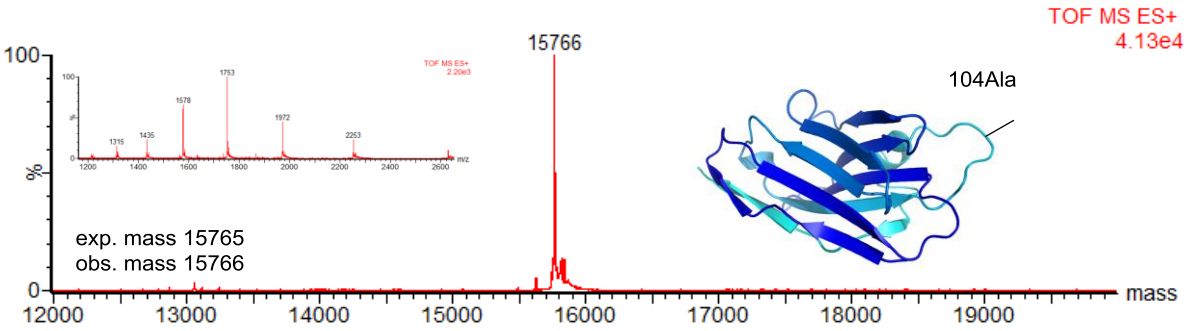

Figure 2.22. Mass spectrum (MS) for WT-cAb-Lys3. Expected mass 15765, observed mass 15766.

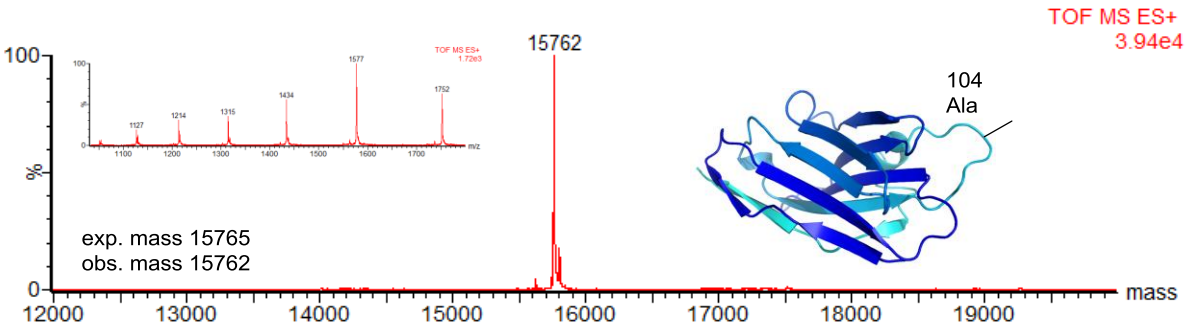

Figure 2.23. WT-cAb-Lys3 following reduction with DTT then reaction with Ellman's reagent.

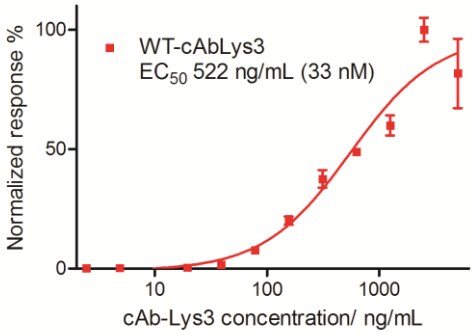

Figure 2.24. ELISA for WT-cAb-Lys3. 20 μg/mL antigen lysozyme was used with a starting concentration of 2500 ng/mL for WT-cAb-Lys3. Anti-polyhistidine-alkaline phosphatase conjugate then alkaline phosphatase substrate was used for detection of binding.

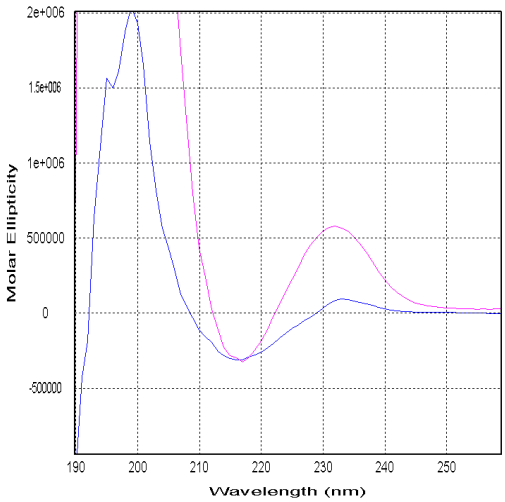

Figure 2.25. CD spectra for WT-cAb-Lys3 (pink) and cAb-Lys3-Cys104 (blue).

cAb-Lys3-Cys104

After establishing that the disulfide bonds in WT-cAb-Lys3 were inert to reaction, full characterisation of the mutant cAb-Lys3-Cys104 was carried out. Initially, a mass higher than expected (116 Da) was observed (**Figure 2.26**). cAb-Lys3-Cys104 was treated with DTT, and gratifyingly the expected mass was observed (**Figure 2.27**). As reducing with DTT resulted in the correct mass, it could be deduced that a disulfide PTM had occurred during mammalian expression. This is very likely to have been *S*-cysteinylation as previously reported by Gadgil and co-workers of a free cysteine in the CDR3 loop in MAB007.[48] Miao and co-workers have also described cysteinylation at an engineered cysteine site at the periphery of a Fab fragment, to which they added radio-labelled thiols site-selectively via disulfide bond formation following reduction.[49]

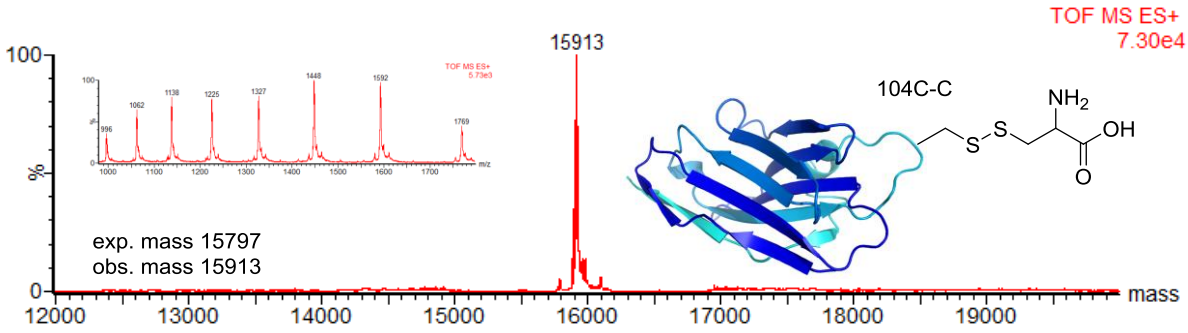

Figure 2.26. cAb-Lys3-Cys104 post purification.

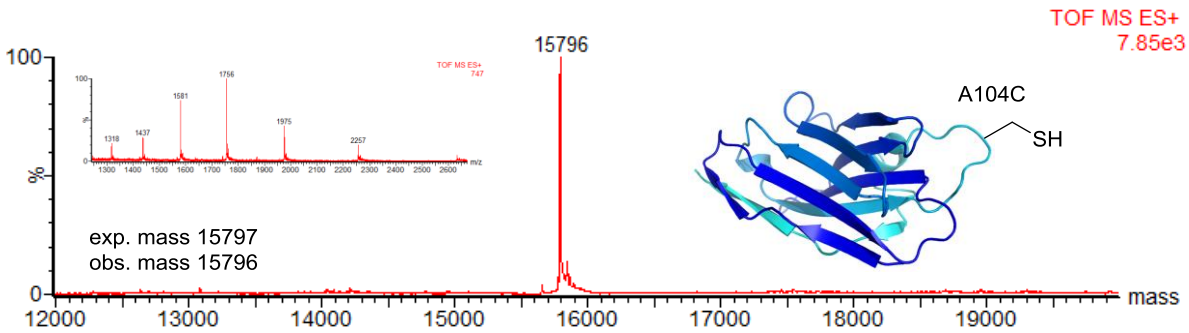

Figure 2.27. cAb-Lys3-Cys104 reduced with DTT.

Reduced cAb-Lys3-Cys104 was then treated with Ellman's reagent to test for the presence of a single reactive cysteine (**Scheme 2.1**), and a mass corresponding to the addition of 1 Ellman's adduct was observed (**Figure 2.28**). From this point forward, cAb-Lys3-Cys104 was always reduced with DTT prior to carrying out chemical modifications.

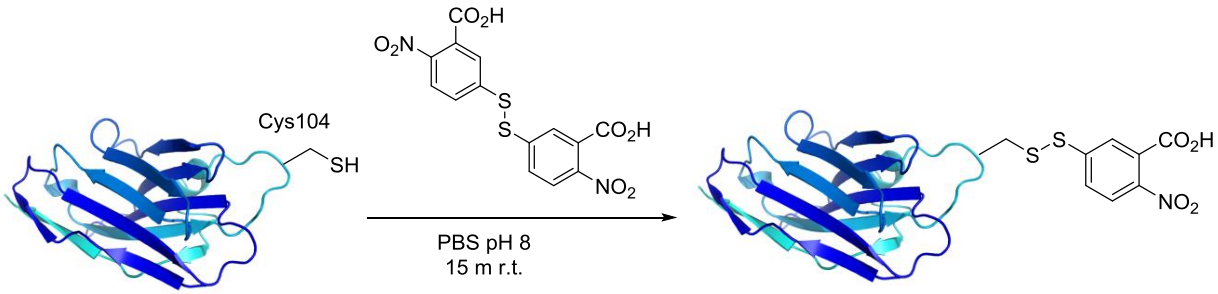

Scheme 2.1. Conditions for treatment of reduced cAb-Lys3-Cys104 with Ellman's reagent.

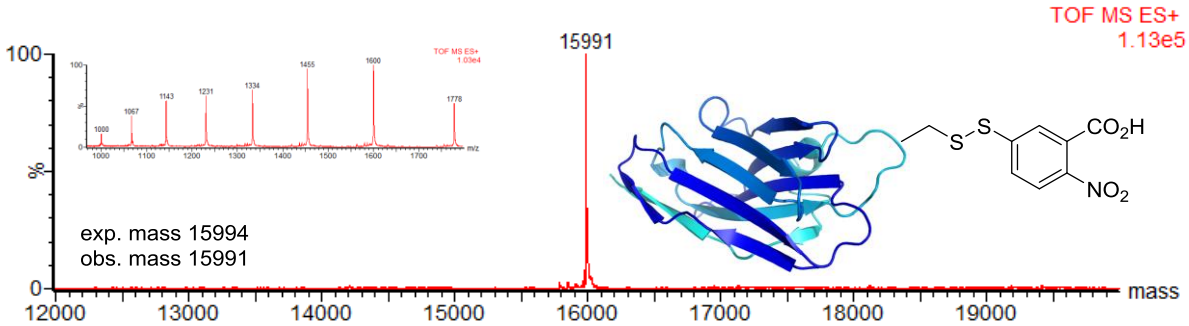

Figure 2.28. Reaction of reduced cAb-Lys3-Cys104 with Ellman's reagent, 15 minutes, room temperature.

The binding ability of cAb-Lys3-Cys104 to lysozyme was tested by ELISA. Binding affinities were found to be decreased compared to the WT, and so a higher initial

concentration of antibody than used with WT-cAb-Lys3 was needed. cAb-Lys3-Cys104 was found to bind at micromolar concentrations (**Figure 2.29**), and also exhibited β-sheet folding as seen by CD (**Figure 2.25**). The decrease in binding compared to WT-cAb-Lys3 can be attributed to a change in residue at a pivotal site,[31] where a key hydrophobic interaction between an alanine and tryptophan has been replaced by a less hydrophobic cysteine.

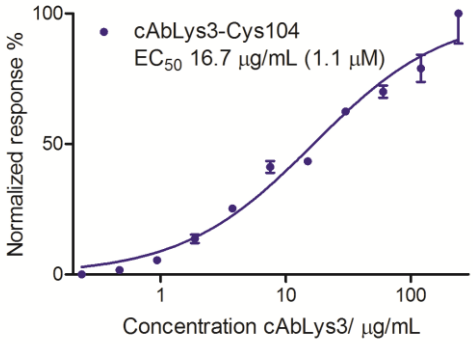

Figure 2.29. ELISA for cAb-Lys3-Cys104. 20 μg/mL antigen lysozyme was used with a starting concentration of 240 μg/mL for cAb-Lys3-Cys104.

Finally, the site of mutation was confirmed by enzymatic digest of the antibodies with endoproteinase Asp-N (Asp-N), then LC-MS/MS analysis of the peptide fragments. Asp-N cleaves at the N-terminus of aspartic and cysteic acid residues. The peptide fragment encompassing position 104 is shown in **Figure 2.30**, and sequencing results for both WT-cAb-Lys3 and cAb-Lys3-Cys104 are shown in **Figure 2.31**. Further analysis is shown in **Experimental Figures 2.1** and **2.2**.

DSTIY**X**SYYECGHGLSTGGYGY

Figure 2.30. Peptide fragment obtained from Asp-N digest of cAb-Lys3. X is alanine for WT-cAb-Lys3 and cysteine for cAb-Lys3-Cys104.

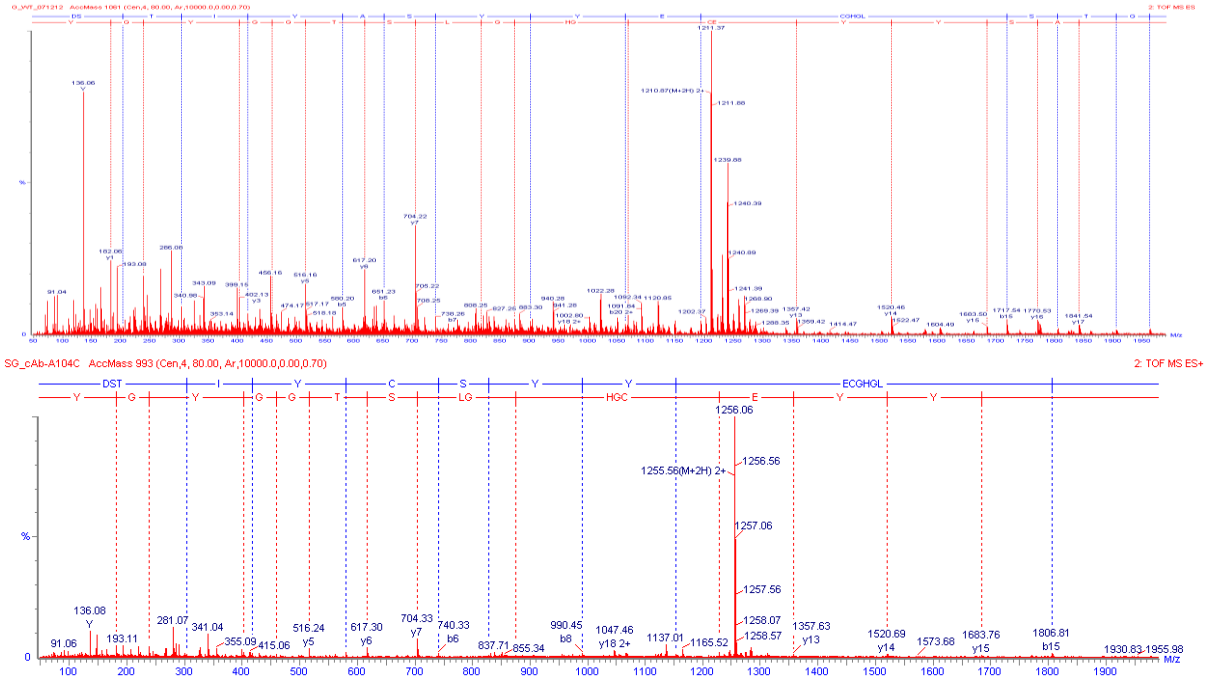

Figure 2.31. LC-MS/MS sequencing data for WT-cAb-Lys3 with alanine at position 104 (top) and cAb-Lys3-Cys104 with cysteine at position 104 (bottom).

2.3 Discussion

The successful expression of a high amount of camelid sdAb WT-cAb-Lys3 and mutant cAb-Lys3-Cys104 in mammalian cells has been described.[47] Although the bacterial expression of soluble sdAbs using the method of exporting to the periplasm under the *pelB* leader sequence developed by Skerra and Pluckthun[34] has been used by others in the pHEN1 vector and variations,[18,31] it was found to be low yielding in *E. coli* BL21(DE3) cells, with protein remaining in inclusion bodies after attempted cell lysis by osmotic shock. This may be due to secretory pathways being overloaded. Interestingly, for cAb-Lys3 in pHEN1, cell lysis by osmotic shock described by others for extracting protein from the periplasm was also found to be unsuccessful on a small scale. Although small scale expression trials varying a number of factors including the extraction method, the use of glucose as a carbon source, induction time and temperature led to soluble His-tagged protein being successfully extracted from cells, it was decided to subclone the cAb-Lys3 gene into a different expression vector pET-22b(+). This vector contains the T7 promoter, compatible with the BL21(DE3) expression strain containing T7 polymerase, and it was also thought expression of cAb-Lys3 and the cysteine mutant using pET-22b(+) may yield higher levels of protein than those obtained in pHEN1 and variants.[18,31] Obtaining a large amount of cAb-Lys3 for chemical modification purposes was required. pET-22b(+) was chosen in particular as like pHEN1, it contains the *pelB* leader sequence for exporting to the periplasm. Additionally Ahmadvand and co-workers used this expression vector for the overexpression of sdAbs to produce 10 – 25 mg/L culture,[12] much more than reported in the pHEN1 system.[18,31] After subcloning of the WT-cAb-Lys3 gene into pET-22b(+), expression under similar conditions to those reported by Ahmadvand were attempted.[12] Unfortunately, protein remained in the cell pellet as inclusion bodies despite carrying out extra osmotic shock steps, as well as trying to control the expression level by decreasing induction temperature, time and IPTG concentration. Trying

to reduce protein expression was attempted as insolubility is caused by a build up of inactive aggregates, which is caused by overproduction during expression.[42,43] As cAb-Lys3 could not be extracted using conventional cell lysis methods to obtain soluble protein, it was decided to purify the protein using denaturing conditions and then attempt its refolding. cAb-Lys3 inclusion bodies have been observed previously.[44] Successful isolation of WT-cAb-Lys3 in denaturing buffer was carried out, however all attempts to refold the protein resulted in precipitate despite the use of various refolding buffer additives, such as oxidised and reduced glutathione for disulfide shuffling, glycerol[45] and arginine.[46] Although bacterial expression systems are generally favoured due to lower costs and ease of production,[34] expression in mammalian cells can lead to higher yields of pure protein,[13] which may outweigh the disadvantages. This was observed with cAb-Lys3 in CHO cells. High levels (90 mg) of both WT-cAb-Lys3 and cAb-Lys3-Cys104 were obtained after expression and purification. The fact that the time taken to express is longer (3 weeks cell incubation times) than with bacteria (generally overnight cell growth) can be considered insignificant, as high levels of soluble antibody were obtained unlike after multiple attempts in *E. coli*. Veggiani and de Marco have previously shown that the co-expression of sdAbs with Erv1p sulfhydryl oxidase increased the yield of sdAbs expressed in bacterial cytoplasm to tens of milligrams per litre.[50] This could have been explored if expression in CHO cells had not been successful. After expression in CHO cells, purification of cell lysate containing secreted cAb-Lys3 by affinity chromatography was facile, and enough antibody was obtained to carry out modification reaction attempts for the duration of the DPhil. As sdAbs are known for their high stabilities,[6,9] extended storage times were not problematic, and no antibody degradation was observed over time.

Two correctly folded and functional sdAb cAb-Lys3 forms were expressed and purified in a eukaryotic expression system not described previously for cAb-Lys3.[47] WT-cAb-Lys3 is

known,[18,31,37–39] and characterisation revealed expected secondary structure, and nanomolar binding to lysozyme. The mutant cAb-Lys3-Cys104 is novel. Again, the expected secondary structure was obtained, and the site of mutation confirmed by proteolytic digest and LC-MS/MS analysis. Lower micromolar binding affinity to lysozyme was identified, showing the importance of position 104 in binding interactions. The alanine at position 104 has been identified as pivotal in binding lysozyme,[36] which is perhaps why a mutation to a chemically different residue causes a change in binding affinity. At pH 8, cAb-Lys3 is negatively charged and lysozyme positive,[38] which is probably why a cysteine residue will not completely diminish binding. Furthermore, the backbone N and O of alanine at position 104 have previously been identified as important in interacting with lysozyme, in a way that mimics the 2-acetamido group of a carbohydrate substrate,[36] an interaction that will still be possible with a different residue. The slightly larger size of the cysteine ($-CH_2S^-$) and perhaps slight decrease in hydrophobicity as compared to alanine ($-CH_3$) may account for the lower level of binding. It would perhaps be interesting to see if mutations at other residues positioned within the CDR3 loop would have similar effects on the binding affinity of cAb-Lys3. More importantly, the reactivity of the two disulfide bonds in cAb-Lys3 was paramount in finding out if cAb-Lys3-Cys104 could be used as a suitable substrate for single site-specific modifications via a cysteine precursor. Gratifyingly, reducing WT-cAb-Lys3 with DTT, then reacting with Ellman's reagent resulted in no change in mass, whereas carrying out the same reaction sequence with the cysteine mutant resulted in a mass change corresponding to the introduction of a single Ellman's adduct. The behaviour of the wild type suggests this is due to the mutation introduced at position 104, and further tests described in Chapters 3 and 4 support the hypothesis that both disulfide bonds in cAb-Lys3 are inert to reduction. This is despite the fact that one of the cysteine residues is at position 109, at the C-terminal end of the CDR3 loop, and involved in stabilising the overall antibody.

2.4 Conclusions

The single-domain antibody cAb-Lys3 and the mutant cAb-Lys3-Cys104 have been expressed and purified in eukaryotic cells in high yields. Initial attempts in both a phagemid vector, and expression vector in *E. coli* were unsuccessful in yielding high amounts of soluble protein. Refolding protein isolated from inclusion bodies was problematic. Once purified, both WT-cAb-Lys3 and cAb-Lys3-Cys104 exhibited expected reactivities, showing that one free cysteine at position 104 was reactive, and not the native disulfide bonds. cAb-Lys3-Cys104 could therefore be taken forward in site-specific chemical modification studies.

2.5 Experimental

Biological Manipulations. Biological manipulations requiring sterile conditions were undertaken in sterile conditions in a HERAsafe KSP12 laminar flow hood (Thermo Scientific).

Agar Plates. LB broth (12.5 g) and agar (7.5 g) were added to water (500 mL). The solution was autoclaved. Once it had cooled down slightly, ampicillin (500 μL, 100 μg/mL) was added. Approximately 20 mL of the solution was poured into petri dishes. They were allowed to set, covered and then stored at 4 °C until needed.

Polymerase Chain Reaction (PCR). The A104C mutation was carried out using the Agilent QuikChange II Site-Directed Mutagenesis Kit. 10x reaction buffer (5 μL), ds DNA template (10 μL, 50 ng), forward oligonucleotide primer (1.7 μL, 125 ng) reverse oligonucleotide primer (1.7 μL, 125 ng), dNTP mix (5 μL) and MQ H_2O (26.6 μL) were added to a thin walled PCR tube and vortexed. *PfuUltra* HF DNA polymerase (1 μL, 2.5 U/ μL) was added to the final volume of 50 μL and the mixture pipetted up and down to ensure homogeneity. PCR was carried out using the cycling parameters shown in **Experimental Table 2.1**.

Temperature/ °C	95	95	55	72	72	4
Time	2 min	30 sec	30 sec	12 min	10 min	∞
		20 cycles				

Experimental Table 2.1. PCR cycling parameters.

Dpn I restriction enzyme (1 μL, 10 U/ μL) was added to the amplification reaction. The reaction was mixed gently and thoroughly by pipetting the solution up and down several times. The reaction was incubated at 37 °C for 1 hour to digest the parental (the nonmutated) supercoiled dsDNA.

Transformation into XL-1 Blue Supercompetent Cells. XL-1 Blue Supercompetent Cells were gently thawed on ice, and then 50 μL aliquoted into a pre-chilled 14 mL BD falcon polypropylene round-bottomed tube. *Dpn* I-treated DNA was transferred to the cells. The reaction was gently swirled to mix, then incubated on ice for 30 minutes. The reaction was heat pulsed for 45 seconds at 42 °C and then placed on ice for 2 minutes. Sterile LB broth or SOC medium (250 μL) preheated to 42 °C was added, and then the reaction was incubated at 37 °C for 1 hour (225 rpm). The transformation reaction was plated onto agar plates containing ampicillin. A pipette cleaned in 70 % ethanol was used to spread varying volumes (25 – 200 μL) of transformation reaction onto the plate. The transformation plates were incubated at 37 °C for a minimum of 16 hours. Plates containing colonies were stored at 4 °C.

Overnight Culture. A single colony was pipetted into sterile LB broth (10 mL) and ampicillin (10 μL, 100 μg/ mL). The reaction was incubated at 37 °C for 16 hours (225 rpm).

Miniprep Plasmid DNA Purification. Miniprep Plasmid DNA purification was carried out using the QIAprep Spin Miniprep Kit. The overnight culture was centrifuged (3,750 rpm, 10 minutes, 4 °C) and the supernatant poured off. Pelleted bacterial cells were resuspended in Buffer P1 (250 μL) and transferred to a microcentrifuge tube. Buffer P2 (250 μL) was added, and the sample mixed thoroughly by inverting the tube 6 times. Buffer N3 (350 μL) was added and mixed immediately and thoroughly by inverting the tube 6 times. The mixture was centrifuged at 13,000 rpm (17,900x*g*) for 10 minutes in a table-top microcentrifuge. The supernatant was pipetted into the QIAprep spin column, and centrifuged for 1 minute. The flow-through was discarded. Buffer PE (750 μL) was added to the QIAprep spin column, and centrifuged for 1 minute. The flow-through was discarded, and the QIAprep spin column centrifuged for 1 minute to remove residual wash buffer. To elute DNA, the QIAprep spin column was placed in a clean 1.5 mL microcentrifuge tube. Water (40 μL) was added to the

centre of the QIAprep spin column, and it was left to stand for 10 minutes, then centrifuged for 1 minute. Pure DNA was stored at -20 °C. Samples for sequencing were prepared at 100 pmol/μL and submitted to the Source BioScience sequencing facility (Oxford).

Protein Expression. A single colony of cAb-Lys3 in *E. coli* BL21(DE3) cells was used to inoculate small starter cultures (10 mL) of sterile LB broth containing ampicillin (100 μg/ mL). This small culture was grown for 16 hours at 37 °C (220 rpm). Small starter culture aliquots (8 mL) were used to inoculate sterile LB broth (800 mL) containing ampicillin (100 μg/ mL). The cells were incubated at 37 °C and the optical density (OD_{600}) was monitored until a value of 0.6 was obtained. Expression was then induced by addition of IPTG (1 mM) and was continued for 16 hours at 25 °C. The cells were harvested by centrifugation (20 minutes, 5,000 rpm, JLA-9.1000 rotor, 4 °C) to give pellets. Cell pellets were snap frozen in liquid nitrogen and stored at -80 °C until required.

Cell Lysis by Osmotic Shock. Cell pellets were thawed and then resuspended in TES buffer (10 mL per cell pellet), and diluted with water (40 mL per cell pellet) on ice. The cell debris was removed from the lysate by centrifugation (30 minutes, 19,000x*g*, JCA-20 rotor, 4 °C).

Protein Purification. Binding buffer was added to the lysate. The protein was purified on an Äkta FPLC coupled to a Frac-900 fraction collector using a 5 mL HisTrap HP (GE Healthcare). After loading the cleared lysate onto the column, the column was washed extensively with binding buffer (30 column volumes). His-tagged protein was eluted from the column using a linear gradient from binding buffer to 100 % elution buffer. All eluent was analysed by SDS-PAGE (NuPage 4 -12 % Bis-Tris gel, Invitrogen) and Western blot to identify the fractions containing the protein. Fractions containing protein were put through a PD-10 desalting column (GE Healthcare) by equilibrating with 25 mL PBS, then eluting with 3.5 mL PBS. Protein concentration was determined using a Nanodrop Spectrometer, and then

snap frozen in liquid nitrogen and stored at -80 °C. In cases where a larger volume of eluent was obtained, fractions were concentrated by VivaSpin (3 or 5 kDa MWCO, Sartorius Stedim) and then desalted.

SDS-PAGE. Novex Bis-Tris gels (Invitrogen) were used (4 – 12 %). Gels were placed in the gel tank, and the gel tank filled with MES running buffer (800 mL, prepared from 20x concentrate, Invitrogen). Samples for the gel were prepared by adding sample (15 μL) to 6x dye (3 μL), and denaturing at 90 °C for 5 – 10 minutes. Approximately 10 μL of this denatured sample was loaded into the gel. Where the sample was a cell pellet, a small amount of the pellet was scraped into a microcentrifuge tube and 10 – 20 μL water added to obtain a diluted suspension. The gel was run at 200V for 50 minutes or the time taken for the dye to reach the bottom of the well.

Staining with Coomassie Brilliant Blue. Coomassie Brilliant Blue Stain (20 mL, Bio-Rad) was added to the gel. It was allowed to develop for 1 hour on an orbital rocker then rinsed with water.

Western Blot. SDS-PAGE was carried out on desired fractions. Transfer buffer (100 mL) was added, and the gel placed on an orbital shaker for 30 minutes. 6 pieces of filter paper were cut to the size of the gel and pre-wet in transfer buffer. The membrane was pre-wet by dipping in methanol, then water. An air tight 'sandwich' was formed by layering 3 pieces of filter paper, gel, membrane, and then 3 more pieces of filter paper. Alternatively, the iBlot device (Invitrogen) was used to transfer the gel to the membrane (p3 program, 7 minutes). In the meantime, a solution of BSA (2.5 g, bovine serum albumin) in TBST (50 mL) was prepared. This was added to the membrane to block it, and placed on an orbital shaker for 1 hour. A solution of BSA (2.5 g) and anti-polyHistidine-Alkaline Phosphatase (8 μL, Sigma) in TBST (50 mL) was added to the membrane and placed on an orbital shaker at 4 °C

overnight. The membrane was rinsed with TBST 3 times at 4 °C. The membrane was then rinsed with water. BCIP/NBT substrate (5 – 10 mL, Sigma) was added and incubated with the membrane for 10 minutes. The membrane was rinsed with water, and then placed between two acetate sheets and scanned in.

Expression Trials. A single colony of cAb-Lys3 in *E. coli* BL21(DE3) cells was used to inoculate small starter cultures (5 mL) of sterile LB broth containing ampicillin (100 μg/ mL). This small culture was grown for 16 hours at 37 °C (220 rpm). Small starter culture aliquots (200 μL) were used to inoculate sterile LB broth (10 mL) containing ampicillin (100 μg/ mL). The cells were incubated at 37 °C (220 rpm) and the optical density (OD_{600}) was monitored until a value of 0.6 was obtained. Expression was then induced by addition of IPTG (1 mM) and incubation was continued for the desired time at the desired temperature (220 rpm). The cells were harvested by centrifugation (8 minutes, 8,000 rpm, 4 °C).

For cell lysis with BugBuster (Novagen), the cell pellet was resuspended in BugBuster MasterMix (5 mL per gram wet cell paste), and pipetted up and down until homogenous. The lysate was rocked for 20 minutes at room temperature, and then harvested to remove cell debris (16,000x*g*, 20 minutes, 4 °C). In the case where sonication was used, lysate was sonicated for bursts of 2 x 30 seconds with a wait of 1 minute in between.

Restriction Digests. Restriction enzymes were purchased from NEBiolabs. All necessary components were mixed in a thin walled PCR tube, pipetted up and down then incubated at 37 °C for 3 hours.

Ligations. All necessary components were mixed in a thin walled PCR tube, pipetted up and down then incubated at 16 °C overnight (T4 DNA ligase) or 25 °C for 1 hour (Quick Ligase). Both ligation enzymes were purchased from NEBiolabs.

Gel Extraction Kit (Qiagen). The DNA fragment was excised from the agarose gel with a clean scalpel and then weighed in a Falcon tube. Three volumes of Buffer QG was added to 1 volume of gel (100 mg ≈ 100 μL). The gel/buffer solution was incubated at 50 °C for 10 minutes (or until the gel was completely dissolved) with occasional vortexing. 1 volume of isopropanol was added to the solution, and then the solution applied to a QIAquick column and centrifuged for 1 minute (13,200 rpm). Flow through was discarded, and 0.75 mL Buffer PE was added and centrifuged for 1 minute. Flow through was discarded and the column centrifuged for an additional minute. DNA was eluted by adding 40 μL MQ H_2O to the QIAquick column over a clean microcentrifuge tube, standing for 10 minutes and then centrifuging for 1 minute.

PCR Purification Kit (Qiagen). 5 volumes of Buffer PB was added to 1 volume of the PCR sample and mixed. The solution was applied to a QIAquick column and centrifuged for 1 minute (13,200 rpm). Flow through was discarded, and 0.75 mL Buffer PE was added and centrifuged for 1 minute. Flow through was discarded and the column centrifuged for an additional minute. DNA was eluted by adding 40 μL MQ H_2O to the QIAquick column over a clean microcentrifuge tube, standing for 10 minutes and then centrifuging for 1 minute.

DNA Agarose Gel Electrophoresis. 0.3 g agarose was added to 50 mL TAE buffer in a conical flask and heated in a microwave until the agarose dissolved completely. Once cool enough to touch, 4 μL ethidium bromide was added. The solution was poured into a gel holder and allowed to set for 30 minutes. The gel was covered with 200 mL TAE buffer. Samples containing 5x DNA loading dye were prepared and loaded into the gel. The gel was run at 100 V for approximately 1 hour. DNA bands were visualised under UV (366 nm).

Isolation and Denaturation of Inclusion Bodies. The cell pellet was resuspended in ice cold TES (10 mL per litre of cell culture) and then diluted 5 fold with ice cold water. The resulting

suspension was stirred on ice for 30 minutes. Cells were harvested by centrifugation (19,000x*g*, 30 minutes, 4 C) and the supernatant poured off. The cell pellet was resuspended in 100 % BugBuster Protein Extraction Reagent (5 mL per gram of wet cell paste, BBPER, Novagen) and the solution was pipetted up and down until homogenous. The solution was rocked at room temperature for 20 minutes and centrifuged (16,000*x*g, 20 minutes, 4 °C). The addition of BBPER, incubation and harvesting was repeated once more with 100 %, then once with 10 % and three more times with 5 %. Denaturing was performed by resuspending washed inclusion bodies in denaturing buffer (5 mL per gram inclusion body). The denaturing solution was stirred overnight at room temperature and then centrifuged to pellet the cellular debris (10,000*x*g, 30 minutes, room temperature).

Purification under Denaturing Conditions. Lysate was added to Ni-NTA HisBind resin (1 mL resin per 4 mL lysate, Novagen) and incubated at room temperature for 2 hours before loading onto the column. Flow through was collected and then the resin washed and eluted with denaturing buffer at pH 6.3, 5.9 and 4.5. Fractions were analysed by SDS-PAGE and Western blot. Fractions containing pure His-tagged protein were combined.

Dilution Refolding. Denatured protein (100 μL) was added dropwise to a stirring solution of the relevant buffer (10 mL). After two minutes of stirring, the solution was concentrated by VivaSpin (3 or 5 kDa MWCO).

Gigaprep. A starter culture of 5 mL LB containing kanamycin (50 μg/mL) was inoculated with a single colony of WT-cAb-Lys3/cAb-Lys3-Cys104 from a freshly streaked plate (XL-1 Blue Supercompetent Cells) and incubated for 8 hours at 37 °C (220 rpm). The starter culture was diluted by adding 1 mL to 500 mL LB in a 2 L flask. Cells were grown for 12 – 16 hours at 37 °C (220 rpm). Cells were harvested by centrifugation (6,000*x*g, 15 minutes, 4 °C), and resuspended in Buffer P1 containing RNase A and LyseBlue (125 mL). Buffer P2 (125 mL)

was added and the resulting solution mixed thoroughly by vigorously inverting 4 – 6 times then incubating at room temperature for 5 minutes. Chilled Buffer P3 was added and the resulting solution mixed immediately by vigorously inverting 4 – 6 times and then incubating on ice for 30 minutes. Cells were harvested (≥ 20,000*xg*, 30 minutes, 4 °C) twice with supernatant containing plasmid DNA being removed. A QIAGEN-tip10000 was equilibrated by applying Buffer QBT (75 mL). The supernatant containing plasmid DNA was applied to the QIAGEN-tip, and it was allowed to enter the resin by gravity flow. The resin was washed with Buffer QC (600 mL), and eluted with Buffer QF (100 mL). DNA was precipitated by adding isopropanol (70 mL) to the eluted DNA. After a quick mixing step, it was centrifuged immediately (≥ 15,000*xg*, 30 minutes, 4 °C), and the supernatant carefully decanted. A pellet could be seen. The pellet was washed with 70 % ethanol (10 mL) and centrifuged (≥ 15,000*xg*, 30 minutes, 4 °C). Again, the supernatant was decanted carefully. The pellet was air dried for 15 minutes, then dissolved in a suitable volume of MQ H_2O. The concentration was measured by Nanodrop. A 4 mg aliquot was taken and added to 1/10 volume of 5 M NaCl and 2.5 volumes 100 % ethanol. The solution was shaken gently, and precipitation of DNA could be seen. The solution was stored at – 20 °C overnight, along with 80 % ethanol solution. Precipitated DNA was centrifuged (1300 rpm, 10 minutes, 4 °C), supernatant decanted, and then 80 % ethanol added. Precipitated DNA was centrifuged again (1300 rpm, 10 minutes, 4 °C). In a sterile environment, the supernatant was decanted and 1 mL sterile filtered MQ H_2O added to the DNA pellet. The DNA was allowed to resuspend completely at 4 °C overnight.

Transfection and Expression of cAb-Lys3 in CHO cells.[47] CHO cells were grown in 1 L chemically defined CHO medium in a 3 L flask for 1 week at 37 °C with shaking. Cells were harvested by centrifugation (450 g, 15 minutes, 4 °C) and the supernatant decanted. Pelleted cells were resuspended in Earle's balanced salt solution (EBSS, 20 mL, Sigma), and then

harvested by centrifugation (450*x*g, 15 minutes, 4 °C). Pelleted cells were then resuspended in EBSS (2 mL) containing the vector for cAb-Lys3 (4 mg total DNA in UCB vector). The solution was made up to 10 mL with EBSS and kept on ice. This was split into 800 µL aliquots and the cells electroporated at 300 V. Transfected cells were added to Gibco CD CHO medium (Invitrogen), and 1 L medium was incubated with shaking in a 3 L flask at 37 °C for 1 day, and then at 32 °C for 13 days. CD CHO medium was prepared by preheating all components to 37 °C, followed by the addition 100× GlutaMAX (10 mL, Invitrogen) and antibiotic-antimycotic (2 mL, contains 10,000 units of penicillin (base), 10,000 µg of streptomycin (base), and 25 µg of amphotericin B/ml utilizing penicillin G (sodium salt), streptomycin sulfate, and amphotericin B as Fungizone® Antimycotic in 0.85% saline, Invitrogen). Cells were harvested by centrifugation (450*x*g, 15 minutes, 4 °C), and the supernatant taken to the purification step. Protein purification was carried out on an Äkta FPLC coupled to a Frac-900 fraction collector. A 5 mL HisTrap HP was equilibrated with 5 column volumes of binding buffer before sample loading. The column was washed with 2 column volumes of binding buffer to remove excess unbound protein before a step to 100 % elution buffer over 5 column volumes. Protein was detected by UV absorbance at 280 nm. A flow rate of 5 mL/min was used. Flow through and eluted fractions were analysed by SDS-PAGE and Western blot. Fractions containing protein were concentrated (Vivaspin) and buffer exchanged (PD10) into PBS, pH 8. 90 mg each of WT-cAb-Lys3 and cAb-Lys3-Cys104 was obtained in total. Protein was split into 1 mg/mL aliquots, snap frozen in liquid N_2 and stored at – 80 °C.

Protein Modification and Mass Spectrometry. MQ purified water was used for protein and cellular manipulations. Protein concentrations were determined by Nanodrop. Liquid chromatography-mass spectrometry (LC-MS) was performed on a Micromass LCT (ESI-TOF-MS) coupled to an Agilent 1100 Series HPLC using a Phenomenex Jupiter 5 µm C4

column (250 × 4.6 mm). Water (solvent A) and acetonitrile (solvent B), each containing 1% formic acid by volume, were used as the mobile phase at a flow rate of 1.0 mL/min. The gradient was programmed as follows: 95% A for 5 min to desalt and then a linear gradient to 100% B over 15 min followed by 100% B for an additional 5 min. A linear gradient over 10 minutes back to 95% A was used to re-equilibrate the column. The electrospray source was operated with a capillary voltage of 3.2 kV and a cone voltage of 25 V. Nitrogen was used as the nebulizer and desolvation gas at a total flow of 600 l/hr. Under these conditions, all protein material typically co-eluted in a single peak between 13 and 18 minutes. For reaction analysis, the mass spectra for all protein material in this peak were combined using MassLynx software (v. 4.1 from Waters). Mass spectra were then calibrated using a calibration curve constructed from a minimum of 17 matched peaks from the multiply charged ion series of equine myoglobin obtained at a cone voltage of 25V. The calibrated, combined ion series was deconvoluted using a maximum entropy algorithm that is preinstalled on the MassLynx software.

ELISA. Each well of a 96-well plate (Greiner Bio-one half-area high-binding plates) was coated with 1 μg of hen egg white lysozyme (Sigma), and incubated at 4 °C overnight. All subsequent steps were performed at room temperature. The plate was washed four times with PBS (pH 7.4) containing 0.05% Tween20 (Sigma), blocked for 90 minutes with 3% BSA in PBS and then washed once with PBS (pH 7.4) containing 0.05% Tween20. Antibody (0.48 mg/mL in 1% BSA, 0.02% Tween20 in PBS) dilutions were made across the plate for final concentrations of 240 μg/mL to 234 ng/mL. The plate was incubated with gentle rocking for 2 hours. Unbound antibody was removed by washing four times with PBS (pH 7.4) containing 0.05% Tween20. The secondary antibody (Anti-polyHistidine-alkaline phosphatase conjugate) was prepared at a 1:1000 dilution in PBS (pH 7.4) and 50 μL was added to each well. The plate was incubated with gentle rocking for 1 hour. Each well was

then washed with 50 μL of diethanolamine buffer (Phosphatase substrate kit, Thermo Scientific). PNPP phosphatase substrate (Phosphatase substrate kit, Thermo Scientific) was prepared by dissolving one tablet in 6 mL of diethanolamine buffer. 50 μL of the PNPP substrate solution was added to each well and incubated for 15 min. After this time, absorbance was measured at 405 nm. Absorbance was plotted against concentration. Sigmoidal regression analysis and normalisation was carried out using GraphPad Prism 5.01.

CD. CD measurements were made using a Chirascan spectropolarimeter fitted with a Peltier temperature controller. Protein solutions were each made up in PBS at pH 8. CD spectra were measured in a 1 mm quartz cuvette at room temperature using a scan rate of 50 nm/min, 1 nm interval, 1 nm bandwidth and a response time of 0.5 s. After baseline correction, ellipticities in deg were converted to molar ellipticities (deg cm^2 dmol-res^{-1}) by normalizing for the concentration of peptide bonds and path length.

Protein Digestion Analysis by LC-MS/MS. Peptides were analysed using a nanoLC-MS/MS system with nanoLockspray (nanoAcquity Synapt-HDMS; Waters Corporation, Milford, MA, USA). Peptide digests were injected from a sample manager and trapped on a 5 μm symmetry C18 column (180μm x 20 mm) and washed for 1 min at 15 μl/min with mobile phase A (0.1% formic acid). Peptides were then separated and eluted for MS analysis using a 90 min reverse phase gradient at 400 nl/min (0.1–60% ACN over 70 min) on a BEH 130 C18 1.7μm particle size 75μm x 150mm nanoAcquity UPLC column. The column temperature was set at 300°C. The reference for the nanolockspray was set to the 13C peak of reserpine at a concentration of 3 mg/L flowing at 20 μL/min. The reference was constantly infused and sampled at 10 sec intervals. The eluted peptide spectra were ionised using nano-electrospray and measuring using a Synapt-HDMS (Quadrupole-Time of Flight mass spectrometer). The sample was analyzed in positive, V mode over a mass range between 140–4300 m/z with a

scan time of 1s. The on-line eluted peptides were analyzed using a MSe method collecting MS data with a low collision energy (6 eV) and MS/MS data using collision enery ramping between 15 and 35 volts. Spectra were processed using ProteinLynx and Biolynx (Waters Corporation, Milford, MA, USA).

Asp-N digests. cAb-Lys3 (100 µL, 0.2 mg/mL in ammonium bicarbonate pH 8.5) was heated to 95 °C for 15 minutes, reduced with DTT (5 mM) at 60 °C for 15 minutes, then alkylated with iodoacetamide (15 mM) for 15 minutes at room temperature. Endoproteinase Asp-N from *Pseudomonas fragi* mutant strain (0.1 µg, 2.5 µL, Sigma) was added to the protein solution, and then shaken at 37 °C overnight.

a

Untitled
Associated Datafile: SG_cAb_AspN_081112 (50 - 1990 amu)
AspN:-/D

Frag#	Res#	Sequence	Theor (Bo)	[M+H]	[M+2H]	[M+3H]
D4	90-98	(E)DTAIYYBAA(D)	1046.44	1047.45	524.23	349.82
D2	62-72	(A)DSVKGRFTISQ(D)	1236.65	1237.65	619.33	413.22
D3	73-89	(Q)DNAKNTVYLLMNSLEPE(D)	1949.94	1950.95	975.98	650.99
D5	99-120	(A)DSTIYASYYEBGHGLSTGGYGY(D)	2419.99	2421.00	1211.00	807.67
D3-4	73-98	(Q)DNAKNTVYLLMNSLEPEDTAIYYBAA(D)	2978.37	2979.38	1490.19	993.80
D6	121-146	(Y)DSWGQGTQVTVSRENLYFQGHHHHHH(-)	3093.41	3094.42	1547.71	1032.14

b

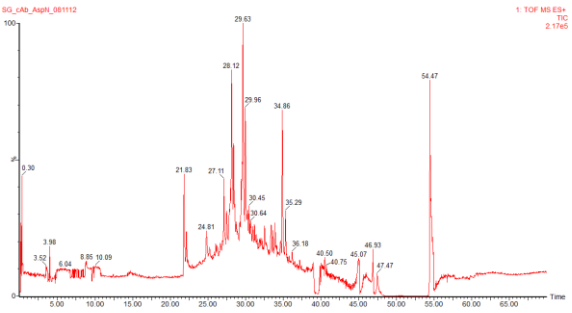

c

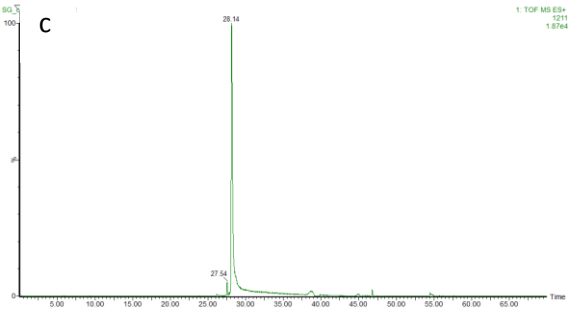

d

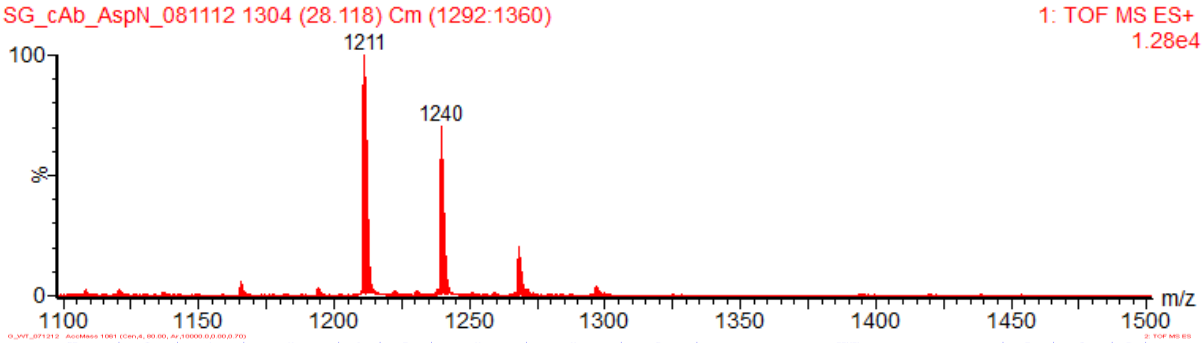

e

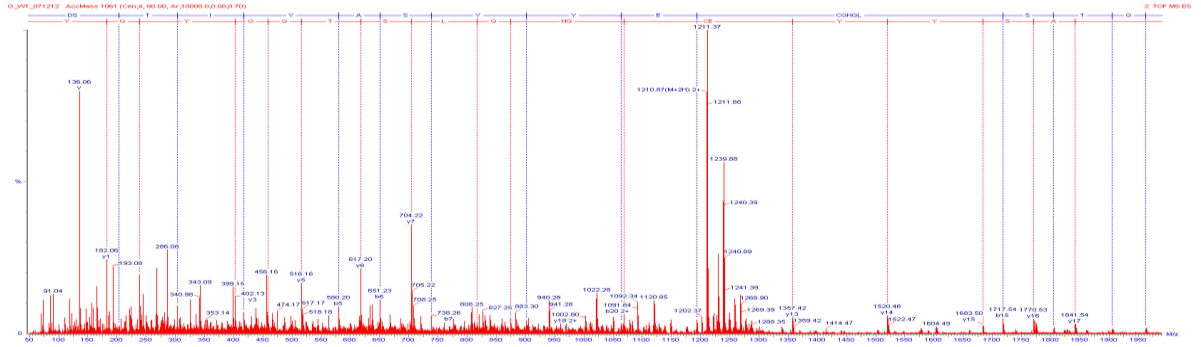

Experimental Figure 2.1. Enzymatic digest of WT-cAb-Lys3 (Ala104) and sequencing. a) Expected sequences and theoretical masses of the peptides resulting from digestion of WT-cAb-Lys3 with Asp-N. Masses identified in the mass spectrum integrated over the whole LC-MS chromatogram are highlighted in black (ΔDa = 0.1). B corresponds to carboxymethylamide cysteine. b) LC-MS chromatogram. c) Extracted mass chromatogram for the theoretical mass $[D5+2H]^{2+}$: M = 1211.0. d) MS of peak at 28.14 minutes. e) MS/MS of peptide D5, Ala is observed at position 104.

a

Associated Datafile: SG_cAb-A104C (50 - 1990 amu)
AspN:-/D

Frag#	Res#	Sequence	Theor (Bo)	[M+H]	[M+2H]	[M+3H]
D4	90-98	(E)DTAIYYBAA(D)	1046.44	1047.45	524.23	349.82
D2	62-72	(A)DSVKGRFTISQ(D)	1236.65	1237.65	619.33	413.22
D3	73-89	(Q)DNAKNTVYLLMNSLEPE(D)	1949.94	1950.95	975.98	650.99
■D5	99-120	(A)DSTIYBSYYEBGHGLSTGGYGY(D)	2508.98	2509.99	1255.50	837.34
D6	121-146	(Y)DSWGQGTQVTVSRENLYFQGHHHHHH(-)	3093.41	3094.42	1547.71	1032.14
D1	1-61	(-)DVQLVESGGGSVQAGGSLRLSBAASGYTIGPYBMGWFRQAPGKEREGVAAINMGGGITYYA(D)	6331.12	6332.13	3166.57	2111.38

b

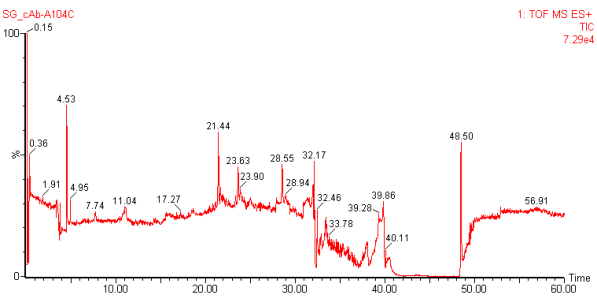

c

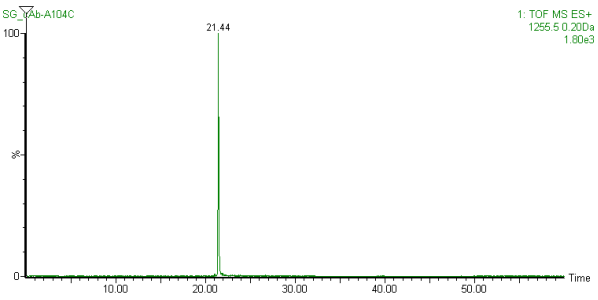

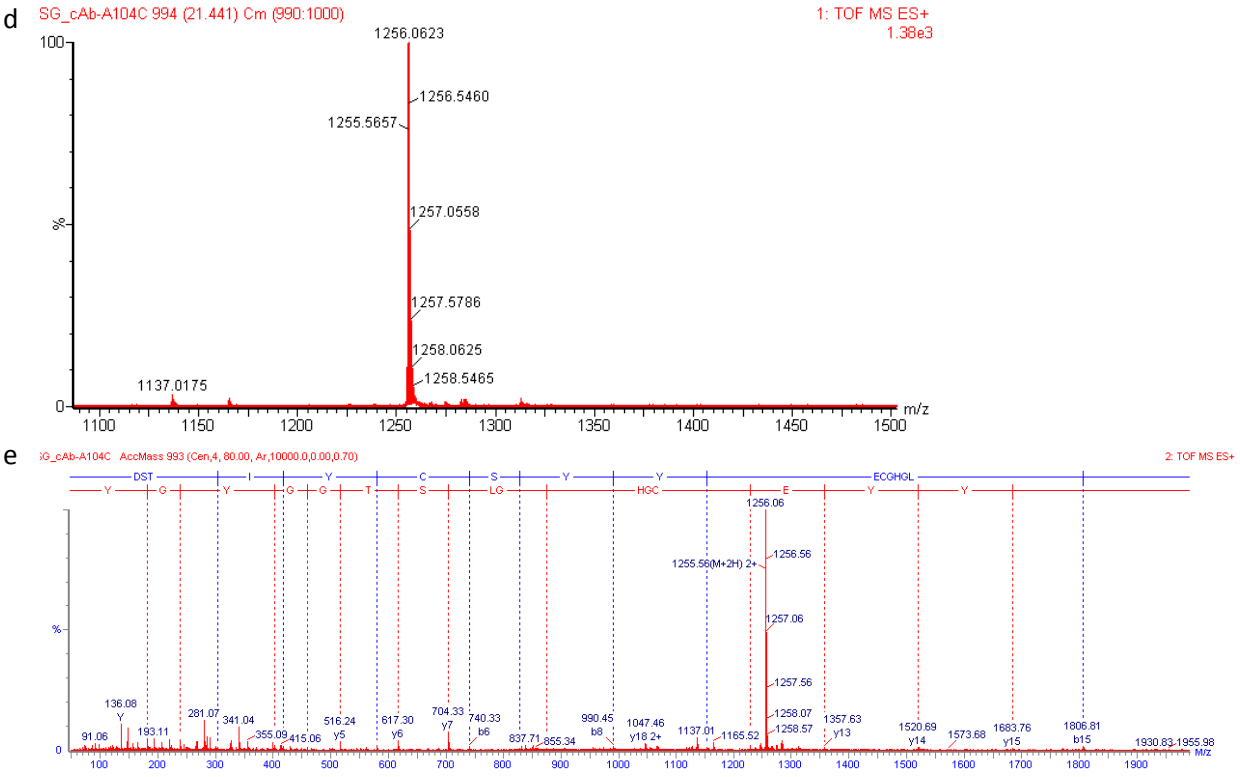

Experimental Figure 2.2. Enzymatic digest of cAb-Lys3-Cys104 and sequencing. a) Expected sequences and theoretical masses of the peptides resulting from digestion of cAb-Lys3-Cys104 with Asp-N. Masses identified in the mass spectrum integrated over the whole LC-MS chromatogram are highlighted in black (ΔDa = 0.1). B corresponds to carboxymethylamide cysteine. b) LC-MS chromatogram. c) Extracted mass chromatogram for the theoretical mass $[D5+2H]^{2+}$: M = 1255.50. d) MS of peak at 21.44 minutes. e) MS/MS of peptide D5, Cys is observed at position 104.

Reducing with DTT. DTT (1.2 mg, 7.8 μmol) was added to 0.5 mL of cAb-Lys3 (WT or Cys104, c = 1 mg/mL, PBS pH 8) and shaken (600 rpm) at room temperature for 5 minutes. After this time, the protein solution was passed through a PD minitrap (GE Healthcare), previously equilibrated with PBS (pH 8), eluting with 1 mL of the same buffer. The reduced protein was used immediately.

Reaction with Ellman's Reagent. A stock solution of Ellman's reagent was prepared by dissolving 0.6 mg in 108 μL PBS pH 8. A 75 μL aliquot cAb-Lys3 (WT or Cys104, c = 0.5 mg/mL in PBS, pH 8) was diluted with 75 μL PBS, pH 8. A 10 μL aliquot of the Ellman's

reagent stock solution was added to the diluted protein. The solution was shaken (600 rpm) at room temperature for 15 minutes.

Buffer Recipes

TES 5x	TBST
0.1 M Tris-HCl	10 mM Tris-HCl
0.5 mM EDTA	150 mM NaCl
0.5 M sucrose	0.05% Tween

Binding buffer	Elution buffer
50 mM imidazole	1 M imidazole
0.14 M NaCl	0.14 M NaCl
2 mM $MgCl_2$	2 mM $MgCl_2$
50 mM EDTA	50 mM EDTA
20 mM Tris-HCl, pH 8.0	20 mM Tris-HCl, pH 8.0

Transfer buffer	TAE
192 mM glycine	40 mM Tris base
25 mM Tris-HCl, pH 8.3	20 mM acetic acid
1.3 mM SDS	1 mM EDTA
20 % (v/v) methanol	

Denaturing buffer	Refolding buffer
8 M urea	20 mM HEPES
0.2 M sodium phosphate	150 mM NaCl

0.01 M Tris-HCl	3 mM GSH
	0.3 mM GSSG
	1 mM EDTA, pH 7

Binding buffer for purification of mammalian expression	Elution buffer for purification of mammalian expression
50 mM sodium phosphate	50 mM sodium phosphate
300 mM NaCl	300 mM NaCl
10 mM imidazole, pH 8	250 mM imidazole, pH 8

2.6 Chapter 2 References

1. Hamers-Casterman, C., Atarhouch, T., Muyldermans, S., Robinson, G., Hamers, C., Songa, E. B., Bendahman, N., Hamers, R. Naturally occurring antibodies devoid of light chains. *Nature* **363,** 446–448 (1993).

2. Greenberg, A., Avila, D., Hughes, M. A new antigen receptor gene family that undergoes rearrangement and extensive somatic diversification in sharks. *Nature* **374,** 168–173 (1995).

3. Eyer, L., Hruska, K. Single-domain antibody fragments derived from heavy-chain antibodies: a review. *Vet. Med. (Praha).* **57,** 439–513 (2012).

4. Paalanen, M. M. I., Ekokoski, E., El Khattabi, M., Tuominen, R. K., Verrips, C. T., Boonstra, J., Blanchetot, C. The development of activating and inhibiting camelid V_HH domains against human protein kinase C epsilon. *Eur. J. Pharm. Sci.* **42,** 332–339 (2011).

5. Saerens, D., Ghassabeh, G. H., Muyldermans, S. Single-domain antibodies as building blocks for novel therapeutics. *Curr. Opin. Pharmacol.* **8,** 600–608 (2008).

6. Harmsen, M. M., De Haard, H. J. Properties, production, and applications of camelid single-domain antibody fragments. *Appl. Microbiol. Biotechnol.* **77,** 13–22 (2007).

7. van der Linden, R. H. J., Frenken, L. G. J., de Geus, B., Harmsen, M. M., Ruuls, R. C., Stok, W., de Ron, L., Wilson, S., Davis, P., Verrips, C. T. Comparison of physical chemical properties of llama V_HH antibody fragments and mouse monoclonal antibodies. *Biochim. Biophys. Acta - Protein Struct. Mol. Enzymol.* **1431,** 37–46 (1999).

8. Pérez, J. M. J., Renisio, J. G., Prompers, J. J., van Platerink, C. J., Cambillau, C., Darbon, H., Frenken, L. G. J. Thermal Unfolding of a Llama Antibody Fragment: A Two-State Reversible Process. *Biochemistry* **40,** 74–83 (2000).

9. Dumoulin, M., Conrath, K., van Meirhaeghe, A., Meersman, F., Heremans, K., Frenken, L. G. J., Muyldermans, S., Wyns, L., Matagne, A. Single-domain antibody fragments with high conformational stability. *Protein Sci.* **11,** 500–515 (2002).

10. Ewert, S., Cambillau, C., Conrath, K., Plückthun, A. Biophysical Properties of Camelid V_HH Domains Compared to Those of Human V_H3 Domains. *Biochemistry* **41,** 3628–3636 (2002).

11. Vu, K., Ghahroudi, M., Wyns, L., Muyldermans, S. Comparison of llama V_H sequences from conventional and heavy-chain antibodies. *Mol. Immunol.* **34,** 1121–1131 (1997).

12. Ahmadvand, D., Rahbarizadeh, F., Vishteh, V. K. High-expression of monoclonal nanobodies used in the preparation of HRP-conjugated second antibody. *Hybridoma* **27,** 269–276 (2008).

13. Bazl, M. R., Rasaee M. J., Foruzandeh, M., Rahimpour, A., Kiani, J., Rahbarizadeh, F., Alirezapour, B., Mohammadi, M. Production of chimeric recombinant single-domain antibody-green fluorescent fusion protein in Chinese hamster ovary cells. *Hybridoma* **26,** 1–9 (2007).

14. Marks, J. D., Hoogenboom, H. R., Griffiths, A. D., Winter, G. Molecular evolution of proteins on filamentous phage. Mimicking the strategy of the immune system. *J. Biol. Chem.* **267,** 16007–16010 (1992).

15. Borrebaeck, C. A. K. *Antibody engineering : a practical guide*. (Freeman, 1992).

16. Griffiths, A. D. Production of human antibodies using bacteriophage. *Curr. Opin. Immunol.* **5,** 263–267 (1993).

17. Winter, G., Griffiths, A. D., Hawkins, R. E., Hoogenboom, H. R. Making antibodies by phage display technology. *Annu. Rev. Immunol.* **12,** 433–455 (1994).

18. Arbabi Ghahroudi, M., Desmyter, A., Wyns, L., Hamers, R., Muyldermans, S. Selection and identification of single-domain antibody fragments from camel heavy-chain antibodies. *FEBS Lett.* **414,** 521–526 (1997).

19. Tanha, J., Dubuc, G., Hirama, T., Narang, S. A., MacKenzie, C. R. Selection by phage display of llama conventional V_H fragments with heavy-chain antibody V_HH properties. *J. Immunol. Methods* **263,** 97–109 (2002).

20. Rahbarizadeh, F., Rasaee, M. J., Forouzandeh-Moghadam, M., Allameh, A.-A. High expression and purification of the recombinant camelid anti-MUC1 single-domain antibodies in *Escherichia coli*. *Protein Expr. Purif.* **44,** 32–38 (2005).

21. Frenken, L. G. J, van der Linden, R. H. J., Hermans, P. W. J. J., Bos, J. W., Ruuls, R. C., de Geus, B., Verrips, C. T. Isolation of antigen specific Llama V_HH antibody fragments and their high level secretion by *Saccharomyces cerevisiae*. *J. Biotechnol.* **78,** 11–21 (2000).

22. O'Brien, P. M., Aitken, R. *Antibody Phage Display*. **178,** Humana Press, 2001.

23. Thomassen, Y. E., Meijer, W., Sierkstra, L. & Verrips, C. T. Large-scale production of V_HH antibody fragments by *Saccharomyces cerevisiae*. *Enzyme Microb. Technol.* **30,** 273–278 (2002).

24. Rahbarizadeh, F., Rasaee, M. J., Forouzandeh, M., Allameh, A.-A. Over expression of anti-MUC1 single-domain antibody fragments in the yeast *Pichia pastoris*. *Mol. Immunol.* **43,** 426–435 (2006).

25. Sethuraman, N., Stadheim, T. A. Challenges in therapeutic glycoprotein production. *Curr. Opin. Biotechnol.* **17,** 341–346 (2006).

26. Joosten, V., Gouka, R. J., van den Hondel, C. A. M. J. J., Verrips, C. T., Lokman, B. C. Expression and production of llama variable heavy-chain antibody fragments (V_HHs) by *Aspergillus awamori*. *Appl. Microbiol. Biotechnol.* **66,** 384–392 (2005).

27. Korouzhdehy, B., Dadmehr, M., Piri, I., Rahbarizadeh, F. Expression of biological active V_HH camelid single-domain antibody in transgenic tobacco. *African J. Biotechnol.* **10,** 4234–4241 (2011).

28. Conrad, U., Plagmann, I., Malchow, S., Sack, M, Floss, D. M., Kruglov, A. A., Nedospasov, S. A., Rose-John, S, Scheller, J. ELPylated anti-human TNF therapeutic single-domain antibodies for prevention of lethal septic shock. *Plant Biotechnol. J.* **9,** 22–31 (2011).

29. Pollithy, A., Romer, T., Lang, C., Müller, F. D., Helma, J., Leonhardt, H., Rothbauer, U., Schüler, D. Magnetosome expression of functional camelid antibody fragments (nanobodies) in *Magnetospirillum gryphiswaldense*. *Appl. Environ. Microbiol.* **77,** 6165–6171 (2011).

30. Zou, X., Smith, J. A., Nguyen, V. K., Ren, L., Luyten, K., Muyldermans, S., Brüggemann, M. Expression of a dromedary heavy chain-only antibody and B cell development in the mouse. *J. Immunol.* **175,** 3769–3779 (2005).

31. Desmyter, A., Transue, T. R., Ghahroudi, M. A., Ti, M-H, D., Poortmans, F., Hamers, R., Muyldermans, S., Wyns, L. Crystal structure of a camel single-domain VH antibody fragment in complex with lysozyme. *Nat. Struct. Biol.* **3,** 803–811 (1996).

32. Decanniere, K., Transue, T. R., Desmyter, A., Maes, D., Muyldermans, S., Wyns, L. Degenerate interfaces in antigen-antibody complexes. *J. Mol. Biol.* **313,** 473–478 (2001).

33. Hoogenboom, H. R., Griffiths, A. D., Johnson, K. S., Chiswell, D. J., Hudson, P., Winter, G. Multi-subunit proteins on the surface of filamentous phage: methodologies for displaying antibody (Fab) heavy and light chains. *Nucleic Acids Res.* **19,** 4133–4137 (1991).

34. Skerra, A., Pluckthun, A. Assembly of a functional immunoglobulin Fv fragment in *Escherichia coli. Science* **240,** 1038–1041 (1988).

35. Teh, Y.-H. A., Kavanagh, T. A High-level expression of Camelid nanobodies in *Nicotiana benthamiana. Transgenic Res.* **19,** 575–586 (2010).

36. Transue, T. R., De Genst, E., Ghahroudi, M. A, Wyns, L., Muyldermans, S. Camel single-domain antibody inhibits enzyme by mimicking carbohydrate substrate. *Proteins* **32,** 515–522 (1998).

37. Cortez-Retamozo, V., Lauwereys, M., Hassanzadeh, G., Gobert, M., Conrath, K., Muyldermans, S., De Baetselier, P., Revets, H. Efficient tumor targeting by single-domain antibody fragments of camels. *Int. J. Cancer* **98,** 456–462 (2002).

38. Dejaegere, A., Choulier, L., Lafont, V., De Genst, E., Altschuh, D. Variations in antigen-antibody association kinetics as a function of pH and salt concentration: a QSAR and molecular modeling study. *Biochemistry* **44,** 14409–14418 (2005).

39. Freyhult, E. K., Andersson, K., Gustafsson, M. G. Structural modeling extends QSAR analysis of antibody-lysozyme interactions to 3D-QSAR. *Biophys. J.* **84,** 2264–2272 (2003).

40. De Genst, E., Handelberg, F., Van Meirhaeghe, A., Vynck, S., Loris, R., Wyns, L., Muyldermans, S. Chemical basis for the affinity maturation of a camel single-domain antibody. *J. Biol. Chem.* **279,** 53593–53601 (2004).

41. Chalker, J. M., Bernardes, G. J. L., Lin, Y. A., Davis, B. G. Chemical modification of proteins at cysteine: opportunities in chemistry and biology. *Chem. Asian J.* **4,** 630–640 (2009).

42. Rudolph, R., Lilie, H. *In vitro* folding of inclusion body proteins. *FASEB J* **10,** 49–56 (1996).

43. Gribskov, M., Burgess, R. R. Overexpression and purification of the sigma subunit of *Escherichia coli* RNA polymerase. *Gene* **26,** 109–118 (1983).

44. French, A. C. Site-selective chemical modification of antibodies. *DPhil Thesis*, University of Oxford (2009).

45. Meng, F., Park, Y., Zhou, H. Role of proline, glycerol, and heparin as protein folding aids during refolding of rabbit muscle creatine kinase. *Int. J. Biochem. Cell Biol.* **33,** 701–709 (2001).

46. Buchner, J., Rudolph, R. Renaturation, Purification and Characterization of Recombinant Fab Fragments Produced in *Escherichia coli. Bio/Technology* **9,** 157–162 (1991).

47. Chalker, J. M., Gunnoo, S. B., Boutureira, O., Gerstberger, S. C., Fernandez-Gonzalez, M., Bernades, G. J. L., Griffin, L., Hailu, H., Schofield, C. J., Davis, B. G. Methods for converting cysteine to dehydroalanine on peptides and proteins. *Chem. Sci.* **2,** 1666-1676 (2011).

48. Gadgil, H. S., Bondarenko, P. V., Pipes, G. D., Dillon, T. M., Banks, D., Abel, J, Kleeman, G. R., Treuheit, M. J. Identification of cysteinylation of a free cysteine in the Fab region of a recombinant monoclonal IgG1 antibody using Lys-C limited proteolysis coupled with LC/MS analysis. *Anal. Biochem.* **355,** 165–174 (2006).

49. Miao, Z., McCoy, M., Singh, D. Cysteinylated protein as reactive disulfide: an alternative route to affinity labeling. *Bioconjugate Chem.* **19,** 15–19 (2007).

50. Veggiani, G., de Marco, A. Improved quantitative and qualitative production of single-domain intrabodies mediated by the co-expression of Erv1p sulfhydryl oxidase. *Protein Expr. Purif.* **79,** 111–114 (2011).

Chapter 3: Towards Demonstrating the 'Chemical Affinity Maturation' of cAb-Lys3

'It is clear that the introduction of a double bond at the active site allows the possibility for the preparation of new types of derivatives...'

Strumeyer, White and Koshland, 1963.

3.1 Introduction

3.1.1 Dehydroalanine

Natural occurrence of dehydroalanine

Dehydroalanine (Dha) is a naturally occurring, although uncommon, 2,3-unsaturated amino acid. It is found in lantibiotics – lanthionine-containing antibiotics – which are polypeptides comprising 19 – 38 amino acids that undergo extensive post-translational modification (PTM) during production by Gram-positive bacteria, giving rise to a wealth of unusual amino acids.[1–3] Lantibiotics are produced as gene-encoded precursor peptides, and then a wide range of PTMs generate the active antimicrobial moieties. For example, serine undergoes enzymatic dehydration to give Dha, and then stereoselective intramolecular addition of a proximate cysteine to Dha forms a thioether-linked bridge, the core of the lanthionine structure (**Scheme 3.1**). This modification is present in Nisin, discovered in 1928,[4] and to date the most widely studied lantibiotic. In another lantibiotic, lactocin S, Dha formed after dehydrogenation of serine is reported to undergo stereospecific hydrogenation to alanine.[5]

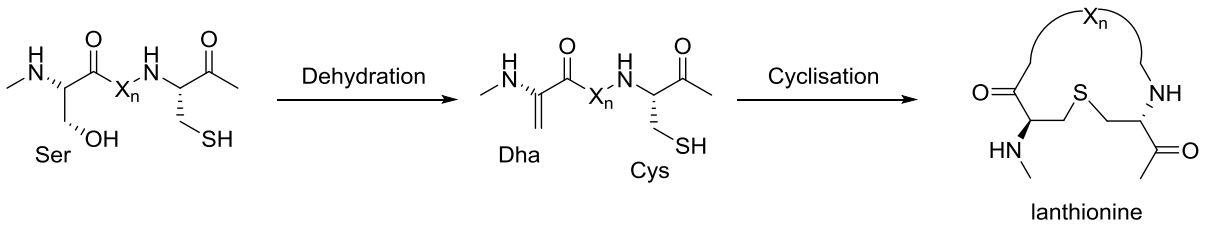

Scheme 3.1. Formation of the lanthionine (thioether linkage) within a lantibiotic.

Dha also occurs in proteins – for instance, tyrosine is converted to Dha in thyroglobulin during thyroid hormone biosynthesis (**Scheme 3.2**).[6,7]

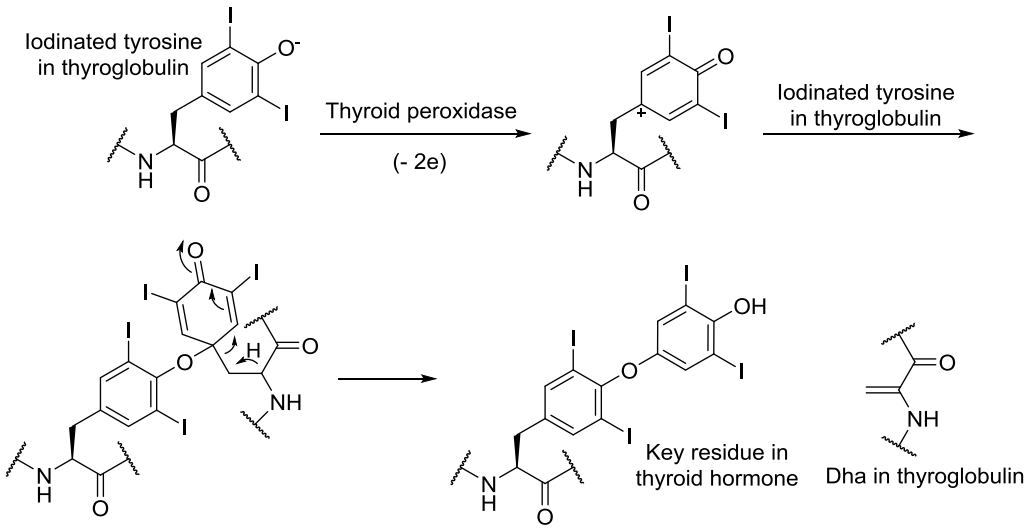

Scheme 3.2. Mechanism for the formation of Dha within the thyroglobulin.

Previous reports on the chemical installation of dehydroalanine into proteins

In 1966, seminal work by both the Bender and Koshland laboratories demonstrated the use and potential of converting one amino acid residue to another in a protein using site-selective chemical modification (**Scheme 3.3**).[8,9] They both reacted phenylmethanesulfonyl fluoride (PMSF) with a serine in the active site of subtilisin, which could then undergo displacement with a thioacetate ion to give cysteine. Nowadays, mutagenesis to the twenty naturally occurring amino acids can be carried out routinely at a genetic level, but the pioneering work

was key in showing the potential of site-selective chemical modification in the elucidation and manipulation of protein function.

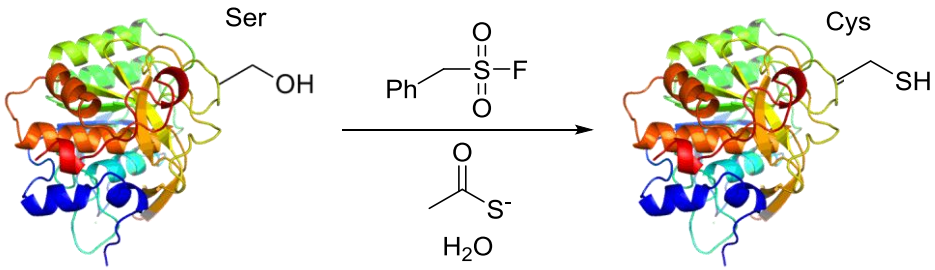

Scheme 3.3. Site-selective conversion of serine in the active site of subtilisin to cysteine.

Earlier than this, Koshland reported the first example of the introduction of Dha in the protease chymotrypsin.[10] The site of modification was at the active site serine, which was believed to be a key nucleophilic residue for enzyme catalysis, despite the substrates being hydroxylic, and therefore harbouring the same reactivity. By converting the serine only to Dha, they wanted to see if they still had an active enzyme – or if the loss of nucleophilicity at this site resulted in a loss of activity. Sure enough, the anhydro chymotrypsin was inactive. Their method was based on previous observations by Photaki, who had converted serine to Dha on an amino acid level by tosylation and subsequent treatment with base to drive β-elimination,[11] and also work by Fahrney, who had used PMSF before elimination.[12] The Koshland lab reacted chymotrypsin with ^{14}C-labelled PMSF, and then drove the β-elimination using a high pH (**Scheme 3.4**). Site-selectivity could be achieved as the protein contained only one serine. The reaction was monitored by measuring the increase (on sulfonyl bond formation), then decrease (on elimination) in radioactivity.[10]

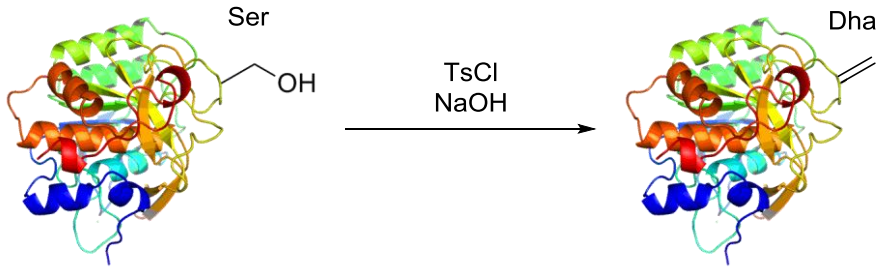

Scheme 3.4. Site-selective conversion of serine to Dha in chymotrypsin.

Koshland's work was pioneering in demonstrating the potential and applicability in introducing non-natural amino acids at key residues in proteins. In their publication, they stated that 'it is clear that the introduction of a double bond at the active site allows the possibility for the preparation of new types of derivatives', and it is the application of this principle to an antibody that forms the basis for the work described in this thesis. They recognised that any changes at an active site of a protein need to cause minimal disruption, as the activity of key residues may be more sensitive to changes. However, their method relies on a high pH for elimination, and also a unique serine residue – making it less likely to be generally applicable to a wide range of proteins.

In 1977, Lawton also described the introduction of Dha into a protein, with the aim of mapping cysteine residues. He therefore used cysteine as a precursor, and the Cyssor reagent (2-Methyl-N^1-benzenesulfonyl-N^4-(bromoacetyl)quinonediimide).[13] Following the formation of a labile sulfonium ion after dialkylation of cysteine with Cyssor reagent, elimination led to Dha (**Scheme 3.5a**). Dha was then hydrolysed by heating with acetic acid, and the fragments obtained after this chemical digest analysed. The use of an insoluble reagent makes it difficult to apply to proteins, as buffered aqueous media is preferred to prevent protein precipitation. Similarly and more recently, Okamoto and co-workers observed the formation of Dha during their synthesis of complex glycopeptides.[14] They saw a cyclised intermediate resulting from alkylation of cysteine during reaction with a diethyl ester of *meso*-2,5-dibromoadipic acid,

and then elimination to give Dha (**Scheme 3.5b**). Alternatively, the lab of van der Donk have recently undertaken an enzymatic route to Dha, taking inspiration from lantibiotic formation in nature.[1] Here, they phosphorylated a serine residue using the enzyme LctM, which also catalysed subsequent elimination to Dha (**Scheme 3.5c**).[3,15] Although the work was elegant, the peptides require a leader sequence to be susceptible to conversion.

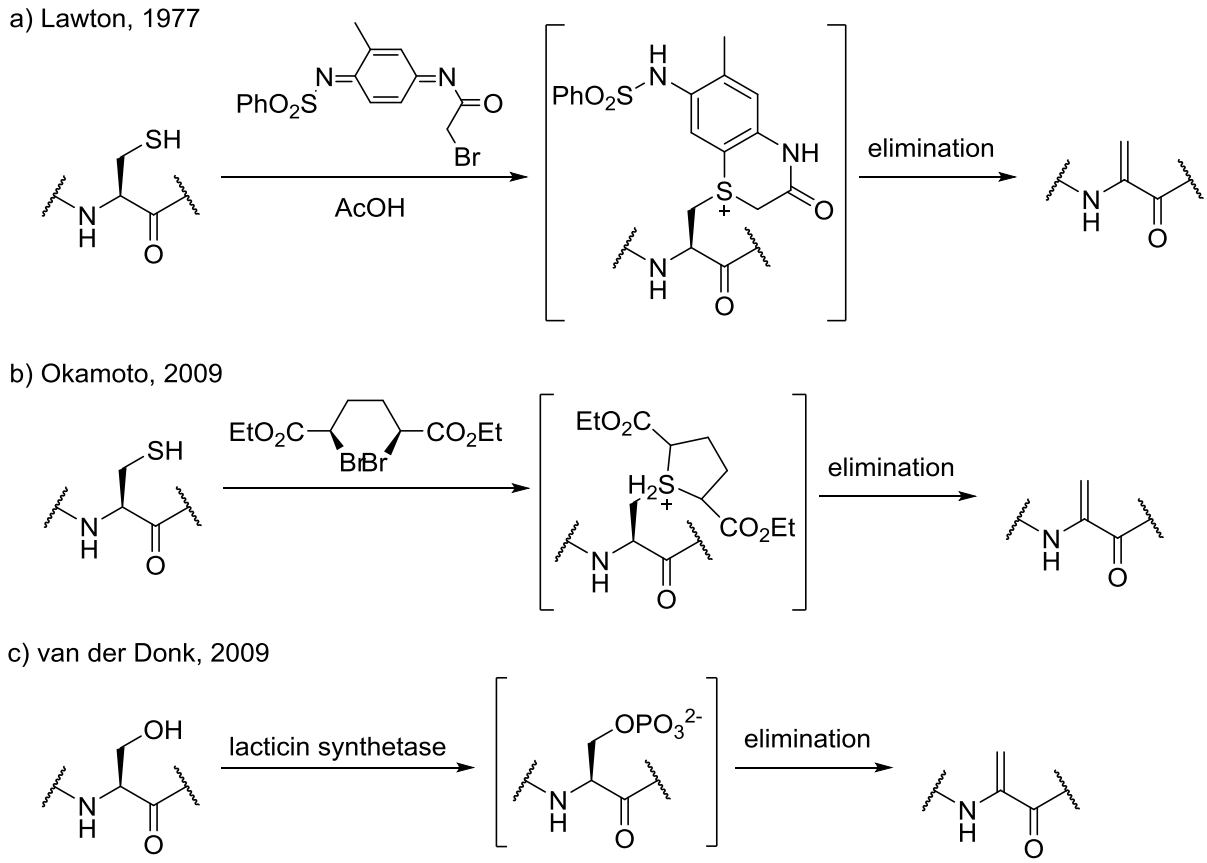

Figure 3.5. Previous routes to Dha.[13–15]

Extensive studies into establishing a general method for the chemical incorporation of dehydroalanine into proteins using cysteine as a precursor have been carried out in our group.[16,17] Two methods that have been attempted with cAb-Lys3-Cys104 are oxidative elimination and bis-alkylation-elimination. Oxidative elimination methods require harsh conditions incompatible with many proteins. In Mabuni's report, the elimination of alkyl cysteine sulfoxide occurs after refluxing in xylene.[18] Somewhat milder conditions were

applied in our group on a single cysteine mutant of the protease SBL-S156C (SBL – Subtilisin *Bacillus Lentus*). Here, a sulfinimine (the nitrogen analogue of sulfoxides), Tamura's reagent, *O*-mesitylenesulfonylhydroxylamine (MSH, **3.1**) acted as an electrophilic N source. The inspiration for applying this method for converting cysteine to Dha was based on Matsu's observation that syn-elimination following formation of the phenyl sulfide could be driven at low temperatures in water,[19] conditions much more compatible with proteins. Although selectivity was observed for reaction on SBL-S156C,[20] MSH is a common oxidising and aminating agent,[20] which decreased the method's potential to be generally applicable to other proteins. The alternative bis-alkylation-elimination method developed on SBL-S156C, uses a more soluble form of the reagents used by Lawton and later Okamoto,[13,14] and therefore may be more general. In addition, the use of cysteine as a precursor is desirable when considering application of a general method to multiple proteins as its natural occurrence is low,[21] it is uniquely reactive in comparison to other proteinogenic amino acids and installation using standard mutagenesis techniques is facile.

Mimicking post-translational modifications using dehydroalanine as a precursor

A myriad of PTMs are present in proteins, and vital to mediating multiple essential processes.[22] In particular, histones, proteins which bind to DNA in chromatin, undergo a wide range of PTMs, which are necessary for regulating chromatin structure and transcription and DNA replication and repair. These include lysine methylation, acetylation, ubiquitination, succinylation, serine and threonine phosphorylation and glycosylation, arginine methylation and deamination as well as many more.[23] The study of these diverse PTMs are imperative to gaining understanding of histone behaviour,[24,25] and synthetic routes towards producing proteins bearing these modifications (and effective mimics) contributes to achieving this.[23] In our group, the incorporation of Dha at a single site in a histone protein (H3) was able to act as

a precursor for the addition of a range of thiol nucleophiles, forming PTM mimics recognisable by primary antibodies specific to native PTMs (**Scheme 3.6**).[23]

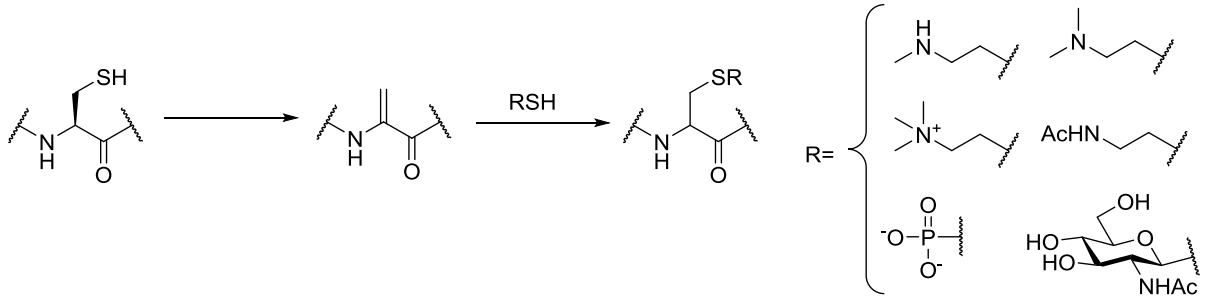

Scheme 3.6. Chemical route to PTM mimics via dehydroalanine on H3.[23]

This work addressed the issue that on forming Dha, a conjugate addition is likely to comprise an epimeric mixture, a feature uncommon in nature. Davis and co-workers demonstrated that this result does not exclude the possibility for further transformation at Dha, as natural function is retained to a degree high enough for successful mimicry. The successful processing of a potentially epimeric phosphorylation mimic is described in Chapter 4. In this chapter however, the addition of thiol nucleophiles to dehydroalanine in cAb-Lys3 is described as a potential method for the introduction of non-natural amino acids for increasing antibody affinities.

For the purposes of site-selective chemical modification of proteins, Dha is invaluable as a synthetic precursor, acting as a unique electrophilic centre. The nucleophilic addition of thiols can lead to *S*-linked PTM mimics,[23,26] and numerous non-natural amino acids. Extending the 'toolkit' of possible transformations on Dha are desirable and preliminary investigations into the development of reactions forming other linkages such as carbon-carbon bond formations have been carried out.[17] The introduction of non-natural amino acids to the CDR3 loop of the sdAb cAb-Lys3 via Dha using two methods are described in this chapter.

3.1.2 Carbon-carbon bond formation in aqueous media and proteins, and the use of transition metals

The ability to form carbon-carbon bonds forms the essence of organic synthesis, and in particular, mediating these transformations in aqueous media has received much attention.[27,28] Organic reactions in aqueous media are of importance to those interested in Green Chemistry for environmental and economic reasons.[29] Practically, the use of water is safer and simpler than working with flammable anhydrous organic solvents, and the number of steps in a synthetic route may be reduced as the need for protection and deprotection steps is less for acidic-hydrogen-containing species. In addition, reactions developed in the absence of organic solvent may be applicable to proteins – where in many cases, protein stability in solution is compromised by the presence of organic solvent. Furthermore, application to *in vitro* and *in vivo* settings may be problematic if an organic solvent is required.

Transition metal-catalysed methods for covalent protein modification

Metal-mediated transformations in aqueous media have been explored on small molecule substrates extensively.[27,28] As well as the advantage of transformations proceeding in the absence of organic solvent, they can occur under mild conditions and with excellent functional group tolerance,[30] thus potentially with the preservation of the structure and function of the protein. The use of transition metal complexes on proteins have been used to carry out covalent protein modifications in a site-selective manner, predominantly targeting aromatic residues.[30] For example, Kodadek and others have reported the use of high valent transition metal complexes for oxidative protein cross-linking initiated by the extraction of a single electron from the aromatic ring of tyrosine, and subsequent coupling to proximate functionality.[31] Francis has demonstrated the use of rhodium carbenoids for labelling the indole functionality of tryptophan,[32] and a π-allyl palladium complex to functionalise tyrosine

residues.[33] Although the methodologies developed are impressive and demonstrate the compatibility of metals with proteins, in the examples mentioned above and others,[30] endogenous amino acid residues are targeted, and thus site-selectivity but not specificity is achieved.[34] In protein modification strategies, the use of non-natural amino acids allows modification at a single site, and coupling with transition metal catalysis has and continues to lead to the development of methodology applicable in a general sense. The use of non-natural amino acids for modification targeting single sites potentially allows specific labelling in complex environments, such as in crude cell lysate and on the surface of living cells.

Transition metal-catalysed chemical modification of proteins via non-natural amino acids forming carbon-carbon bonds

Transition metals are known to catalyse couplings between otherwise unreactive functional groups, making them attractive targets for site-specific protein modifications.[30] Palladium-catalysed cross couplings, in particular the Suzuki-Miyaura method in which an aryl halide is activated by a boronic acid or ester, forming an organometallic intermediate that can react selectively with a functional group on the desired coupling partner has been used extensively in our group for site-specific protein labelling.[35] Here, the non-natural and orthogonally reactive amino acid *p*-iodophenylalanine was genetically incorporated into maltose binding protein (MBP) using the stop codon suppression method,[36] and could be selectively reacted with furan-3-boronic acid using a water soluble palladium catalyst.[35] The methodology has also been used to couple a monodisperse polyethylene glycol (PEG) boronic acid moiety to a protein bearing a genetically encoding *p*-iodophenylalanine residue,[37] for selective cell-surface labelling with fluorescent boronic acids,[38] and for the generation of synthetic *O*-glycosylation mimics on cell surfaces.[39] Another method for carbon-carbon bond formation is olefin metathesis catalysed by the ruthenium-based Grubb's catalyst.[40] Again, the orthogonality of the reaction components allows the application to proteins for modification

in a site-specific manner. In our group, proteins have been labelled with a range of functional groups using olefin cross-metathesis via a chemically installed *S*-allyl cysteine residue.[41–45] Alam and co-workers reported the use of indium in protein modification.[46] They functionalised an N-terminal aldehyde of horse heart myoglobin (introduced using the method of Scheck and Francis, **Figure 1.7, Chapter 1**[47]) with allyl bromide in the presence of indium, and state that the terminal olefin moiety introduced can be used for further modification, for example by metathesis.[40]

Zinc-mediated additions to α,β-unsaturated compounds

Zinc (Zn), and a wealth of organozinc reagents are known to show a high tolerance to many functional groups[48] and are of the utmost importance in catalysing and mediating many organic transformations.[49] The Zn-mediated radical addition of saturated alkyl iodides to α,β-unsaturated carbonyl compounds is one example. This Barbier-type reaction was first pioneered by Luche in 1986.[50] Before this, Luche and co-workers demonstrated the allylation of aldehydes or ketones using tin or zinc (**Scheme 3.7a**).[51,52] In these studies, they found that carrying out the allylation in saturated aqueous ammonium chloride (sat. aq. NH_4Cl) enhanced the rate of reaction, thus supporting the hypothesis that ammonium ions activate zinc. For the corresponding alkylation with non-activated alkyl halides, the reaction did not proceed unless a metal was present – this may be due to the high ionisation potential of the halides, meaning that the transfer of electrons from the zinc is required. A zinc-copper couple was used to mediate the conjugate 1,4-addition of alkyl halides (iodides and bromides), where copper is reported to activate zinc.[50] In addition, the use of sonication was found to greatly enhance the rate of reaction (**Scheme 3.7b**).[53] The reaction is believed to proceed via a free radical mechanism on the metal surface, whereby there is a single electron transfer from the metal to the halide, followed by addition of the alkyl group to the unsaturated system, and finally work up in aqueous media (**Scheme 3.7c**). This mechanism has since not

been disputed. Roth and co-workers have previously explored the diastereoselectivity of the reaction,[54] and some groups more recently have carried out alkylations on amino acid systems.[48,55,56]

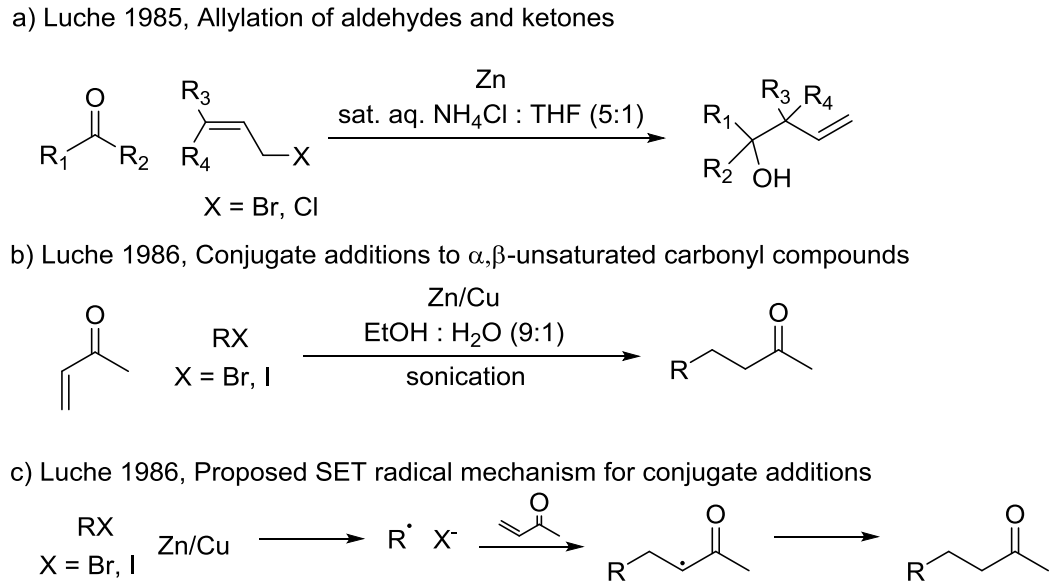

Scheme 3.7. Zn-mediated allylations and conjugate additions pioneered by Luche and co-workers.[50,57,58]

In 2002, Huang and co-workers described the conjugate addition of short chain alkyl groups to electron deficient α-phthalimidoacrylate derivatives mediated by zinc in sat. aq. NH_4Cl to form α-amino acid derivatives (**Scheme 3.8a**). They found water was essential for the reaction, and enhanced when sat. aq. NH_4Cl was used.[55] Since Luche's initial report,[50] little had been reported on the activation of C-X bonds of alkyl halides in water due to the instability of the resulting alkyl organometallic reagents in aqueous environments. Also, the Zn-mediated carbon radical addition to glyoxylic imines and hydrazones was described under very similar conditions (**Scheme 3.8b**).[48,56] The camphorsultam group was used as a chiral auxiliary to allow the disastereoselective synthesis of amino acid derivatives.

a) Huang 2002, Conjugate addition of alkyl halides to α-phthalimidoacrylate derivatives

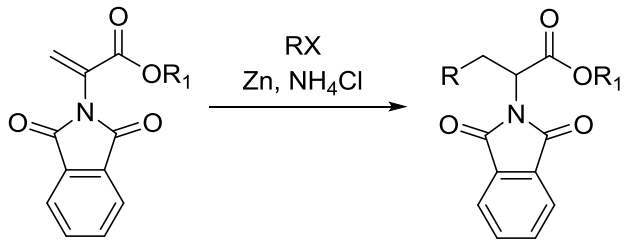

b) Naito 2003, Conjugate additions of 2-PrI to a glyoxylic oxime ether

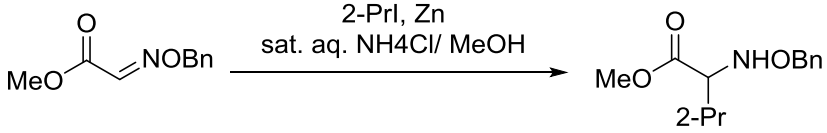

Scheme 3.8. Application of Zn-mediated alkylations on amino acid derivatives.[48,55]

To date, there is no application of this reaction using zinc to non-functionalised amino acids (and proteins). Previously, it was thought that if the conjugate addition could be carried on a single Dha residue (α,β-unsaturated carbonyl system), it may be possible in a protein. Dha provides a suitable site for conjugate additions, the utility of which has been demonstrated with thiol nucleophiles.[16,23] Previously, the Zn-mediated alkylation has been found to be successful with a range of iodide substrates on an amino acid level using AcDhaOMe (**Scheme 3.9**).[17]

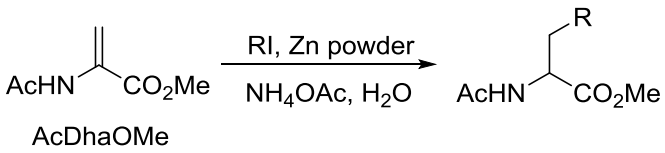

Scheme 3.9. Zn-mediated addition of alkyl iodides to dehydroalanine.

The reactions were highly exothermic, and the only side reaction observed was the reduction of the radical intermediate before alkylation could take place. The methodology has also been applied to the protein SBL-156Dha. The Zn-mediated alkylation of Dha was possible using a range of iodide substrates, forming natural and non-natural residues, natural PTMs and several homologues. The methodology is not without limitations however. The conversion

was found to be unsuccessful with aromatic iodides, probably due to the high energy required to generate an aryl radical. Conversion to glutamic acid and glutamine using iodoacetic acid and iodoacetamide respectively was also unsuccessful. It was hypothesised this may have been due to the substrates being reduced to the corresponding enolates and being quenched by protonation at a rate faster than radical formation. Furthermore, with SBL and a histone protein, it appeared that hydrolysis at Dha is a competing reaction during the exothermic modification.[17]

The crystal structure of cAb-Lys3 in complex with lysozyme reveals that alanine at position 104 at the tip of the CDR3 loop points towards a tryptophan within the active site of lysozyme (**Figure 3.1**).[59]

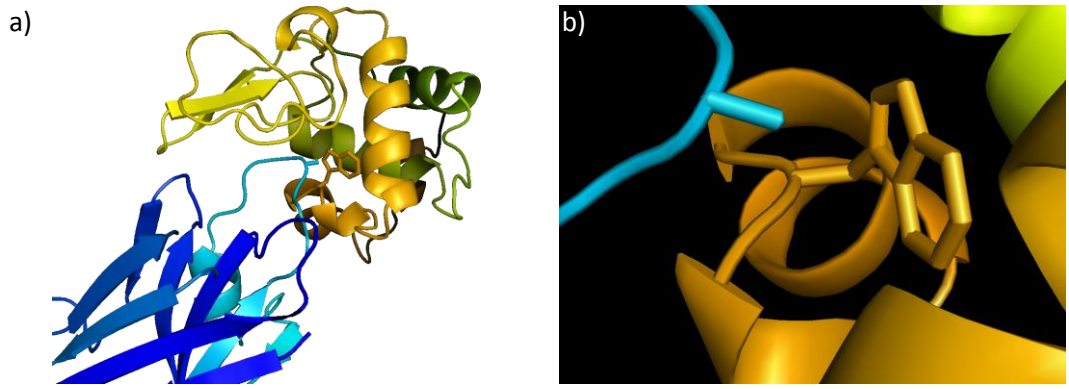

Figure 3.1. a) cAb-Lys3 (blue) in complex with lysozyme (yellow),[59] b) zoom showing cAb-Lys3-Ala104 pointing towards Trp (lysozyme). pdb 1mel.

In the previous chapter, it was shown that this site is pivotal in binding, as the mutation of alanine 104 to cysteine resulted in a decrease in binding from nanomolar affinity to micromolar affinity. It was hypothesised that if Dha could be installed at position 104 of cAb-Lys3 via the mutant precursor cAb-Lys3-Cys104, further reaction by zinc-mediated alkylation with short chain alkyl iodides (or the conjugate addition of short chain alkyl thiols) may allow the modulation of function (binding to antigen) by decreasing the space and increasing hydrophobic character between cAb-Lys3 position 104 and lysozyme tryptophan,

thus creating a more potent antibody. This site-specific chemically-mediated conversion to a non-natural amino acid would demonstrate the concept of a chemical mutation,[17,60] and if successful at increasing the binding affinity of cAb-Lys3, the concept of 'Chemical Affinity Maturation'. Affinity maturation *in vivo* is a complex process by which B-cells produce antibodies with increasing binding affinities following the primary immune response. After the primary immune response, there is an enhanced occurrence of point mutations in the immunoglobulin variable region V genes, which proceed by somatic hypermutation (SHM).[61] Affinity maturation can be mimicked *in vitro*, for example by phage display methods,[62] and has previously been carried out on cAb-Lys3, with the aim of creating an antibody with the highest possible binding affinity.[63] In the work described here, we aimed not to mimic the process, but to develop an alternative chemical approach to increasing the binding affinity of an antibody by the introduction of non-natural functionality at a specific site within cAb-Lys3.

In this chapter, the first examples of site-specific chemical modifications on an sdAb cAb-Lys3 are described. Initially, Dha was installed at position 104 of cAb-Lys3.[16] To our knowledge, this is the first example of the installation of a non-natural amino acid into the binding region of an antibody since photoaffinity labelling studies carried out in the 1970s (**Section 1.3.4, Chapter 1**). The reactivity of Dha in cAb-Lys3 was subsequently tested with a range of short chain alkyl thiols. Conjugate additions were found to be chemically successful, but unfortunately resulted in a loss of antibody function. The Zn-mediated addition of short chain alkyl iodides was then attempted on cAb-Lys3-Dha104. Although some promising results were obtained, overall, cAb-Lys3 was found to be unstable to the necessary reaction conditions, and a reproducible method for the Zn-mediated alkylation of Dha in cAb-Lys3 could not be developed.

3.2 Results

3.2.1 Site-specific chemical installation of dehydroalanine into cAb-Lys3

As described in **Section 2.2.1, Chapter 2**, mutagenesis was carried out to introduce cysteine at position 104 for the site of modification. Single reactivity at position 104 was tested by proteolytic digest and subsequent LC-MS/MS analysis, and reaction with Ellman's reagent to eliminate the possibility that the native disulfide bonds were capable of reacting.

Reactions with MSH 3.1

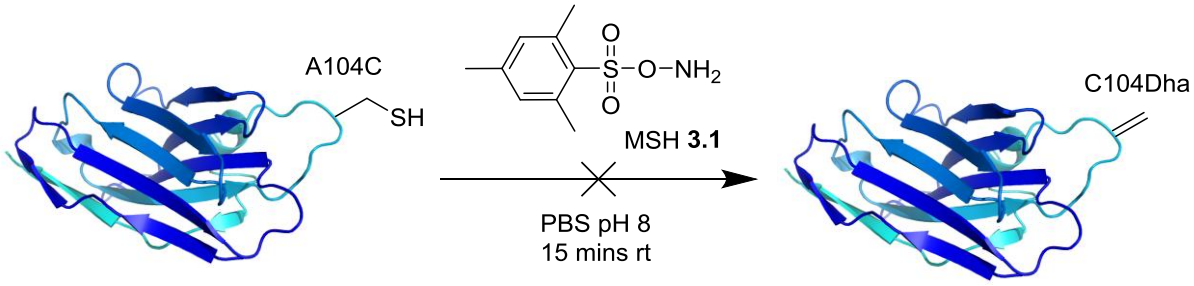

Scheme 3.10. Treatment of cAb-Lys3-Cys104 with **3.1**.

Initially, cAb-Lys3-Cys104 was treated with *O*-mesitylenesulfonylhydroxylamine (**3.1**, MSH), used previously for the site-selective oxidative elimination of cysteine to Dha in SBL-S156C.[20] The reaction was attempted in phosphate buffered saline (PBS) buffer at pH 8 to allow elimination (**Scheme 3.10**). However, the treatment of cAb-Lys3-Cys104 with just 10 eq. **3.1** led to unclean MS with unidentifiable peaks (**Experimental Figure 3.1**).

Whilst **3.1** proved to be a suitable selective reagent for the conversion of cysteine to Dha on SBL-S156C, it is important to consider that it is a highly reactive oxidising and aminating agent.[64,65] A further study into chemical methods to form Dha revealed that MSH is capable of aminating methionine, aspartate, glutamate and histidine residues (**Scheme 3.11**).[16] Although these conversions are reversible in the presence of reducing agent at higher pHs

(but not for histidine), it is not desirable to have any side reactions taking place during site-selective protein modifications. Furthermore, in this study MSH was found to deaminate and reduce lysine and N-terminal residues, which although sounds counterintuitive, a mechanism may be suggested. Initial amination of the ε-amino group of lysine results in a hydrazine, before further oxidation to the mono-substituted diimide and the ultimate loss of nitrogen (**Scheme 3.11**).[66] A similar 'hydrodeamination'[67] was observed with hydroxylamine-*O*-sulfonic acid.[68] Considering the wealth of side reactions possible when treating proteins with MSH, Dha formation via the alternative bis-alkylation-elimination route was explored.

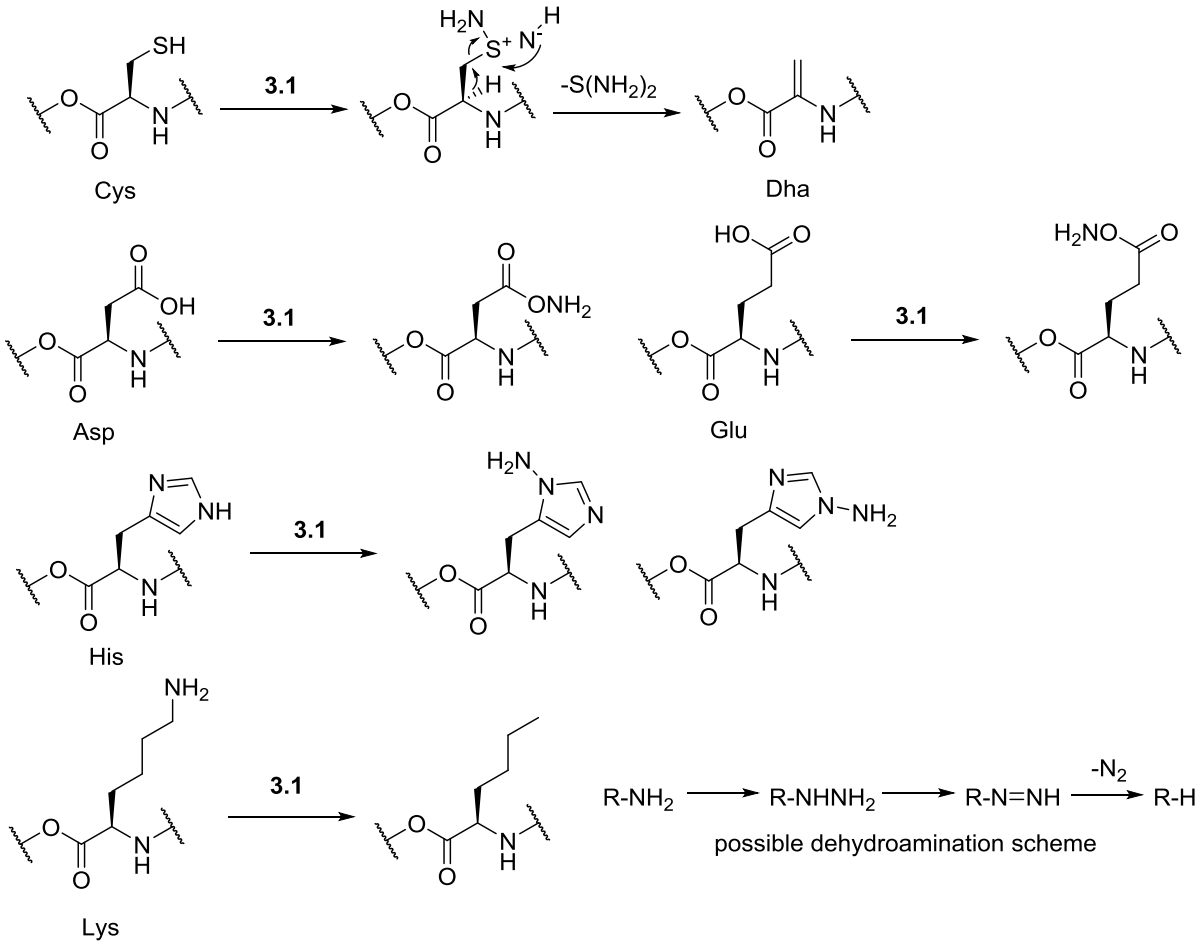

Scheme 3.11. Oxidation elimination mechanism for the conversion of cysteine to dehydroalanine. Possible amination reactions at aspartate, glutamate and histidine side chains. Deamination of lysine and possible sequence.

Reactions with 1,4-diiodobutane 3.2

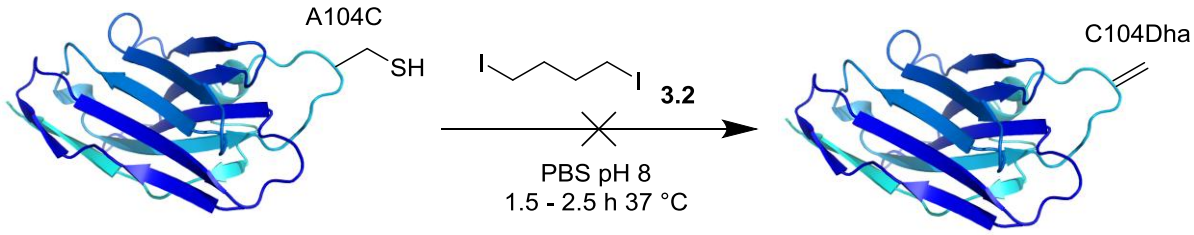

Scheme 3.12. Treatment of cAb-Lys3-Cys104 with reagent **3.2**.

The insoluble 1,4-diiodobutane **3.2** was dissolved in a small volume of organic solvent, and then added to cAb-Lys3-Cys104. A number of attempts were made to drive the formation of Dha forwards such as varying organic co-solvents and amounts (DMF, DMSO, 0 – 17 %) and incubation times (> 1 hour). Unfortunately, in all attempts only starting material was identified by analysis by LC-MS (selected conditions shown in **Table 3.1**). It was decided to proceed with the partially soluble bisamide derivative of 1,4-dibromobutane **3.3**.

Entry	3.2/ μL	DMF/ μL (%)	Observations by MS
1	3	0 (0)	s.m. at 2 hours.
2	3	10 (9)	s.m. at 2 hours.
3	3	10 DMSO (9)	s.m. at 2 hours.

Table 3.1. Reaction conditions for cAb-Lys3-Cys104 with **3.2**. In each condition, 100 μL cAb-Lys3-Cys104 (3.2 nmol, 0.5 mg/mL) was used. Reactions were incubated at 37 °C. s.m. – starting material.

Reactions with dibromo reagent 3.3

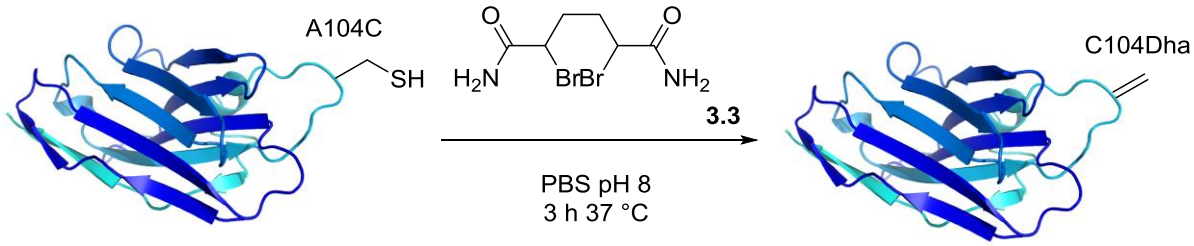

Scheme 3.13. Treatment of cAb-Lys3-Cys104 with **3.3** forming cAb-Lys3-Dha104.

Dibromo reagent **3.3** is structurally similar to 1,4-diiodobutane but partially soluble probably due to the introduction of two terminal amide groups. **3.3** was solubilised in DMF, and a

portion corresponding to 2,000 eq. added to cAb-Lys3-Cys104. After 30 minutes at room temperature, a mass corresponding to the intermediate shown in **Scheme 3.14** could be seen (**Figure 3.2**), and continued incubation at 37 °C for 2 hours resulted in complete consumption of starting material and intermediate (**Figure 3.3**).

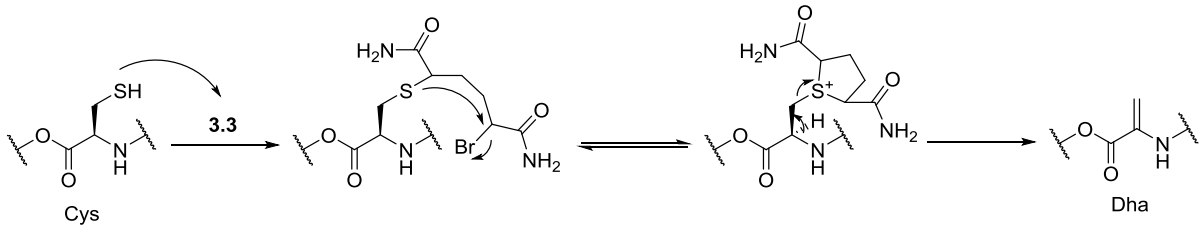

Scheme 3.14. Bis-alkylation elimination mechanism for the conversion of Cys to Dha with reagent **3.3**.

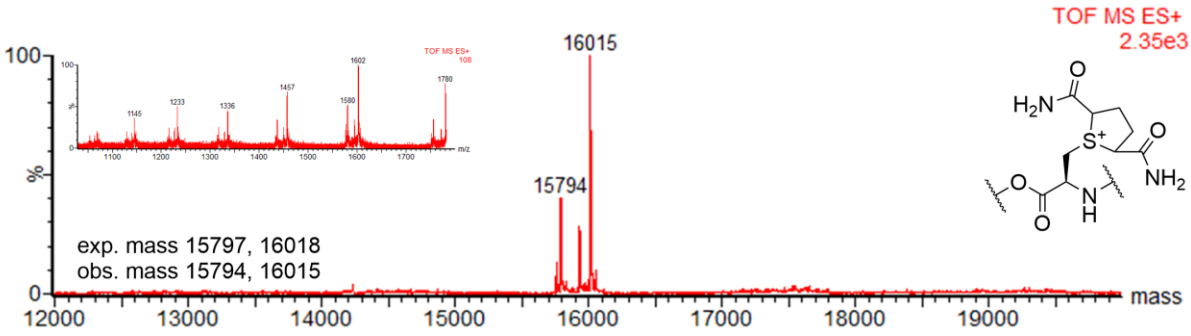

Figure 3.2. MS at 30 minutes of cAb-Lys3-Cys104 incubation with reagent **3.3**.

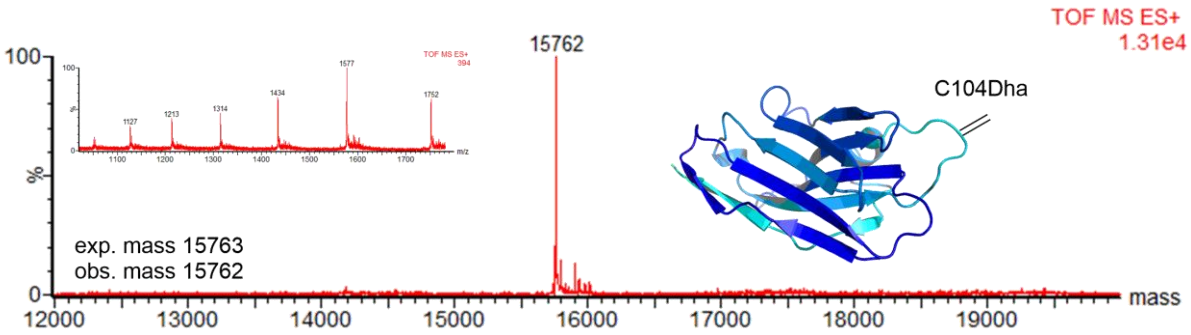

Figure 3.3. cAb-Lys3-Dha104 formation after 2 hours at 37 °C (following room temperature incubation for 30 minutes, **Figure 3.2**).

In the interest of keeping all chemical protein modification steps as ambient as possible, and as a large excess of reagent **3.3** was used in the first instance, a mass corresponding to 100 eq.

of reagent **3.3** was added to cAb-Lys3-Cys104 in the absence of any organic co-solvent. It could be seen that the reagent was only partially soluble. Gratifyingly after 3 hours at 37 °C, full conversion to cAb-Lys3-Dha104 was seen (**Figure 3.4**). cAb-Lys3-Dha104 can be made reliably and routinely using this method with no organic co-solvent with no evidence of side reactions at any other residues than cysteine.

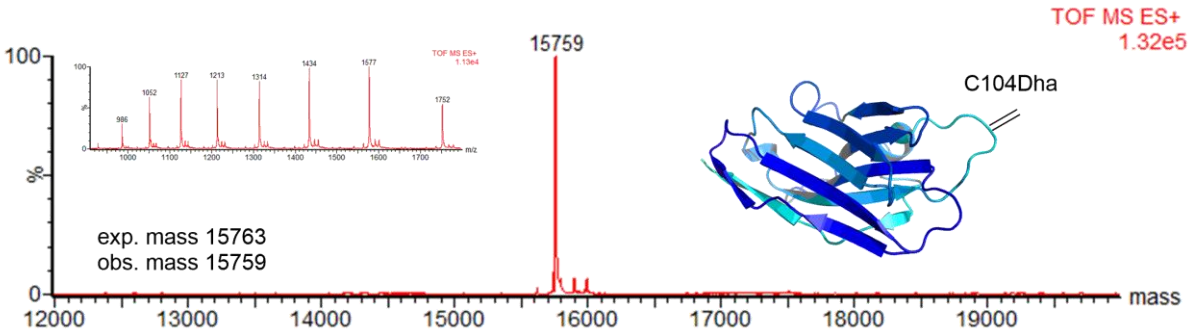

Figure 3.4. The formation of cAb-Lys3-Dha104 after 3 hours at 37 °C in the absence of organic co-solvent.

To ensure that position 104 was the site of modification, cAb-Lys3-Dha104 was subjected to enzymatic digest by Asp-N and subsequent LC-MS/MS analysis. Only position 104 was found to be modified (**Experimental Figure 3.2**). The reactivity of Dha at position 104 of cAb-Lys3 was tested chemically by reaction with β-mercaptoethanol (**Scheme 3.15**). After 1 hour at 37 °C, full conversion to the thioether linked cAb-Lys3 was seen (**Figure 3.5**). As a further control, WT-cAb-Lys3 was also reduced with DTT, reacted with **3.3** and then β-mercaptoethanol (**Scheme 3.16**). At all steps, no increase in mass corresponding to any reaction was seen (**Figure 3.6**), and no decrease in ion count was detected. This implies that structurally, cAb-Lys3 is stable to reaction conditions.

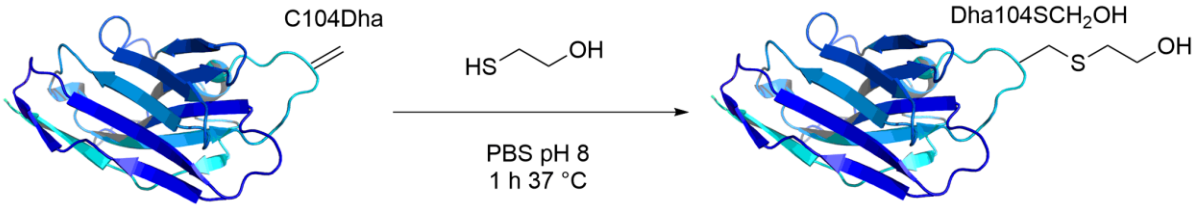

Scheme 3.15. Treatment of cAb-Lys3-Dha104 with β-mercaptoethanol.

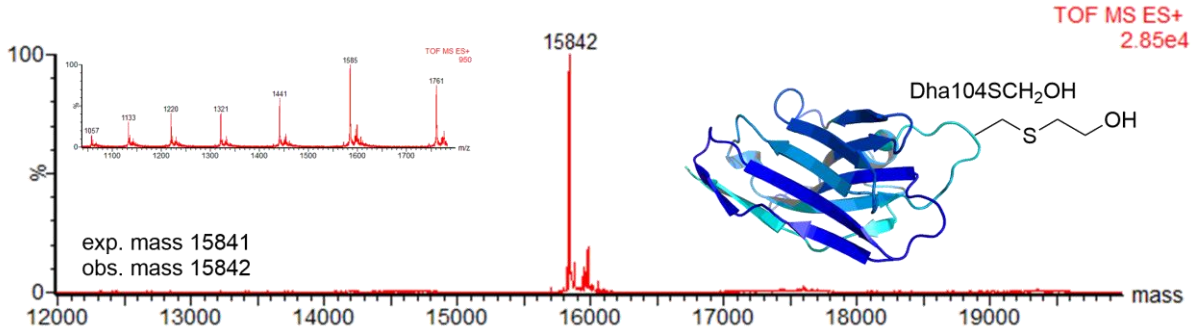

Figure 3.5. Treatment of cAb-Lys3-Dha104 with β-mercaptoethanol.

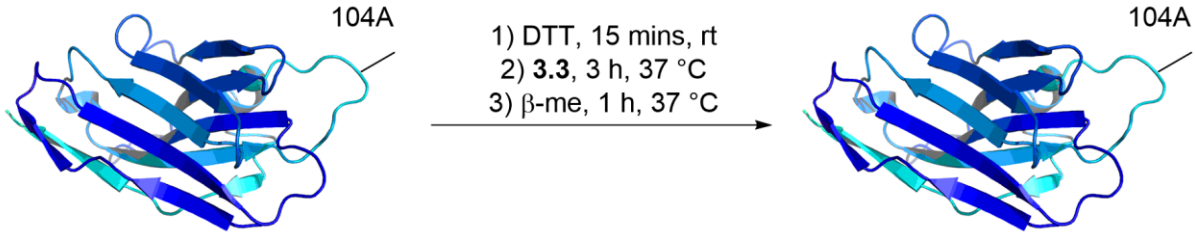

Scheme 3.16. Treatment of WT-cAb-Lys3 under identical conditions to those used on cAb-Lys3-Cys104.

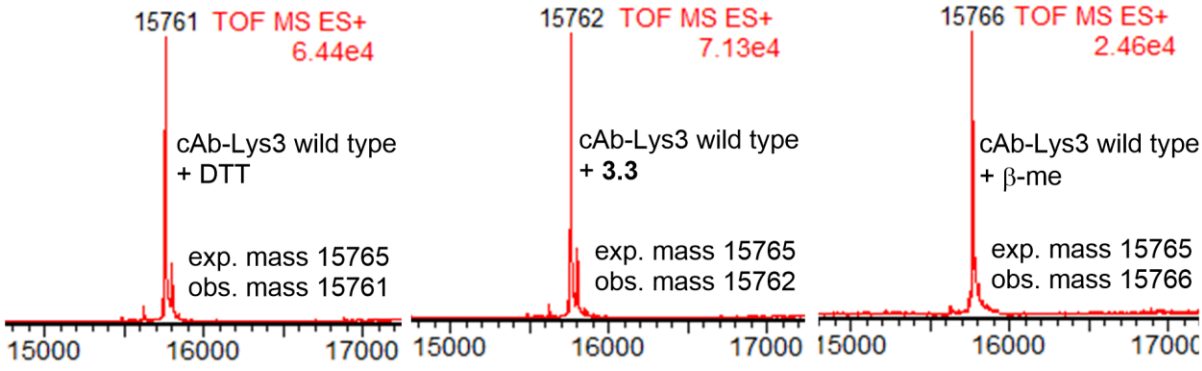

Figure 3.6. Resulting MS for WT-cAb-Lys3 treated under the conditions shown in Scheme **3.16**.

cAb-Lys3-Dha104 was tested for binding to lysozyme by ELISA. Interestingly, no binding was observed. In the experiment, cAb-Lys3-Dha104 was run alongside both WT-cAb-Lys3

and also WT-cAb-Lys3 that had been treated with DTT and **3.3** (steps 1 and 2 of **Scheme 3.16**). WT-cAb-Lys3 was found to bind as expected (both reacted and non-reacted forms), but cAb-Lys3-Dha104 did not (**Figure 3.7**). The secondary structure of the cAb-Lys3 forms were also tested by CD – all forms showed β-sheet folding (**Figure 3.8**). The lack of binding by Dha to lysozyme may be down to the effect of introducing an sp^2 hybridised carbon at position 104 instead of sp^3, and therefore imposing conformational constraint in the loop, inhibiting binding.[69] The effect of the conversion to Dha on the overall structure of cAb-Lys3 was also tested by ^{1}H NMR. cAb-Lys3-Dha104 was found to be folded along with WT-cAb-Lys3 and the mutant cAb-Lys3-Cys104 (**Experimental Figures 3.3 – 3.5**), confirming that the overall protein structure is stable to reaction conditions, and that lack of binding of modified forms is probably due to the introduction of this non-natural residue at the single site.

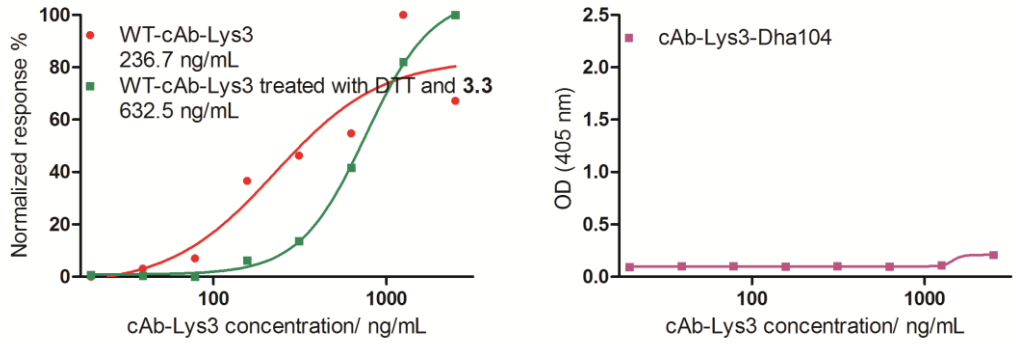

Figure 3.7. ELISA of WT-cAb-Lys3, WT-cAb-Lys3 treated with DTT and reagent **3.3**, and cAb-Lys3-Dha104.

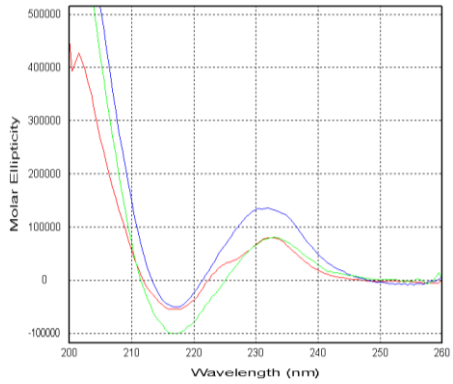

Figure 3.8. CD spectra for cAb-Lys3 forms. Red: WT-cAb-Lys3, blue: WT-cAb-Lys3 treated with DTT and reagent **3.3**, green: cAb-Lys3-Dha104.

Following the successful installation of Dha at position 104 of cAb-Lys3, further modifications with the aim of modulating binding affinity were developed.

3.2.2 Conjugate addition of alkyl thiols to cAb-Lys3-Dha104

In WT-cAb-Lys3, the CDR3 loop protrudes into a hydrophobic cleft in lysozyme. In particular, an alanine at position 104 mediates hydrophobic interactions with a tryptophan residue (**Figure 3.1**). The alanine was mutated to cysteine, and then further converted to Dha, which can act as a unique electrophilic site. The addition of thiol nucleophiles has been carried out previously in the group, in particular to form a range of PTM mimics.[16,20,23,70] Initially the conjugate addition of short chain alkyl thiols (**Scheme 3.17**) was used to see if extending the carbon chain would lead to closer contact with the tryptophan in lysozyme thus increasing binding affinities – demonstrating the concept of 'Chemical Affinity Maturation'.

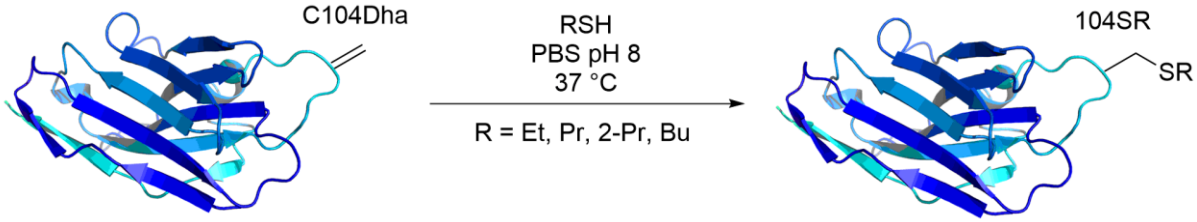

Scheme 3.17. The conversion of Dha to cAb-Lys3-SR104 using short chain alkyl thiols.

Initially, ethanethiol (EtSH) and propanethiol (PrSH) were used as substrates for conjugate additions. Both reagents are insoluble and highly volatile, which makes the addition of small amounts (a few μL) to proteins problematic. Only starting material could be observed by LC-MS when adding one portion of neat thiol. The use of DMF as a co-solvent did not help in forming product. Portion wise addition (3 x 20 μL) of reagent was found to help, and full conversion to the desired products could be detected for EtSH, PrSH and 2-propanethiol (2-PrSH) within 2.5 hours at 37 °C in the absence of any organic co-solvent (**Figures 3.9, 3.10 and 3.11**). Multiple attempts to react butanethiol (BuSH) with Dha were unsuccessful. It was decided to proceed with probing the binding affinities of the other cAb-Lys3-SR104 forms (SEt104, SPr104 and S-2Pr104) to see if extra methylene units could strengthen binding affinities. Addition at a single site was observed during the reactions. Efforts to confirm the site of modification at position 104 by proteolytic digest and LC-MS/MS analysis were unsuccessful, but chemical tests described later were used to deduce the position of modification as 104 (**Figures 3.16a** and **3.16b**).

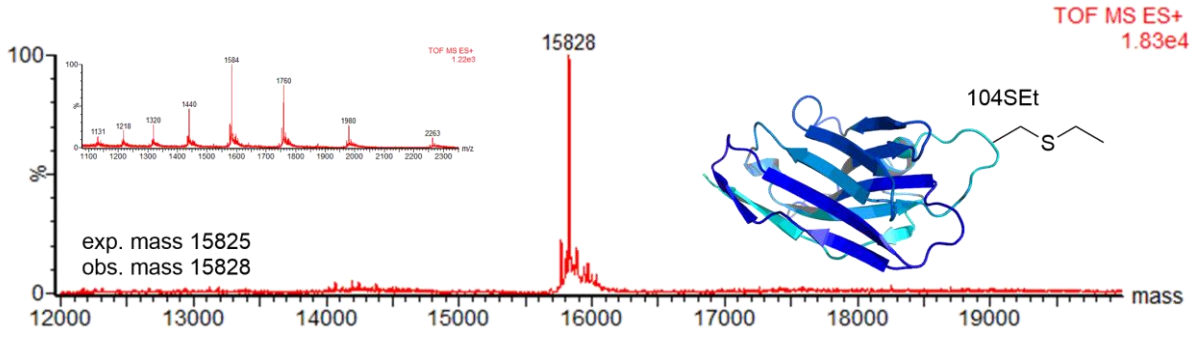

Figure 3.9. Conversion to cAb-Lys3-SEt104 after 2.5 hours at 37 °C.

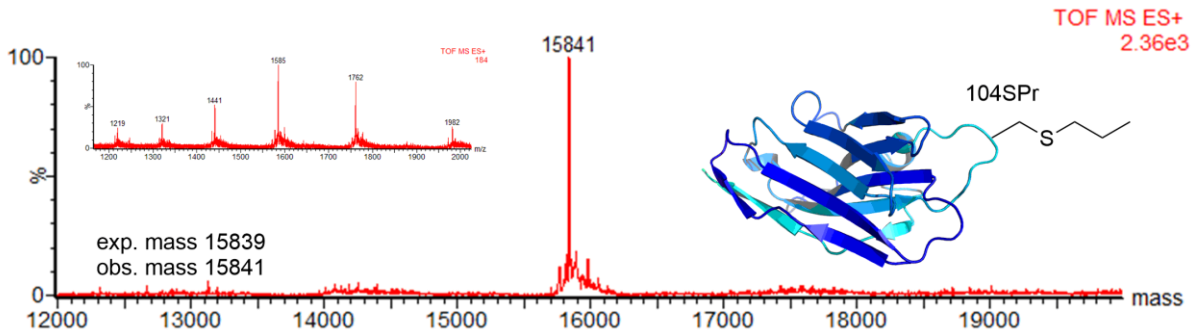

Figure 3.10. Conversion to cAb-Lys3-SPr104 after 2.5 hours at 37 °C.

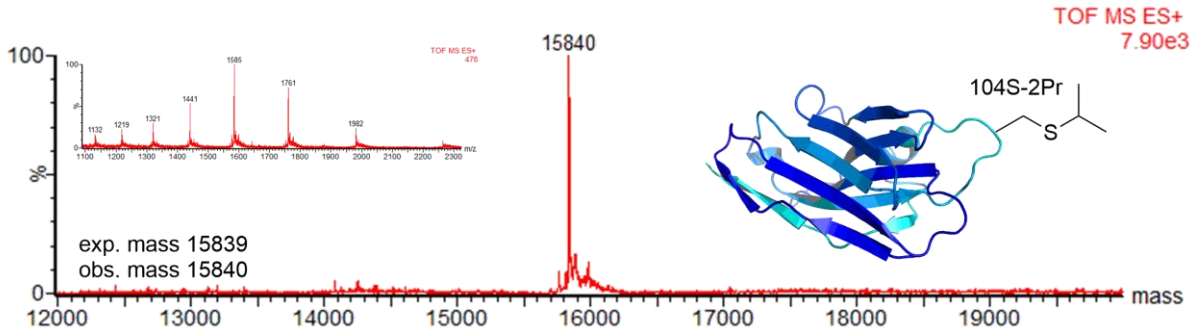

Figure 3.11. Conversion to cAb-Lys3-S-2Pr104 after 2.5 hours at 37 °C.

An efficient and reproducible protocol was developed for the conjugate addition of the short chain alkyl thiols EtSH, PrSH and 2-PrSH to cAb-Lys3-Dha104. Despite the insolubility of the reagents, full conversion could occur in the absence of any organic co-solvent. Next, the effects of the modifications on the binding ability to lysozyme were tested.

Investigating the effects of conjugate thiol addition on cAb-Lys3 binding

After a desalting step, ELISAs were carried out alongside WT-cAb-Lys3 using lysozyme as the antigen (as shown in **Figure 2.24, Chapter 2**). Unfortunately, the presence of the chemically installed alkyl sulfide groups appeared to diminish any binding capability of the antibody. The assays were repeated at the same conditions, and at higher initial antibody concentrations, but still no binding was observed. ELISA data resembled the negative control, where no lysozyme was coated onto the wells (**Figure 3.12**).

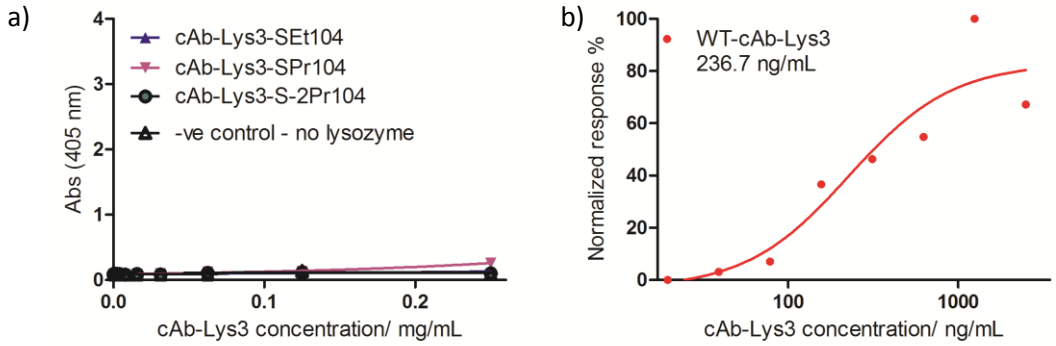

Figure 3.12. a) ELISA of modified cAb-Lys3. Where position 104 has been modified by EtSH, PrSH or 2-PrSH, binding ability is diminished, b) ELISA of WT-cAb-Lys3.

To further probe binding, modified antibodies including 104Dha were subjected to Hydrogen Deuterium Exchange with Mass Spectrometry MS (HDX) analysis.[71] Here, non-covalent interactions can be probed by the exchange of amide hydrogens with deuterium. The results obtained were in keeping with the ELISA data – no binding was observed for the modified antibodies (**Experimental Section**).

In order to investigate whether lack of binding was due to non-desired side reactions (perhaps at internal disulfide bonds) and or changes in protein conformation over the multiple reaction steps, detailed controls were carried out as depicted in **Scheme 3.18**.

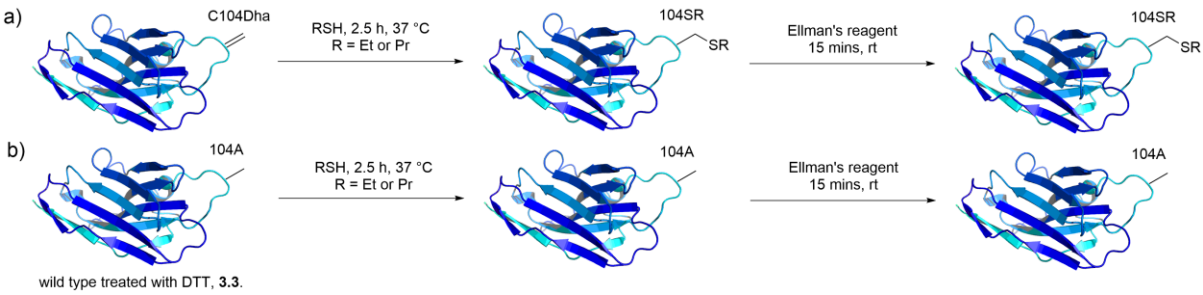

Scheme 3.18. Detailed controls for investigating the addition of EtSH and PrSH to 104Dha and WT-cAb-Lys3.

After the first step of thiol addition to cAb-Lys3-Dha104 and WT-cAb-Lys3, LC-MS and ELISA was used to confirm reactions (and lack of for WT-cAb-Lys3), and retaining of binding ability. The desired masses were observed by LC-MS (data for WT-cAb-Lys3 shown

in **Figures 3.13** and **3.14**), indicating a single addition at a non-native residue. ELISA revealed that WT-cAb-Lys3 treated with alkyl thiols did not diminish binding ability (**Figure 3.15**). This implied that internal disulfide bonds and all other accessible residues are inert to reduction.

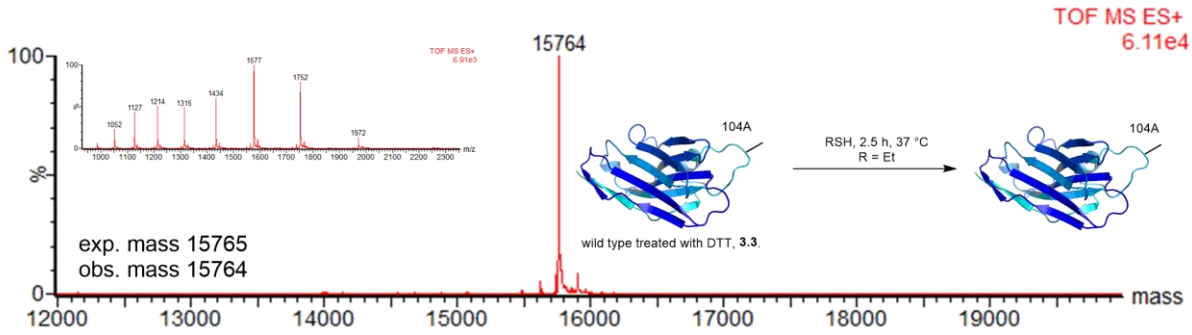

Figure 3.13. Treatment of WT-cAb-Lys3 with DTT, reagent **3.3** and EtSH.

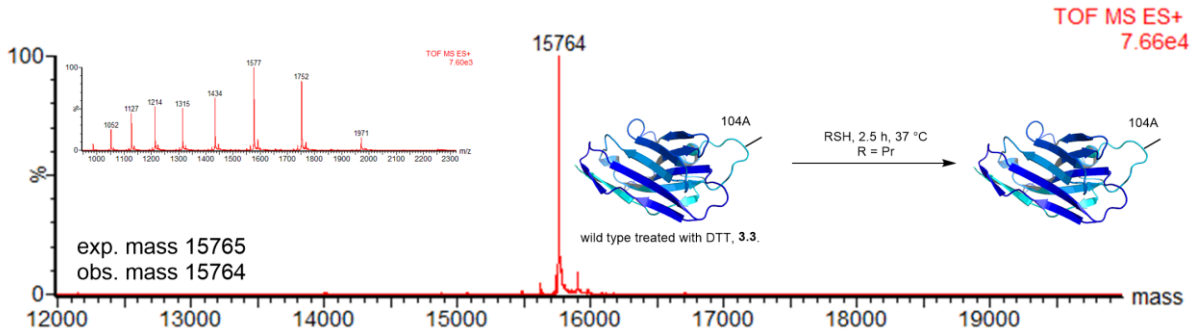

Figure 3.14. Treatment of WT-cAb-Lys3 with DTT, reagent **3.3** and PrSH.

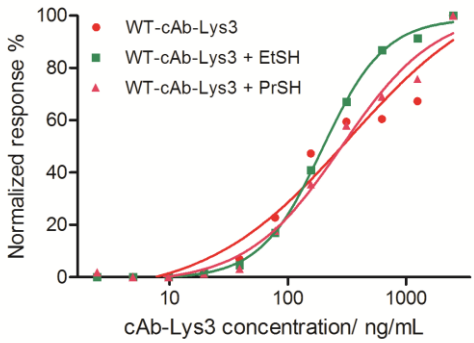

Figure 3.15. WT-cAb-Lys3 after undergoing 3 reaction steps – with DTT, **3.3** and RSH (R = Et, Pr).

Next, cAb-Lys3 treated with alkyl thiols were subjected to treatment with Ellman's reagent to test for consumption of free thiol as a way of deducing that modification had occurred at position 104 via Dha and not at the native disulfide bonds. No changes in mass were detected for both cAb-Lys3-SR104 and WT-cAb-Lys3 (**Figure 3.16**). Finally, all antibodies subjected to reaction conditions were tested for secondary structure by CD (**Figure 3.17**).

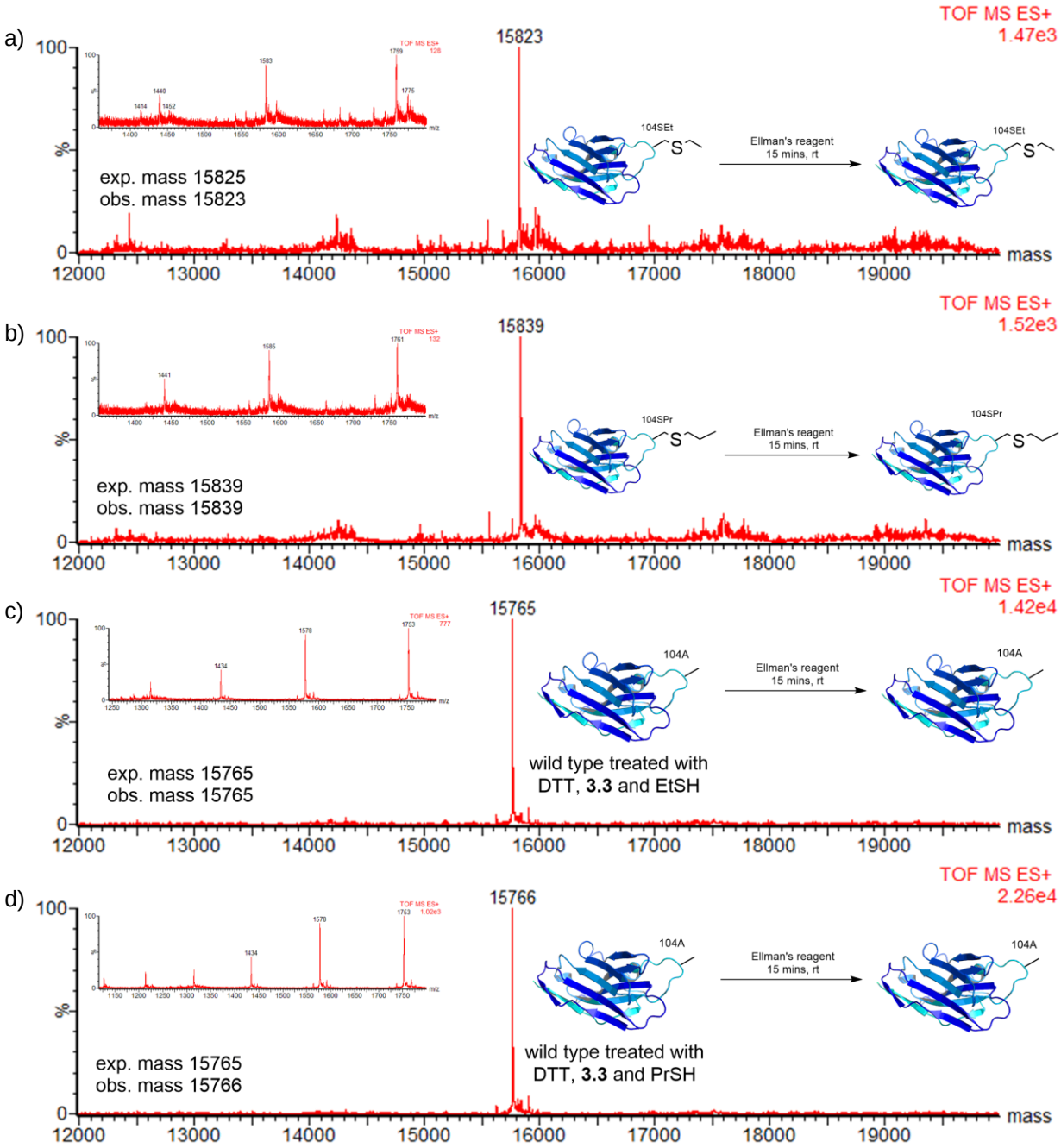

Figure 3.16. Control Ellman's reactions.

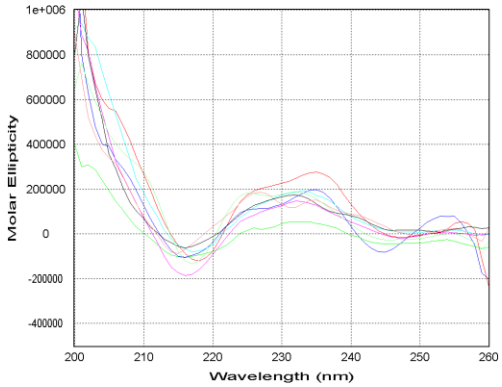

Figure 3.17. CD spectra of cAb-Lys3. Red: cAb-Lys3-SEt104, blue: cAb-Lys3-SPr104, bright green: WT-cAb-Lys3 + EtSH, turquoise: WT-cAb-Lys3 + PrSH, pink: cAb-Lys3-SEt104 + Ellman's, black: cAb-Lys3-104Pr + Ellman's, orange: WT-cAb-Lys3 + EtSH + Ellman's, green: WT-cAb-Lys3 + PrSH + Ellman's.

3.2.3 S_N2 reactions between cAb-Lys3-Cys104 and short chain alkyl iodides

The conversion of cysteine to Dha means that subsequent products arising from conjugate addition may be present as an epimeric mixture (**Scheme 3.19a**). This probably depends on the steric hindrance imposed by neighbouring residues to the site of modification. Direct addition to cysteine however, will result in retention of stereochemistry (**Scheme 3.19b**).

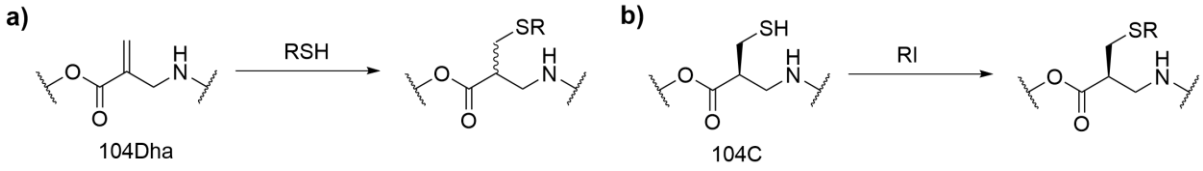

Scheme 3.19. a) Conjugate additions of thiols to Dha, b) direct addition to Cys.

As it was not known if epimerisation might be a reason for the complete diminishing of binding ability of cAb-Lys3 after thiol addition, S_N2 additions of short chain alkyl iodides were carried out directly on cAb-Lys3-Cys104, with the aim of retaining the L-stereochemistry (**Scheme 3.20**). Single-site additions with iodoethane (EtI) and iodopropane (PrI) were successful (**Figures 3.18** and **3.19**), but unsuccessful with 2-iodopropane, where protein loss was observed by LC-MS. Reactions were also unsuccessful with iodomethane. Multiple adducts of mass higher than expected were observed (data not shown), perhaps due

to methylation at non-desired side chains. In fact, WT-cAb-Lys3 control reactions discussed later do support this hypothesis.

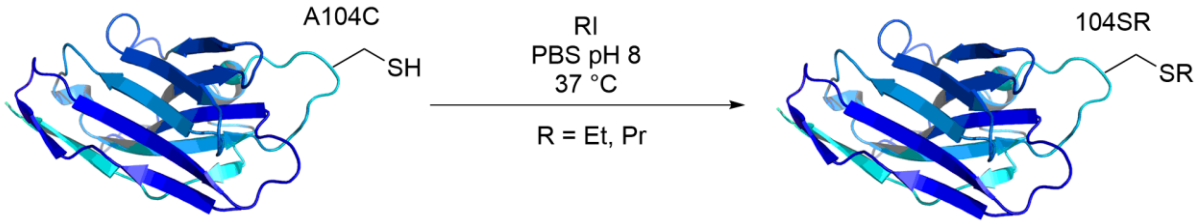

Scheme 3.20. Treatment of cAb-Lys3-Cys104 with EtI and PrI.

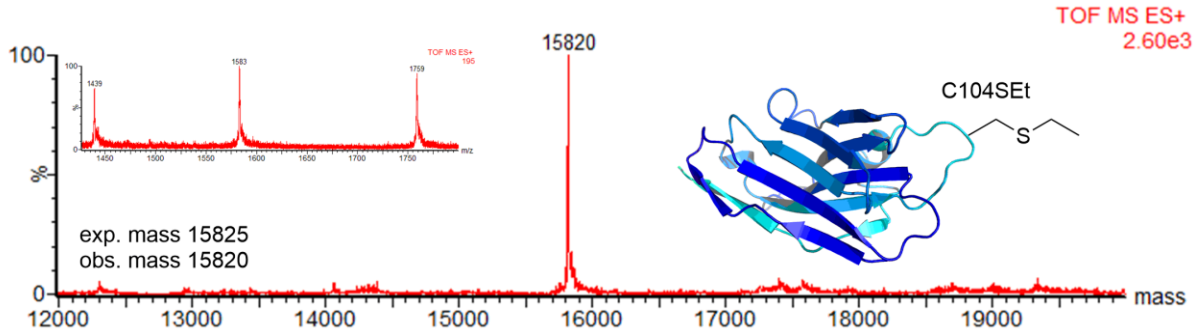

Figure 3.18. Formation of cAb-Lys3-Cys104SEt by treatment of cAb-Lys3-Cys104 with EtI.

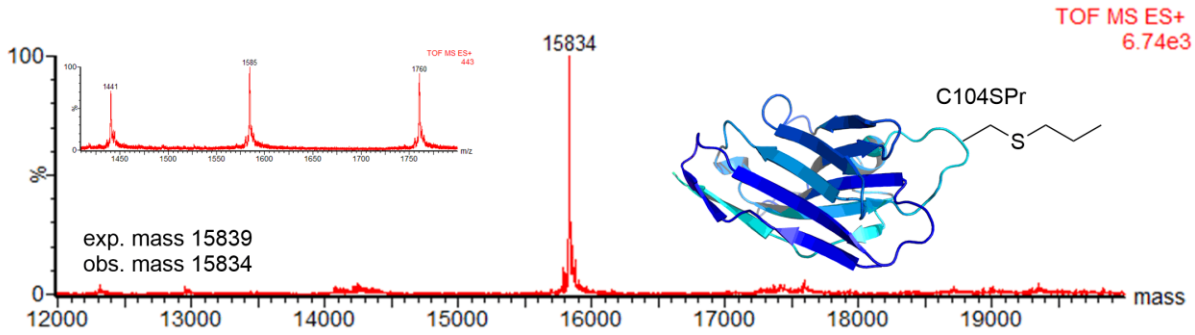

Figure 3.19. Formation of cAb-Lys3-Cys104SPr by treatment of cAb-Lys3-Cys104 with PrI.

As with all protein chemical modifications described so far, alkyl iodide addition was carried out in the absence of any organic co-solvent. To check that all free thiol had been consumed, Ellman's reagent was reacted with cAb-Lys3-Cys104SEt, and no reaction was observed (**Figure 3.20**).

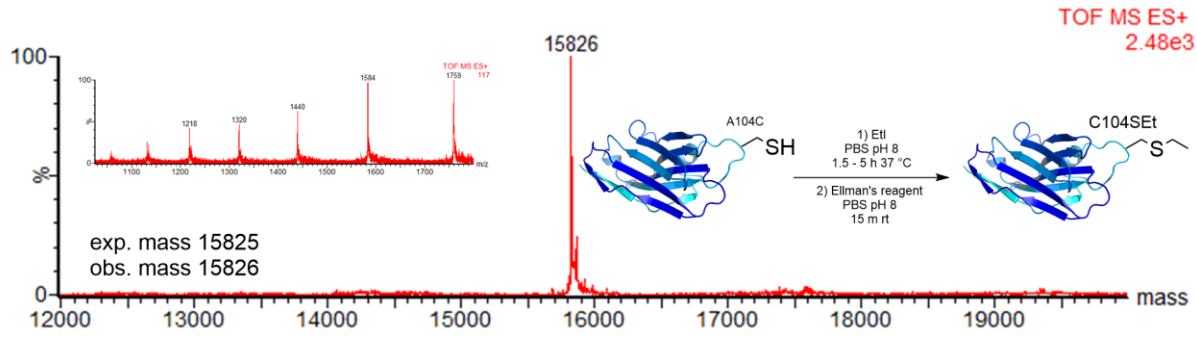

Figure 3.20. Treatment of cAb-Lys3-Cys104SEt with Ellman's reagent.

Binding of the cAb-Lys3-104-sulfide products to lysozyme at high concentrations was tested alongside WT-cAb-Lys3 by Surface Plasmon Resonance (SPR). WT-cAb-Lys3 was found to bind with a K_d (dissociation constant) of 100 nm, in keeping with the literature.[59] Data obtained under the same conditions for both cAb-Lys3-Cys104SEt and cAb-Lys3-Cys104SPr was slightly ambiguous. Dissociation constants calculated were less than that of WT-cAb-Lys3, and the shape of the association and disassociation curves were suggestive of binding down to a 'bulk effect', in which data is affected by small molecules present. In particular, results like this are obtained when running buffers vary in different samples.[72] These results were obtained despite a desalting step post-reaction (see **Experimental Figures 3.6 – 3.9** for more details). The same modified antibodies were subjected to an ELISA, and no binding was observed.

The reactions were repeated, and purification of the modified antibodies done by multiple desalting steps, or dialysis against PBS. In both cases, no binding by ELISA was observed. The secondary structure of the modified antibodies was tested by CD, and β-sheet structure was observed (**Figure 3.21**).

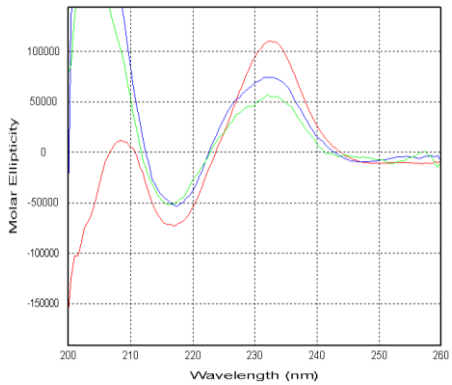

Figure 3.21. CD spectra for WT-cAb-Lys3 (red), and cAb-Lys3 modified by reaction with EtI (blue) and PrI (green).

As a further test to confirm a single site of modification, control reactions where WT-cAb-Lys3 was treated with various short chain alkyl iodides (iodomethane (MeI), 2-iodopropane (2-PrI), EtI and PrI) were carried out (as in **Scheme 3.20**). Considering that alkylations at cysteine in cAb-Lys3-Cys104 were selective, it was surprising to see multiple proteins were obtained during these reactions (**Figures 3.22 – 3.25**). The reacted antibodies were tested for binding by ELISA. Interestingly, binding was preserved in the modified WT-cAb-Lys3 forms, indicating that modifications away from position 104 of the CDR3 loop are possible without comprising binding capability (**Figure 3.26**). The retention of binding after non-site specific alkylations also confirmed that loss of binding with cAb-Lys3 forms modified at position 104 were a result of modifying this position.

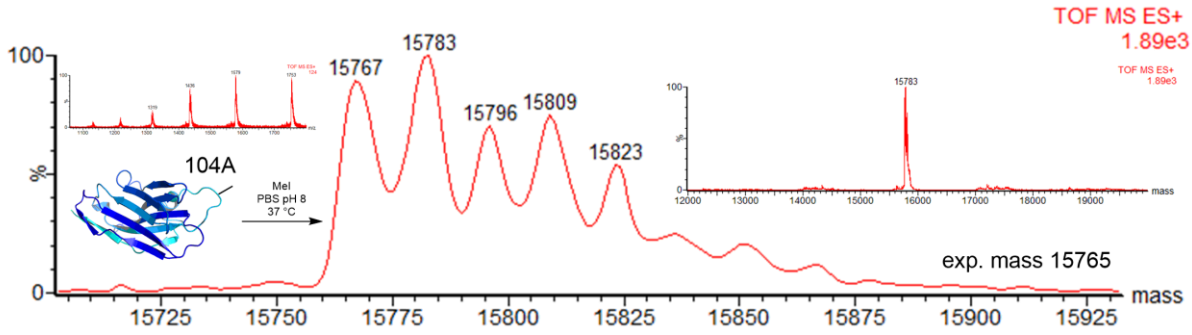

Figure 3.22. Treatment of WT-cAb-Lys3 with MeI. Multiple proteins in increments of 14 – 16 Da are observed. This may be methylation (15 Da).

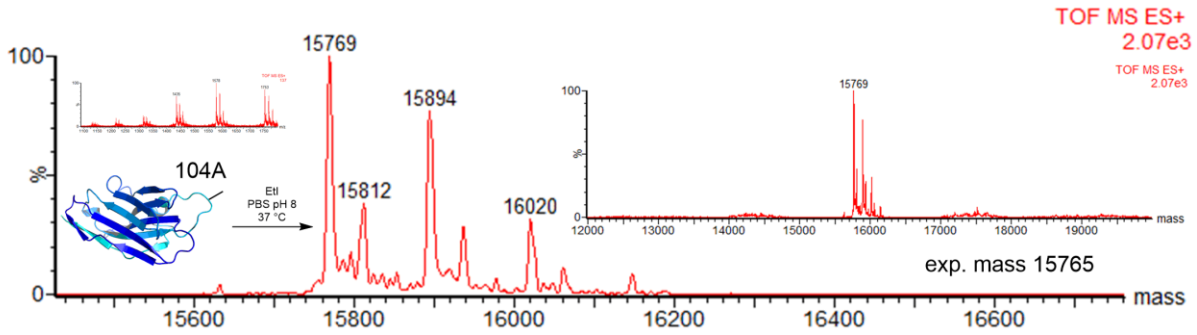

Figure 3.23. Multiple proteins are observed after the treatment of WT-cAb-Lys3 with EtI.

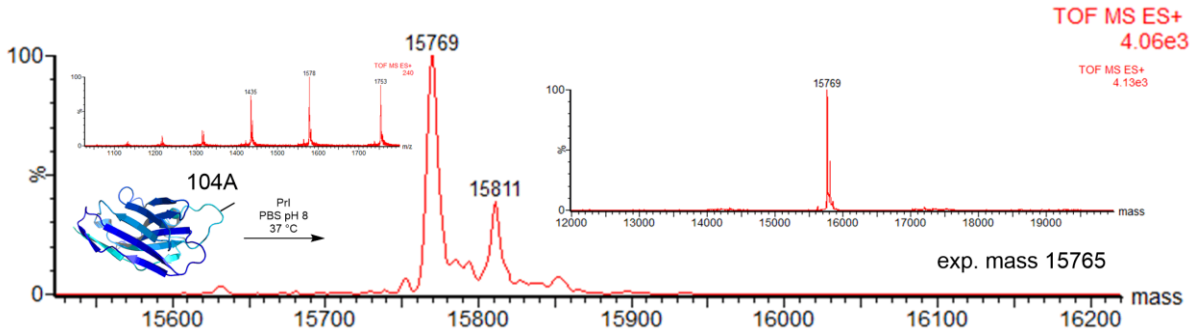

Figure 3.24. Treatment of WT-cAb-Lys3 with PrI. An extra protein at + 42 Da is observed. This may correspond to a single alkylation (39 Da).

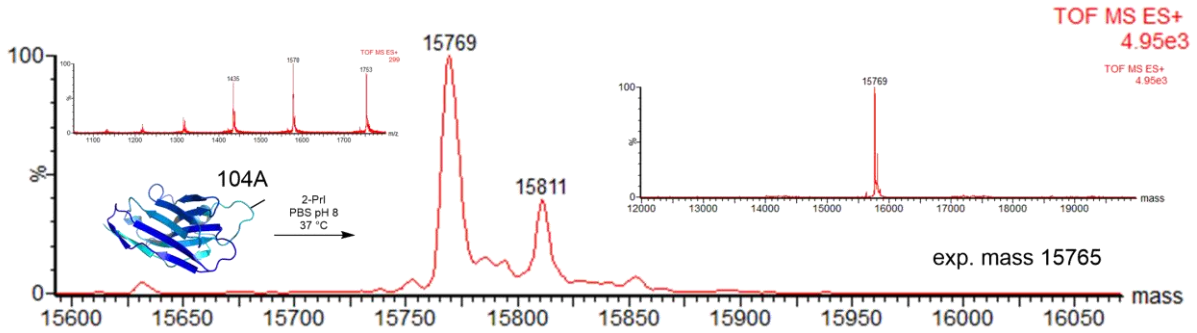

Figure 3.25. Treatment of WT-cAb-Lys3 with 2-PrI. An extra protein at + 42 Da is observed. This may correspond to a single alkylation (39 Da).

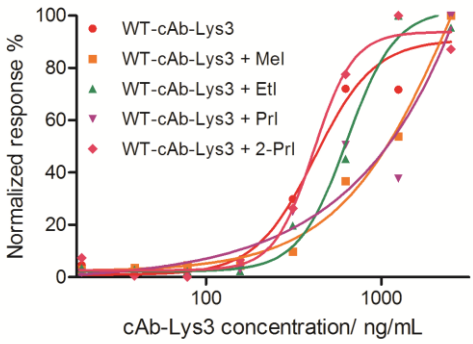

Figure 3.26. ELISA of WT-cAb-Lys3 treated with various short chain alkyl iodides.

cAb-Lys3-SR104 has been formed using two methods – by the addition of short chain alkyl thiols to cAb-Lys3-Dha104 and by the addition of short chain alkyl iodides to cAb-Lys3-Cys104. Unfortunately, in both cases, the modifications led to the diminishing of binding. Next, an alternative method forming carbon-carbon bonds for extending the number of methylene units at position 104 was attempted.

3.2.4 Zinc-mediated radical alkylations on cAb-Lys3-Dha104

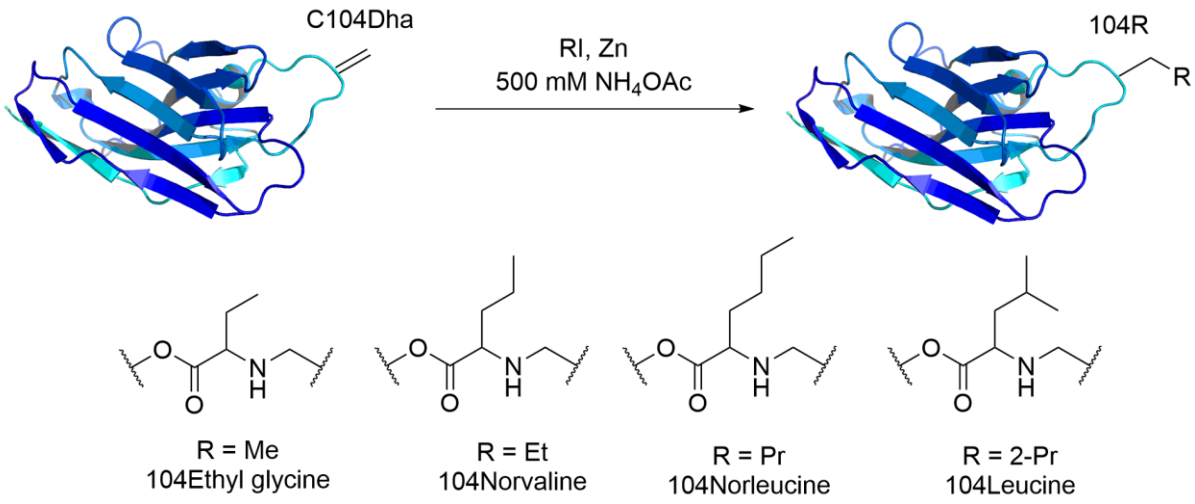

Scheme 3.21. Zinc-mediated alkylations and desired products.

The reaction in **Scheme 3.21** was attempted on cAb-Lys3-Dha104 as a method for extending the carbon chain at position 104. If successful, the method would be the first example to chemically introduce carbon-carbon bonds in this manner in a protein, potentially forming a

number of non-natural amino acids. Previously, the reaction has been tested on an amino acid level and with the protein SBL with various alkyl iodides.[17] For our purpose of extending the methylene unit chain for modulating the binding affinity of cAb-Lys3, the alkyl iodides MeI, EtI, PrI and 2-PrI were used in reaction attempts.

Initially, cAb-Lys3-Dha104 (formed as shown in **Section 3.2.1**), was buffer exchanged into 500 mM ammonium acetate, pH 6. It was thought that the use of a lower pH would prevent the non-selective alkylation observed previously on WT-cAb-Lys3. Antibody was incubated with 10,000 eq. zinc (Zn) and 12,000 eq. alkyl iodide for 15 minutes at room temperature. By LC-MS, no protein was detected where PrI was used, and starting material was observed for the reactions with MeI and EtI (**Figure 3.27**). Comparing the spectra obtained by LC-MS for cAb-Lys3-104Dha and the reaction using EtI showed that a significant amount of protein loss had occurred (as well as no product formation).

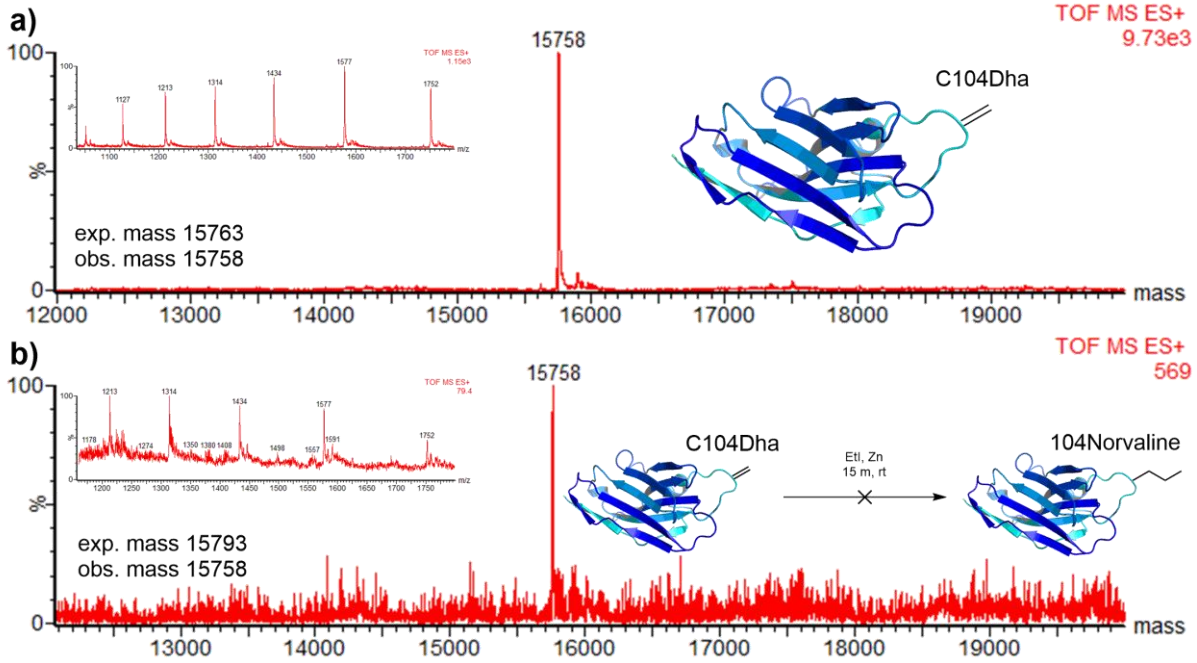

Figure 3.27. a) cAb-Lys3-Dha104, b) After incubation with zinc (10,000 eq.) and EtI (12,000 eq.), no product is observed as well as a decrease in ion count.

Based on the above result that the Zn-mediated alkylation was somehow detrimental to the antibody, the behaviour of cAb-Lys3 under the reaction conditions were tested by SDS-PAGE. WT-cAb-Lys3 and cAb-Lys3-Cys104 were incubated with 250 and 2,500 eq. Zn. By SDS-PAGE, bands appeared to be progressively fainter as the number of Zn equivalents was increased (**Figure 3.28**). This implied that Zn had a detrimental effect on the native antibody. It was speculated that Zn may be oxidising in the acidic medium to Zn^{2+} and coordinating to the His tag.

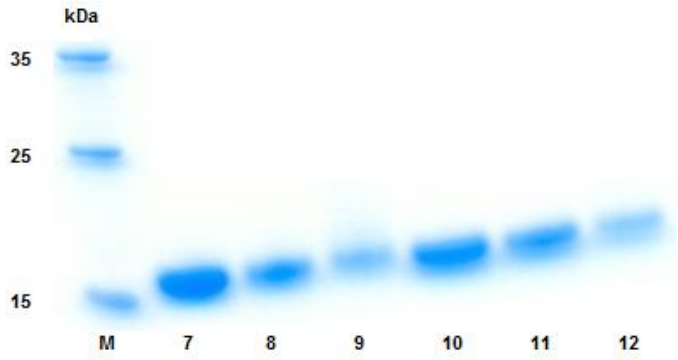

Figure 3.28. WT-cAb-Lys3 and cAb-Lys3-Cys104 was incubated with Zn. 7: WT-cAb-Lys3, 8: WT-cAb-Lys3 + 250 eq. Zn, 9: WT-cAb-Lys3 + 2500 eq. Zn, 10: cAb-Lys3-Cys104, 11: cAb-Lys3-Cys104 + 250 eq. Zn, 12: cAb-Lys3-Cys104 + 2,500 eq. Zn.

Next, cAb-Lys3-Dha104 was incubated under various conditions. By SDS-PAGE, it could be seen that incubation with 2,500 and 25,000 eq. Zn resulted in complete loss of protein (lanes 3 and 4, **Figure 3.29**). A band could still be seen when antibody was incubated with just MeI (lane 5). In complete reaction conditions (cAb-Lys3-Dha104, Zn and MeI, lane 6), a very faint band could be seen. This may be due to Zn only or an effect of the whole reaction.

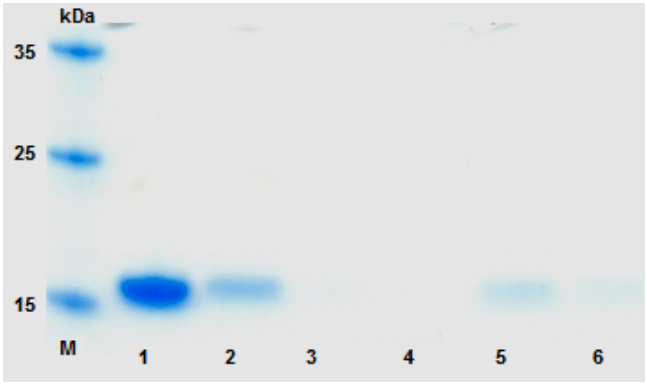

Figure 3.29. cAb-Lys3-Dha104 was incubated with varying amounts of Zn and or MeI. 1: cAb-Lys3-Cys104, 2: cAb-Lys3-Dha104, 3: cAb-Lys3-Dha104 + 2,500 eq. Zn, 4: cAb-Lys3-Dha104 + 25,000 eq. Zn, 5: cAb-Lys3-Dha104 + MeI, 6: cAb-Lys3-Dha104 + 2,500 eq. Zn + MeI.

The SDS-PAGE experiments implied that incubation with increasing amounts of Zn was progressively detrimental to cAb-Lys3, which may be due to coordination to the C-terminal His tag. It was therefore decided to cleave the His tag before further investigation into the Zn-mediated alkylation.

His tag cleavage of cAb-Lys3 (WT and C104)

Prior to the C-terminal His tag of cAb-Lys3 is the amino acid sequence `ENLYFQG` which is the cleavage site for tobacco etch virus (TEV) protease. Three different proteases were used, all containing His tags, such that separation of enzyme and antibody after cleavage could be easily achieved by affinity chromatography. AcTEV protease, TurboTEV protease and TEV protease expressed and purified in-house[1] were used for His tag cleavage. Further details are described in the **Experimental Section** (**Experimental Figures 3.10 – 3.12**). cAb-Lys3-Cys104 with no His tag was tested for reactivity with Ellman's reagent (**Experimental Figure 3.13**) and reagent **3.3** forming Dha at position 104 (**Experimental Figure 3.14**). Only cAb-Lys3 with no His tag was used for further optimisations of Zn-mediated alkylations.

[1] Expressed and purified by Phin Chooi (BGD)

Zinc-mediated alkylations on cAb-Lys3-Cys104 with no His tag

Before proceeding with reaction attempts, the stability of cleaved cAb-Lys3-Cys104 towards zinc at both pH 8 and 6 was tested by SDS-PAGE. Gratifyingly, no decrease in band intensities were observed after incubation with 500 and 5,000 eq. Zn (**Figure 3.30**). Furthermore, cAb-Lys3-Dha104 was incubated with 15,000 eq. Zn at room temperature and 37 °C. Samples after 30 minutes show the same intensity by LC-MS (data not shown), and by SDS-PAGE, showing that zinc alone is not responsible for protein loss (**Figure 3.31**).

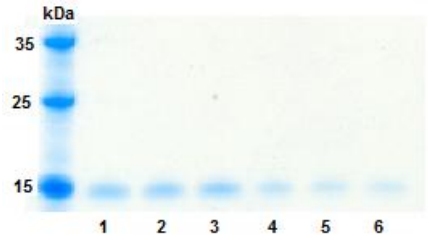

Figure 3.30. SDS-PAGE of cleaved cAb-Lys3-Cys104 with varying amounts of zinc. 1: cAb-Lys3-Cys104 (PBS, pH 8), 2: 500 eq. Zn, 3: 5,000 eq. Zn, 4: cAb-Lys3-Cys104 (500 mM NH4OAc, pH 6), 5: 500 eq. Zn, 6: 5,000 eq. Zn, 1 – 3 PBS pH 8, 4 – 6 NH_4OAc, pH 6. Bands in lanes 4 – 6 are less intense as a buffer exchange step resulted in a decrease in protein concentration.

Figure 3.31. 1: cAb-Lys3-Cys104, 2: reduced cAb-Lys3-Cys104, 3: cAb-Lys3-Dha104, 4: cAb-Lys3-Dha104 in 500 mM NH_4OAc pH 6, 5: cAb-Lys3-Dha104 + 15,000 eq. Zn, rt, 30 minutes, 6: cAb-Lys3-Dha104 +15,000 eq. Zn, 37 °C, 30 minutes.

Low equivalents of Zn and MeI

At first, it was decided to see if lower equivalents of both Zn (500 eq.) and alkyl iodide (in this case MeI, 1,000 eq.) would be sufficient for the reaction forming cAb-Lys3-Etg104 (ethyl glycine, **Scheme 3.21**) in 500 mM NH_4OAc, pH 6. Based on previous observations that the reaction is rapid and exothermic,[17] the reaction was analysed by LC-MS after only 10 minutes at room temperature. Only starting material was observed. A further 1000 eq. MeI

was added, and the reaction incubated overnight, after which only starting material remained. Based on a lack of reaction observed for lower equivalents of reagents, it was decided to proceed with higher numbers of equivalents of both Zn and alkyl iodide. For MeI in particular, a much larger excess may be required due to difficulties in forming an unstable methyl radical intermediate.[50] Furthermore, the alkyl iodide substrates have low boiling points, meaning that loss by evaporation is possible.

High excesses of Zn and EDTA Scavenging

Entry	RI	Temperature
1	MeI	r.t.
2	MeI	37 °C
3	Benzyl iodide	r.t.
4	Benzyl iodide	37 °C

Table 3.2. cAb-Lys3-Dha104 (250 μL, 0.9 nmol, c = 0.06 mg/mL, 500 mM NH_4OAc, pH 5.5), Zn (7 mg, 100,000 eq.), 3 x 10 μL RI over 20 minutes (500,000 eq.), 2 hours. In all cases, protein precipitate was observed, and no protein could be detected by LC-MS.

No protein was observed in any conditions tested in **Table 3.2**, indicating that extremely high excess of reagents relative to antibody were not successful in driving the reaction forward. Precipitate was also visible under the conditions. From this result, it was possible to ascertain that the reaction conditions were having some effect on the antibody, meaning that there may be potential to scale equivalents down and identify possible conditions where precipitation is minimised and reaction maximised.

Next a range of alkyl and aromatic iodides were tested with a lower number of Zn equivalents (10,000). The same high excess of alkyl and aromatic iodides was used as previous results showed that iodide was not detrimental to antibody stability (**Figure 3.29**), and they are volatile or insoluble. Conditions are specified in **Table 3.3**.

Entry	RI
1	2-Iodotoluene
2	PrI
3	EtI
4	2-iodobenzoic acid
5	3-iodobenzoic acid

Table 3.3. cAb-Lys3-Dha104 (200 μL, 0.8 nmol, c = 0.06 mg/mL, 500 mM NH_4OAc, pH 5.5), Zn (0.5 mg, 10,000 eq.), 3 x 10 μL RI over 20 minutes (500,000 eq.), 1 hour, room temperature. In all cases, protein precipitate was observed, and no protein could be detected by LC-MS.

Unfortunately the decrease in Zn did not help in preventing loss of protein by precipitation in any of the conditions specified in **Table 3.3**. In order to see if Zn coordination to the antibody was responsible for the loss in signal by LC-MS, EDTA (100 μL, 100 mM) was added to reaction aliquots in an attempt to compete for Zn coordination.[35] By SDS-PAGE, no protein bands were observed implying that the hypothesis of metal coordination was untrue or that EDTA is not an effective scavenger for the purpose. To investigate this further, a much lower concentration of EDTA (18 mM) was used for scavenging. Reactions were set up as shown in **Figure 3.32**. 10 minutes after Zn (10,000 eq.) and either 6 or 30 μL 2-PrI was added to cAb-Lys3-Dha104, 18 mM EDTA was added, and then the reactions analysed by SDS-PAGE.

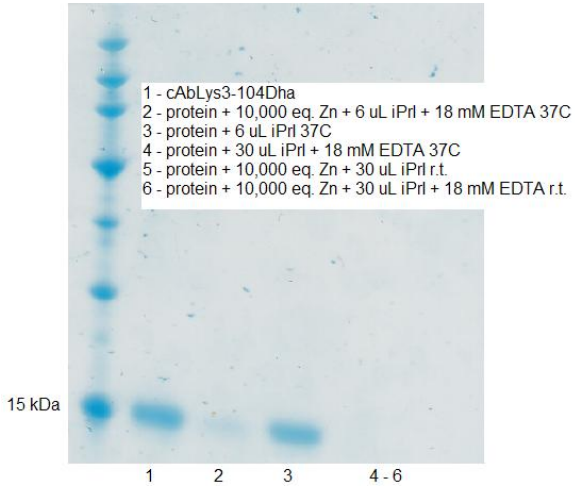

Figure 3.32. cAbLys3 (500 mM NH_4OAc, pH 6) incubation under Zn alkylation conditions.

From the SDS-PAGE in **Figure 3.32**, it can be seen that a low amount of alkyl iodide has no effect on the intensity of the protein band (lane 3, **Figure 3.32**), but when the amount is

raised, a loss of protein is observed (lane 4, **Figure 3.32**). Furthermore, the presence of EDTA in a reaction attempt does not help in preventing protein precipitation (lanes 2 and 6, **Figure 3.32**). From this point, lower equivalents of alkyl iodide were used in reaction attempts. As a test to establish if EDTA itself was having a detrimental effect on the stability of the protein, cAb-Lys3-Dha104 was incubated with increasing concentrations of EDTA and Zn (10,000 eq.). No decrease in band intensity was observed by SDS-PAGE (**Figure 3.33**).

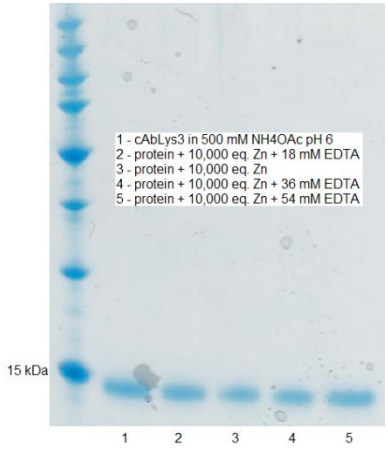

Figure 3.33. cAbLys3 (500 mM NH_4OAc, pH 6) incubation with Zn and EDTA.

Reactions at 37 °C

In light of the temperature being increased, a lower number of equivalents of zinc and alkyl iodides were used for attempted alkylations. Unfortunately, no reaction was observed (**Table 3.4**).

Entry	RI
1	2-PrI
2	MeI
3	EtI

Table 3.4. cAb-Lys3-Dha104 (250 μL, 4.2 nmol, c = 0.25 mg/mL, 500 mM NH_4OAc, pH 6), RI (2 μL, 5,000 eq.), Zn (0.3 – 1 mg, 1,000 – 3,000 eq.), 4 hours, 37 °C. In all cases, starting material was observed at 2 hours, and no protein was detectable at 4 hours.

Unfortunately, an increase in temperature and decrease in reagent equivalents was unsuccessful in driving the reaction forward and preventing protein precipitation after extended incubation times.

Portionwise addition of alkyl iodides

Due to the volatile nature of the alkyl iodides, it was thought portionwise addition to antibody over the single addition of an excess may help drive the reaction. For the substrate 2-PrI, portionwise addition to cAb-Lys3-Dha104 was investigated with increasing number of portions. Conditions are shown in **Table 3.5**.

Entry	2-PrI
1	1 x 2 μL
2	2 x 2 μL
3	3 x 2 μL
4	4 x 2 μL

Table 3.5. cAb-Lys3-Dha104 (250 μL, 4.2 nmol, c = 0.25 mg/mL, 500 mM NH_4OAc, pH 5.5), Zn (2 – 3 mg, 7,000 – 10,000 eq.), n x 2 μL RI every 5 minutes (n x 5,000 eq.), 2 hours, 37 °C. 3 – 6 cond. In all cases, protein precipitate was observed, and no protein could be detected by LC-MS.

Portionwise addition of substrate did not help in obtaining product. Precipitate was still observed in the reactions, implying that the antibody is not stable to reaction conditions. As a test to confirm that the precipitate forming was in fact protein, precipitate was isolated from the reaction buffer by centrifugation, and resuspended in clean buffer. SDS-PAGE of samples corresponding to entries 1 – 4 in **Table 3.5** revealed that protein just under 15 kDa was present although bands are faint (**Figure 3.34**). Further analysis of precipitate solubilised in guanidinium hydrochloride (5 M, 50 mM Tris-HCl, pH 8) by LC-MS did reveal low amounts of starting material (cAb-Lys3-104Dha).

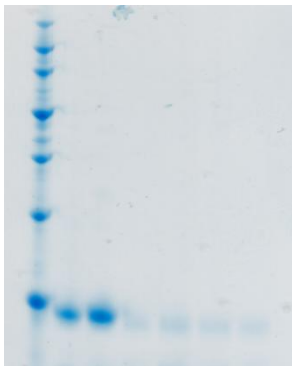

Figure 3.34. Lane 1 reduced cAb-Lys3-Cys104, lane 2 cAb-Lys3-Dha104, lanes 3 – 6 entries 1 – 4 (**Table 3.5**) solubilised precipitate after 30 minutes.

In another reaction attempt (conditions specified in **Table 3.6**), reaction was observed. As in other cases a decrease in ion count (and therefore protein loss) was seen, but unusually, some protein could still be observed after 24 hours at 37 °C. In other attempts, just an hour reaction time resulted in complete losses of protein. The cAb-Lys3-Cys104 that the reaction was carried out on contained a truncated antibody form from too long an incubation with TEV protease. The mass of the truncated form increased with each modification step.

Entry	2-PrI/ μL (n eq.)	Observations by MS
1	0.5 + 1 (3,500 eq.)	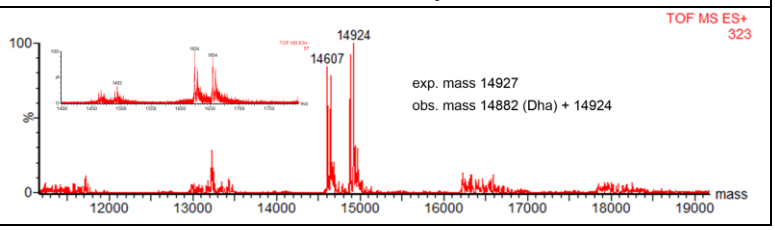

Table 3.6. cAb-Lys3-Dha104 (250 μL, 4.2 nmol, c = 0.25 mg/mL, 500 mM NH_4OAc, pH 6), Zn (0.5 mg, 2,000 eq.), 24 hours, 37 °C.

Although the ion count has decreased in the above spectrum, product formation had occurred. Further incubation led to no increase of product formation. Detection of product and starting material in some cases prompted continued investigation into the Zn-mediated alkylations. In another experiment, the portionwise addition of a total of 12,000 eq. 2-PrI was directly compared to the use of 5,000 and 13,000 eq. Zn (**Table 3.7**). Using the slightly higher amount of 5,000 eq. Zn lead to partial conversion as observed in **Table 3.7**, but on increasing

to 13,000 eq, complete conversion to desired product was obtained, albeit with a large decrease in ion count.

Entry	Zn/ mg (n eq.)	Observations by MS
1	1.7 (5,000 eq.)	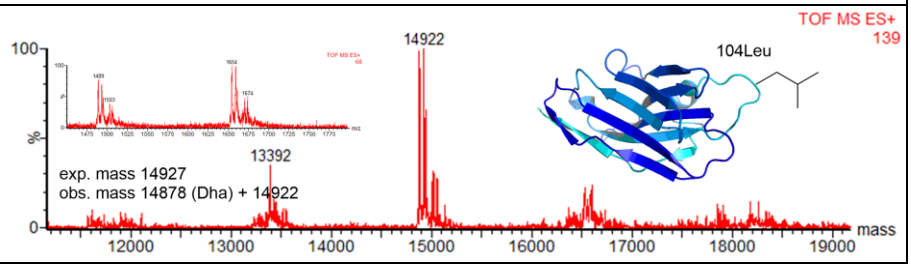
2	4.6 (13,000 eq.)	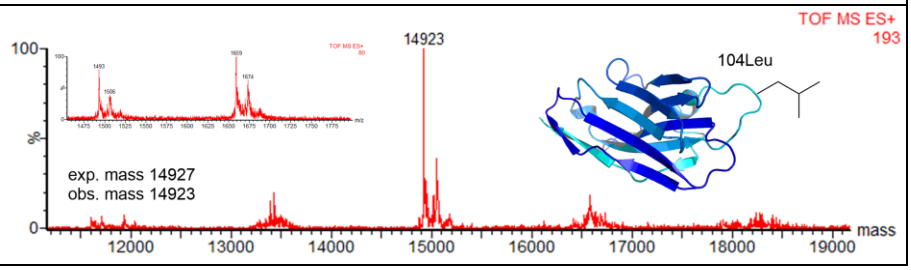

Table 3.7. cAb-Lys3-Dha104 (500 µL, 5.4 nmol, c = 0.16 mg/mL, 500 mM NH_4OAc, pH 6), 3 x 2 µL 2-PrI every 10 minutes (3 x 4,000 eq.), 40 minutes, r.t.

Promisingly, product formation to cAb-Lys3-Leu104 was observed in both cases, also with a decrease in ion intensity. Complete consumption of Dha was seen for entry 2, **Table 3.7**, whereas approximately 50 % conversion was observed for entry 1, where less Zn was used. The results were promising. Based on these results, similar conditions were applied to the primary alkyl iodides, MeI, EtI and PrI. Unfortunately, protein was not observed by LC-MS. Considering that the rate of reaction is likely to be less as compared to the secondary 2-PrI, longer reaction times were allowed which unfortunately led to complete precipitation.

For this reason, the formation of cAb-Lys3-Norvaline104 (cAb-Lys3-Dha104 + EtI, Scheme **3.21**) was attempted using a similar amount of Zn (10,000 eq. and 15,000 eq.), but a higher number of equivalents of the less reactive iodide, EtI (3 x 30,000 eq. over 5 minutes) and a higher temperature of 37 °C in 500 mM ammonium acetate (500 µL, 3.7 nmol protein). Each reaction was run in parallel. For the case with 10,000 eq. Zn, no protein was detected after 10 minutes. However, where 15,000 eq. was used, full conversion to cAb-Lys3-Norvaline104

was observed after 1.5 hours (**Figure 3.35**). Unfortunately, this conversion was accompanied by an extremely low ion count of 35.1. The fact that no protein was detected by LC-MS where 10,000 eq. Zn was used, and a small amount where 15,000 eq. was used demonstrated the lack of reliability and reproducibility of the application of the Zn-mediated alkylation to cAb-Lys3-Dha104. Modifying multiple reaction factors on the whole did not give clear insights into finding suitable reaction conditions for each alkyl iodide substrate, and thus further experiments and optimisations were required.

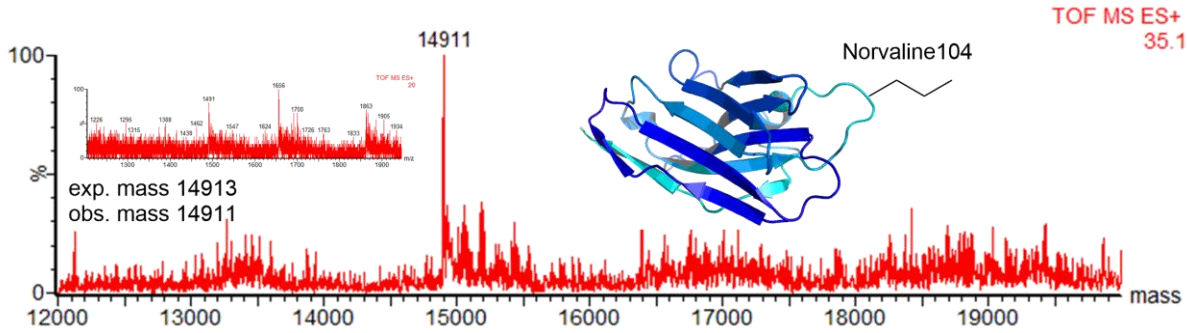

Figure 3.35. Formation of cAb-Lys3-Norvaline104. cAb-Lys3-Dha104 (500 µL, 3.7 nmol, 500 mM NH_4OAc, Zn (15,000 eq.), EtI (3 x 30,000 eq. over 5 minutes), 37 °C.

Use of concentrated cAb-Lys3-Dha104 and varying equivalents

For this, a 10 x more concentrated aliquot of antibody corresponding to 40 nmol was used for a single reaction with EtI and Zn (5,000 eq.) to see if signal by LC-MS could be improved, even with some protein precipitation. Initially, a much lower amount of iodide equivalents was used (2,000 eq.). After 15 minutes at room temperature, analysis by LC-MS revealed that starting material remained with no loss of ion count, indicating that the EtI addition was insufficient. However, the addition of a further 8,000 eq. resulted in protein precipitation, and loss of any signal by LC-MS.

Varying NH_4OAc buffer pH

The Zn-mediated conversion of cAb-Lys3-Dha104 to cAb-Lys3-Leu104 (using 2-PrI) was carried out in parallel at a range of pHs (**Table 3.8**).

Entry	500 mM NH_4OAc, pH	Observations by MS
1	4	No protein by LC-MS, protein precipitate observed.
2	4.5	No protein by LC-MS, protein precipitate observed.
3	6	Low amounts of s.m. by LC-MS, protein precipitate observed.
4	6.5	Low amounts of s.m. by LC-MS, protein precipitate observed.
5	7	Low amounts of s.m. by LC-MS, protein precipitate observed.
6	7.5	Low amounts of s.m. by LC-MS, protein precipitate observed.

Table 3.8. cAb-Lys3-Dha104 (100 μL, 0.54 nmol, c = 0.1 mg/mL), Zn (0.4 – 0.7 mg, 10,000 eq.), 3 x 1 μL RI (3 x 20,000 eq.), 10 minutes, 37 °C.

Based on the results above, a suitable pH that drove the reaction and minimised precipitation (and therefore loss of protein) was not identified.

500 mM NH_4OAc, pH 4 and low temperature

Next, reaction at a lower temperature was attempted. It was thought this may help to prevent loss of iodide by evaporation, and perhaps promote radical formation and addition. Within 1 hour of reaction at the lower temperature of 4 °C, no protein was observed by LC-MS. In this attempt, 4 nmol of cAb-Lys3-Dha104 was reacted in NH4OAc (pH 4) with Zn (6,000 eq.) and 2-PrI (5,000 eq.).

Further Zn-mediated alkylations at 4 °C

Further reactions were carried out at a lower temperature with similar equivalents of zinc and 2-PrI used previously, and at pH 6. This was because although protein precipitation was the general observation during reaction attempts, in some cases some product formation was observed but ion counts were always greatly lower. It was decided to see if a lower temperature may prevent significant protein loss, but not the reaction proceeding (**Table 3.9**).

Entry	2-PrI/ μL (n eq.)
1	2 (1,000 eq.)
2	4 (2,000 eq.)

Table 3.9. cAb-Lys3-Dha104 (500 μL, 16.8 nmol, c = 0.5 mg/mL, 500 mM NH_4OAc, pH 6), Zn (1 mg, 1,000 eq.), 1 hour, 4 °C. In both cases, protein precipitate was observed and no protein was detectable by LC-MS.

Lowering the temperature proved unsuccessful in obtaining any desired product of alkylation. It is also important to note that lowering the number of equivalents of Zn 10-fold (10,000 to 1,000 eq.) still resulted in precipitate being observed.

Varying buffer concentration

Ammonium ions are reported to activate Zn and allow the reaction to proceed.[50,55] As modifying the buffer pH did not help with preventing protein loss, it was hypothesised that a decrease in concentration of ammonium ions may help to control this. A range of reactions were set up varying buffer concentration, temperature and the overall addition time and number of equivalents of 2-PrI. The number of equivalents of Zn was kept constant (**Table 3.10**).

Entry	NH4OAc pH 6	Temperature	2-PrI (n x μL)	Addition time	Observations
1	50 mM	37 °C	4 x 1	30 mins	s.m
2	50 mM	r.t.	5 x 2	10 mins	1 h – s.m., overnight – protein precipitate
3	50 mM	37 °C	5 x 2	10 mins	1 h – s.m., overnight – protein precipitate
4	100 mM	r.t.	5 x 2	10 mins	1 h – s.m., overnight – protein precipitate
5	100 mM	37 °C	5 x 2	10 mins	1 h – s.m., overnight – protein precipitate
6	250 mM	37 °C	4 x 1	30 mins	1 h – s.m., overnight – protein precipitate

Table 3.10. cAb-Lys3-Dha104 (500 μL, 1.3 nmol, c = 0.04 mg/mL, NH_4OAc, pH 6), Zn (0.8 mg, 10,000 eq.), overnight.

In entry 1 (**Table 3.10**), a low concentration of buffer as well as a longer addition time of 2-PrI resulted in no conversion to product and also no decrease in ion count. It was decided to try and drive the reaction using the same buffer concentration of 50 mM, but shorten the

addition time at both room temperature and 37 °C (entries 2 and 3, **Table 3.10**). However, this resulted in no desired reaction and a loss of protein detection after prolonged incubation. Similar results were observed with 100 mM buffer (entries 4 and 5, **Table 3.10**). Following these observations, it was decided to increase the buffer concentration to 250 mM, but lengthen the addition time of 2-PrI. Unfortunately, no conversion to product was observed, and a decrease in ion count was seen, implying that the identification of conditions to minimise protein precipitation and drive the reaction was still difficult.

Alternative source of ammonium ions

The Zn-mediated alkylation of cAb-Lys3-104Dha with 2-PrI was attempted with PBS buffered to pH 6.5 with NH_4Cl. As mentioned before, ammonium ions play a key role in the reaction, and are thought to activate zinc metal.[50,55] Unfortunately, no conversion to product was observed, and as previous attempts, a loss of protein occurred. In this attempt, cAb-Lys3-Dha104 was incubated with 40,000 eq. Zn, and 3 x 2 μL 2-PrI was added over 10 minutes at 37 °C.

Alkylation attempts using UV radiation

Previously, radical addition of glycosyl thiols to alkenes (via homoallylglycine) on proteins under UV irradiation have been carried out in the group.[73] It was hypothesised that it may be possible to form the desired alkyl radical for addition to Dha under similar conditions. To test the stability of cAb-Lys3 under such conditions, WT antibody was incubated in a UV reactor (λ_{max} 365 nm) for 6 hours. Samples were taken at various time points and analysed by SDS-PAGE. Unfortunately, as shown in **Figure 3.36**, the intensity of the band for antibody decreased over time, implying that cAb-Lys3 was unstable to UV irradiation and therefore not a suitable protein substrate for UV-mediated radical formation.

Figure 3.36. WT-cAb-Lys3 incubated under UV conditions. Lane 1: 0 m, lane 2: 10 m, lane 3: 30 m, lane 4: 1 h, lane 5: 1.5 h, lane 6: 2 h.

Sonication and desalting of samples before analysis

When Luche first reported the Zn-mediated alkylation reaction,[50] he also reported that sonication enhanced the rate of reaction for small molecules.[53] For this reason, it was thought that sonication of the antibody with the reaction components (zinc and alkyl iodide) may rapidly drive the reaction before precipitation of the protein could occur. Before attempting the reaction, the stability of cAb-Lys3 was tested by subjecting WT-cAb-Lys3 to sonication for 15 minutes. Gratifyingly, samples analysed by LC-MS before and after sonication show similar high ion counts, indicating that the antibody is stable to sonication. Following this, reactions with sonication were attempted (**Table 3.11**).

Entry	Sonication	Observations
1	yes	Protein precipitate
2	no	Protein precipitate

Table 3.11. cAb-Lys3-Dha104 (500 μL, 2.9 nmol, c = 0.09 mg/mL, NH_4OAc, pH 6), Zn (1.8 mg, 10,000 eq.), 5 μL 2-PrI (25,000 eq), 15 minutes, room temperature.

An alkylation with sonication was set up in parallel to one without. Unfortunately, sonication proved unsuccessful in driving the alkylation forward and preventing protein precipitation. Furthermore, samples were desalted before analysing by LC-MS in case the high concentration of small molecules was inhibited protein detection. This did not prove effective in detection, implying that the lack of resulting protein after incubation in reaction conditions was the primary reason for the low detection levels.

Pure Zn

It is known that commercially available Zn can contains trace amounts of other metals and other impurities, so it was decided to wash Zn with 10% hydrochloric acid, water and acetone before use. Reactions with washed Zn were set up as shown in **Table 3.12**. Samples were taken at 10 and 30 minutes for analysis by LC-MS. It was also attempted to desalt samples before analysing.

Entry	RI/μL
1	0.3 EtI
2	0.5 EtI
3	1 EtI
4	1 2-PrI
5	3 2-PrI

Table 3.12. cAb-Lys3-Dha104 (200 μL, 1.7 nmol, c = 0.13 mg/mL, NH_4OAc, pH 6), Zn (0.5 mg, 5,000 eq.), 30 minutes, room temperature. In all cases, protein precipitate is observed, and no protein is detectable by LC-MS.

Unfortunately, the use of washed Zn did not help in preventing protein loss during the reaction. A range of equivalents of EtI (2,000 – 7,000 eq.) and 2-PrI (5,000 – 17,000 eq.) were used.

Zinc-copper-mediated alkylations

As well as ammonium ions being reported to be required for the activation of Zn, copper is also thought to do the same.[50] Based on the negative results obtained with the use of Zn alone, it was decided to try the reactions with zinc-copper couple (Zn/Cu) under similar conditions to those described previously, and also with gluconic acid as an alternative metal scavenger to EDTA.

Zn/Cu-mediated alkylation with PBS buffered with NH_4Cl

cAb-Lys3-Dha104 in PBS buffered with NH_4Cl was incubated with 5.2 mg Zn/Cu and 3 x 2 μL 2-PrI. Interestingly, at 30 minutes, 1 and 2 hours, a number of adducts were observed by LC-MS (**Figure 3.37**). The adducts had a mass difference of ~ 126, which corresponds to the

combined mass of Zn and Cu. This implied that the alloy was coordinating to the antibody, and may have provided evidence of this process causing protein precipitation as the ion count did decrease (**Figure 3.37**). Gluconic acid was added as a competing chelator for Zn.[74] After 1 hour, no protein was detected. However the reaction was repeated with the addition of gluconic acid at the beginning. Conversion to the desired product was observed after overnight incubation, albeit with a very low ion count (**Figure 3.38**).

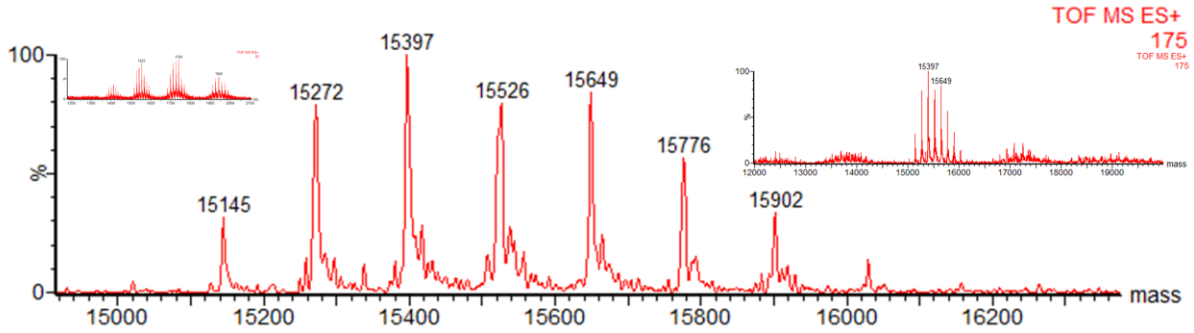

Figure 3.37. cAb-Lys3-Dha104 (PBS buffered with NH_4Cl), 5.2 mg Zn/Cu, 3 x 2 μL 2-PrI, 2 hours, 37 °C.

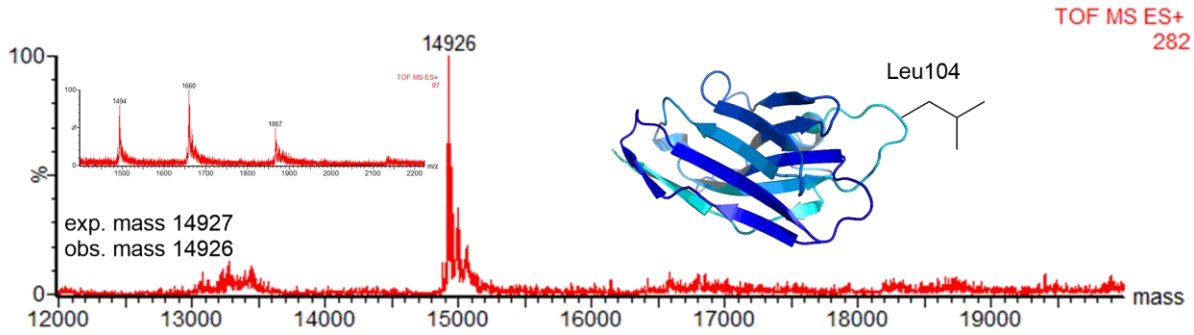

Figure 3.38. cAb-Lys3-Dha104 (PBS buffered with NH_4Cl), 5.2 mg Zn/Cu, 3 x 2 μL 2-PrI, overnight, 10% gluconic acid, 37 °C.

Zn/Cu-mediated alkylation in 500 mM NH_4OAc pH 6

The reaction was attempted with cAb-Lys3-Dha104 in 500 mM NH_4OAc pH 6 with 4.6 mg Zn/Cu and 3 x 1 μL 2-PrI added over 1 hour. Slower addition of the iodide was carried out to see if precipitation could be controlled. Effervescence and subsequent loss of protein detection was observed. No adducts of Zn/Cu coordinating to antibody could be detected in

this buffer. Again, 10 % gluconic acid was added to the reaction, and a product peak was seen after 6.5 hours (**Figure 3.39**). Although the ion count is much lower than the starting material, it can be said that gluconic acid plays a positive role in competing for Zn coordination. Unfortunately, no conversion to the desired products was observed when the same conditions were applied to reaction with MeI and EtI.

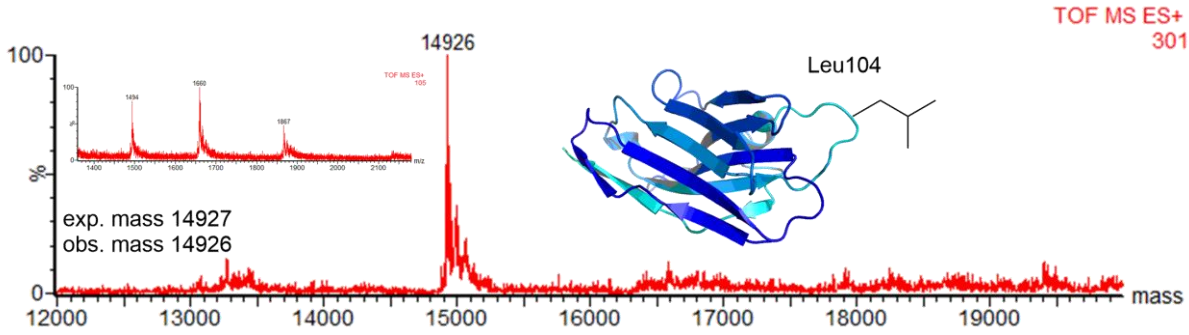

Figure 3.39. cAb-Lys3-Dha104 (500 mM NH_4OAc), 4.6 mg Zn/Cu, 3 x 1 µL 2-PrI, 6.5 hours, 10% gluconic acid, 37 °C.

Exploration of buffer pH and amount of gluconic acid

Based on the promising result above, the reaction was attempted with 2-PrI at lower pHs and with a range of gluconic acid volumes (**Table 3.13**).

Entry	500 mM NH4OAc, pH	Gluconic acid	Observations
1	4	0	No protein by LC-MS, protein precipitate.
2	4	2%	4 h – s.m., overnight – protein precipitate.
3	4	20%	No protein by LC-MS, protein precipitate.
4	6	2%	1 h – s.m. + product, low ion count, overnight – conversion, low ion count.
5	6	20%	4 h – s.m. + product, low ion count, overnight – no protein by LC-MS, protein precipitate.

Table 3.13. cAb-Lys3-Dha104 (500 µL, 3.4 nmol, c = 0.1 mg/mL), Zn/Cu (7 mg), 5 x 2 µL 2-PrI over 30 minutes, overnight, 37 °C.

The data in **Table 3.13** show that a higher amount of gluconic acid (20 %) does not result in a higher amount of antibody recovery (entries 3 and 5). This may be because a large amount of

a Zn chelator may inhibit the reaction. Also, the reaction is unsuccessful at pH 4 (entries 1 – 3, **Table 3.13**). Although conversion is observed at pH 6 with 2 % gluconic acid, loss of protein by precipitation is still high (Entry 4, **Table 3.13**).

Use of a radical initiator

Vazo44 has been used as a radical initiator previously.[73] Its potential in the context of driving this alkylation of 2-PrI to cAb-Lys3-Dha104 was explored according to the conditions in **Table 3.14**.

Entry	Vazo44/ mg	Zn/Cu/ mg	Observations
1	4.5	0	No protein by LC-MS, protein precipitate.
2	4.5	5	No protein by LC-MS, protein precipitate.

Table 3.14. cAb-Lys3-Dha104 (250 μL, 3.4 nmol, c = 0.2 mg/mL, 500 mM NH_4OAc, pH 6, 3 x 2 μL 2-PrI over 10 minutes, 45 minutes, 37 °C.

Vazo44 was not a suitable radical initiator with and without the presence of Zn/Cu as complete loss of antibody was observed within 45 minutes (**Table 3.14**). The repeated result of a loss of protein under radical conditions provides further evidence that cAb-Lys3 is not a suitable substrate for radical-mediated reactions.

Zn/Cu-mediated alkylation with sonication

As attempted with zinc previously, reaction using sonication was carried out according to the conditions described in **Table 3.15**. Unfortunately, no protein could be detected by LC-MS after 15 minutes at room temperature.

Entry	Sonication
1	yes
2	no

Table 3.15. cAb-Lys3-Dha104 (500 μL, 2.9 nmol, c = 0.09 mg/mL, NH_4OAc, pH 6), Zn/Cu (1.8 mg), 5 μL 2-PrI (25,000 eq), 15 minutes, room temperature. In both cases, protein precipitate is observed and no protein is detectable by LC-MS.

Zn/Cu-mediated alkylation with primary alkyl iodides

Although 2-PrI was used in most attempts as a model substrate for the alkylation due to its higher reactivity, the successful addition of both MeI and EtI would give rise to the non-natural amino acids ethyl glycine and norvaline respectively, inaccessible by other means. Similar conditions found to prevent complete loss of antibody in reaction of cAb-Lys3-Dha104 with 2-PrI described earlier were used, and low amounts of gluconic acid were used to act as a competitor for zinc chelation (**Table 3.16**).

Entry	EtI/ μL	Gluconic acid	Observations
1	1	0	s.m. by LC-MS, lower ion count + protein precipitate.
2	1	0.5%	s.m. by LC-MS, lower ion count + protein precipitate.
3	3	0	s.m. by LC-MS, lower ion count + protein precipitate.
4	3	0.5%	s.m. by LC-MS, lower ion count + protein precipitate.
5	3	5%	s.m. by LC-MS, lower ion count + protein precipitate.
6	3 x 0.3 over 50 minutes	0	50 mins - s.m. by LC-MS, no decrease in ion count.
7	3 x 1 over 50 minutes	0	1 h 50 mins - s.m. by LC-MS, no decrease in ion count.

Table 3.16. cAb-Lys3-Dha104 (200 μL, 1.3 nmol, c = 0.13 mg/mL, 500 mM NH_4OAc, pH 6), Zn/Cu (0.5 mg), 30 minutes unless otherwise stated, r.t.

At first, slightly milder reaction conditions of low equivalents of EtI and Zn/Cu as well as carrying out the reactions at room temperature were used as shown in **Table 3.16**. This was to see if the reaction could proceed rapidly with minimal protein loss. However, only starting material with a much lower ion count was observed for all conditions. Additionally, samples taken at 10 and 30 minutes were desalted before analysis, which did not help detection levels. Gluconic acid did not help to prevent the loss of protein. Also, the portionwise addition of very low volumes of EtI was insufficient in driving the reaction (entries 6 and 7, **Table 3.16**).

Entry	RI/ μL	Zn/Cu/ mg	Observations
1	MeI 3 x 2 over 10 minutes	2	1 h and overnight – s.m. and lower ion count, protein precipitate.

2	EtI 3 x 2 over 10 minutes	2	1 h and overnight – s.m. and lower ion count, protein precipitate.
3	MeI 3 x 10 Over 20 minutes	4	1 h – s.m. and lower ion count, overnight – no protein detected by LC-MS, protein precipitate.
4	EtI 3 x 10 Over 20 minutes	4	1 h – s.m. and lower ion count, overnight – no protein detected by LC-MS, protein precipitate.
5	MeI 50	4	1 h – s.m. and lower ion count, overnight – no protein detected by LC-MS, protein precipitate.
6	EtI 50	4	1 h – s.m. and lower ion count, overnight – no protein detected by LC-MS, protein precipitate.

Table 3.17. cAb-Lys3-Dha104 (500 µL, 0.7 nmol, c = 0.02 mg/mL, 500 mM NH_4OAc, pH 6), Zn/Cu (4 mg), 2 % gluconic acid, overnight, 37 °C.

Following this, low portionwise amounts of primary alkyl iodide and double the amount of Zn/Cu were tested at 37 °C (entries 1 and 2, **Table 3.17**). Here, conversion to desired product was not observed. Both MeI and EtI are more volatile and less reactive than 2-PrI. To compensate for this, higher portions were added (entries 3 and 4, **Table 3.17**). Unfortunately, no conversion to product as well as a loss of antibody was seen for both substrates, with complete loss after overnight incubation. Additionally, the addition of a single, large portion of MeI and EtI did not help in driving the desired reaction on cAb-Lys3-Dha104 and precipitate was observed (entries 5 and 6, **Table 3.17**).

Zn/Cu-mediated alkylation with 2-bromopropane

It was hypothesised that use of the slightly less reactive 2-bromopropane (2-PrBr) may help with loss of protein over the course of the reaction. Conditions used are described in **Table 3.18**.

Entry	2-PrBr/ µL	Temperature	Observations
1	1	r.t.	1 h and overnight – s.m. and lower ion count, protein precipitate.
2	2	r.t.	1 h and overnight – s.m. and lower ion count, protein precipitate.
3	1	37 °C	1 h – s.m. and lower ion count, overnight – no protein detected by LC-MS, protein precipitate.
4	2	37 °C	1 h – s.m. and lower ion count, overnight – no protein detected by LC-MS, protein precipitate.

Table 3.18. cAb-Lys3-Dha104 (100 μL, 2.7 nmol, c = 0.37 mg/mL, 500 mM NH_4OAc, pH 6), Zn/Cu (1 mg).

3.2.5 Indium-mediated alkylations

Indium (In) has long been known to be able to mediate chemical transformations in aqueous medium,[75,76] and in 2009, Shen and co-workers reported a method for the conjugate addition of unactivated alkyl iodides to α,β-unsaturated carbonyl compounds using indium/copper in water.[77] Unlike zinc, indium has been used on proteins before, where it was used to mediate the addition of allyl bromide to N-terminal aldehydes.[46]

It was decided to see if the conditions could be applied to the alkylation of cAb-Lys3-Dha104 with 2-PrI. Initially, the stability of cAb-Lys3 in the conditions used in the publication (In/CuI/$InCl_3$, 6:3:0.1) was tested. cAb-Lys3-Cys104 was incubated with 10,000 eq. In, and the corresponding amounts of CuI and $InCl_3$ at both room temperature and 37 °C. Samples at various time points were analysed by SDS-PAGE, and no decrease in band intensity was observed, implying stability (**Figure 3.40**). cAb-Lys3-Cys104 containing the C-terminal His tag was also tested under In conditions, and bands are progressively fainter, implying metal coordination to protein (**Figure 3.41**).

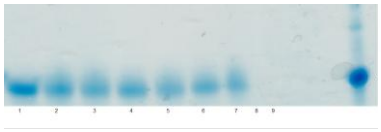

Figure 3.40. Incubation of cAbLys3-A104C under metal conditions. Metal refers to 10,000 eq. In and CuI/$InCl_3$ (6:3:0.1). Lane 1: cAb-Lys3-Cys104 (Ab), lane 2: Ab + metal, r.t., 1 h, lane 3: Ab + metal, 37 °C 1 h, lane 4: Ab + metal, r.t., 2 h, lane 5: Ab + metal, 37 °C, 2 h, lane 6: Ab + metal, r.t., 2.5 h, lane 7: Ab + metal, 37 °C, 2.5 h.

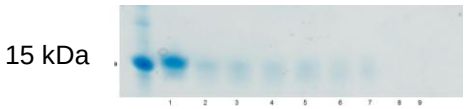

Figure 3.41. Incubation of cAbLys3 wild type (His). Metal refers to 10,000 eq. In and CuI/$InCl_3$ (6:3:0.1). Lane 1: WT-cAb-Lys3 (Ab), lane 2: Ab + metal, r.t., 30 m, lane 3: Ab + metal, 37 °C 30 m,

lane 4: Ab + metal, r.t., 1 h, lane 5: Ab + metal, 37 °C, 1 h, lane 6: Ab + metal, r.t., 2.5 h, lane 7: Ab + metal, 37 °C, 2.5 h.

Following this, the alkylation was attempted with cAb-Lys3-Dha104 (with no His tag) in both PBS (pH 7.4) and 500 mM ammonium acetate pH 6.0, with 10,000 eq. In/CuI/$InCl_3$ (6:3:0.1) and 2-PrI. Unfortunately, no product formation was seen in either buffer. Reactions were allowed to proceed for 2 days, by which time starting material only with a slight decrease in ion count was observed.

3.3 Discussion

In this chapter, combining the concept of affinity maturation of antibodies with that of site-specific protein modification has been attempted.

It was possible to site-specifically introduce Dha in the CDR3 loop of cAb-Lys3, which then proved successful as an electrophilic precursor for subsequent conjugate additions with a range of short chain alkyl thiols. These modified sulfide-containing antibody forms were characterised by LC-MS and CD. In Chapter 2, it was shown that the internal disulfide bonds of cAb-Lys3 were inert to reaction, and this was further proven by testing WT-cAb-Lys3 under the conditions used to modify cAb-Lys3-Dha104. No changes in mass were observed in the control reactions, and WT-cAb-Lys3 used retained binding to lysozyme. This proved that the site of reaction was position 104 only. The modification to the sulfide groups resulted in a diminishing of binding ability to antigen lysozyme, and thus, the concept of 'Chemical Affinity Maturation' was not proven. It is not known why the single modification caused such a drastic change in behaviour. As shown in Chapter 2, the mutation from an alanine at position 104 of cAb-Lys3 to cysteine did result in a decrease of binding affinity, and perhaps the further addition of methylene units added too much steric hindrance to allow the CDR3 loop to fit into the active site cleft of lysozyme. It can be postulated that the modification may have caused a change in the overall conformation of the loop, but as the loop itself is quite flexible, it was thought that obtaining a crystal structure of the modified cAb-Lys3 forms may not provide insight into reasons for the loss of binding. Using Dha as a precursor means that products arising from subsequent reactions may be epimeric, and only one of the diastereomers may have been active. This effect has not yet been studied on proteins, and is likely to be dependent on each protein in question. Slightly higher amounts of antibody were subjected to ELISAs, but still no binding to lysozyme was observed, implying that the

problem is the new chemical group introduced and not the conformation. To further test this, the same sulfide-containing cAb-Lys3 forms were synthesised by adding short chain alkyl iodides directly to cAb-Lys3-Cys104. By ELISA, no binding was observed, and by SPR also, supporting the hypothesis that the chemical modification itself is responsible for the lack of binding. When cAb-Lys3-Cys104 was reacted with the alkyl iodides EtI and PrI, only single addition was observed. However, for control experiments where alkyl iodides were added to WT-cAb-Lys3, non-selective alkylation was observed. This shows that the reaction at cysteine proceeds at a faster rate than the non-selective sites. The alkylated WT-cAb-Lys3 forms retained binding to lysozyme, despite being modified; reiterating the fact that the residue position 104 is pivotal to binding, but modifications may be carried out at other sites with the retention of binding, and that the presence of the non-natural residues at position 104 is responsible for the loss of binding. Following the loss of binding on reactions of cAb-Lys3-Dha104 with short chain alkyl thiols, it was decided to proceed with another method for extending the number of methylene units within the CDR3 loop at position 104. The zinc-mediated alkylation to α,β-unsaturated systems pioneered by Luche,[50] and carried out on electron deficient amino acid derivatives since[55,56] was attempted as a potential method for extending the number of methylene units at position 104 by carbon-carbon bond formation. The reaction had been carried out previously in the group on the protein SBL, but a major side reaction of suspected hydrolysis at Dha was observed.[17] Investigations into this are ongoing in the group. During reaction attempts with cAb-Lys3, hydrolysis at Dha was not observed. Instead, the antibody appeared to be unstable to the required reactions conditions. Multiple factors were tested, including buffer concentration and pH, reagent equivalents, zinc and zinc-copper, temperature, time, sonication and zinc chelating reagents. Unfortunately, a reliable and reproducible method could not be found with any of the alkyl iodide substrates tested (MeI, EtI, 2-PrI), and protein precipitation occurred in every condition. Each reaction

attempt was analysed by LC-MS, and either no protein could be detected, or a small amount was – indicating significant protein loss as a result of the attempted reaction. The antibody was stable to incubation with the reaction components individually, but once they were all present, precipitation occurred. The reaction is known to be highly exothermic,[17,50] and this may explain why protein was lost. The results here show that the zinc-mediated alkylation of cAb-Lys3 is not a suitable choice for modifications. The modification of proteins using zinc has not been described previously. The reaction was also attempted with indium, but no conversion or significant loss of protein was observed. Given the increased popularity of the use of transition metals for protein modifications,[30] perhaps an alternative metal may be more suitable, and or a less exothermic reaction. The aim of this project was to try and create a more potent antibody by increasing the strength of the non-covalent hydrophobic interactions within the binding space. Perhaps a covalent strategy may be more useful and perhaps generally applicable, where non-natural amino acids are introduced in the CDR3 loop of the antibody, but also in the antigen epitope, and subsequent orthogonal cross-linking may be successful in strengthening interactions. If successful, the Zn-mediated alkylation of cAb-Lys3-Dha104 with 2-PrI could have led to the formation of an epimeric mixture of cAb-Lys3-Leu104. Therefore, the effect of epimerisation on binding may be explored further by carrying out a genetic mutation at position 104 to leucine, and testing its binding capability to lysozyme.

3.4 Conclusions

The site-specific chemical installation of dehydroalanine into the CDR3 loop of cAb-Lys3 has been described. After optimisation, a facile method for Dha incorporation was found using ambient conditions. cAb-Lys3-Dha104 was found to be a suitable electrophilic species for the addition of various short chain alkyl thiols. Although the modifications forming cAb-Lys3 sulfide adducts were chemically successful, the incorporation of these non-natural groups resulted in the complete inhibition of binding to antigen lysozyme. The modified cAb-Lys3 forms retained β-sheet structure, which led us to conclude that an unfavourable change in the conformation of the CDR3 loop or interactions may have been the cause of this. Next, a Zn-mediated radical addition of alkyl iodides to cAb-Lys3-Dha104 was attempted. A wealth of conditions were used, but on the whole, antibody was found to be unstable to the required reaction conditions.

3.5 Experimental

cAb-Lys3-Cys104 + DTT. Disulfide at position 104 was reduced with DTT. DTT (1.2 mg, 7.8 μmol) was added to 0.5 mL of cAb-Lys3 (wild type or A104C, c = 1 mg/mL, PBS pH 8.0) and shaken (600 rpm) at room temperature for 5 minutes. After this time, the protein solution was passed through a PD minitrap (GE Healthcare), previously equilibrated with PBS (pH 8.0), eluting with 1 mL of the same buffer. The reduced protein was used immediately.

cAb-Lys3-Cys104 + MSH 3.1. A solution of MSH **3.1** was prepared in DMF (2 mg in 1.4 mL). 12.5 μL of this solution was added to reduced cAb-Lys3-Cys104 (250 μL, 7.9 nmol, c = 0.5 mg/mL, PBS pH 8). After 10 minutes of shaking (600 rpm) at room temperature, the reaction was analysed by LC-MS.

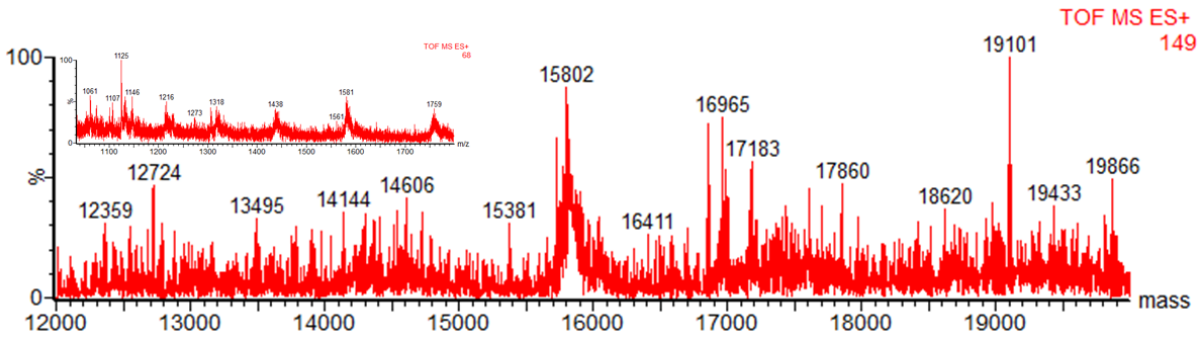

Experimental Figure 3.1. MS for cAb-Lys3-Cys104 + 10 eq. MSH **3.1**. Peaks are unidentifiable and ion count is low indicating multiple reactions and also protein degradation.

cAb-Lys3-Cys104 + 1,4-diiodobutane 3.2. cAb-Lys3-Cys104 was reduced as described above. 1,4-diiodobutane **3.2** (3 μmol, 22.7 μmol, 7,000 eq.) was added to DMF/ DMSO, vortexed, and added to the protein aliquot (cAb-Lys3-Cys104, 100 μL, 3.2 nmol, c = 0.5 mg/mL, PBS pH 8). The resulting emulsion was vortexed and then shaken vigorously (600 rpm) at 37 °C for 2 hours. Aliquots were analysed by LC-MS, no conversion to product was observed.

cAb-Lys3-Cys104 + dibromo reagent 3.3 (with DMF as a co-solvent). The dibromo derivative (100mg, 0.33 mmol) was dissolved in 1.2 mL DMF. 20 μL was added to reduced cAb-Lys3-Cys104 (100 μL, 3.2 nmol, c = 0.5 mg/mL, PBS pH 8) and the resulting solution shaken vigorously (600 rpm) at room temperature for 30 minutes. An aliquot was taken for LC-MS (exp. mass 16018, obs. mass 16015). The reaction mixture was then shaken vigorously at 37 °C for 2 hours. An aliquot was analysed by LC-MS. Full conversion to Dha was observed.

cAb-Lys3-Cys104 + dibromo reagent 3.3 (no co-solvent). 3.3 (1.2 mg, 3.3 μmol, 100 eq.) was added to a 1.5 mL plastic tube. An aliquot of the reduced cAb-Lys3-Cys104 prepared above (990 μL, 31.3 nmol, c = 0.5 mg/mL, PBS pH 8) was added to the same tube. The reaction was shaken (600 rpm) at 37 °C for 3 hours. The reaction was then cooled to room temperature and insoluble material was removed by centrifugation (1 minute, 16K g). LC-MS analysis of the supernatant revealed full conversion to a protein with a mass corresponding to the formation of dehydroalanine.

cAb-Lys3-Dha104 + β-Mercaptoethanol. To cAb-Lys3-Dha104 (250 μL, 4.0 nmol, c = 0.25 mg/mL, PBS pH 8) was added β-mercaptoethanol (5 μL, 70.4 μmol, 17,000 eq.) and the reaction shaken for 1 hour at 37 °C, after which the reaction was analysed by LC-MS.

cAb-Lys3-Dha104 + RSH. To cAb-Lys3-Dha104 (500 μL, 15.9 nmol, c = 0.25 mg/mL) was added 3 x 20 μL RSH (EtSH, PrSH, 2-PrSH) over 30 minutes while shaking (600 rpm) at 37 °C. Reactions were continued for a further 2 hours. LC-MS revealed full conversion to the cAb-Lys3-sulfide adducts. Reactions were desalted through a PD10 minitrap. All manipulations using thiols were carried out in a fume hood, and waste washed in a bleach bath before disposal.

Wild type controls. WT-cAb-Lys3 was treated in exactly the same way as described for the reactions of the mutant cAb-Lys3-Cys104.

Test with Ellman's reagent. The same protocol as described in Chapter 2 was used.

ELISA. ELISA was carried out according to the protocol described in Chapter 2.

Asp-N Digest and LC-MS/MS Analysis of cAb-Lys3-Dha104. The same protocol used in **Chapter 2 Experimental Section** was followed.

cAb-Lys3-Dha104

a **Associated Datafile: SG_104DHA_071212 a (50 - 1990 amu)**
AspN:-/D

Frag#	Res#	Sequence	Theor (Bo)	[M+H]	[M+2H]	[M+3H]
D4	90-98	(E)DTAIYYBAA(D)	1046.44	1047.45	524.23	349.82
D2	62-72	(A)DSVKGRFTISQ(D)	1236.65	1237.65	619.33	413.22
D3	73-89	(Q)DNAKNTVYLLMNSLEPE(D)	1949.94	1950.95	975.98	650.99
■D5	99-120	(A)DSTIYZSYYEBGHGLSTGGYGY(D)	2417.97	2418.98	1210.00	807.00
D6	121-146	(Y)DSWGQGTQVTVSRENLYFQGHHHHHH(-)	3093.41	3094.42	1547.71	1032.14
D1	1-61	(-)DVQLVESGGGSVQAGGSLRLSBAASGYTIGPYBMGWFRQAPGKEREGVAAINMGGGITYYA(D)	6331.12	6332.13	3166.57	2111.38

b

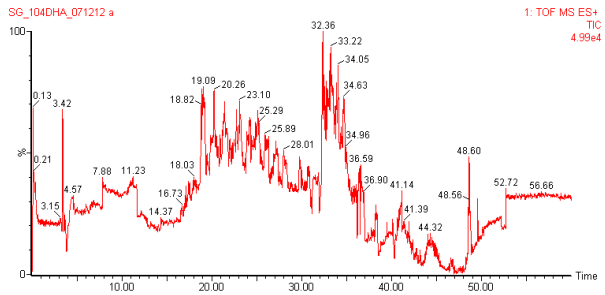

c

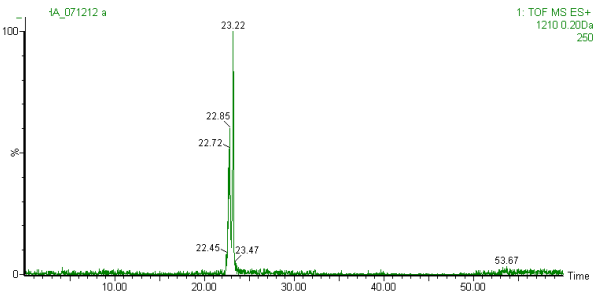

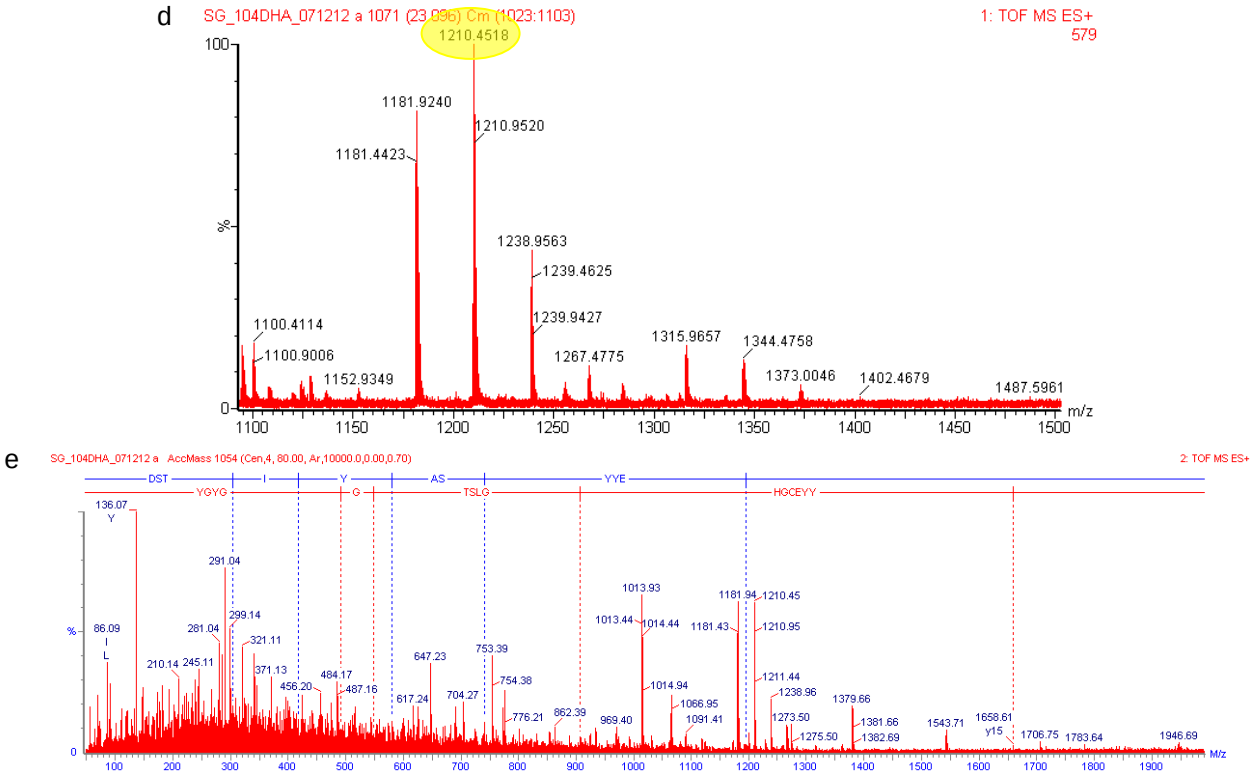

Experimental Figure 3.2. Enzymatic digest of cAb-Lys3-Dha104 and sequencing. a) Expected sequences and theoretical masses of the peptides resulting from digestion of cAb-Lys3-Dha104 with Asp-N. Masses identified in the mass spectrum integrated over the whole LC-MS chromatogram are highlighted in black (ΔDa = 0.1). B corresponds to carboxymethylamide cysteine, Z is Dha. b) LC-MS chromatogram. c) Extracted mass chromatogram for the theoretical mass $[D5+2H]^{2+}$: M = 1210.00. d) MS of peak at 22.72 – 23.22 minutes. e) MS/MS of peptide D5, Dha (denoted as A) is observed at position 104.

HDX MS. (Performed and analysed by Rachel Garlish (UCB))

Samples were prepared as described above and concentrated to:

Lysozyme at 100 µM, cAb-Lys3-SEt104 at 100 µM, cAb-Lys3-SPr104 at 100 µM, cAb-Lys3-Dha104 at 100 µM, WT-cAb-Lys3 at 100 µM.

The samples were desalted 3 times using Zeba desalting columns and Ammonium Acetate (100mM, adjusted to pH8). The samples were run on the LCT Premier Mass Spectrometer at a source pressure of 3.5.

WT-cAb-Lys3

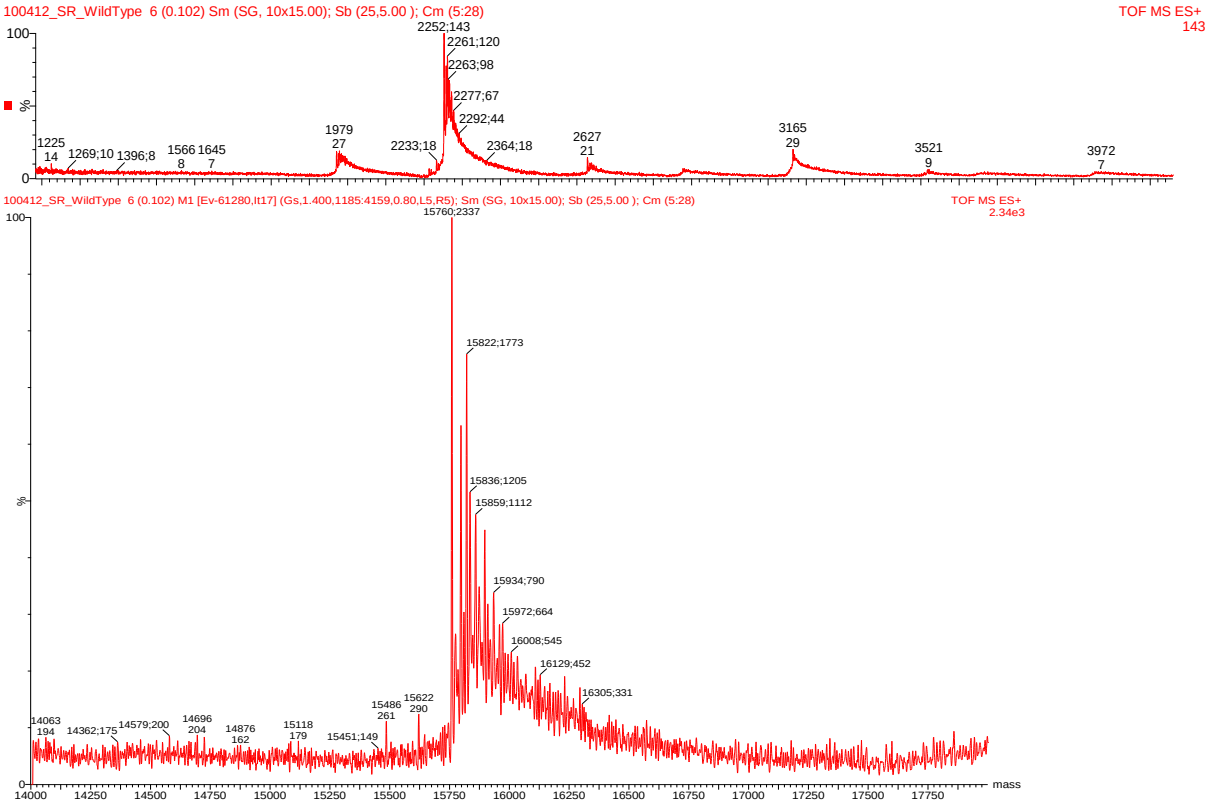

Spec. 13 : WT-cAb-Lys3 (100µM) Top is m/z spectrum, bottom is deconvoluted mass.

cAb-Lys3-Dha104

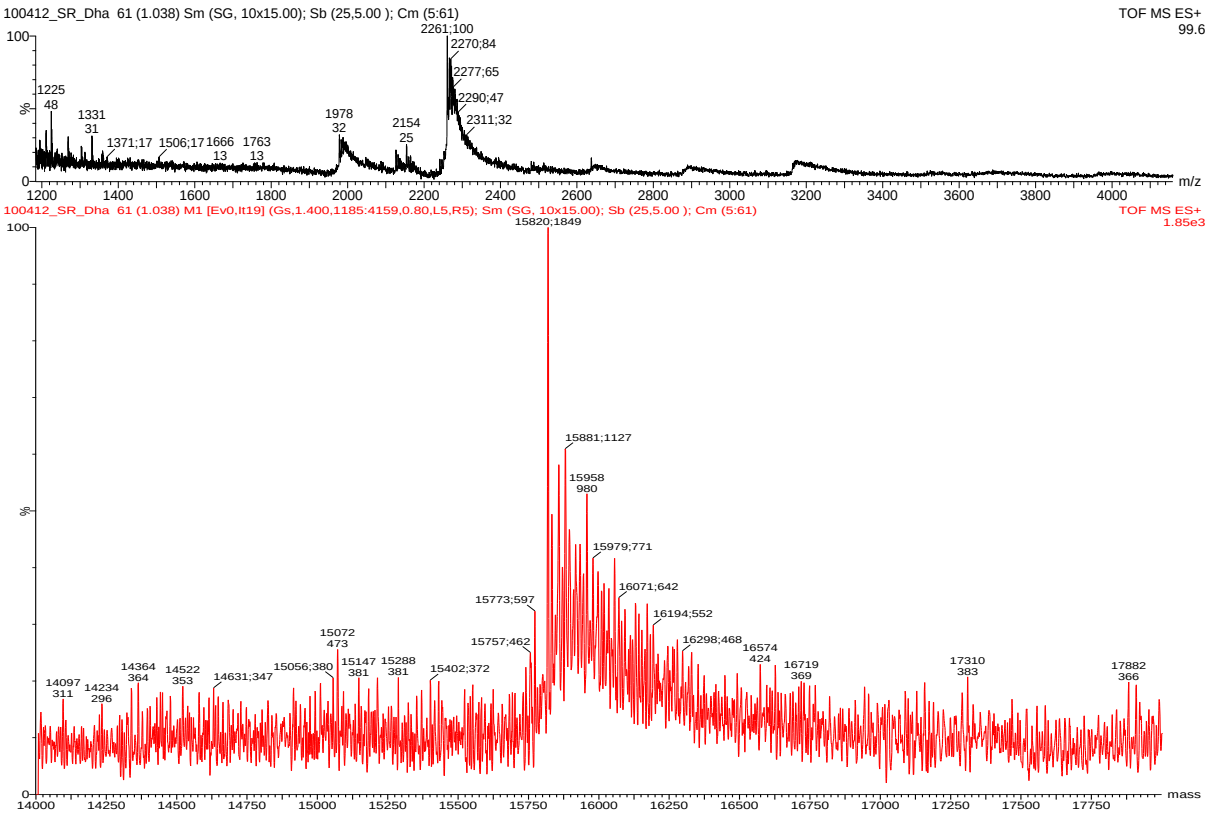

Spec. 14 : cAb-Lys3-Dha104 (100µM) Top is m/z spectrum, bottom is deconvoluted mass.

cAb-Lys3-SEt104

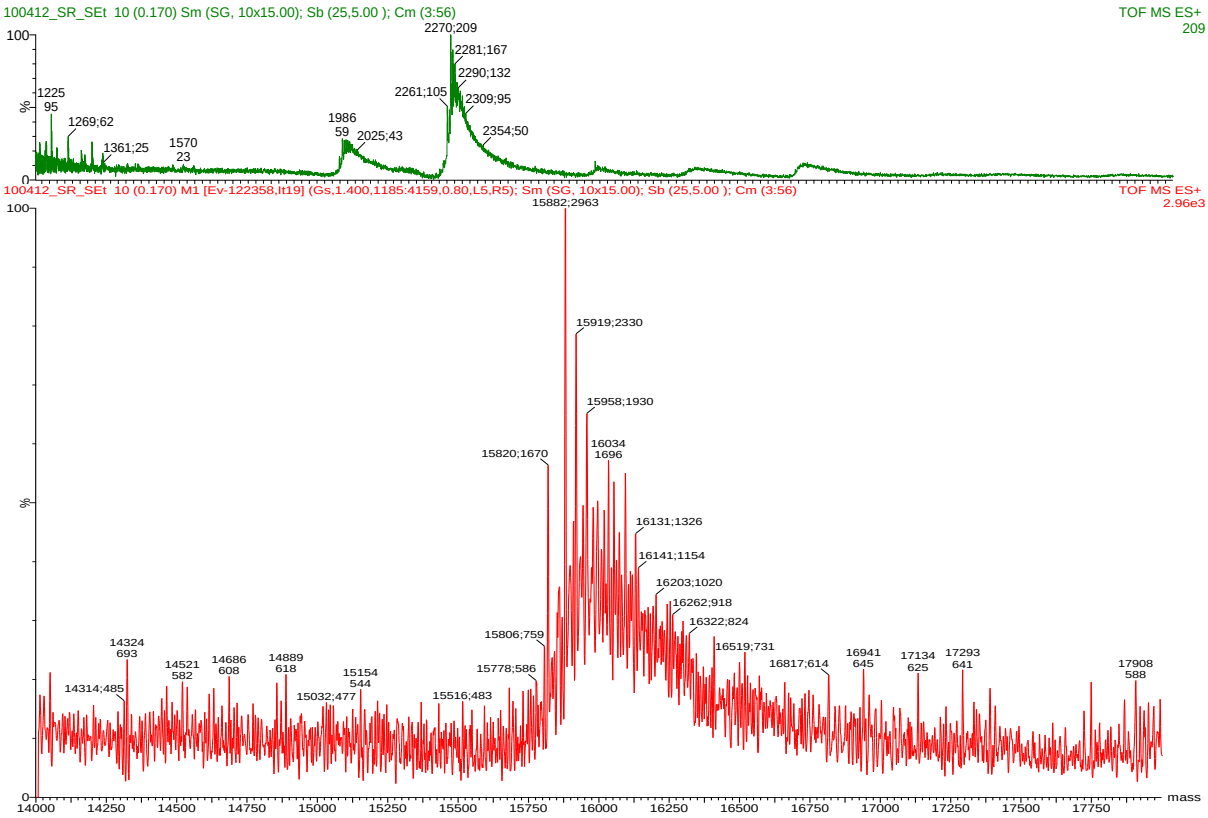

Spec. 15 : cAb-Lys3-SEt104 (100µM) Top is m/z spectrum, bottom is deconvoluted mass.

cAb-Lys3-SPr104

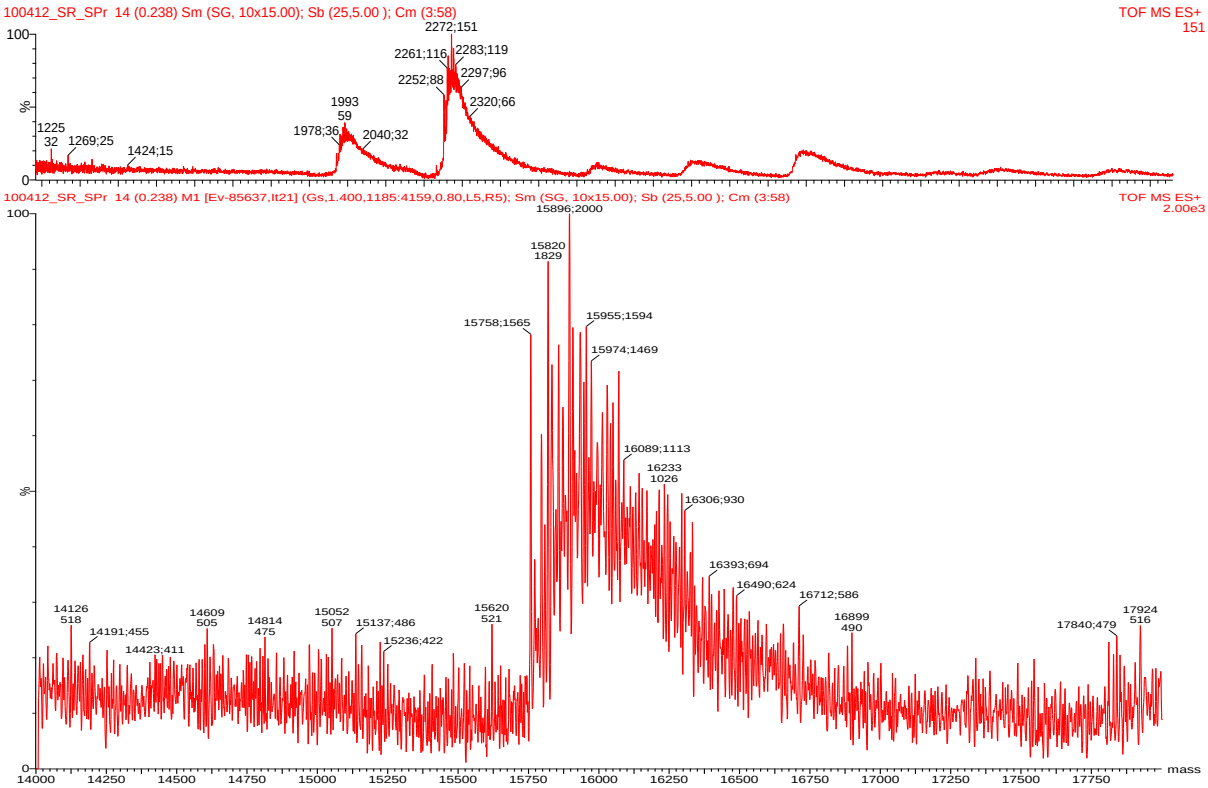

Spec. 16 : cAb-Lys3-SPr104 (100µM) Top is m/z spectrum, bottom is deconvoluted mass.

Next, the four antibodies were mixed 1:1 with lysozyme that had been diluted to 20µM and 10µM.

WT-cAb-Lys3

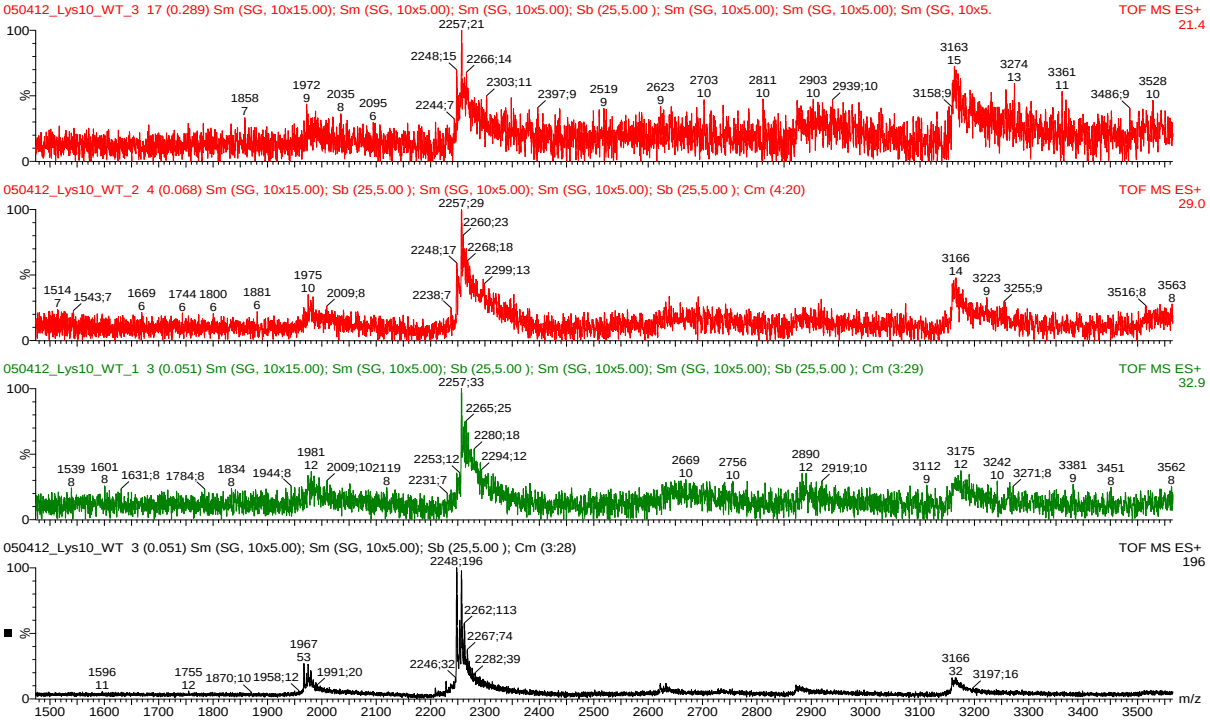

Spec. 17 : WT-cAb-Lys3 (100µM) with Lysozyme (10µM).
Incubation and pressure from top to bottom : 2 hours, pressure 2.7, 1 hour 30 minutes, pressure 3.0, 1 hour, pressure 3.6, no incubation, pressure 3.6.
No lysozyme or lysozyme + WT-cAb-Lys3 peaks can be seen in the spectrum.

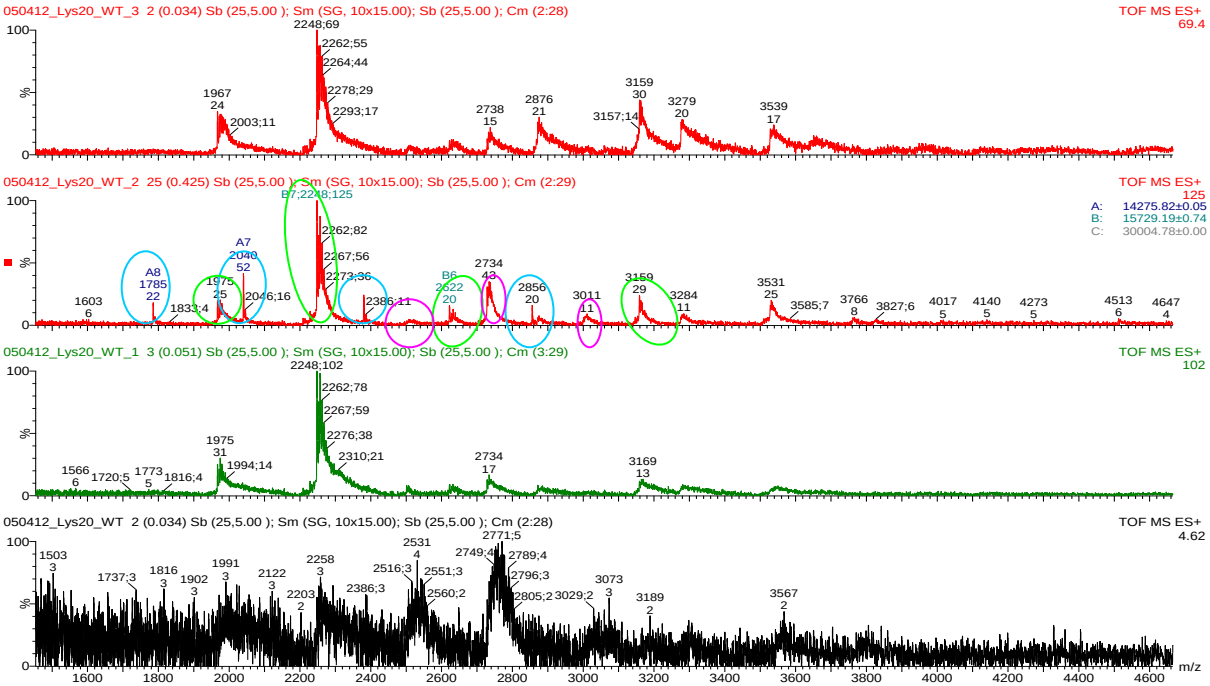

Spec. 18 : WT-cAb-Lys3 (100µM) with Lysozyme (20µM).
Incubation and pressure from top to bottom : 2 hours, pressure 2.7, 1 hour 30 minutes, pressure 3.0, 1 hour, pressure 3.6, no incubation, pressure 3.6.
For the spectrum with incubation 1 hour 30 minutes at pressure 3.0 peaks can be seen for the lysozyme alone (blue), WT-cAb-Lys3 alone (green) and for lysozyme + WT-cAb-Lys3 (purple).

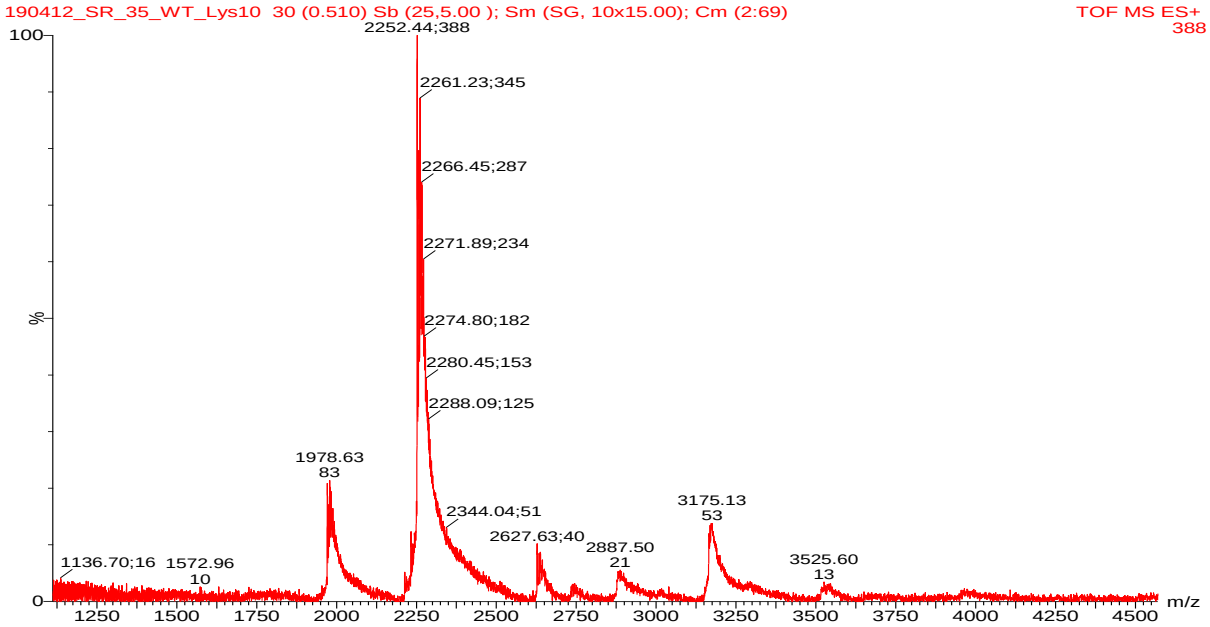

Spec. 19 : WT-cAb-Lys3 (100µM) with Lysozyme (10µM).
Incubated for 2 days and run at pressure 3.5. Only WT-cAb-Lys3 peaks seen.
Deconvoluted mass 15760.

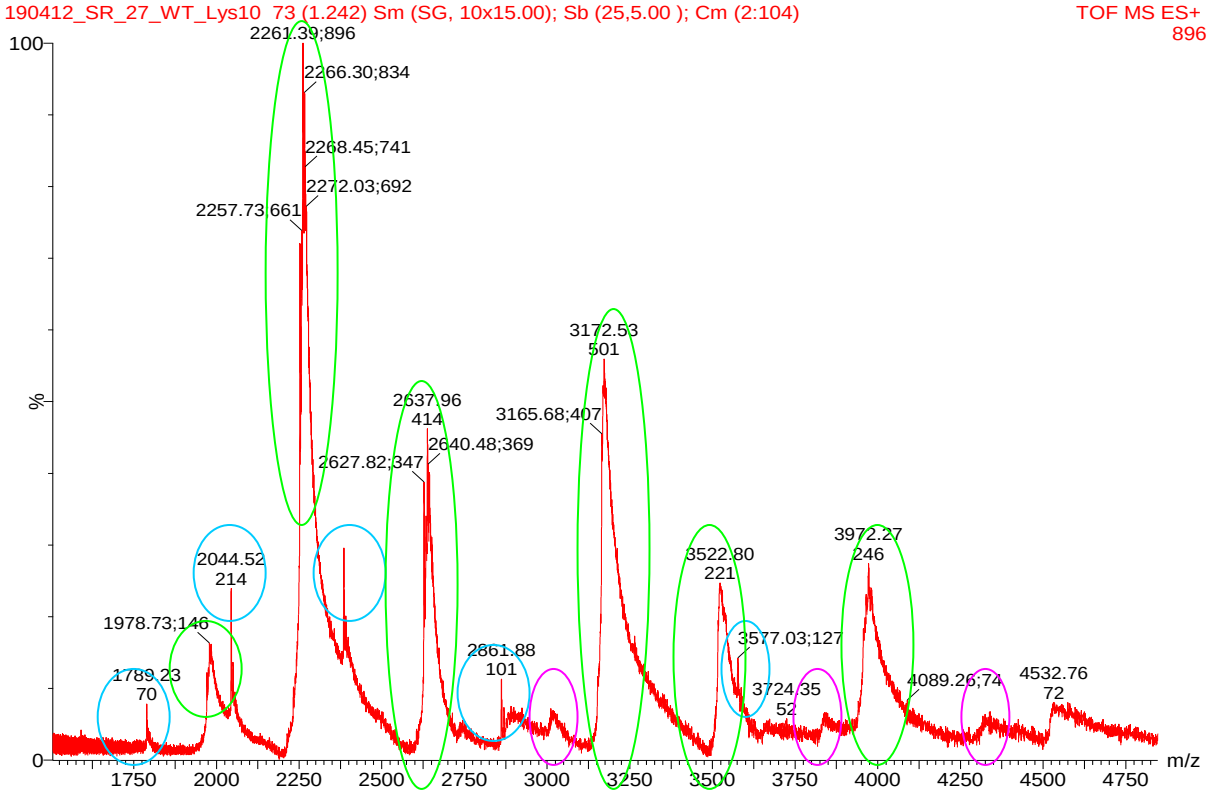

Spec. 20 : WT-cAb-Lys3 (100µM) with Lysozyme (10µM).
Incubated for 2 days and run at pressure 2.7.
Peaks can be seen for the lysozyme alone (blue), WT-cAb-Lys3 alone (green) and for lysozyme + WT-cAb-Lys3 (purple).
The bound peaks are very small and could be clearly deconvoluted.
cAb-Lys3-Dha104

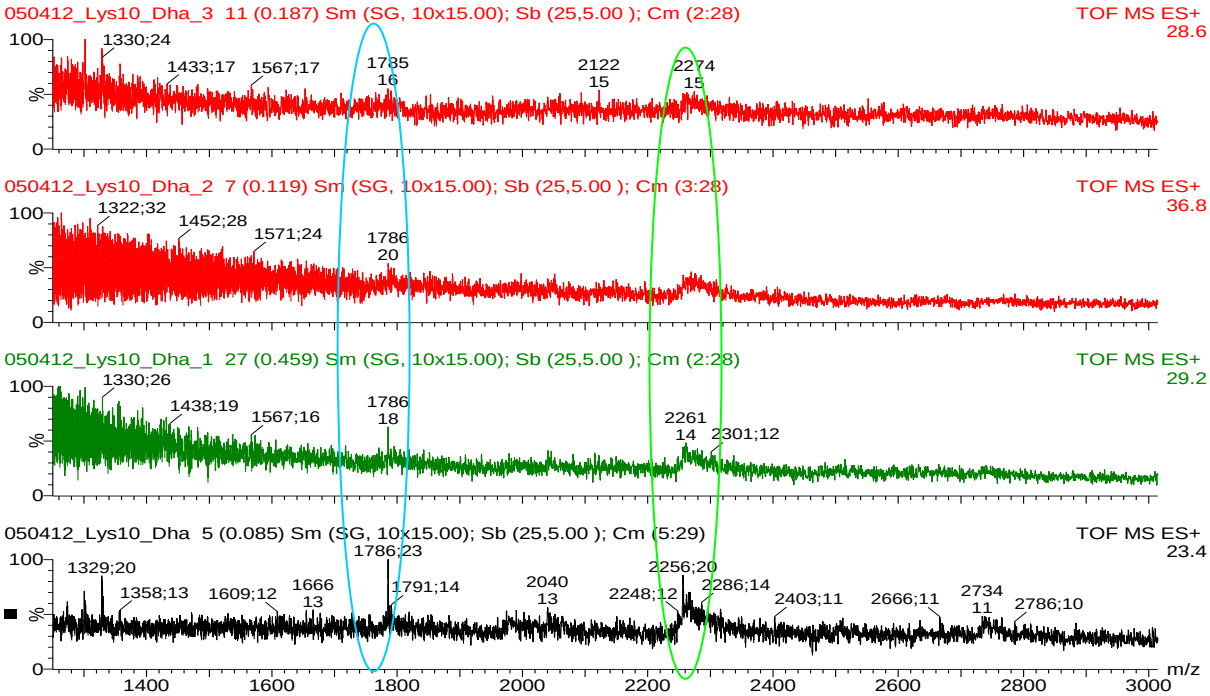

Spec. 21 : cAb-Lys3-Dha104 (100µM) with Lysozyme (10µM).
Incubation and pressure from top to bottom : 2 hours, pressure 2.7, 1 hour 30 minutes, pressure 3.0, 1 hour, pressure 3.6, no incubation, pressure 3.6.
The spectra are all very noisy, in the no incubation spectra there is one peak for lysozyme (blue) and one for the cAb-Lys3-Dha104 (green). These get more difficult to see as the incubation time increases.

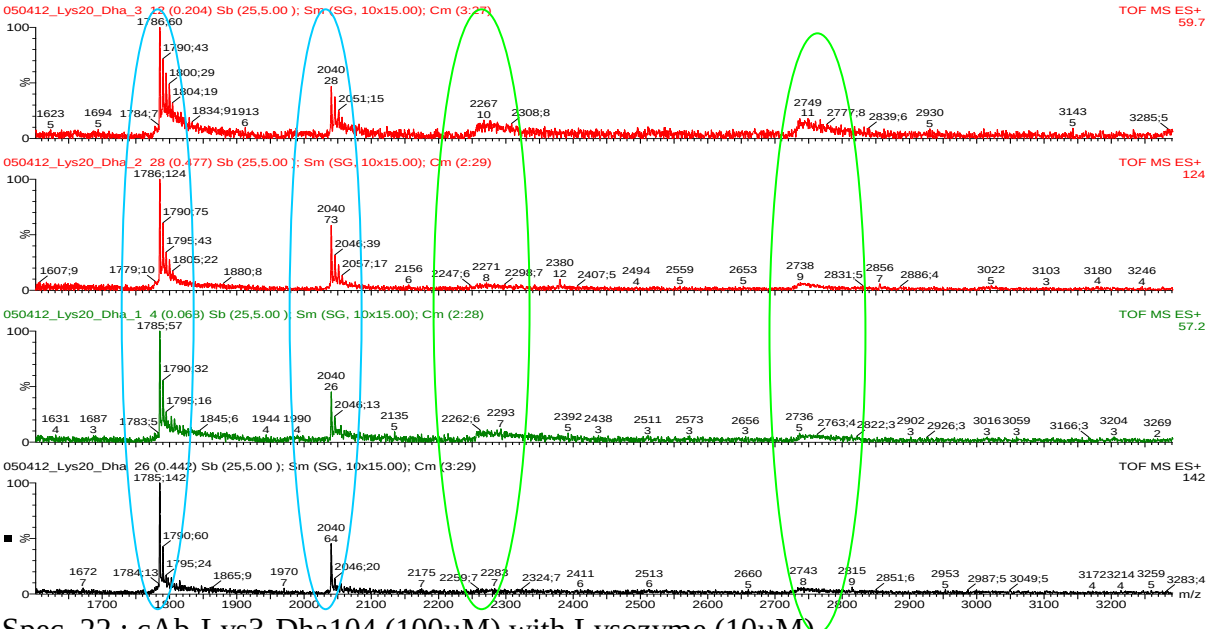

Spec. 22 : cAb-Lys3-Dha104 (100µM) with Lysozyme (10µM).
Incubation and pressure from top to bottom : 2 hours, pressure 2.7, 1 hour 30 minutes, pressure 3.0, 1 hour, pressure 3.6, no incubation, pressure 3.6.
The lysozyme peaks can be seen clearly (blue) but the cAb-Lys3-Dha104 peaks (green) are difficult to determine, especially with shorter incubation time.

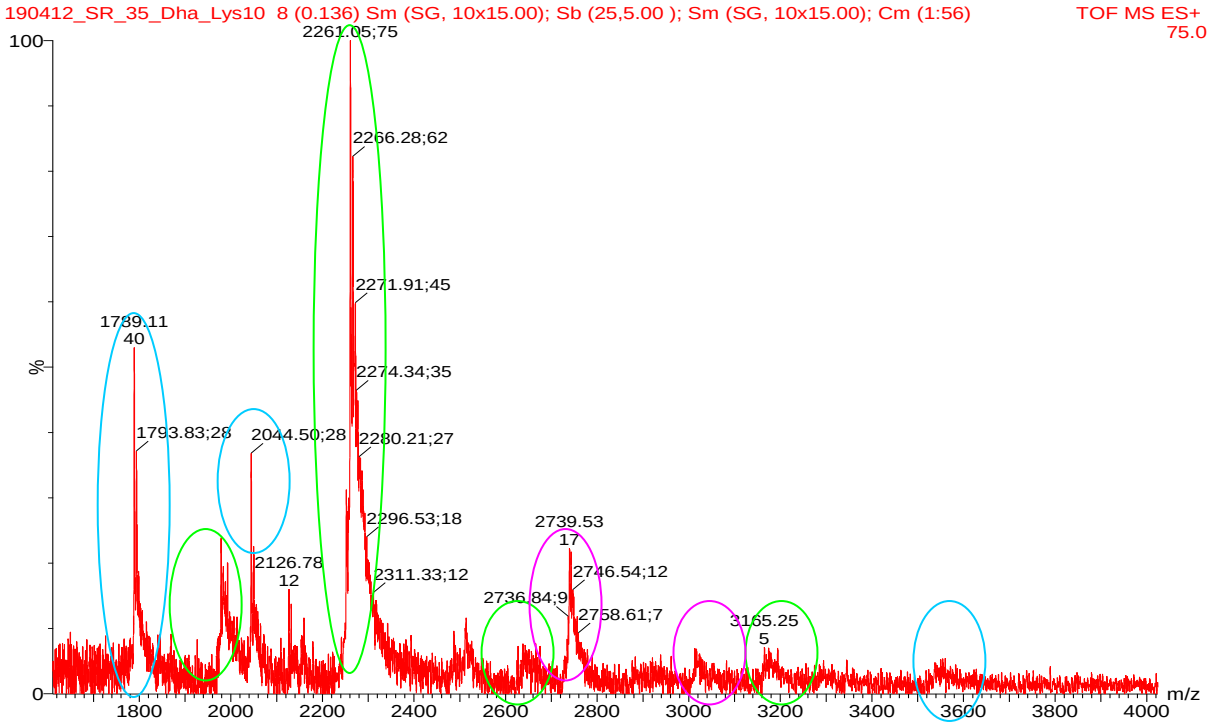

Spec. 23 : cAb-Lys3-Dha104 (100µM) with Lysozyme (10µM).
Incubated for 2 days and run at pressure 3.5. Peaks can be seen for the lysozyme (blue) and the cAb-Lys3-Dha104 (green) and some small peaks indicate there may be a small amount of complex (purple) but this is difficult to quantify due to the noise.

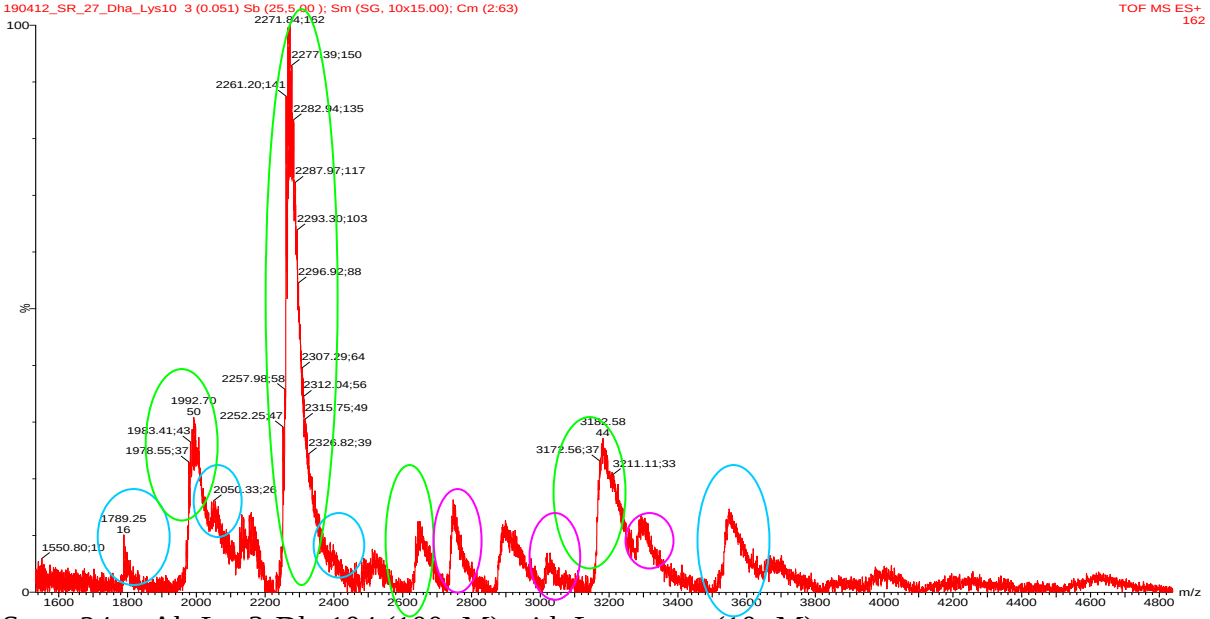

Spec. 24 : cAb-Lys3-Dha104 (100µM) with Lysozyme (10µM).
Incubated for 2 days and run at pressure 2.7. Peaks can be seen for the lysozyme (blue) and the cAb-Lys3-Dha104 (green) and some small peaks indicate there may be a small amount of complex (purple). Deconvolutiong gave a small, broad, peak around a mass of 30000 which would indicate that cAb-Lys3-Dha104 is binding to Lysozyme.

cAb-Lys3-SEt104

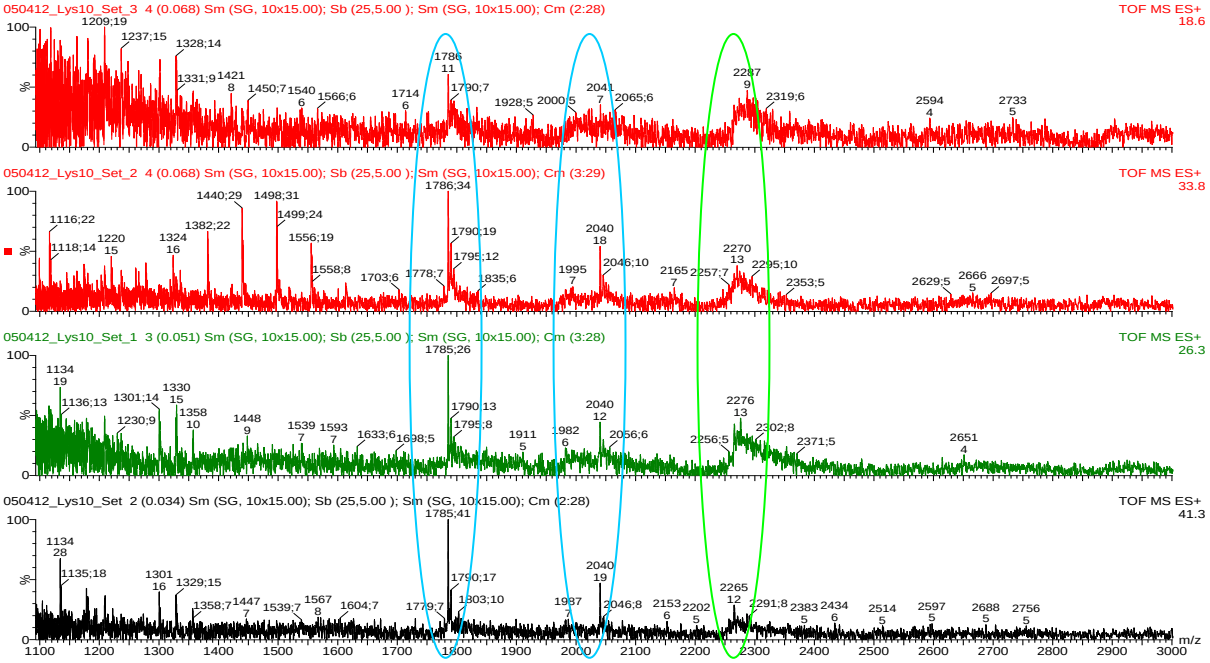

Spec. 25 : cAb-Lys3-SEt104 (100µM) with Lysozyme (10µM).
Incubation and pressure from top to bottom : 2 hours, pressure 2.7, 1 hour 30 minutes, pressure 3.0, 1 hour, pressure 3.6, no incubation, pressure 3.6.
The lysozyme peaks can be clearly seen (blue) but the cAb-Lys3-SEt104 peaks are more broad and noisy (green).

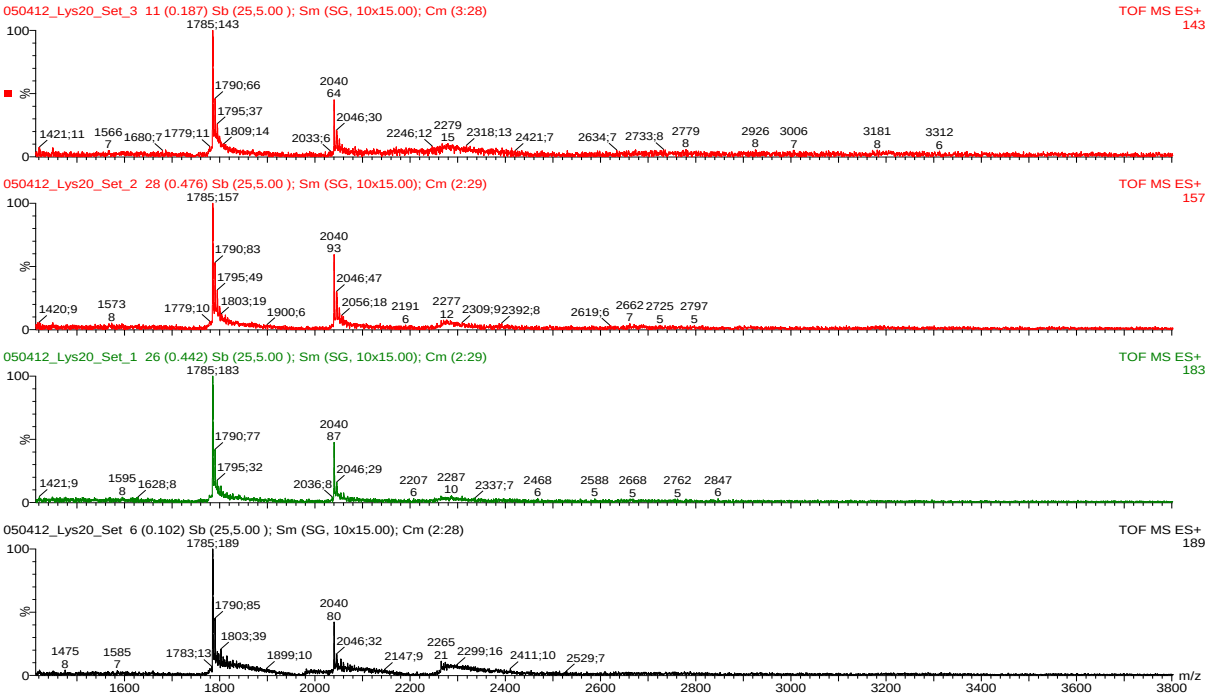

Spec. 26 : cAb-Lys3-SEt104 (100µM) with Lysozyme (20µM).
Incubation and pressure from top to bottom : 2 hours, pressure 2.7, 1 hour 30 minutes, pressure 3.0, 1 hour, pressure 3.6, no incubation, pressure 3.6.
The spectra are the same as for the 10µM Lysozyme but with less noise.

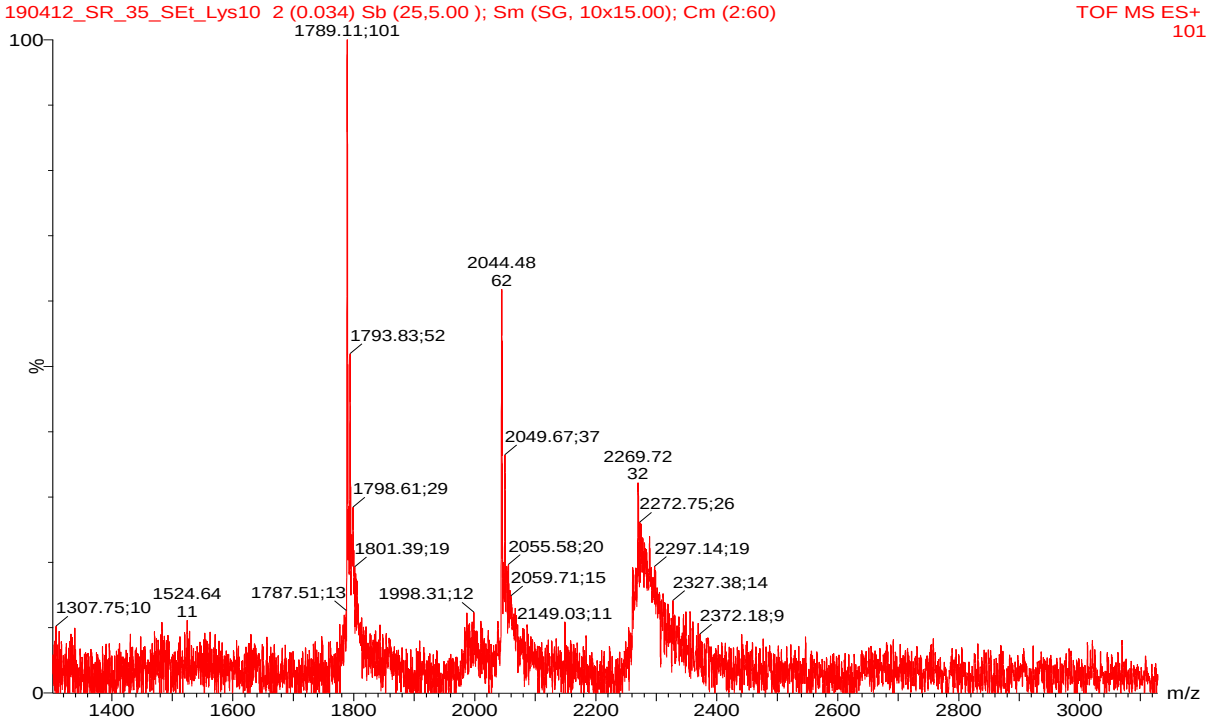

Spec. 27 : cAb-Lys3-SEt104 (100µM) with Lysozyme (10µM).
Incubated for 2 days and run at pressure 3.5.
No binding.

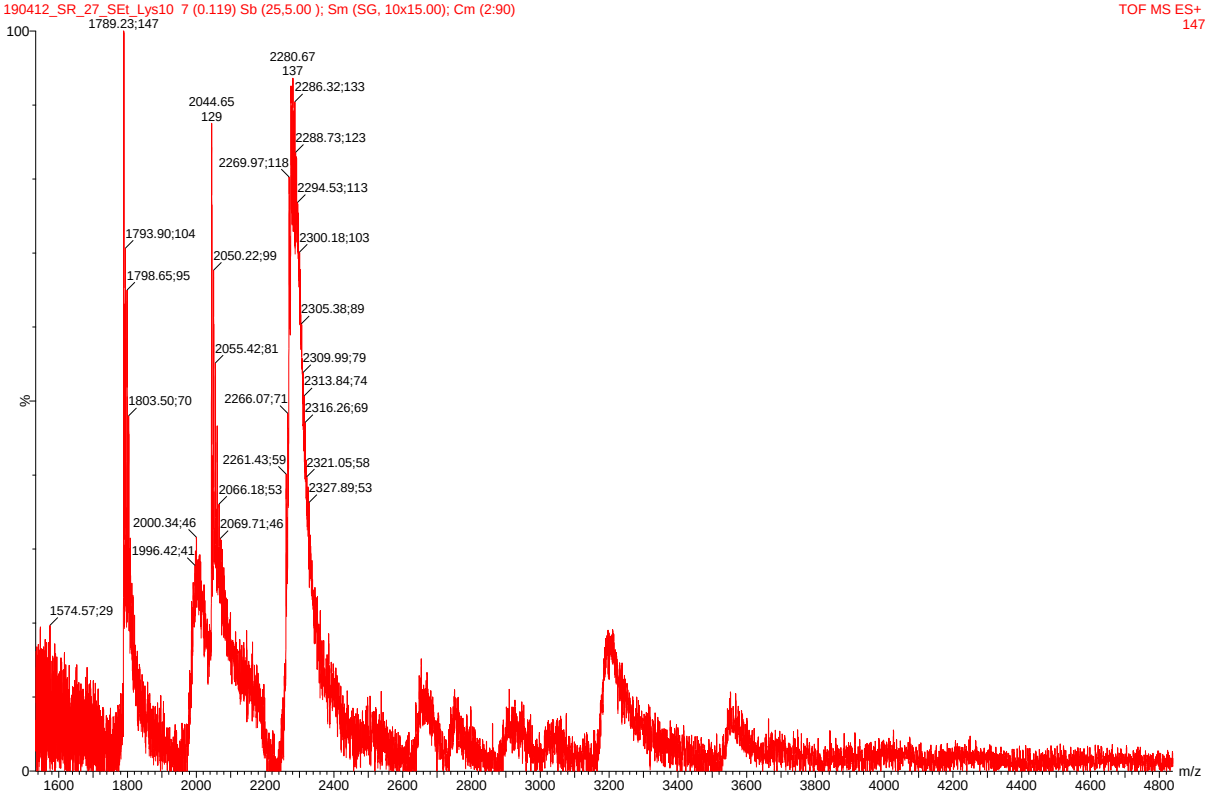

Spec. 28 : cAb-Lys3-SEt104 (100µM) with Lysozyme (10µM).
Incubated for 2 days and run at pressure 2.7.
No binding.
Spr

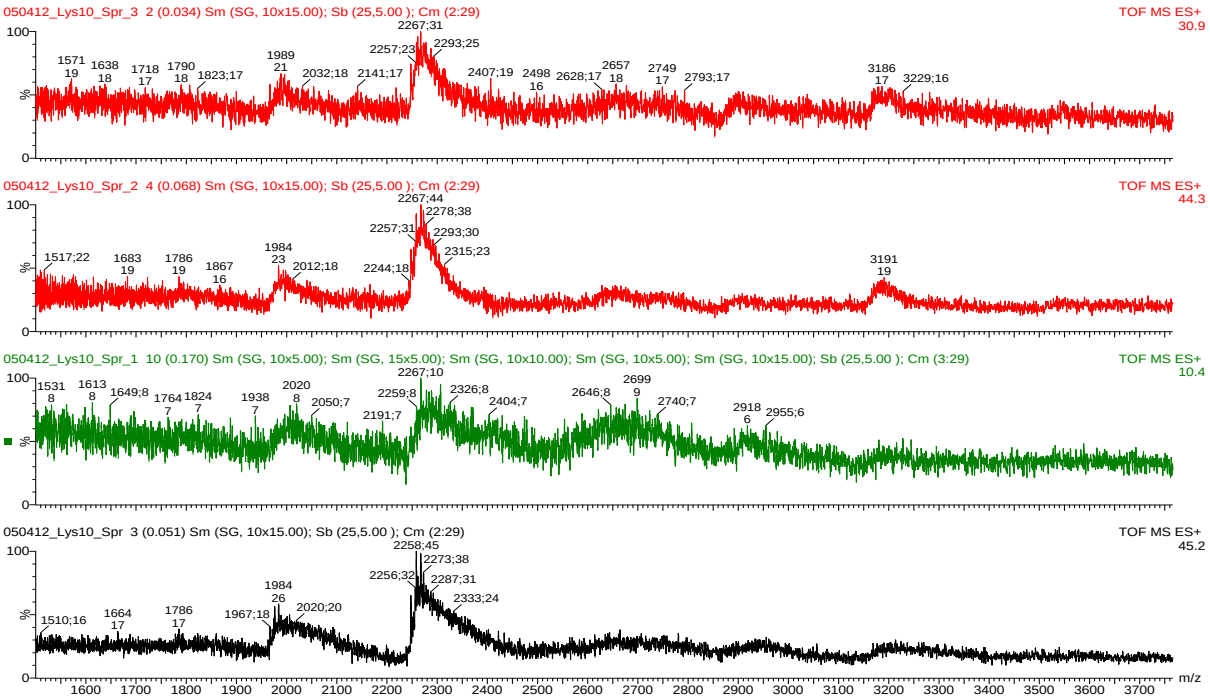

Spec. 29 : cAb-Lys3-SEt104 (100µM) with Lysozyme (10µM).
Incubation and pressure from top to bottom : 2 hours, pressure 2.7, 1 hour 30 minutes, pressure 3.0, 1 hour, pressure 3.6, no incubation, pressure 3.6.
Only very broad and noisy Spr peaks can be seen.

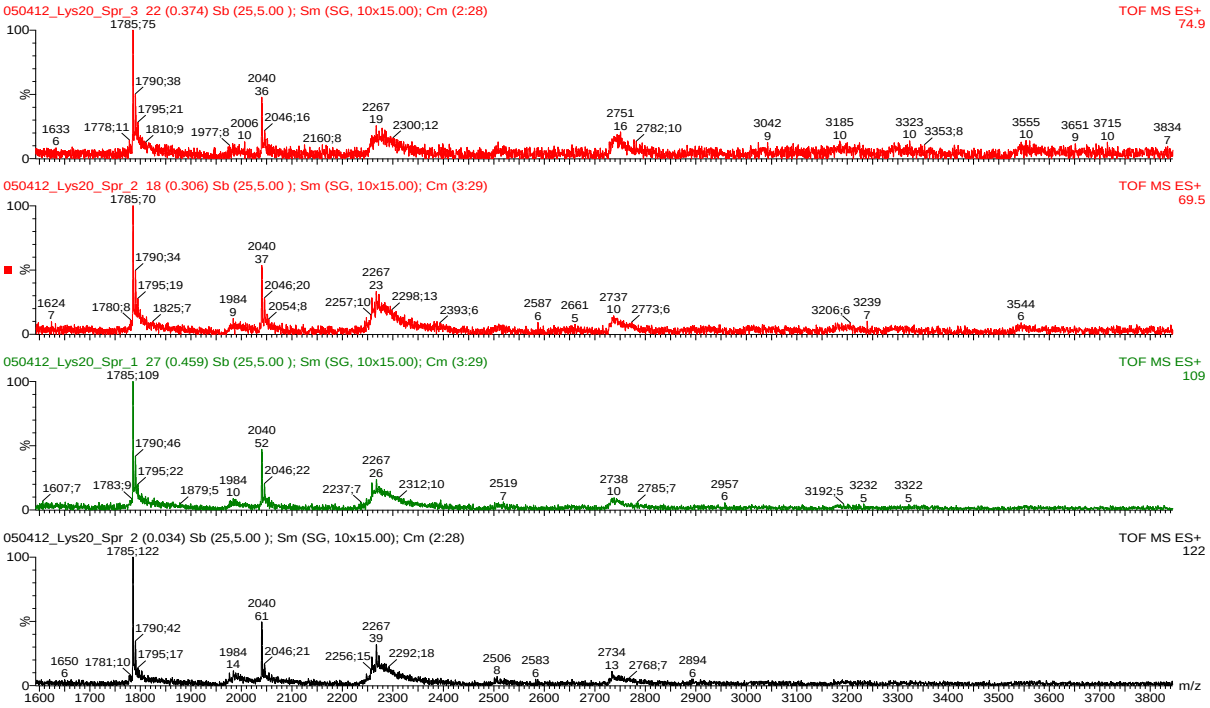

Spec. 30 : cAb-Lys3-SEt104 (100µM) with Lysozyme (20µM).
Incubation and pressure from top to bottom : 2 hours, pressure 2.7, 1 hour 30 minutes, pressure 3.0, 1 hour, pressure 3.6, no incubation, pressure 3.6.
Peaks for both the lysozyme and the cAb-Lys3-SEt104 can now be seen, no binding is seen.
cAb-Lys3-SPr104

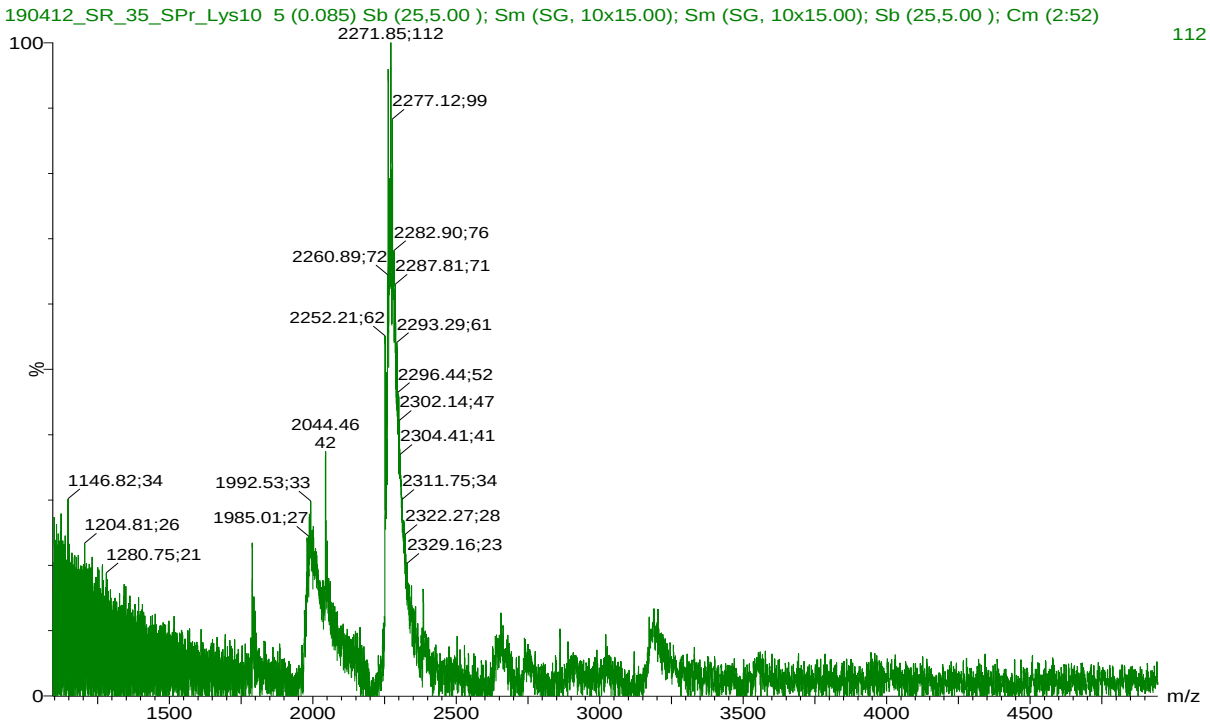

Spec. 31 : cAb-Lys3-SPr104 (100µM) with Lysozyme (10µM).
Incubated for 2 days and run at pressure 3.5.
No binding.

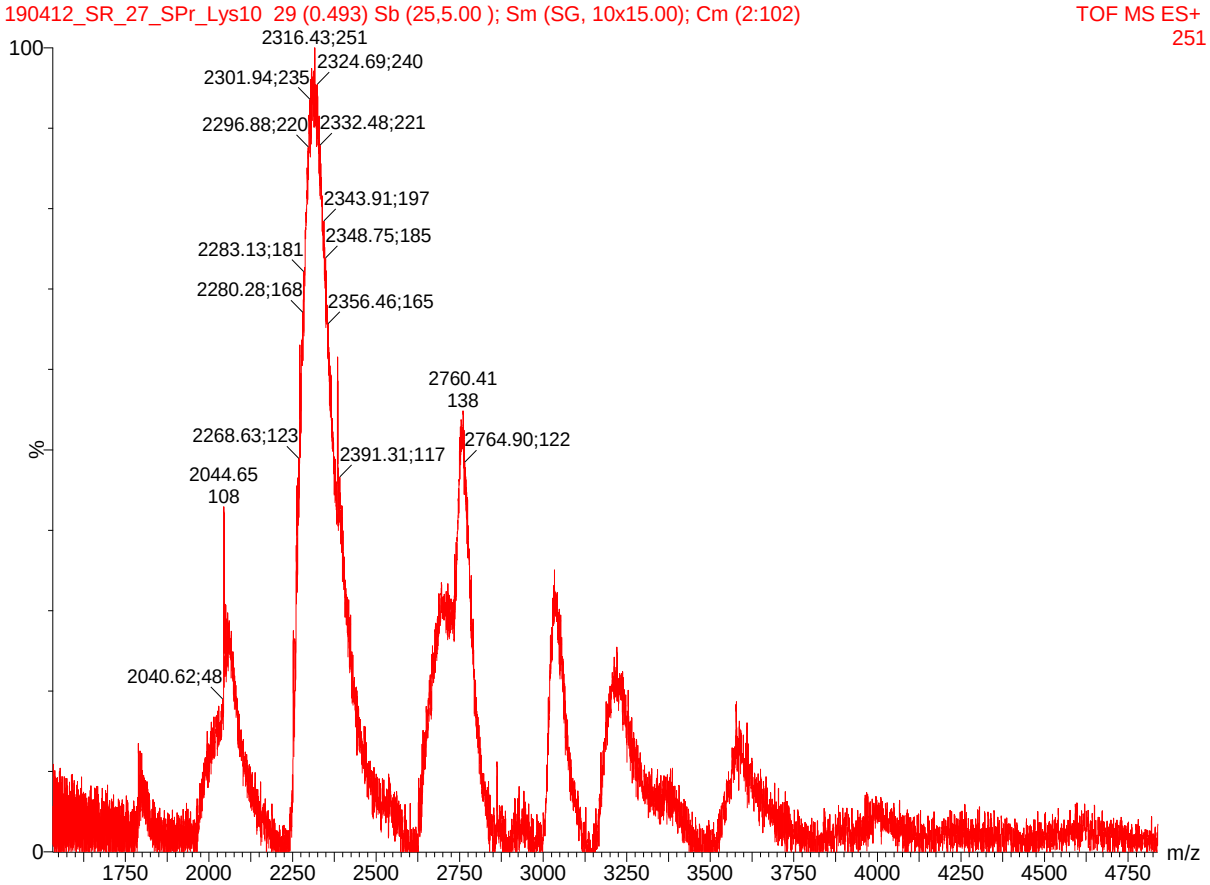

Spec. 32 : cAb-Lys3-SPr104 (100µM) with Lysozyme (10µM).
Incubated for 2 days and run at pressure 2.7.
No binding.

Conclusions of HDX studies

WT-cAb-Lys3 binds the most clearly, though this is still small and difficult to quantify. cAb-Lys3-Dha104 is the only one out of the other 3 antibodies to show any binding, it only binds weakly, even in a 10:1 ratio.

^{1}H NMR of WT-cAb-Lys3, cAb-Lys3-Cys104 and cAb-Lys3-Dha104 (carried out with Dr. Tim Claridge (University of Oxford))

^{1}H NMR was performed on WT-cAb-Lys3, cAb-Lys3-Cys104 and cAb-Lys3-Dha104 on a Bruker AVIII 700 with ^{1}H TCI cryoprobe (700 MHz). Spectra are all very similar apart from expected minor changes from chemical differences at position 104. There are signals at 0 – 2 ppm, indicative of folded protein. This positive result indicates that the modification does not denature the protein. For cAb-Lys3-Dha104, protein was desalted 5 times, to decrease signals by small molecules. Signals are less intense in this sample due to differences in concentration after multiple desalting columns.

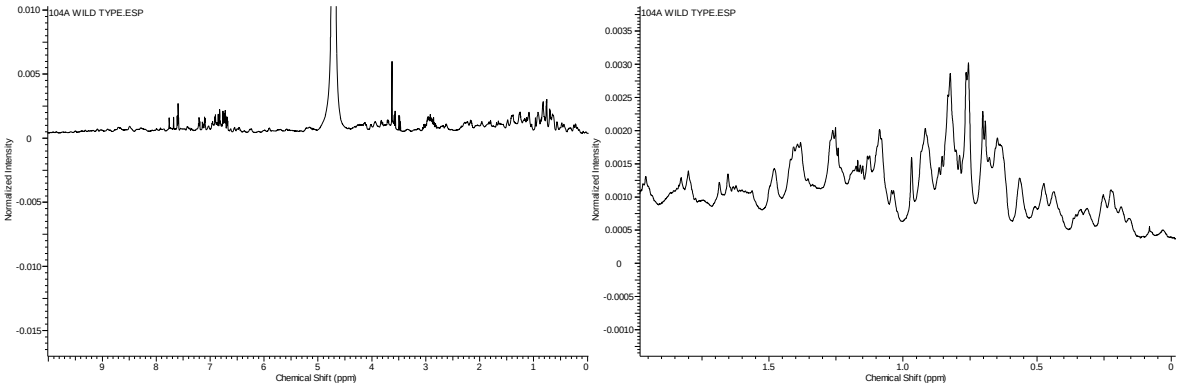

Experimental Figure 3.3. ^{1}H NMR of WT-cAb-Lys3. Left: 0 – 9 ppm, right: zoom of 0 – 2 ppm.

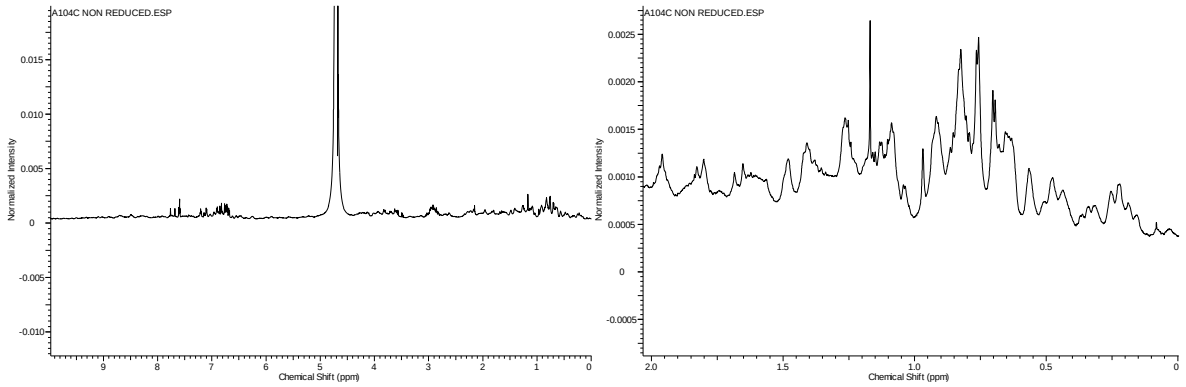

Experimental Figure 3.4. ^{1}H NMR of cAb-Lys3-Cys104. Left: 0 – 9 ppm, right: zoom of 0 – 2 ppm.

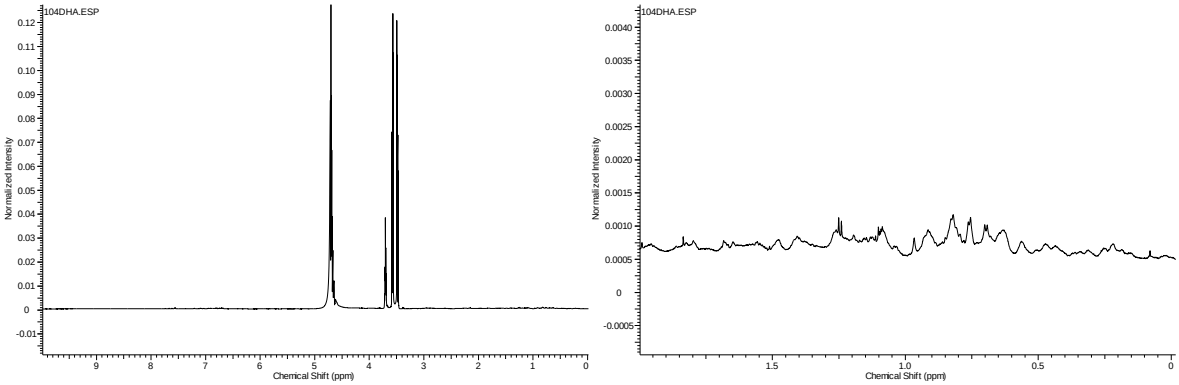

Experimental Figure 3.5. ^{1}H NMR of cAb-Lys3-Dha104. Left: 0 – 9 ppm, right: zoom of 0 – 2 ppm.

cAb-Lys3-Cys104 + RI. To cAb-Lys3-Cys104 (500 μL, 63.3 nmol, c = 2 mg/mL) was added 3 x 20 μL RI (EtI, PrI) over 30 minutes while shaking (600 rpm) at 37 °C. Reactions were continued for a further 1 – 5 hours. LC-MS revealed full conversion to the cAb-Lys3-sulfide adducts. Reactions were desalted through a PD10 minitrap.

SPR (carried out with Dr. Terry Baker (UCB))

Lysozyme was immobilised onto a chip (made up of 4 flow cells) in varying concentrations (0, 0.5, 1 and 2 μg/mL) by amine coupling chemistry (EDC/NHS activation and then ethanolamine deactivation). After the addition of each cAb-Lys3 derivative, the chip was

cleaned with HCl. cAb-Lys3 was added in concentrations from 0.316 – 1000 nM. On off curves and dissociation constants were generated on Biacore software.

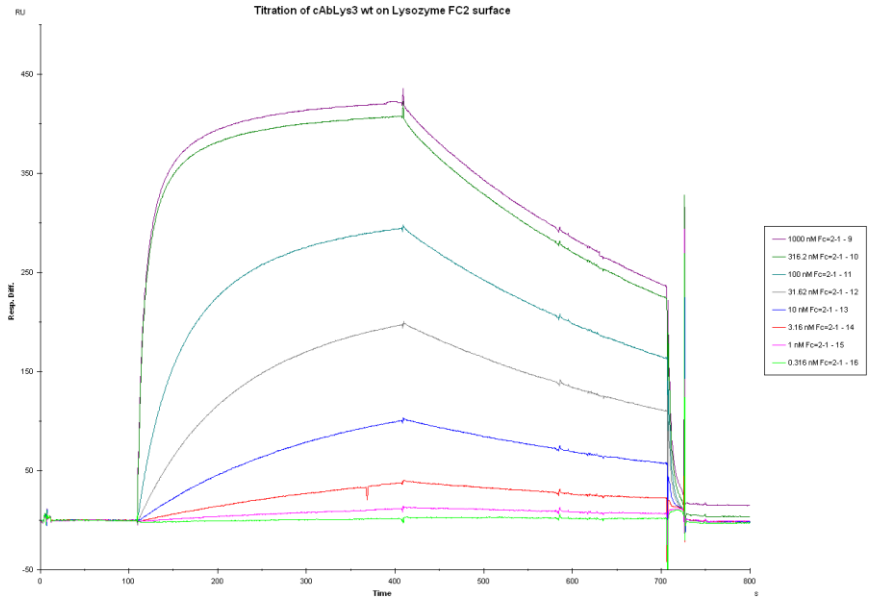

Experimental Figure 3.6. Association and dissociation curves for WT-cAb-Lys3, k_d = 100 nm.

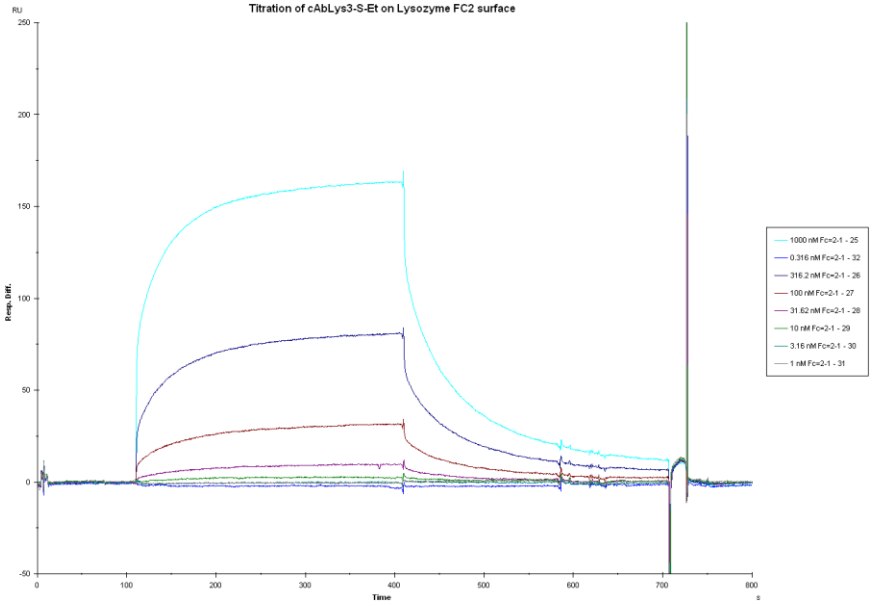

Experimental Figure 3.7. Association and dissociation curves for cAb-Lys3-SEt104, k_d = 502 nm.

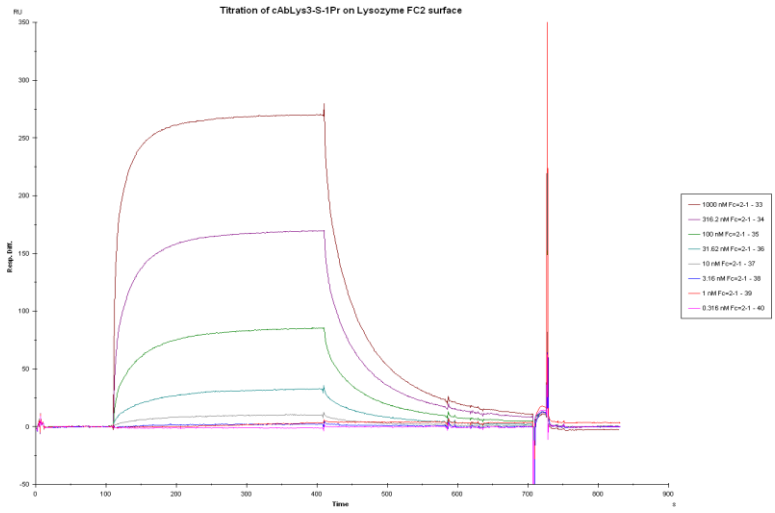

Experimental Figure 3.8. Association and dissociation curves for cAb-Lys3-104S-1Pr, k_d = 240 nm. 'Zero controls' were carried out where just PBS was added to the flow cells immobilised with lysozyme. No binding was observed.

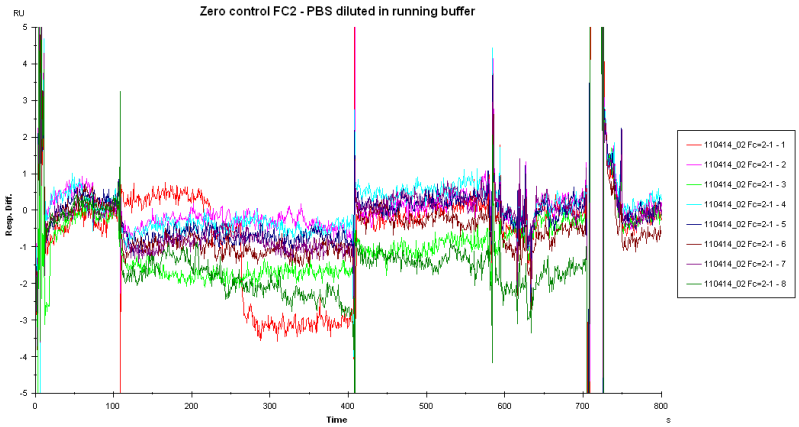

Experimental Figure 3.9. 'Zero controls'. Experiments carried out with just PBS over lysozyme, no binding.

His tag cleavage

AcTEV protease (Invitrogen)

WT-cAb-Lys3 or cAb-Lys3-Cys104 (0.5 mL, c = 1 mg/mL PBS, pH 8) was incubated with 158 U AcTEV at 30 °C overnight (600 rpm). Antibody was separated from enzyme by affinity chromatography. Antibody eluted in the flow through was concentrated by VivaSpin

and buffer exchanged into PBS, pH 8 (**Experimental Figure 3.10**). Antibody was stored at – 80 °C.

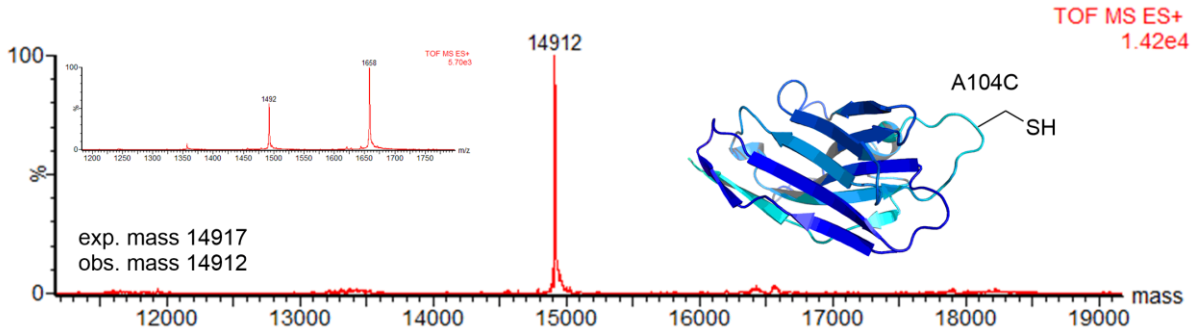

Experimental Figure 3.10. cAb-Lys3-Cys104 with His tag removed by AcTEV protease.

TurboTEV protease (Eton Biosciences)

In initial experiments, prolonged incubation of cAb-Lys3 with TurboTEV led to precipitation and subsequent loss of protein. Conditions were therefore optimised monitoring the reaction over time. TurboTEV (20 µL, 400 U) was added to WT-cAb-Lys3 or cAb-Lys3-Cys104 (0.5 mL, c = 1 mg/mL PBS, pH 8), and shaken (600 rpm) at room temperature. SDS-PAGE of samples at various time intervals indicated that full cleavage is observed at 2 hours (**Experimental Figure 3.11**). These conditions were subsequently used routinely. Antibody was separated from enzyme by affinity chromatography. Antibody eluted in the flow through was concentrated by VivaSpin and buffer exchanged into PBS, pH 8. Antibody was stored at – 80 °C.

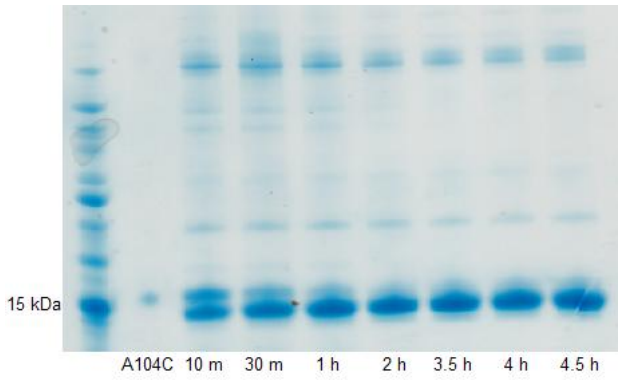

Experimental Figure 3.11. Monitoring TurboTEV action on cAb-Lys3-Cys104 over time. A single band below cAb-Lys3-Cys104 is observed at 2 hours.

TEV protease[2]

cAb-Lys3-Cys104 (1 mL, c = 1 mg/mL PBS, pH 8) was incubated with TEV (9 μL, 3.8 mg/mL) at room temperature overnight (600 rpm), after which a band by SDS-PAGE lower than s.m. was observed (**Experimental Figure 3.12**) Antibody was separated from enzyme by affinity chromatography. Antibody eluted in the flow through was concentrated by VivaSpin and buffer exchanged into PBS, pH 8. Antibody was stored at – 80 °C.

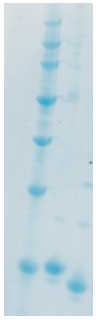

Experimental Figure 3.12. Action of TEV protease on cAb-Lys3-Cys104. Lane 1: marker, lane 2: cAb-Lys3-Cys104 with His tag, lane 3: cAb-Lys3-Cys104 treated with TEV.

cAb-Lys3-Cys104 (His tag cleaved) was tested for reactivity with Ellman's reagent and dibromo reagent **3.3** using established conditions. Full reactivity was observed (Experimental Figures **3.x** and **3.x**).

[2] Expressed and purified by Phin Chooi (BGD) using a construct from the Structural Genetics Consortium (SGC).

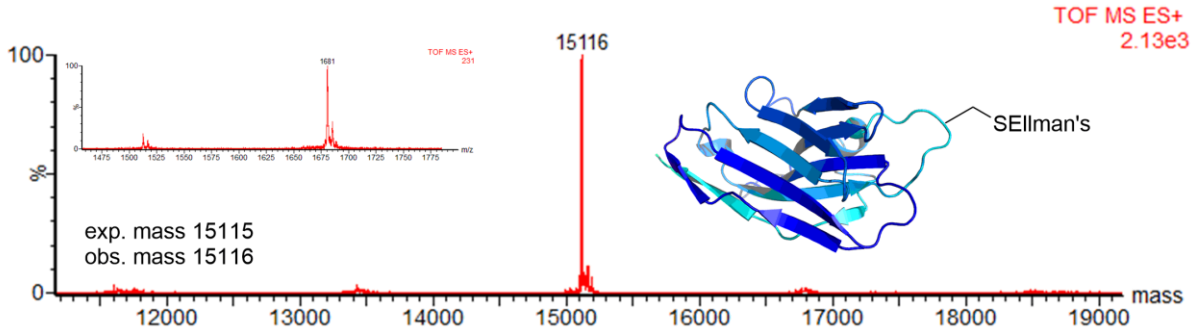

Experimental Figure 3.13. cAb-Lys3-Cys104Ellman's can be formed on antibody containing no His tag.

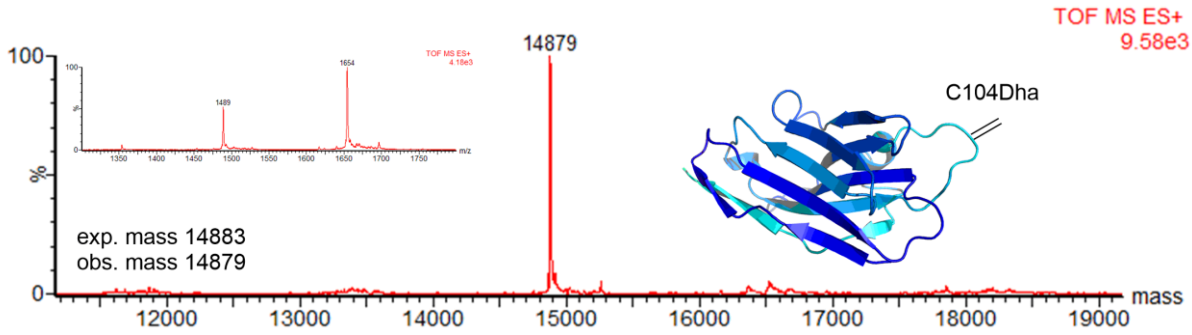

Experimental Figure 3.14. cAb-Lys3-Dha104 can be formed using reagent **3.3** on antibody containing no His tag.

3.6 Chapter 3 References

1. Jung, G. Lantibiotics-ribosomally synthesized biologically active polypeptides containing sulfide bridges and α,β-didehydroamino acids. *Angew. Chem. Int. Ed. Engl.* **30,** 1051–1068 (1991).

2. Jack, R. W., Jung, G. Lantibiotics and microcins : polypeptides with unusual chemical diversity. *Curr. Opin. Chem. Biol.* **4,** 310–317 (2000).

3. Willey, J. M., van der Donk, W. A. Lantibiotics: peptides of diverse structure and function. *Annu. Rev. Microbiol.* **61,** 477–501 (2007).

4. Rogers, L A, Whittier, E. O. Limiting factors in the lactic fermentation. *J. Bacteriol.* **16,** 211–229 (1928).

5. Skaugen, M., Nissen-Meyer, J., Jung, G., Stevanovic, S., Sletten, K., Abildgaard, C. I. M., Nes, I. F. *In vivo* conversion of L-Serine to D-Alanine in a ribosomally synthesized polypeptide. *J. Biol. Chem.* **269,** 27183–27185 (1994).

6. Gavaret, J., Nunez, J., Cahnmann, H. J. Formation of dehydroalanine residues during thyroid hormone synthesis in thyroglobulin. *J. Biol. Chem.* **255,** 5281–5285 (1980).

7. Gavaret, J., Cahnmann, H. J., Nunez, J. Thyroid hormone synthesis in thyroglobulin. *J. Biol. Chem.* **256,** 9167–9173 (1981).

8. Polgar, L., Bender, M. A new enzyme containing a synthetically formed active site. thiol-subtilisin. *J. Am. Chem. Soc.* **4331,** 3153–3154 (1966).

9. Neet, K. E., Koshland, D. E. The conversion of serine at the active site of subtilisin to cysteine: A "chemical mutation." *Proc. Natl. Acad. Sci. U. S. A.* **56,** 1606–1611 (1966).

10. Strumeyer, D. H., White, W. N., Koshland, D. E. Role of serine in chymotrypsin action. Conversion of the active site serine to dehydroalanine. *Biochemistry* **50,** 931–935 (1963).

11. Photaki, I. Transformation of serine to cysteine. β-Elimination reactions in serine derivatives. *J. Am. Chem. Soc.* **85,** 1123–1126 (1963).

12. Fahrney, D. E., Gold, A. M. Sulfonyl fluorides as inhibitors of esterases. I. Rates of reaction with acetylcholinesterase, α-Chymotrypsin and Trypsin. *J. Am. Chem. Soc.* **85,** 997–1000 (1963).

13. Holmes, T. J. Jr., Lawton, R. G., Lawton, R. Cysteine modification and cleavage of proteins with 2-methyl-N1-benzenesulfonyl-N4-bromoacetylquinonediimide. *J. Am. Chem. Soc.* **99,** 1984–1986 (1977).

14. Okamoto, R., Souma, S., Kajihara, Y. Efficient substitution reaction from cysteine to the serine residue of glycosylated polypeptide: repetitive peptide segment ligation strategy and the synthesis of glycosylated tetracontapeptide having acid labile sialyl-T_N antigens. *J. Org. Chem.* **74,** 2494–2501 (2009).

15. Oman, T. J., van der Donk, W. A. Insights into the mode of action of the two-peptide lantibiotic haloduracin. *ACS Chem. Biol.* **4,** 865–874 (2009).

16. Chalker, J. M., Gunnoo, S. B., Boutureira, O., Gerstberger, S. C., Fernandez-Gonzalez, M., Bernades, G. J. L., Griffin, L., Hailu, H., Schofield, C. J., Davis, B. G. Methods for converting cysteine to dehydroalanine on peptides and proteins. *Chem. Sci.* **2,** 1666-1676 (2011).

17. Chalker, J. M. Reaction Engineering for Protein Modification : Tools for Chemistry and Biology. *DPhil Thesis,* University of Oxford (2011).

18. Rich, D. H., Tam, J., Mathiaparanam, P., Grant, J. A., Mabuni, C. General synthesis of didehydroamino-acids and peptides. *J. C. S. Chem. Comm.* 897–898 (1974).

19. Matsuo, J., Kozai, T., Ishibashi, H. Mild preparation of alkenes from phenyl sulfides: one-pot elimination of phenylthio group via sulfilimine at ambient temperature. *Org. Lett.* **8,** 6095–6098 (2006).

20. Bernardes, G. J. L., Chalker, J. M., Errey, J. C., Davis, B. G. Facile conversion of cysteine and alkyl cysteines to dehydroalanine on protein surfaces: versatile and switchable access to functionalized proteins. *J. Am. Chem. Soc.* **130,** 5052–5053 (2008).

21. Chalker, J. M., Bernardes, G. J. L., Lin, Y. A., Davis, B. G. Chemical modification of proteins at cysteine: opportunities in chemistry and biology. *Chem. Asian J.* **4,** 630–640 (2009).

22. Seo, J., Lee, K. Post-translational modifications and their biological functions : proteomic analysis and systematic approaches. *J. Biochem. Mol. Biol.* **37,** 35–44 (2004).

23. Chalker, J. M., Lercher, L., Rose, N. R., Schofield, C. J., Davis, B. G. Conversion of cysteine into dehydroalanine enables access to synthetic histones bearing diverse post-translational modifications. *Angew. Chem. Int. Ed. Engl.* **51,** 1835–1839 (2012).

24. Strahl, B. D., Allis, C. D. The language of covalent histone modifications. *Nature* **403,** 41–45 (2000).

25. Jenuwein, T., Allis, C. D. Translating the histone code. *Science* **293,** 1074–1080 (2001).

26. Van Kasteren, S. Synthesis of post-translationally modified proteins. *Biochem. Soc. Trans.* **40,** 929–944 (2012).

27. Li, C. Organic reactions in aqueous media-with a focus on carbon-carbon bond formation. *Chem. Rev.* **93,** 2023–2035 (1993).

28. Li, C.-J. Organic reactions in aqueous media with a focus on carbon-carbon bond formations: a decade update. *Chem. Rev.* **105,** 3095–3165 (2005).

29. Li, C.-J., Trost, B. M. Green chemistry for chemical synthesis. *Proc. Natl. Acad. Sci. U. S. A.* **105,** 13197–13202 (2008).

30. Antos, J. M., Francis, M. B. Transition metal catalyzed methods for site-selective protein modification. *Curr. Opin. Chem. Biol.* **10,** 253–262 (2006).

31. Kodadek, T., Duroux-Richard, I., Bonnafous, J.-C. Techniques: Oxidative cross-linking as an emergent tool for the analysis of receptor-mediated signalling events. *Trends Pharmacol. Sci.* **26,** 210–217 (2005).

32. Antos, J. M., Francis, M. B. Selective tryptophan modification with rhodium carbenoids in aqueous solution. *J. Am. Chem. Soc.* **126,** 10256–10257 (2004).

33. Tilley, S. D., Francis, M. B. Tyrosine-selective protein alkylation using π-allylpalladium complexes. *J. Am. Chem. Soc.* **128,** 1080–1081 (2006).

34. Baslé, E., Joubert, N., Pucheault, M. Protein chemical modification on endogenous amino acids. *Chem. Biol.* **17,** 213–227 (2010).

35. Spicer, C. D., Davis, B. G. Palladium-mediated site-selective Suzuki-Miyaura protein modification at genetically encoded aryl halides. *Chem. Commun. (Camb).* **47,** 1698–1700 (2011).

36. Liu, D. R., Magliery, T. J., Pastrnak, M., Schultz, P. G. Engineering a tRNA and aminoacyl-tRNA synthetase for the site-specific incorporation of unnatural amino acids into proteins *in vivo*. *Proc. Natl. Acad. Sci. U. S. A.* **94,** 10092–10097 (1997).

37. Dumas, A. Spicer, C. D., Gao, Z., Takehana, T., Lin, Y. A., Yasukohchi, T., Davis, B. G. Self-liganded Suzuki-Miyaura coupling for site-selective protein PEGylation. *Angew. Chem. Int. Ed. Engl.* **52,** 3916–3921 (2013).

38. Spicer, C. D., Triemer, T., Davis, B. G. Palladium-mediated cell-surface labeling. *J. Am. Chem. Soc.* **134,** 800–803 (2012).

39. Spicer, C. D., Davis, B. G. Rewriting the bacterial glycocalyx via Suzuki-Miyaura cross-coupling. *Chem. Commun. (Camb).* **49,** 2747–2749 (2013).

40. Chatterjee, A. K., Choi, T.-L., Sanders, D. P., Grubbs, R. H. A general model for selectivity in olefin cross metathesis. *J. Am. Chem. Soc.* **125,** 11360–11370 (2003).

41. Lin, Y. A., Chalker, J. M., Floyd, N., Bernardes, G. J. L., Davis, B. G. Allyl sulfides are privileged substrates in aqueous cross-metathesis: application to site-selective protein modification. *J. Am. Chem. Soc.* **130,** 9642–9643 (2008).

42. Lin, Y. A., Chalker, J. M., Davis, B. G. Olefin metathesis for site-selective protein modification. *Chembiochem* **10,** 959–969 (2009).

43. Chalker, J. M., Lin, Y. A., Boutureira, O., Davis, B. G. Enabling olefin metathesis on proteins: chemical methods for installation of *S*-allyl cysteine. *Chem. Commun. (Camb).* 3714–3716 (2009).

44. Lin, Y. A., Chalker, J. M., Davis, B. G. Olefin cross-metathesis on proteins: investigation of allylic chalcogen effects and guiding principles in metathesis partner selection. *J. Am. Chem. Soc.* **132,** 16805–16811 (2010).

45. Lin, Y. A., Boutureira, O., Lercher, L., Bhushan, B., Paton, R. S., Davis, B. G. Rapid cross-metathesis for reversible protein modifications via chemical access to Se-allyl-selenocysteine in proteins. *J. Am. Chem. Soc.* **135,** 12156-12159 (2013).

46. Alam, J., Keller, T. H., Loh, T.-P. Indium mediated allylation in peptide and protein functionalization. *Chem. Commun. (Camb).* **47,** 9066–9068 (2011).

47. Scheck, R. A., Francis, M. B. Regioselective labeling of antibodies through N-terminal transamination. *ACS Chem. Biol.* **2,** 247–251 (2007).

48. Ueda, M., Miyabe, H., Nishimura, A., Naito, T. Zinc-mediated radical reaction of glyoxylic oxime ether and hydrazone in aqueous media : asymmetric synthesis of α-amino acids. *Tetrahedron:Asymmetry* **14,** 2857–2859 (2003).

49. Wu, X.-F., Neumann, H. Zinc-catalyzed organic synthesis: C-C, C-N, C-O bond formation reactions. *Adv. Synth. Catal.* **354,** 3141–3160 (2012).

50. Petrier, C., Dupuy, C., Luche, J. Conjugate additions to α,β-unsaturated carbonyl compounds in aqueous media. *Tetrahedron Lett.* **27,** 3149–3152 (1986).

51. Petrier, C., Einhorn, J., Luche, J. L. Selective tin and zinc mediated allylations of carbonyl compounds in aqueous media. *Tetrahedron Lett.* **26,** 1449–1452 (1985).

52. Einhorn, C., Luche, J. Selective allylation of carbonyl compounds in aqueous media. *J. Organomet. Chem.* **322,** 177–183 (1987).

53. Luche, J. L., Allavena, C. Ultrasound in organic synthesis 161. Optimisation of the conjugate additions to α,β-unsaturated carbonyl compounds in aqueous media. *Tetrahedron Lett.* **29,** 5369–5372 (1988).

54. Roth, M., Damm, W., Giese, B. The Curtin-Hammett principle: Stereoselective radical additions to alkenes. *Tetrahedron Lett.* **37,** 351–354 (1996).

55. Huang, T., Keh, C. C. K., Li, C.-J. Synthesis of alpha-amino acid derivatives and amines via activation of simple alkyl halides by zinc in water. *Chem. Commun. (Camb).* 2440–2441 (2002).

56. Ueda, M., Miyabe, H., Sugino, H., Naito, T. Zinc-mediated carbon radical addition to glyoxylic imines in aqueous media for the synthesis of α-amino acids. *Org. Biomol. Chem.* **3,** 1124–1128 (2005).

57. Petrier, C., Einhorn, J., Luche, J. L. Selective tin and zinc mediated allylations of carbonyl compounds in aqueous media. *Tetrahedron Lett.* **26,** 1449–1452 (1985).

58. Petrier, C., Luche, J. Allylzinc reagents additions in aqueous media. *J. Org. Chem.* **50,** 910–912 (1985).

59. Desmyter, A., Transue, T. R., Ghahroudi, M. A., Ti, M-H, D., Poortmans, F., Hamers, R., Muyldermans, S., Wyns, L. Crystal structure of a camel single-domain V_H antibody fragment in complex with lysozyme. *Nat. Struct. Biol.* **3,** 803–811 (1996).

60. Chalker, J. M., Davis, B. G. Chemical mutagenesis: selective post-expression interconversion of protein amino acid residues. *Curr. Opin. Chem. Biol.* **14,** 781–789 (2010).

61. Delves, P., Martin, S., Burton, D., Roitt, I. *Roitt's Essential Immunology*. (Wiley-Blackwell, 2006).

62. Winter, G., Griffiths, A. D., Hawkins, R. E., Hoogenboom, H. R. Making antibodies by phage display technology. *Annu. Rev. Immunol.* **12,** 433–455 (1994).

63. De Genst, E., Handelberg, F., Van Meirhaeghe, A., Vynck, S., Loris, R., Wyns, L., Muyldermans, S. Chemical basis for the affinity maturation of a camel single domain antibody. *J. Biol. Chem.* **279,** 53593–53601 (2004).

64. Johnson, C. R., Kirchhoff, R. A., Corkins, H. G. Chemistry of sulfoxides and related compounds. XLIX. Synthesis of optically active sulfoximines from optically active sulfoxides. *J. Org. Chem.* **39,** 2458–2459 (1974).

65. Mendiola, J., Rincon, J. A., Mateos, C., Soriano, J. F., de Frutos, O. Niemeier, J. K., Davis, E. M. Preparation, use, and safety of O-mesitylenesulfonylhydroxylamine. *Org. Process Res. Dev.* **13,** 263–267 (2009).

66. Kosower, E. M. Monosubstituted diazenes (diimides). Surprising intermediates. *Acc. Chem. Res.* **4,** 193–198 (1971).

67. Doldouras, G. A., Kollonitsch, J. A direct, selective, and general method for reductive deamination of primary amines. *J. Am. Chem. Soc.* **100,** 341–342 (1978).

68. Wallace, R. G. Hydroxylamine-O-sulfonic acid. *Aldrichim. Acta.* **13,** 3 – 11 (1980).

69. Palmer, E. P., Pattaroni, C., Nunami, K., Chadha, R. K., Goodman, M., Wakamiya, T., Fukase, K., Horimoto, S., Kitazawa, M., Fujita, H., Kubo, A., Shiba, T. Effects of dehydroalanine on peptide conformations. *J. Am. Chem. Soc.* **114,** 5634–5642 (1992).

70. Chalker, J. M., Bernardes, G. J. L., Davis, B. G. A "Tag-and-Modify" Approach to Site-Selective Protein Modification. *Acc. Chem. Res.* **44,** 730–741 (2011).

71. Houde, D., Engen, J. R. Conformational analysis of recombinant monoclonal antibodies with hydrogen/deuterium exchange mass spectrometry. *Methods Mol. Biol.* **988,** 269–89 (2013).

72. Guiducci, C. RESONANCE BASED SYSTEMS. 1–27

73. Floyd, N., Vijayakrishnan, B., Koeppe, J. R., Davis, B. G. Thiyl glycosylation of olefinic proteins: *S*-linked glycoconjugate synthesis. *Angew. Chem. Int. Ed. Engl.* **48,** 7798–7802 (2009).

74. Ramachandran, S., Fontanille, P., Pandey, A., Larroche, C. Gluconic Acid : Properties, Applications and Microbial Production. *Food Technol. Biotechnol.* **44,** 185–195 (2006).

75. Li, C., Chan, T. Organometallic reactions in aqueous media with indium. *Tetrahedron Lett.* **32,** 7017–7020 (1991).

76. Li, C., Chan, T. Organic syntheses using indium-mediated and catalyzed reactions in aqueous media. *Tetrahedron* **55,** 11149–11176 (1999).

77. Shen, Z.-L., Cheong, H.-L., Loh, T.-P. Indium/copper-mediated conjugate addition of unactivated alkyl iodides to α,β-unsaturated carbonyl compounds in water. *Tetrahedron Lett.* **50,** 1051–1054 (2009).

Chapter 4: Building Conditionally Functional Synthetic Proteins – Creation of an AND Antibody

'…That chemical affinities govern all biological processes…'

Paul Ehrlich

4.1 Introduction

4.1.1 Antibody therapeutics and the need for protein-based Boolean logic gates

The targeted release of antibody therapeutics specifically at their disease sites may help to prevent side effects encountered from binding antigen in non-target tissue.[1,2] This need for targeted drug delivery was recognised 100 years ago by Paul Ehrlich, who coined the term 'magic bullets' for therapeutics targeting only desired sites.[3] The development of antibodies and fragments as therapeutics is possible largely due to the development of hybridoma technology for the production of monoclonal antibodies (mAbs).[4] Much of the research around antibody therapeutics is towards minimising immunogenicity by humanisation of therapeutics, and also conjugation to enhance therapeutic qualities.[5–7] In this chapter, progress towards a strategy for minimising side effects obtained when an antibody therapeutic encounters target receptors in healthy tissues is described.[1,2]

In 2009, Donaldson and co-workers reported the fusion of two single-chain variable fragments (scFvs) binding to epidermal growth factor receptor (EGFR) at their binding sites with their protein cognate domains via a protease-susceptible linker. This fusion resulted in the 'masking' of the antibody. *In vitro* it was found that fused antibody could not bind to EGFR, but when matrix metalloproteinase 9 (MMP-9, the protease recognising the linker sequence) was added, binding was regained.[8] MMP-9 is an extracellular enzyme and is

frequently overexpressed in epithelial malignancies where EGFR blockade may be beneficial.[9] However, MMP-9 is also secreted at many other sites and this may preclude controlled release of antibody specifically at disease sites. Moreover, applying this strategy to other antibody-antigen systems would require the construction of individual genes encoding for the desired antibody and epitope. Recently, Janssen and co-workers describe a somewhat similar approach for reversibly masking IgG. They formed a non-covalent complex between IgG and a DNA-based ligand which contains a protease-susceptible linker and an epitope sequence at each end. The DNA-based ligand was rigid and blocked binding, but this blocking could be reversed upon treatment with a protease.[10] This approach may be applicable to other multivalent formats. In terms of therapeutic applications, it also has the same limitations as Donaldson's approach[8] in that each new target would require substantial genetic engineering, and the use of a protease active in multiple sites could lead to unpredictable targeting ability.

In both Donaldson and Janssen's work, controlled function was developed by the conversion of an antibody from a biological entity that requires one input for function to one that requires two inputs: antigen and protease. In the absence of one or both inputs, no function can be obtained. This system can be considered to be a Boolean AND logic gate (**Figure 4.1**), where the presentation of two inputs to an entity is necessary for function of that entity.[11]

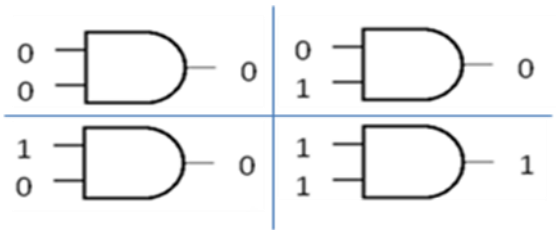

Figure 4.1. Presentation of inputs for AND gate logic.

The development of AND logic gates, and indeed logic gates following other Boolean function (OR, NOT, NOR gates) are receiving increased attention for applications in biotechnology, due to the potential to precisely tune function.[12] In particular, genetic-based Boolean logic gates exploiting the behaviour of nucleic acids have been developed,[12–16] for example for the targeted control of protein synthesis,[17] and growth inhibition of tumour cells.[18] However, as a result of the time 'lag' generated by intervening transcriptional and translational processes, expression-based switches and gates display slow response times that may not be suitable for highly dynamic biological environments, such as at cell surfaces or in tissues. Moreover, DNA-based constructs have been developed for conditional delivery of payloads based on an antigenic input.[19] However, the susceptibility of exposed nucleic-acid based 'robots' to nucleases *in vivo* may prevent widespread application of DNA-based technology. Therefore stable protein-based gates would be preferable, but to date no precise strategy has been developed for the creation of discrete Boolean-gated proteins, and the use of proteins in logic-based control is rare.[20,21] Those examples which have been reported involve the use of proteins and processes directly evolved from nature and typically employ only proteinogenic amino acids.[8,10] The use of non-natural amino acids may provide the ability to specifically control desired function, whilst minimising disturbance to natural processes. Here, we describe the use of synthetic post-translation modification (PTM) mimics[22] at position 104 of cAb-Lys3. This position is known to be pivotal to mediating hydrophobic interactions contributing to a high binding affinity.[23,24] In the previous chapter, it was shown that the introduction of non-natural groups at this position can have detrimental effects on binding, and so exploration into whether this process could be reversible was carried out in order to see if a synthetic AND-gated antibody could be developed.

4.1.2 Glycosylation and glycosidases

The post-translational glycosylation of proteins is ubiquitous within the body, and methods for understanding glycosyl attachment (via glycosyltransferases) and removal (via glycosidases) are important areas of research. The synthesis of glycoside mimics in proteins may help in understanding natural processes, and methods developed within the group for the synthesis of mimics have focused particularly on forming *S*-linked glycosylation mimics via cysteine and dehydroalanine,[25–27] and also naturally occurring *O*-linked forms.[28] In terms of naturally occurring thioglycosides, early reports from Lote and Weiss which identified them in human urine and blood[29] are controversial as the reported sequence does not appear to be part of the human proteome[30] and glycosylation at cysteine is considered rare.[31] More recently, the antimicrobial glycopeptide sublancin has been found to contain a natural glucosyl linkage,[32] and the *S*-glycosyltransferase responsible for glycosylation of the cysteine residue has been identified.[32,33] Other groups have identified multiple forms of cysteine glycosylation in glycopeptides in bacteriocins.[34,35] Synthetic routes to thioglycosides have received much attention in the literature[36] and they are considered hydrolytically stable analogues to their natural *O*-linked counterparts. They have been comprehensively studied for applications in X-ray crystallography and for carbohydrate-based therapeutics and vaccines.[37,38] In general, thioglycosides are considered impervious to hydrolysis. However, both Macauley and co-workers,[39] and Yip and Withers[40] have identified the removal of thioglycosides by glycosidases specific for *O*-glycans. In certain tumour environments, the overexpression of some processing enzymes are known.[9,41–43] Indeed it is thought that higher levels of glycosidases may be expressed and secreted in tumour cells than in non-malignant cells,[41,44,45] or that the enzymes are present at similar levels but differences in cellular pH (cancerous cells can be more acidic) lead to an increase in enzyme activity.[46] As well as *O*-

specific glycosidases, one class of *S*-specific glycosidases, thioglucosidases, are known in plant systems. The thioglucosidases hydrolyse glucosinolates (plant metabolites), and the resulting aglycone undergoes rearrangement to give products such as toxic isothiocyanates – which are thought to contribute to the plants' defence system (**Figure 4.2**).[47] They are also found in some bacterial strains,[48] but as yet no human thioglycosidases have been identified.

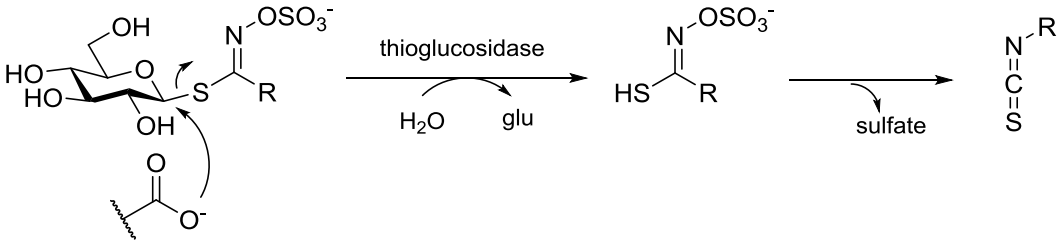

Figure 4.2. Release of glucose from glucosinolates by thioglucosidase.

4.1.3 Phosphorylation and phosphatases

Phosphorylation is another example of a ubiquitous PTM. Phosphorylation is vital to a myriad of cellular processes in the body, and is mediated by kinases (catalysing phosphate attachment) and phosphatases (catalysing phosphate removal). Phosphorylation occurs predominantly on serine, threonine and tyrosine residues[49,50] although the phosphorylation of histidine[51] and arginine[52] residues is also known. Strategies for the chemical installation of phosphate groups onto amino acids is important in gaining an understanding of certain cellular processes.[22,53] Phosphorylation can have drastic effects on protein structure and function,[54–58] a property which has been exploited in the construction of new biomaterials,[59–61] and commonly involves the use of proteinogenic amino acids only. Phosphorylation on cysteine residues is considered rare,[62] although Sun and co-workers have previously identified several global transcriptional regulators in *Staphylococcus aureus* bearing phosphorylated cysteines, and have found this rare PTM to significantly impact on the function of proteins.[63] Phosphorylated cysteine (phosphocysteine, pCys) is a bioisostere of

the more common phosphoserine (pSer), and chemically installed pCys has been shown to be a suitable mimic for pSer: pCys is recognised by pSer-specific antibodies[27] and has been used to investigate kinase activity.[64] Like glycosidases, certain phosphatases are known to be overexpressed and secreted in tumour environments, a characteristic that may potentially be exploited in targeted drug delivery strategies.[42,43]

In this chapter, the concept of an AND antibody is introduced. It is shown that by using a combination of site-specific chemical and enzymatic methods, cAb-Lys3 can be converted into a temporary inhibitory state. Initially, we attempted to demonstrate the concept using glycosyl groups. The successful installation of *S*-linked GlcNAc, glucose and galactose are described. For each glycosylated antibody, binding to lysozyme was inhibited. The glycosylated antibody forms were found to be impervious to glycosidase treatment and so active antibody could not be 'released'. A phosphate group was then installed at position 104 of cAb-Lys3 via Dha, forming pCys. Again the modification was found to inhibit binding of the antibody to lysozyme. This inhibition of binding was relieved by treatment with various phosphatases. In order to achieve binding of cAb-Lys3-pCys104 to lysozyme, both antigen and phosphatase were required, demonstrating the concept of an antibody following Boolean AND logic. The concept was then demonstrated *in vitro* and in mammalian tissue, by the selective directing of cAb-Lys3 to cell surfaces only in the presence of both antigen and phosphatase.

4.2 Results

4.2.1 Binding inhibition using GlcNAc

Synthesis and characterisation of cAb-Lys3-CysGlcNAc104[65]

cAb-Lys3-CysGlcNAc104 was synthesised from cAb-Lys3-Dha104 using GlcNAc with a thiol at the anomeric position (2-acetamido-2-deoxy-1-thio-β-D-glucopyranose, GlcNAc thiol, **Scheme 4.1**).[1] Conversion to glycosylated antibody was possible, but some optimisation was required.

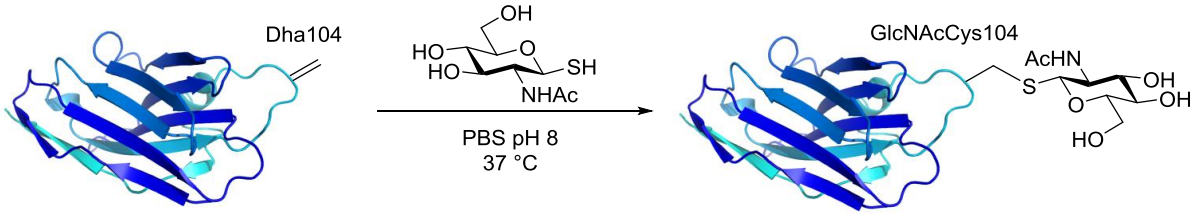

Scheme 4.1. Introduction of GlcNAcCys at position 104 of cAb-Lys3 via a conjugate addition of GlcNAc thiol to cAb-Lys3-Dha104.

Initially, 3,000 eq. of GlcNAc thiol was added to cAb-Lys3-Dha104. After incubation at room temperature for 1.5 hours, LC-MS revealed 50% conversion to the glycosylated antibody (**Figure 4.3**). No further conversion was observed with prolonged incubation.

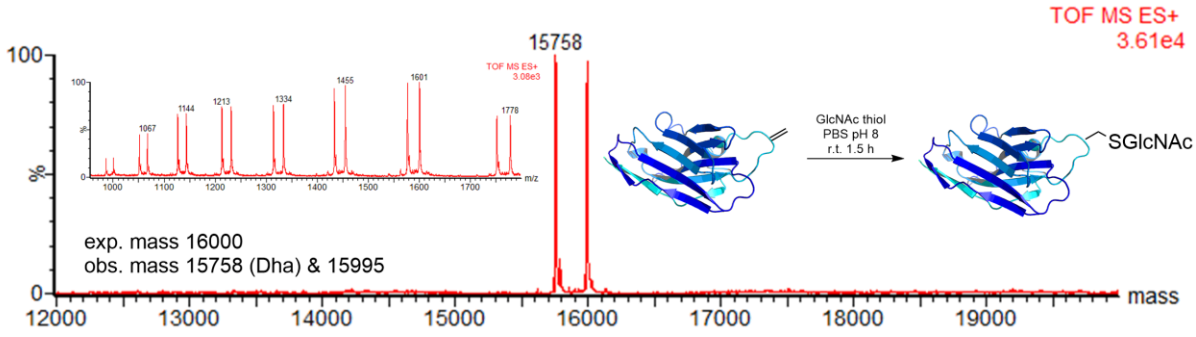

Figure 4.3. Partial conversion to cAb-Ly3-GlcNAcCys104 upon treatment of cAb-Lys3-Dha104 with 3,000 eq. of GlcNAc thiol for 1.5 hours at room temperature.

[1] GlcNAc-SH was kindly donated by Dr. Justin Chalker.[65]

Based on the lack of complete conversion observed, portionwise addition of GlcNAc thiol was attempted. Fresh cAb-Lys3-Dha104 was treated with 2 x 5,000 eq. GlcNAc thiol over 1.5 hours. After 4 hours incubation at 37 °C, approximately 80% conversion to glycosylated antibody was observed (**Figure 4.4**). No further conversion was observed after further incubation.

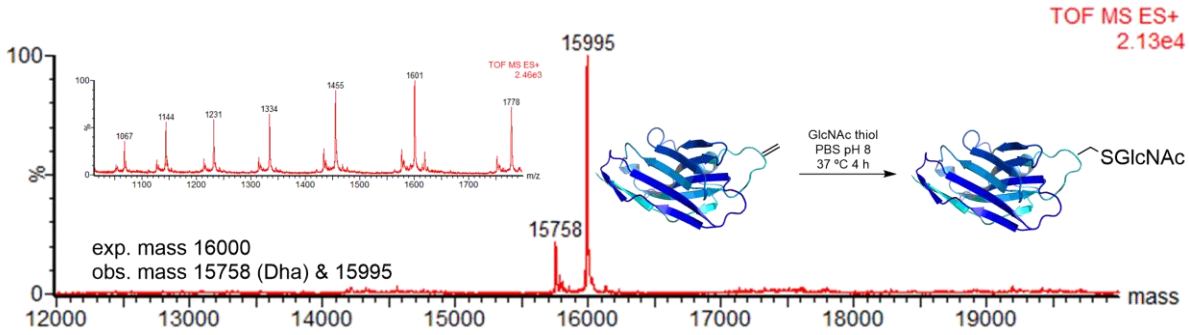

Figure 4.4. 80% conversion to cAb-Lys3-GlcNAcCys104 was observed when cAb-Lys3-Dha104 was treated with 2 x 5,000 eq. of GlcNAc thiol for 4 hours at 37 °C.

The results obtained from the two reaction conditions (i.e. single and double addition of thioglycoside) implied that portionwise addition of GlcNAc thiol was more efficient in driving conversion to the glycosylated antibody. To further test this hypothesis, cAb-Lys3-Dha104 was treated with a large excess of GlcNAc thiol (15,000 eq.) for 3.5 hours at 37 °C. Approximately 60% conversion was observed (**Figure 4.5**), showing that the portionwise addition of GlcNAc thiol is more beneficial than single addition. Prolonged incubation (overnight) did not lead to further conversion. This may be because over the course of the reaction, GlcNAc thiol was gradually being hydrolysed to a lactol, which is no longer nucleophilic enough to attack Dha. Also, the lack of antibody degradation revealed that cAb-Lys3 is robust and stable to prolonged incubation at 37 ºC and shaking (600 rpm).

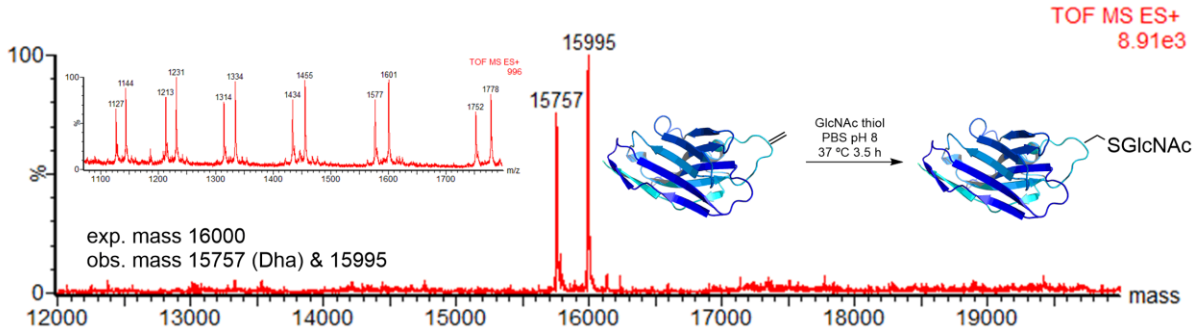

Figure 4.5. 60% conversion to cAb-Lys3-GlcNAcCys104 was observed when cAb-Lys3-Dha104 is treated with a single portion of GlcNAc thiol (15,000 eq.) for 3.5 hours at 37 °C.

It was therefore decided that a combination of the use of a high excess and portionwise addition of GlcNAc thiol should be used to drive the reaction to completion. Indeed, complete conversion to glycosylated product was observed when 10 portions of 2,000 eq. of GlcNAc thiol were added to cAb-Lys3-Dha104 with addition at 15 minute intervals, reaction at 37 °C and monitoring over 10 hours (**Table 4.1**).

Entry	Time/ hours	Observations
1	0	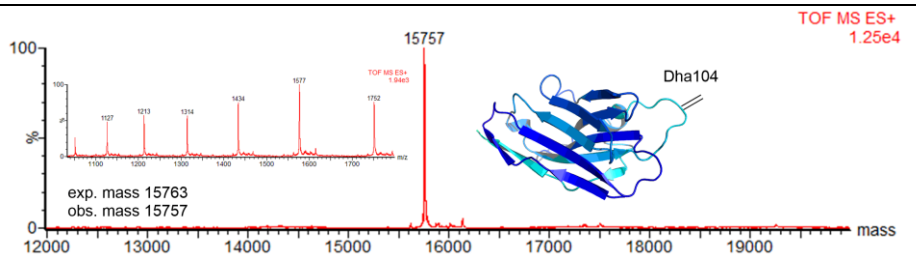
2	1	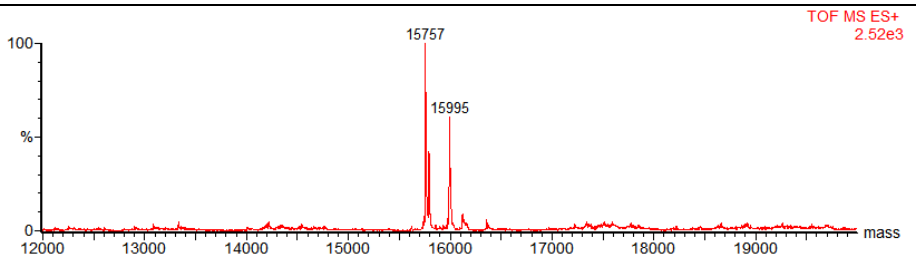
3	4	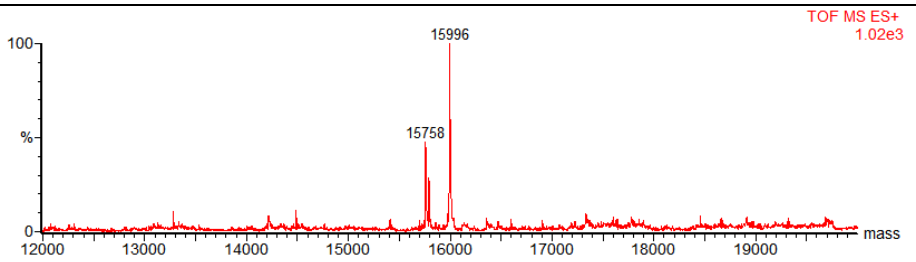

4	7	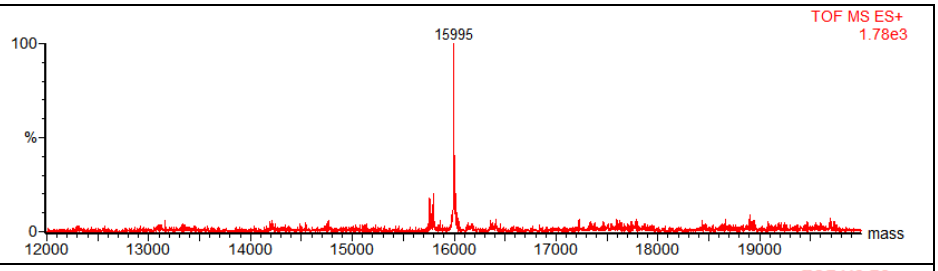
5	10	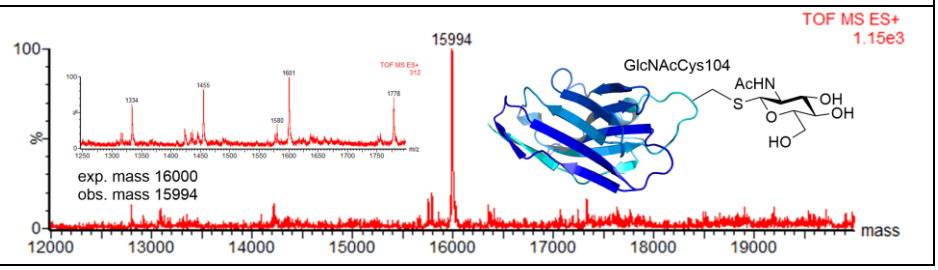

Table 4.1. Reaction progress for cAb-Lys3-Dha104 + 10 x 2,000 eq. of GlcNAc thiol, 37 °C.

Glycosylation at position 104 of cAb-Lys3 was chemically corroborated by reduction with DTT, then β-mercaptoethanol to reveal the presence of free thiol. Gratifyingly, no reaction was observed (**Experimental Figures 4.1** and **4.2**). As the starting material cAb-Lys3-Dha104 had been shown to be able to react with β-mercaptoethanol (**Figure 3.5, Chapter 3**), it could be deduced that all Dha at position 104 had been consumed upon reacting with GlcNAc thiol. Unfortunately, attempts to carry out proteolytic digest and LC-MS/MS analysis on cAb-Lys3-GlcNAcCys104 were unsuccessful. The effect of the introduction of a relatively bulky GlcNAc entity (compared to Ala104 in WT-cAb-Lys3 and Cys104 in the mutant) on antibody activity was investigated by testing binding ability of the antibody to the antigen, lysozyme. ELISA showed that binding was severely diminished in comparison to WT-cAb-Lys3 and cAb-Lys3-Cys104 (**Figure 4.6**). This result is perhaps not surprising considering that the crystal structure of cAb-Lys3 in complex with lysozyme shows predominantly hydrophobic binding in a tight interaction.[23] The polar sugar moiety would be expected to disfavour hydrophobic binding as well as interrupting any tight binding interaction by virtue of its relatively large size. The glycosylated antibody's secondary structure was tested by CD and was found to retain predominant β-sheet character (**Figure**

4.7). As the modification is at the tip of a protruding loop (CDR3) and positioned away from other residues of the CDRs 1 and 2 and the framework region, it is reasonable to speculate that a complete switch in chemical character (hydrophobic to polar) at this position would not affect overall antibody structure.

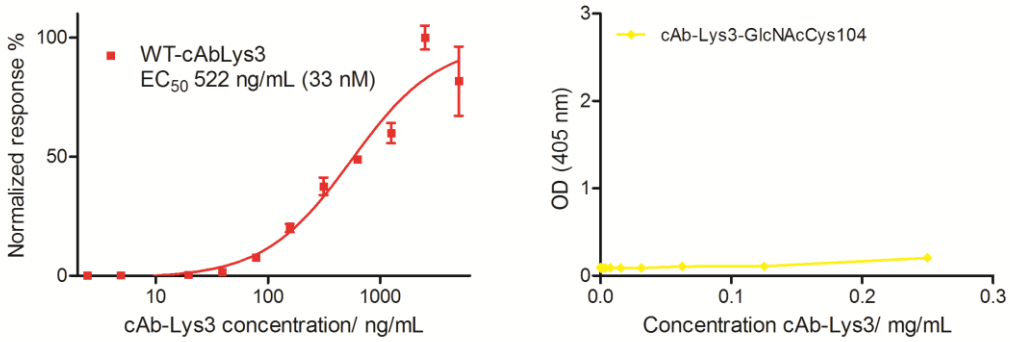

Figure 4.6. ELISA of WT-cAb-Lys3 (left) and cAb-Lys3-GlcNAcCys104 (right).

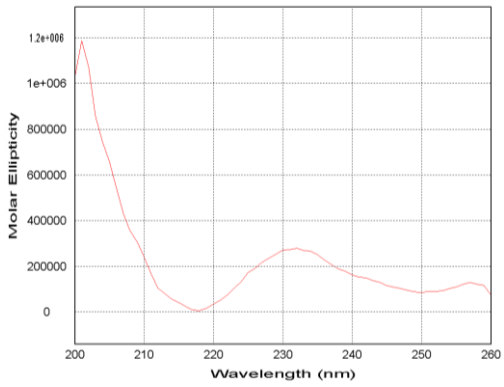

Figure 4.7. CD spectrum for cAb-Lys3-GlcNAcCys104.

A singly glycosylated antibody fragment was synthesised using chemical methods.[65] The location of the modification was elucidated by chemical testing and the modified antibody was found to retain overall secondary structure. The binding ability of the antibody to antigen was found to be diminished which is probably due to the change from hydrophobic to polar character at a key residue involved in binding.[23] Following this binding inhibition, a strategy to remove the GlcNAc moiety in cAb-Lys3 was explored, with the aim of regaining cAb-

Lys3-Cys104and therefore antigen-binding capability – hence providing a method for removing temporary inhibition.[8,10]

Attempted glycosidase removal with *O*-GlcNAcase

Family 84 human *O*-GlcNAcase (hOGA) catalyses the cleavage of *O*-GlcNAc from post-translationally modified proteins. The enzyme acts intracellularly and the mechanism involves anchimeric assistance.[66] The enzyme has previously been found to cleave pNP-*S*-GlcNAc with comparable efficiencies to pNP-*O*-GlcNAc, but without using general acid catalysis.[39]

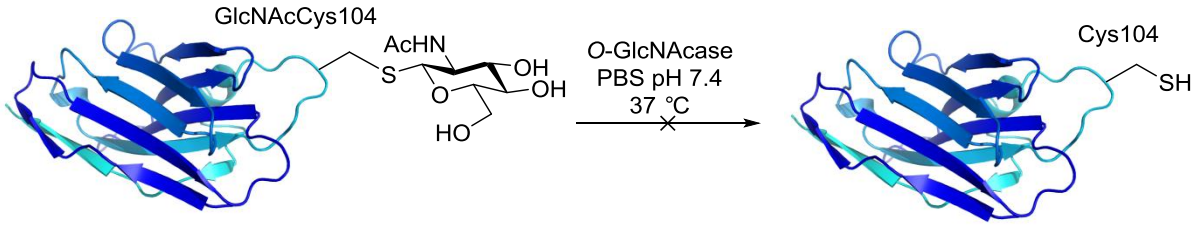

Scheme 4.2. Attempted deglycosylation of the cAb-Lys3 thioglycoside using *O*-GlcNAcase.

Two forms of *O*-GlcNAcase (OGA) were used for the reaction shown in **Scheme 4.2**; SPy 1600, isolated from *Streptococcus pyogenes*,[67] and recombinant human OGA (hOGA).[39]

SPy1600 - *O*-GlcNAcase isolated from *Streptococcus pyogenes*

SPy1600 removes *O*-GlcNAc from a variety of glycoconjugates that are imported into the bacterial cell during pathogenesis. The enzyme was isolated from *Streptococcus pyogenes*, and is reported to also cleave *O*-GlcNAc from eukaryotic proteins.[67] Its ability to cleave *S*-GlcNAc from glycosylated cAb-Lys3 was tested under various conditions (**Table 4.2**).

Entry	cAb-Lys3-GlcNAcCys104	Spy1600 (10.4 mg/mL, 57.84 U/mL)	Eq.	Time	Conditions and observations
1	0.25 mg/mL, 1 mL 15.6 nmol	5 μL plus 5 μL after 1 h, 0.58 U	4	16 hours	15 minutes, 1 h and 16 h: only s.m. observed
2	0.25 mg/mL, 500 μL, 7.8 nmol	6.8 μL, 0.39 U	50	16 hours	Preheated protein 15 minutes, 1 h and 16 h: only s.m. observed
3	0.25 mg/mL, 100 μL, 1.6 nmol	2.8 μL, 0.16 U	100	16 hours	Preheated protein first 15 minutes, 1 h and 16 h: only s.m. observed
4	0.25 mg/mL, 100 μL, 1.6 nmol	5.6 μL, 0.32 U	200	16 hours	Preheated protein first 15 minutes, 1 h and 16 h: only s.m. observed
5	0.25 mg/mL, 100 μL, 1.6 nmol	11.2 μL, 0.64 U	400	16 hours	Preheated protein first 15 minutes, 1 h and 16 h: only s.m. observed
6	0.25 mg/mL, 100 μL, 1.6 nmol	22.4 μL, 1.28 U	800	16 hours	Preheated protein first 15 minutes, 1 h and 16 h: only s.m. observed
7	0.25 mg/mL, 1.75 μL, 0.6 μg	10 μL, 0.6 U	1	2 days	Reaction carried out in Tris-HCL, pH 7.5 15 minutes, 1 h, 16 h and 48 h: only s.m. observed

Table 4.2. Conditions investigated for cleaving *S*-linked GlcNAc from cAb-Lys3 using Spy1600. For entries 1 – 6, 10 mM HEPES, pH 7.6 at 37 °C was used. s.m. is starting material.

Under all conditions investigated, including high enzyme loading and prolonged reaction times, the enzyme Spy1600 showed no activity towards the antibody. It was therefore decided to test the cleavage with the same OGA that Macauley and co-workers used when they observed the removal of *S*-GlcNAc from thioglycosides.[39]

Expression and purification of human *O*-GlcNAcase

Family 84 human OGA (hOGA) was expressed and purified according to the procedure described by Vocadlo and co-workers.[39] The gene encoding hOGA in pET-28a(+) vector was transformed into *E. coli* Tuner(λDE3) cells, and the sequence verified. Protein was expressed in *E. coli* using standard techniques, and following cell lysis by sonication, purified by affinity chromatography (**Figure 4.8**). Fractions containing protein were dialysed against PBS, pH 7.4 (membrane with a MWCO 12 – 14 kDa) to remove low molecular weight

impurities visible by SDS-PAGE (**Figure 4.8**). In total, 0.39 mg/mL (1 mL) protein was obtained as tested by bicinchoninic acid (BCA) assay. The enzymatic activity was tested by reaction with the chromophoric substrate pNP-*O*-GlcNAc (**Figure 4.9**).[39]

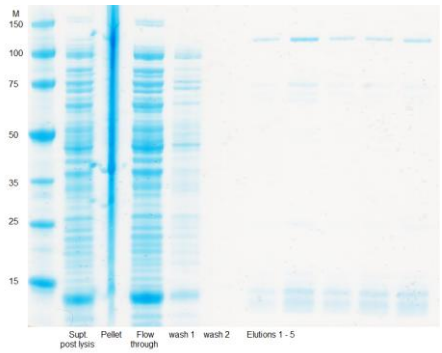

Figure 4.8. Expression and purification of hOGA, mass ~ 102 kDa.

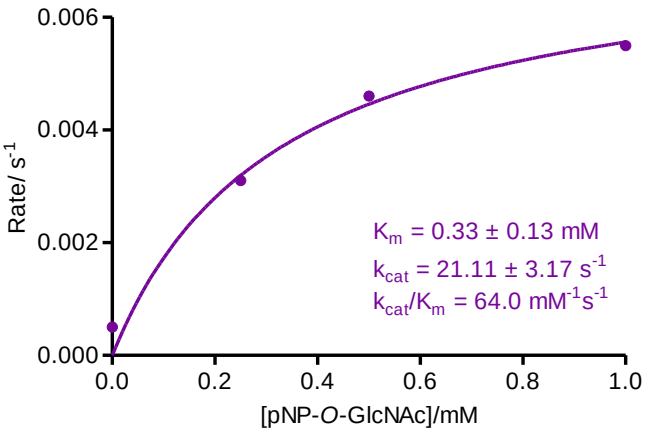

Figure 4.9. hOGA enzymatic activity assay.

Testing the activity of human *O*-GlcNAcase on cAb-Lys3-GlcNAcCys104

Entry	cAb-Lys3-GlcNAcCys104	hOGA (0.39 mg/mL)	Time	Conditions and observations
1	0.5 mg/mL, 500 μL 15.6 nmol	5 μL, 2 μg	16 hours	10 mins, 45 mins and 16 h: only s.m. observed
2	0.5 mg/mL, 100 μL 3.1 nmol	5 μL, 2 μg	16 hours	10 mins, 45 mins and 16 h: only s.m. observed
3	0.5 mg/mL, 500 μL, 15.6 nmol	4 x 5 μL every 15 minutes	16 hours	10 mins, 45 mins and 16 h: only s.m. observed

Table 4.3. Conditions for cleaving *S*-linked GlcNAc from cAb-Lys3 in PBS, pH 7.4 at 37 °C.

hOGA did not show the desired glycosidase activity towards cAb-Lys3-GlcNAcCys104, despite the use of long reaction times, large amounts of enzyme, and portionwise addition of enzyme (**Table 4.3**). Portionwise addition of large amounts of enzyme was attempted as hOGA is known to react slowly and is somewhat unstable.[2] The results indicated that the chemically introduced *S*-GlcNAc was completely stable to glycosidase, in keeping with reports on the enhanced stability of thioglycosides as compared to their *O*-linked analogues.[38]

4.2.2 Binding inhibition using glucose

Synthesis of 1-thio-β-D-glucose and cAb-Lys3-GluCys104

2,3,4,6-Tetra-*O*-acetyl-1-thio-β-D-glucopyranose[3] was treated with sodium methoxide in methanol to remove the acetate groups and give 1-thio-β-D-glucopyranose (glucose thiol, **Scheme 4.3**).

[2] Verbal communication with Professor David Vocadlo.
[3] 2,3,4,6-Tetra-*O*-acetyl-1-thio-β-D-glucopyranose was kindly donated by Arghya Modak.

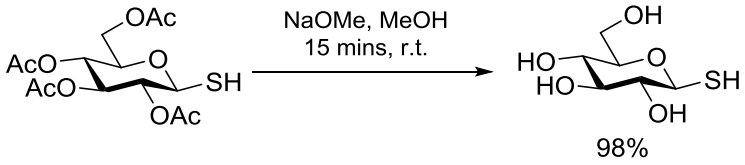

Scheme 4.3. Synthetic route to glucose thiol.

Glucose thiol was coupled to cAb-Lys3-Dha104 via a conjugate addition (**Scheme 4.4**). Initially, 6,000 eq. of glucose thiol was added to cAb-Lys3-Dha104 in 5 portions over 1 hour at 37 °C. The use of a large excess and portionwise addition was attempted due to previous observations that GlcNAc thiol addition to cAb-Lys3-Dha104 was most efficient when conducted in this manner (**Table 4.3**). However, although a mass corresponding to product was observed at 1 hour by LC-MS, the total ion count was substantially lower, indicating loss of antibody. Therefore, the reaction was repeated with 2,000 eq. of glucose thiol, but again a decrease in ion count was observed. Small molecule impurities were removed using a desalting column. Subsequently, the number of equivalents of glucose thiol was reduced to 800, and reactions were carried out at room temperature and at 37 °C. It was found that at room temperature, full conversion to glucosylated antibody was observed after overnight reaction, whereas at 37 °C full conversion was observed with 1 hour. Furthermore, with the lower equivalents of sugar the reaction proceeded without drastic decreases in ion intensity (**Figure 4.10**). The absence of the NHAc group in glucose may improve the reactivity of the anomeric thiol position, as oxazoline formation through neighbouring group participation is no longer possible, and or perhaps due to the electron withdrawing ability of the group.

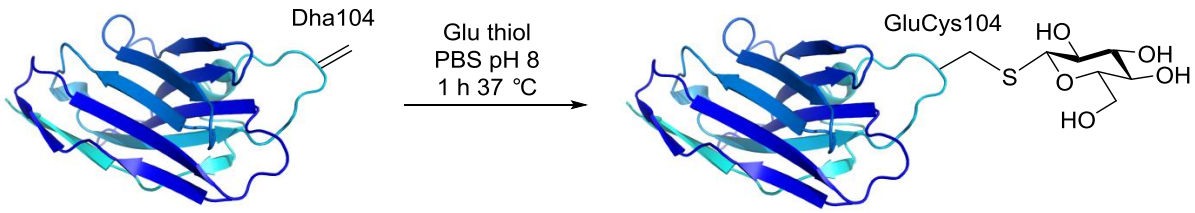

Scheme 4.4. Coupling of cAb-Lys3-Dha104 and glucose thiol forming cAb-Lys3-GluCys104.

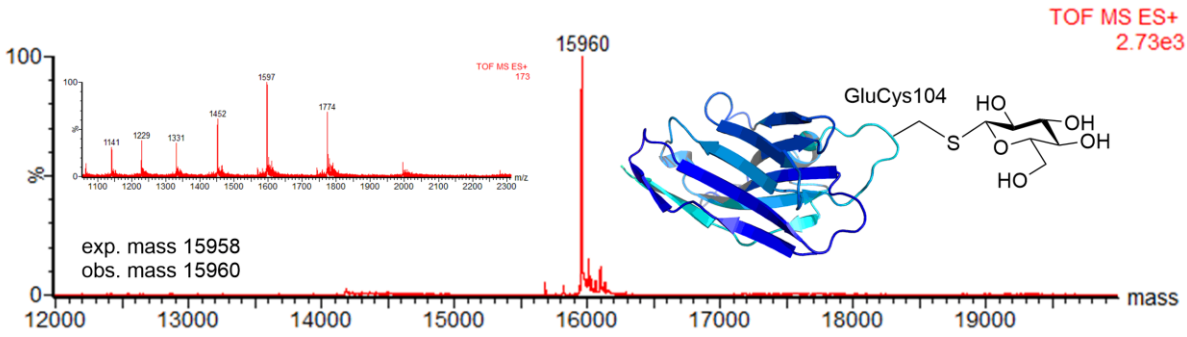

Figure 4.10. cAb-Lys3-Dha104 + 800 eq. of glucose thiol, 1 hour, 37 °C.

As for cAb-Lys3-GlcNAcCys104, the glucosylated antibody, cAb-Lys3-GluCys104 was found to retain predominant β-sheet character as shown by CD (red trace, **Figure 4.11**). The ability of cAb-Lys3 to bind to lysozyme was found to be diminished (ELISA) (red trace, **Figure 4.12**). Chemical corroboration of the location of modification was obtained by testing for the full consumption of free thiol using Ellman's reagent (**Experimental Figure 4.3**). Proteolytic digest and LC-MS/MS analysis was attempted to identify modification at position 104, but was unsuccessful.

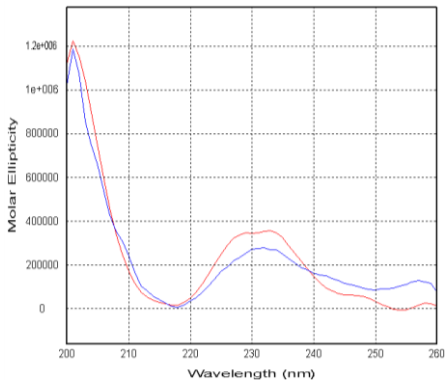

Figure 4.11. CD spectra for glycosylated antibodies show a dip at ~ 215 nm, characteristic of β-sheet folding. Red: cAb-Lys3-GluCys104, blue: cAb-Lys3-GalCys104.

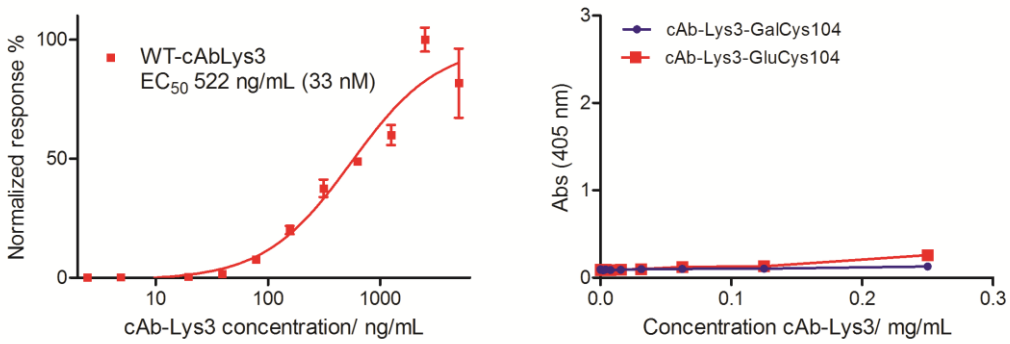

Figure 4.12. ELISA of cAb-Lys3-GluCys104 and cAb-Lys3-GalCys104 with antigen lysozyme.

Treatment of cAb-Lys3-GluCys104 with β-thioglucosidase from Sinapis alba (white mustard) seed

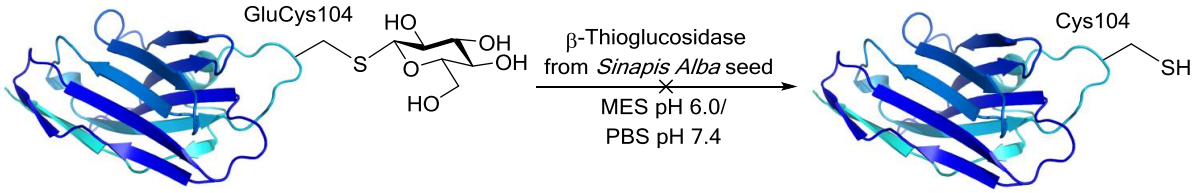

Scheme 4.5. Treatment of cAb-Lys3-GluCys104 with β-thioglucosidase.

The majority of thioglycosides have been reported to be impervious to *O*-glycosidases and so it was decided to investigate whether β-thioglucosidase would be able to act on the glucosylated antibody.[38] In plants β-thioglucosidase are known to cleave glucosinolates releasing toxic compounds (**Figure 4.2**).[47] To our knowledge, the reactivity of β-thioglucosidase on non-natural substrates has never been demonstrated.

The activity of commercially available β-thioglucosidase was tested on the model substrate sinigrin (**Experimental Section**). Following confirmation of activity, cAb-Lys3-GluCys104 was treated with a range of enzyme equivalents in both MES, pH 6.0 (according to manufacturer's guidelines) and PBS, pH 7.4 (physiological pH) as shown in **Table 4.4**.

Entry	cAb-Lys3-GluCys104	mU	U eq.	Observed masses in MES pH 6.0	Observed masses in PBS pH 7.4
1	1.1 nmol	1.1	1	s.m.	s.m.
2	1.1 nmol	2.2	2	s.m.	s.m.
3	1.1 nmol	5.5	5	s.m.	s.m.
4	1.1 nmol	11	10	15273 + s.m.	s.m.
5	1.1 nmol	22	20	15273 + 15410 + s.m.	s.m.
6	1.1 nmol	44	40	14804 + 15273 + 15410 + s.m.	s.m.
7	1.1 nmol	66	60	14804 + 15273 + 15410 + s.m.	s.m.
8	1.1 nmol	88	80	14804 + 15273 + 15410 + s.m.	s.m.
9	1.1 nmol	110	100	14804 + 15273 + 15410 + s.m.	s.m.

Table 4.4. β-Thioglucosidase was prepared as a solution of 0.6 U/mL in either MES, pH 6.0 or PBS, pH 7.4. cAb-Lys3-GluCys104 was treated with enzyme and analysed by LC-MS after 15 minutes incubation at room temperature.

At physiological pH, no reaction of glucosylated antibody was observed (**Table 4.4**). Unfortunately, at pH 6.0, truncation products were observed, none of which corresponded to truncated antibody where glycosidase action may have occurred. An example trace is shown in **Figure 4.13**.

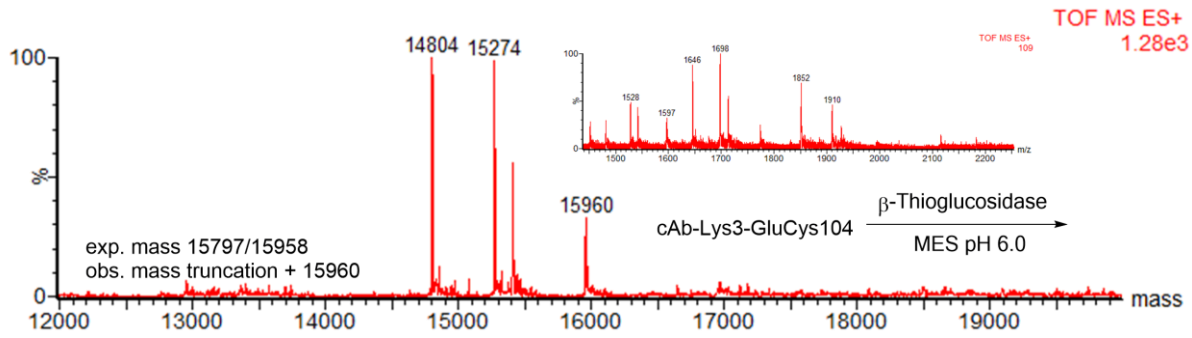

Figure 4.13. Resulting MS when cAb-Lys3-GluCys104 was treated with 100 U eq. β-thioglucosidase for 10 minutes at room temperature in MES, pH 6.0 (entry 9, **Table 4.4**).

In order to test whether truncation could be attributed to impure enzyme,[4] WT-cAb-Lys3 in MES, pH 6.0 was treated with 80 U eq. of β-thioglucosidase. After 10 minutes, extensive truncation was observed as well as some remaining glucosylated antibody (observed mass 15960, **Figure 4.13**). Subsequently it was found that the addition of protease inhibitor prevented this unwanted reaction and so we concluded that the commercial enzyme was contaminated with protease (**Figure 4.14**).

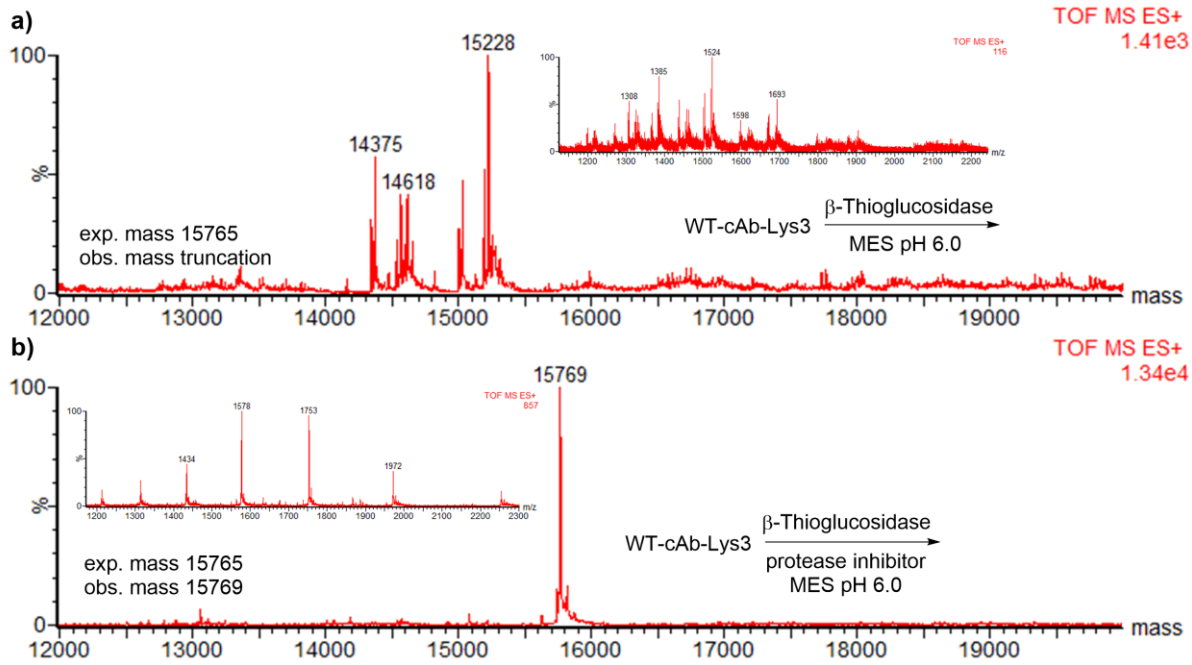

Figure 4.14. a) WT-cAb-Lys3 treated with 80 U eq. β-thioglucosidase, b) WT-cAb-Lys3 treated with 80 U eq. β-thioglucosidase and protease inhibitor.

[4] The manufacturer commented that β-thioglucosidase contains a sugar and anti-oxidant as stabilisers, and may contain other enzymes.

Entry	cAb-Lys3-GluCys104	mU	U eq.	Protease inhibitor/ μL	Observed masses in MES pH 6.0
1	1.1 nmol	1.1	1	0.2	Truncation + s.m.
2	1.1 nmol	2.2	2	1	Majority s.m.
3	1.1 nmol	5.5	5	2	Majority s.m.
4	1.1 nmol	11	10	5	Majority s.m.
5	1.1 nmol	22	20	10	Majority s.m.

Table 4.5. Conditions for cAb-Lys3-GluCys104 + β-thioglucosidase + protease inhibitor. Protease inhibitor was prepared as a solution of 1 tablet in 5 mL water.

By varying the amounts of protease inhibitor, conditions were found under which protease action was inhibited. However, no glycosidase action was observed, suggesting that the glucosylated antibody is stable to β-thioglucosidase (**Table 4.5**).

4.2.3 Binding inhibition using galactose

Synthesis of 1-thio-β-D-galactopyranose and cAb-Lys3-GalCys104

1-Thio-β-D-galactopyranose (galactose thiol) was synthesised in three steps from β-D-galactopyranose pentaacetate. β-D-Galactopyranose pentaacetate was treated with HBr to give the anomeric bromide, followed by displacement of bromide with a thioacetate group, and final deprotection to give 1-thio-β-D-galactopyranose (galactose thiol) (**Scheme 4.6**).

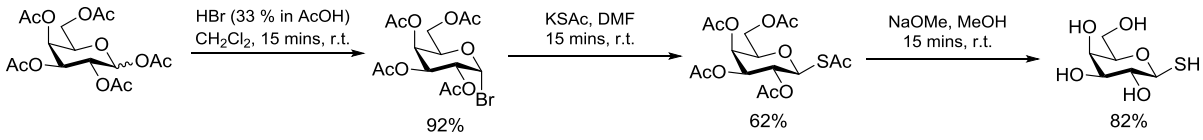

Scheme 4.6. Synthetic route to galactose thiol.

Galactose thiol was coupled to cAb-Lys3-Dha104 via a conjugate addition (**Scheme 4.7**); reaction using 800 eq. of galactose thiol gave full conversion within 2 hours (**Figure 4.15**).

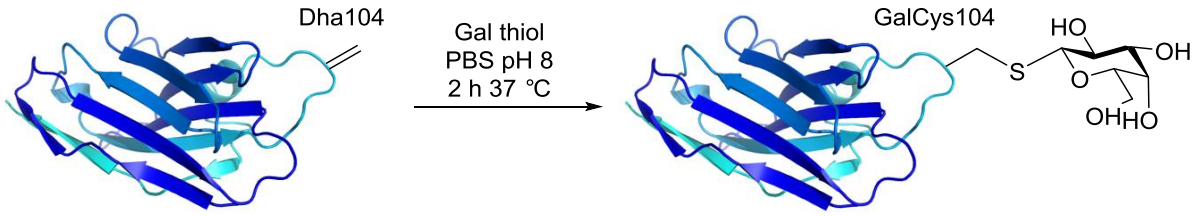

Scheme 4.7. Galactose thiol coupling to cAb-Lys3 via Dha to give cAb-Lys3-GalCys104.

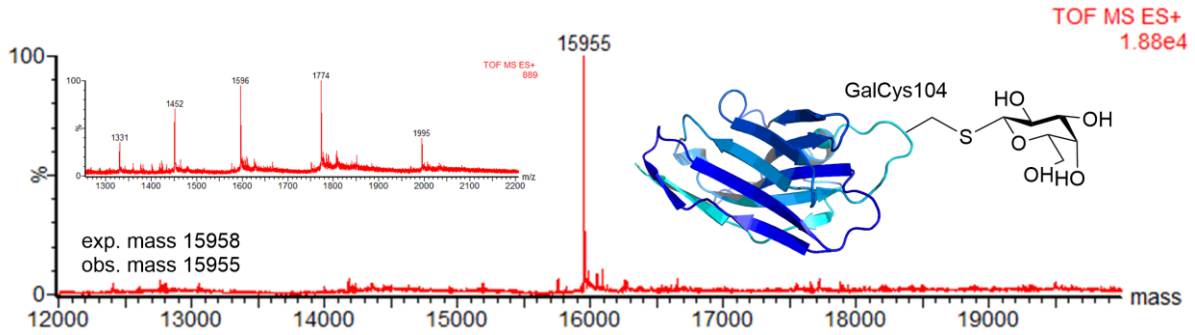

Figure 4.15. cAb-Lys3-Dha104 + 800 eq. galactose thiol, 2 hours, 37 °C.

Galactosylated antibody, cAb-Lys3-GalCys104 was found to retain predominant β-sheet character as tested by CD (blue trace, **Figure 4.11**). As for the other modified cAb-Lys3 constructs, binding ability to lysozyme was diminished (ELISA) (blue trace, **Figure 4.12**). Chemical tests were carried out to elucidate modification at position 104 (**Experimental Figure 4.4**). Proteolytic digest and LC-MS/MS analysis was attempted to identify modification at position 104, but proved unsuccessful.

Treatment of cAb-Lys3-GalCys104 with β-galactosidase from *Aspergillus Oryzae*

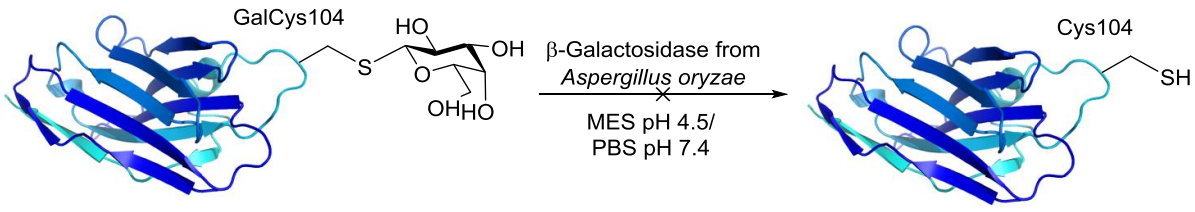

Scheme 4.8. Attempted removal of SGal from cAb-Lys3-GalCys104 using β-galactosidase from *Aspergillus oryzae*.

The activity of the commercially available β-galactosidase was confirmed using the model substrate lactose (**Experimental Section**). Following confirmation of activity, cAb-Lys3-GalCys104 was treated with the enzyme under various conditions as shown in **Table 4.6**.

Entry	cAb-Lys3-GalCys104	mU	U eq.	Observed masses in MES pH 4.5	Observed masses in PBS pH 7.4
1	1.1 nmol	1.1	1	s.m.	s.m.
2	1.1 nmol	2.2	2	s.m.	s.m.
3	1.1 nmol	5.5	5	s.m.	s.m.
4	1.1 nmol	11	10	s.m. + 15820	s.m.
5	1.1 nmol	22	20	s.m. + 15820	s.m.
6	1.1 nmol	44	40	15680 + s.m. + 15820	14800 + s.m.
7	1.1 nmol	66	60	15680 + s.m. + 15820	s.m.
8	1.1 nmol	88	80	15680 + s.m. + 15820	s.m.
9	1.1 nmol	110	100	15545 + 15680 + s.m. + 15820	14545 + 14800 + s.m.

Table 4.6. β-Galactosidase was prepared as a solution of 4.5 U/mL in either MES, pH 4.5 or PBS, pH 7.4. cAb-Lys3-GalCys104 was treated with enzyme, and analysed by LC-MS after 15 minutes at room temperature.

The reaction was conducted at pH 7.4 (physiological) and pH 4.5 (manufacturer's guidelines). At both pH conditions, increasing amounts of truncation were observed proportional to the amount of enzyme used (**Table 4.6**). None of the truncation products corresponded to antibody where glycosidase action may have occurred. An example trace is shown in **Figure 4.16**.

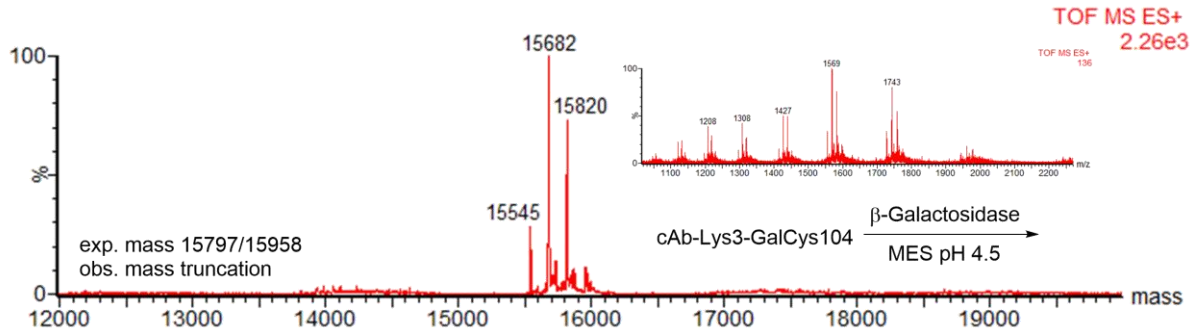

Figure 4.16. Typical MS observed when cAb-Lys3-GalCys104 was treated with 100 U eq. β-galactosidase for 10 minutes at room temperature in MES, pH 4.5 (entry 9, **Table 4.6**).

In order to test whether truncation could be attributed to impurities in the enzyme,[5] WT-cAb-Lys3 in MES, pH 4.5 was treated with 100 U eq. of β-galactosidase. After 10 minutes, extensive truncation was observed and it was found that the addition of protease inhibitor prevented this (**Figure 4.17**).

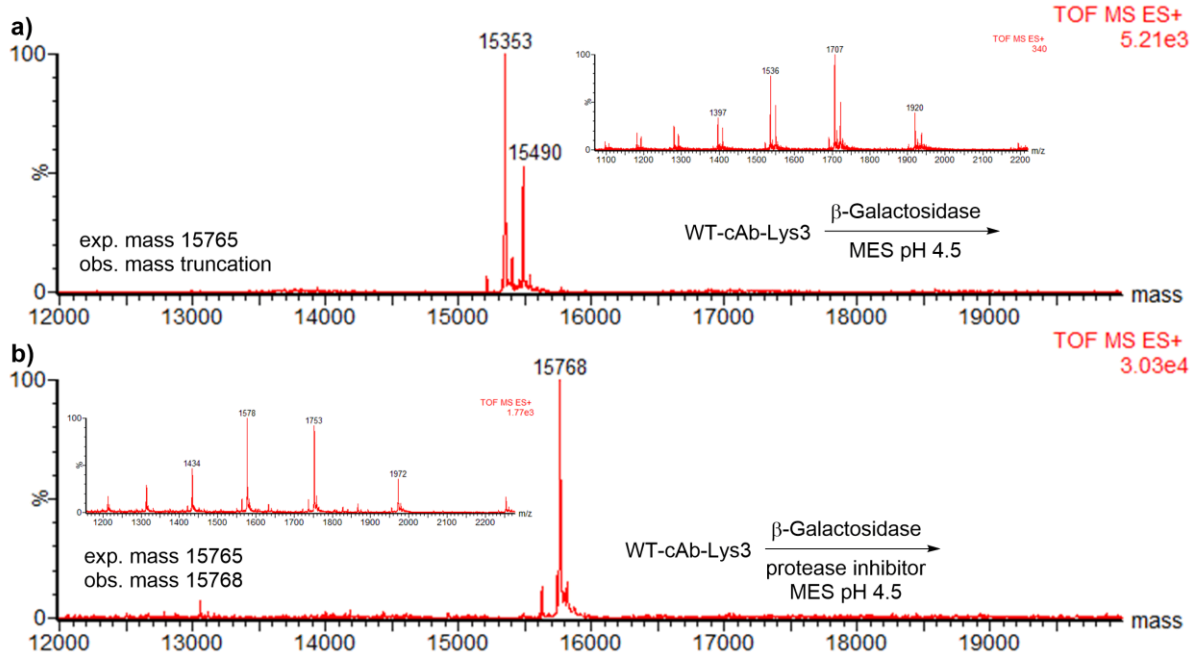

Figure 4.17. a) WT-cAb-Lys3 treated with 100 U eq. β-galactosidase, b) WT-cAb-Lys3 treated with 100 U eq. β-galactosidase and protease inhibitor.

[5] According to the manufacturer, β-galactosidase contains other enzymes that have not been identified.

Entry	cAb-Lys3-GalCys104	mU	U eq.	Protease inhibitor/ μL	Observed masses in MES pH 4.5
1	1.1 nmol	1.1	1	0.2	Truncation + s.m.
2	1.1 nmol	2.2	2	1	Majority s.m.
3	1.1 nmol	5.5	5	2	Majority s.m.
4	1.1 nmol	11	10	5	Majority s.m.
5	1.1 nmol	22	20	10	Majority s.m.

Table 4.7. Conditions for cAb-Lys3-GalCys104 + β-galactosidase + protease inhibitor. Protease inhibitor was prepared as a solution of 1 tablet in 5 mL water.

By varying the amount of protease inhibitor, conditions could be found where protease activity was completely inhibited. However, no conditions were found where glycosidase action was observed, suggesting that the galactosylated antibody was stable to β-galactosidase (**Table 4.7**).

Conclusions for glycosylated antibodies

We were able to attach glucose and galactose to cAb-Lys3 at position 104, forming homogeneous glycosylated antibodies. Removal attempts with β-thioglucosidase and *O*-specific β-galactosidase were unsuccessful, indicating that the glycosylated antibodies are stable to hydrolysis. The stability of the conjugates rendered this approach inappropriate for the development of an AND antibody because we were unable to release the antibody and recapitulate binding activity. Therefore an alternative approach towards an antibody following AND logic was attempted using the thiophosphate group.

4.2.4 Binding inhibition using the thiophosphate group and subsequent removal

Site-specific chemical installation of the thiophosphate group

The thiophosphate group (phosphocysteine, pCys) was introduced at position 104 of cAb-Lys3 via conjugate addition of sodium thiophosphate to cAb-Lys3-Dha104 (**Scheme 4.9**). Optimisation of the reaction was carried out as indicated in **Table 4.8**.

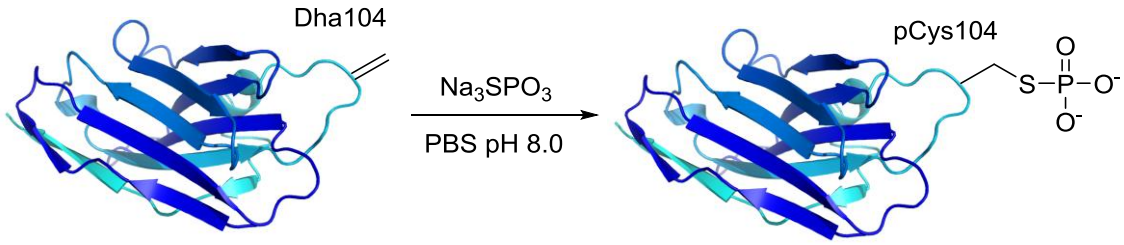

Scheme 4.9. Conjugate addition of sodium thiophosphate to cAb-Lys3-Dha104.

	cAb-Lys3-Dha104	**Na_3SPO_3**	**Conditions**	**Observations**
1	100 µL, 3.2 nmol, 0.5 mg/mL	12.0 mg, 66.7 µmol 20,000 eq.	1 h, 37 °C	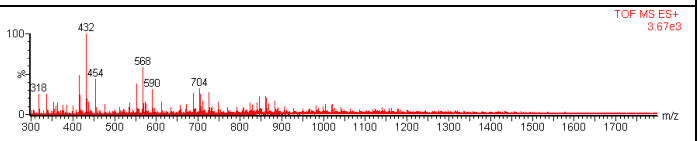
2	100 µL, 3.2 nmol, 0.5 mg/mL	2.3 mg, 12.8 µmol 4,000 eq.	1 h, 37 °C	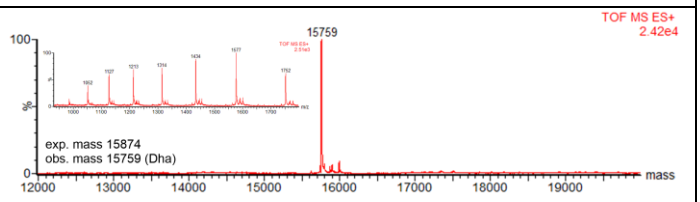
3	100 µL, 3.2 nmol, 0.5 mg/mL	6.7 mg, 37.2 µmol, 10,000 eq.	3 h, 37 °C	1 hour – 30%, 2 hours – 45%, 3 hours – 60% 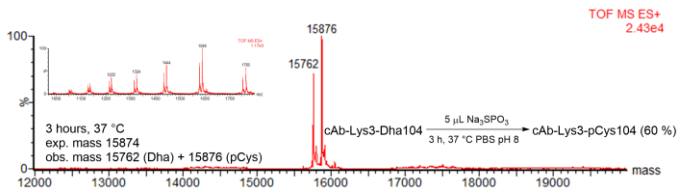
4	100 µL, 3.2 nmol, 0.5 mg/mL	4 x 3.4 mg, 18.9 µmol, 20,000 eq.	16 h, 37 °C	1h30m – 70%, 16 h – full conversion 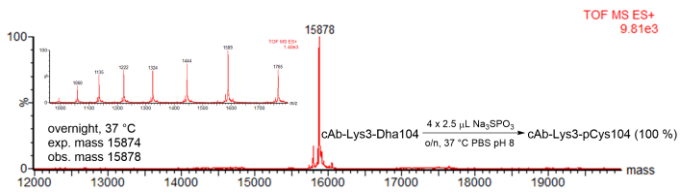

5	100 μL, 3.2 nmol, 0.5 mg/mL	4 x 3.4 mg, 18.9 μmol, 20,000 eq.	16 h, r.t.	1h30m – 50%, 16 h – 70% 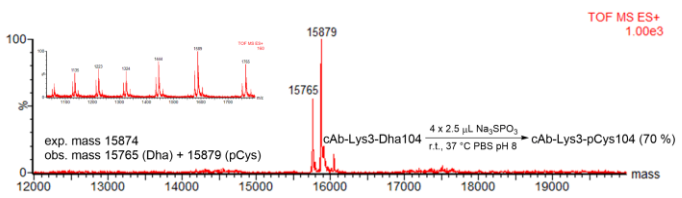

Table 4.8. Optimisation of conditions for the formation of cAb-Lys3-pCys104. Sodium thiophosphate was added as a solution (between 46 and 52 mg Na_3SPO_3 in 18.6 μL water and 20 μL 5 M HCl, pH 8 – 8.5).

Efficient and reproducible installation of the thiophosphate group was observed *via* the portionwise addition of sodium thiophosphate solution at 37 °C (entry 5, **Table 4.8**). As in the addition of GlcNAc thiol to cAb-Lys3-Dha104, the antibody appears to be stable to extended reaction times at higher temperatures. The complete loss of antibody signal upon the addition of 20,000 eq. of thiophosphate in one aliquot indicates that the antibody is unstable to such conditions (entry 1, **Table 4.8**), whereas adding the same number of equivalents of reagent in a portionwise manner led to full conversion without loss of antibody (entries 4 and 5, **Table 4.8**). Furthermore, the difference in reactivity observed when 4,000 eq. (entry 2, **Table 4.8**) and 10,000 eq. (entry 3, **Table 4.8**) of reagent were used demonstrated the need for large excesses. This may be because in solution at pH 8, the sodium thiophosphate forms intermolecular disulfide bonds, and so is gradually consumed. Further investigation into reaction times established that following portionwise addition of sodium thiophosphate, 7 hours at 37 °C was sufficient for full conversion to cAb-Lys3-pCys104 (**Scheme 4.10**).

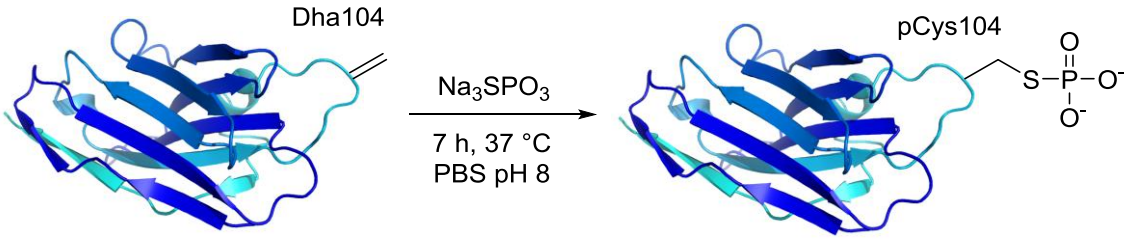

Scheme 4.10. Conversion of cAb-Lys3-Dha104 to cAb-Lys3-pCys104.

As well as characterisation by LC-MS (entry 4, **Table 4.8**), CD analysis indicated that the phosphorylated antibody retained β-sheet structure (**Figure 4.18**). Proteolytic digest and subsequent LC-MS/MS analysis confirmed the site of modification to be position 104 (**Experimental Figure 4.5**).

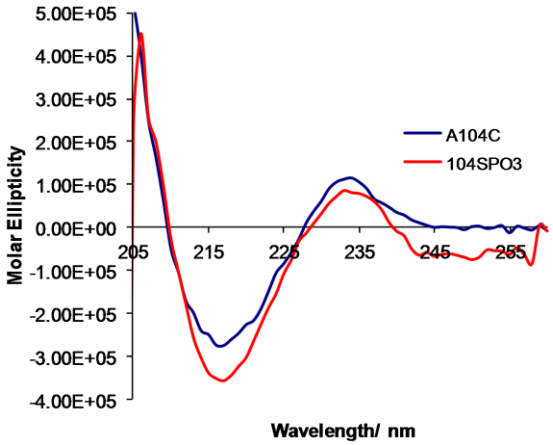

Figure 4.18. CD spectrum of cAb-Lys3-Cys104 and cAb-Lys3-pCys104.

Although phosphorylation is known to cause drastic effects on the overall structure of a protein,[54,55,57,58,68] it is unsurprising that little effect is observed on the structure of cAb-Lys3 as the site of modification is positioned at the tip of the CDR3 loop, which has minimal interactions with neighbouring residues. Indeed, the position of modification was expected to be such that it would affect binding interactions to lysozyme. As mentioned previously, the normal interaction (between 104Ala and Trp) is predominantly hydrophobic.[23] Binding affinity of cAb-Lys3-pCys104 to the antigen lysozyme was tested by ELISA. As expected, antibody binding was found to be severely diminished compared to the WT antibody (**Figure 4.19**).

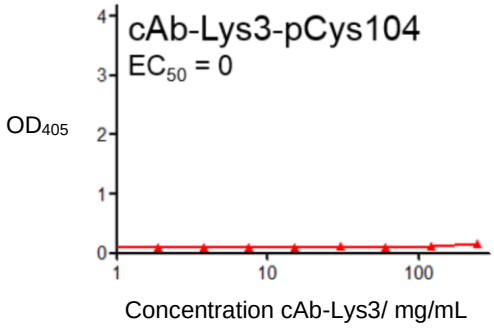

Figure 4.19. cAb-Lys3 binding to lysozyme is severely inhibited following the introduction of the pCys group at position 104.

In conclusion, an inhibited antibody was synthesised under ambient conditions from cAb-Lys3-Dha104. A method by which to remove the inhibiting group and regenerate cysteine at position 104 were investigated next.

Enzymatic removal of chemically installed thiophosphate group from cAb-Lys3-pCys104

λ-Protein phosphatase

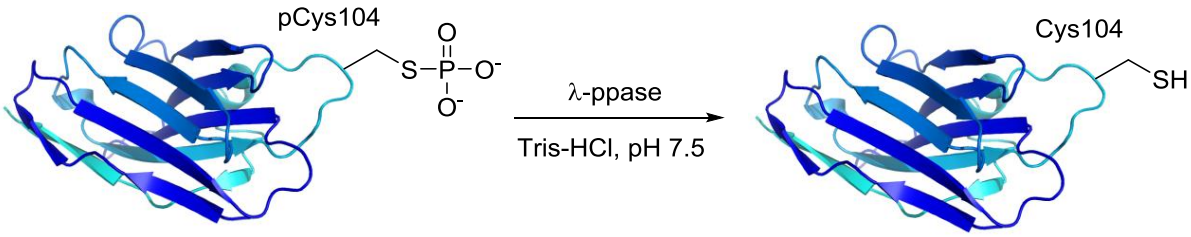

Scheme 4.11. Treatment of cAb-Lys3-pCys104 with λ-protein phosphatase (λ-ppase) regenerating cysteine at position 104.

λ-Protein phosphatase (λ-ppase) is a promiscuous Mn^{2+}-dependent enzyme encoded in the genome of bacteriophage lambda.[69] cAb-Lys3-pCys104 was desalted and buffer exchanged into 50 mM Tris-HCl, and then treated with λ-ppase (**Scheme 4.11**). LC-MS analysis after 90 minutes revealed that some unreacted cAb-Lys3-pCys104 remained and also that cAb-Lys3-Dha104 had formed (**Figure 4.20**). It is thought that the re-formation of cAb-Lys3-Dha104

arose from excess dibromo reagent **3.3** which remained in solution from the prior reaction to form cAb-Lys3-Dha104 (**Figure 3.4, Chapter 3**). As soon as the phosphate group was removed by λ-ppase, the liberated cysteine would react with **3.3** to reform Dha. To test this theory, cAb-Lys3-pCys104 was desalted twice in an attempt to completely remove excess **3.3**, and then treated with λ-ppase. Gratifyingly, clean conversion to cAb-Lys3-Cys104 was observed (**Figure 4.21**). To the best of our knowledge, this is the first example of the use of a phosphatase on an *S*-linked phosphate group, rendering the modification a functional pSer PTM mimic. Furthermore, after conjugate addition to Dha, pCys in cAb-Lys3 is likely to be a diastereomeric mixture. The ratio of diastereomers is likely to be dependent on steric and electronic effects imposed by neighbouring residues.

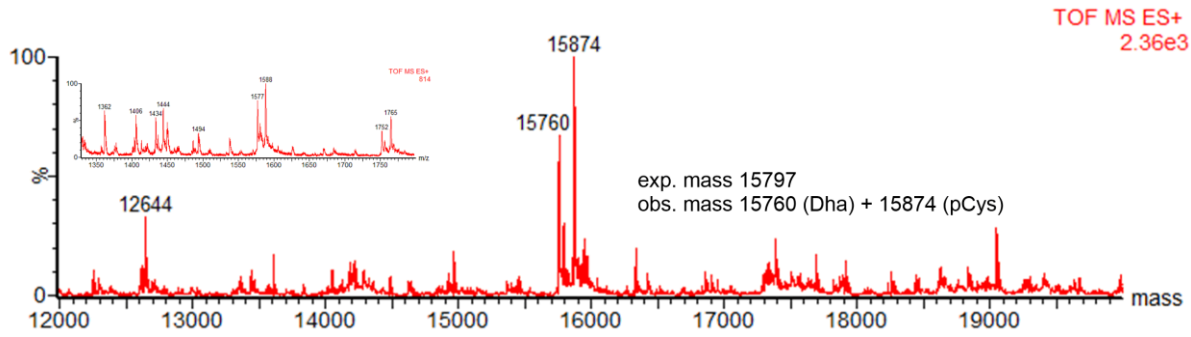

Figure 4.20. On treatment with λ-ppase, regenerated cAb-Lys3-Cys104 appeared to react with excess dibromo reagent **3.3**.

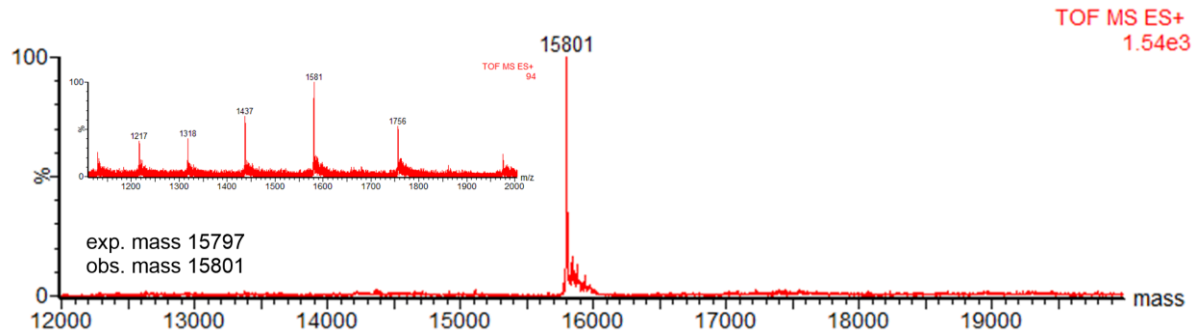

Figure 4.21. Treatment of cAb-Lys3-pCys104 with λ-ppase after two desalting steps gave clean conversion to cAb-Lys3-Cys104.

Next, regenerated cAb-Lys3-Cys104 was tested for binding ability to lysozyme. Binding to lysozyme with micromolar affinity (in the same region as the original mutant) was observed (**Figure 4.22**). No separation of antibody from enzyme was required.

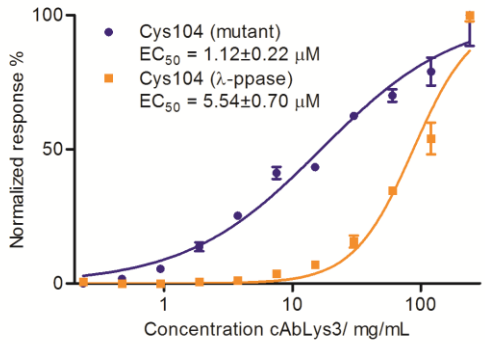

Figure 4.22. ELISA of cAb-Lys3-Cys104 and cAb-Lys3 containing regenerated cysteine at position 104.

Finally, regenerated cAb-Lys3-Cys104 was tested for reactivity by reacting with Ellman's reagent. Full conversion to the expected adduct was observed under identical conditions to those used on the original cysteine mutant (**Figure 4.23**), establishing that full chemical reactivity was restored.

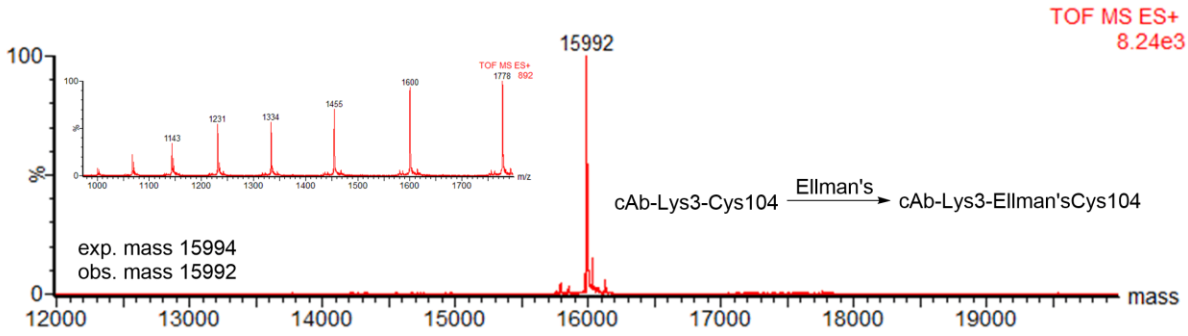

Figure 4.23. Regenerated cAb-Lys3-Cys104 reacts with Ellman's reagent, indicating the presence of a single free thiol.

Enzymatic removal of the thiophosphate group with alternative phosphatases

cAb-Lys3-pCys104 was treated with a range of commercially available phosphatases, with the aim of establishing the generality of the dephosphorylation process. After optimisation, it

was found that a number of phosphatases previously reported to be specific for the *O*-phosphate group[69–73] were active towards the phosphocysteine at position 104 of cAb-Lys3 (**Scheme 4.12**). ELISAs confirmed that antibody containing regenerated cysteine were active in binding to lysozyme at micromolar levels (**Figure 4.24**).

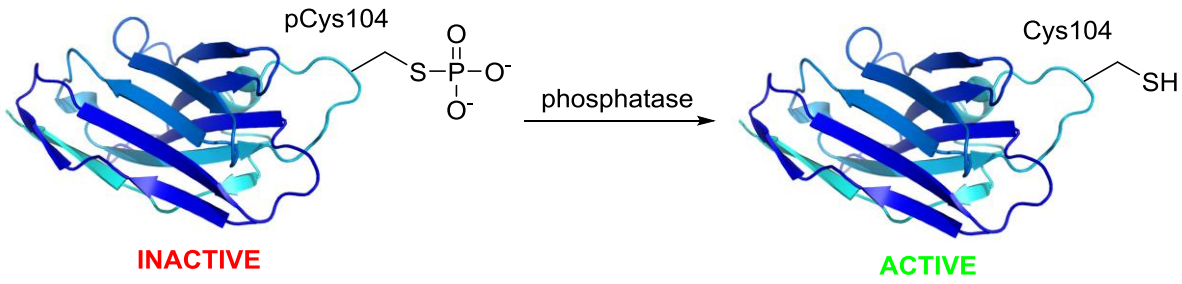

Scheme 4.12. Regeneration of cAb-Lys3-Cys104 by the treatment of cAb-Lys3-pCys104 with a range of phosphatases.

Human placental alkaline phosphatase

The ability of human placental alkaline phosphatase (PLAP) to dephosphorylate cAb-Lys3-pCys104 was of particular interest for potential *in vitro* applications, which are described later in this chapter. Initially, we attempted to cleave cAb-Lys3-pCys104 with PLAP in PBS but no reaction was observed. Phosphate has been reported to potentially inhibit the activity of this enzyme and so the choice of buffer may be responsible for the observed lack of reactivity.[73] In fact, the phosphate ion has been used to purify this enzyme by affinity chromatography, confirming that there is an interaction between the enzyme and phosphate.[73] Therefore we changed reaction conditions and conducted future studies in Tris-HCl buffer. Magnesium (Mg) is reported to be a non-essential activator for the enzyme, prompting us to also investigate this factor.[73] Dephosphorylation of cAb-Lys3-pCys104 by PLAP was investigated using Tris-HCl as the reaction buffer and testing rate acceleration with Mg^{2+}at various enzyme concentrations. Results obtained are summarised in **Table 4.9**.

	Buffer	PLAP	Observations by MS at 1h15m	Observations by MS at 4h45m
1	50 mM Tris-HCl, pH 7.4	0.19 U	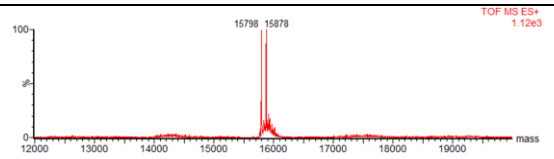	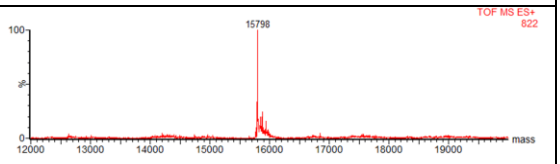
2	50 mM Tris-HCl, pH 7.4	1.13 U	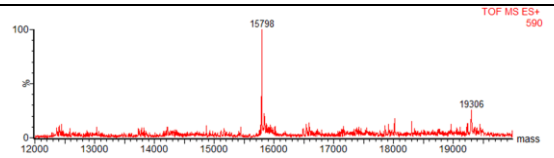	n/a
3	50 mM Tris-HCl, 0.3 mM $MgCl_2$, pH 7.4	0.19 U	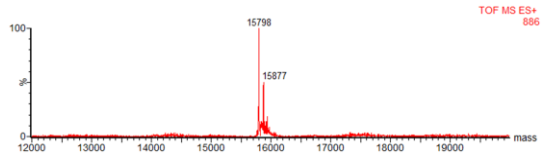	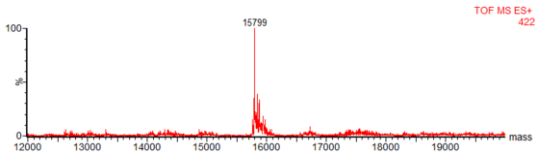
4	50 mM Tris-HCl, 0.3 mM $MgCl_2$, pH 7.4	1.13 U	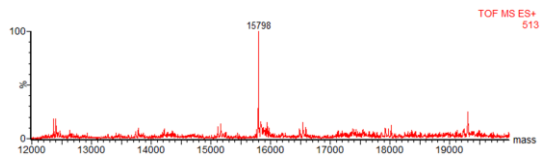	n/a

Table 4.9. Conditions used to investigate the dephosphorylation of cAb-Lys3-pCys104 by PLAP in 50 mM Tris-HCl at pH 7.4. cAb-Lys3-pCys104 exp. mass 15874, cAb-Lys3-Cys104 exp. mass 15797.

The results in **Table 4.9** support previous observations[73] that PBS does indeed inhibit PLAP, as reactions with Tris-HCl led to full conversion in all cases. Unsurprisingly, an increase from 0.19 to 1.13 U PLAP led to faster conversion, whilst the presence of Mg^{2+} was found to accelerate the reaction (entries 1 and 3 at 1 hour 15 minutes, **Table 4.9**).

Alternative Phosphatases

Human acid phosphatase-1 (acp-1), acid phosphatase from potato and alkaline phosphatase from bovine intestinal mucosa (bIMP) were all found to be functional towards cAb-Lys3-pCys104, although each phosphatase was found to work best under different optimal conditions (pH and temperature, **Experimental Figures 6 – 10**). Following removal of the thiophosphate group, the cAb-Lys3 proteins containing a regenerated cysteine at position 104 were submitted to an ELISA, to confirm regeneration of binding. Gratifyingly, all

regenerated forms of cAb-Lys3-Cys104 exhibit micromolar binding affinities to lysozyme (**Figure 4.24**).

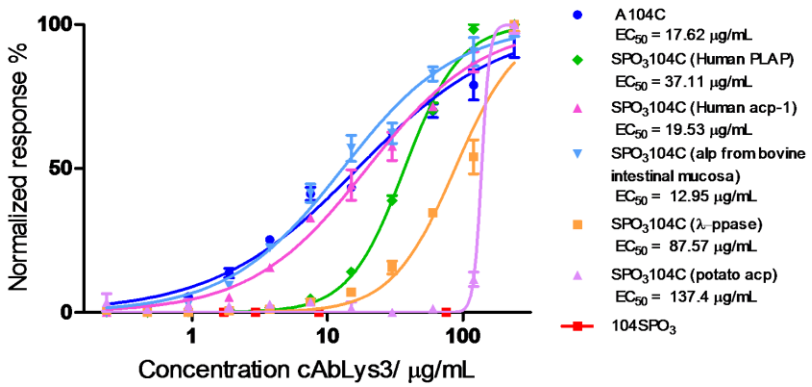

Figure 4.24. cAb-Lys3 containing regenerated Cys at position 104 is able to bind to lysozyme at similar levels as the original mutant.

Comparison of phosphatase activities at physiological conditions

With the aim of investigating the temporary inhibition of cAb-Lys3 *in vitro*, the ability of each of the phosphatases to cleave the thiophosphate group were tested under identical conditions but with a lower number of equivalents of enzyme, and at physiological temperature and pH. Reactions were monitored by LC-MS at 1, 2.5 and 4 hours (**Experimental Figures 11 – 15**). Results revealed that the alkaline phosphatases human PLAP and bIMP were able to cleave the thiophosphate group rapidly at pH 7.4, prompting them to be considered when devising *in vitro* experiments. For both λ-ppase and human acp-1, limited thiophosphate removal was observed, whilst approximately 60% dephosphorylation was observed with acp from potato (**Figure 4.25**).

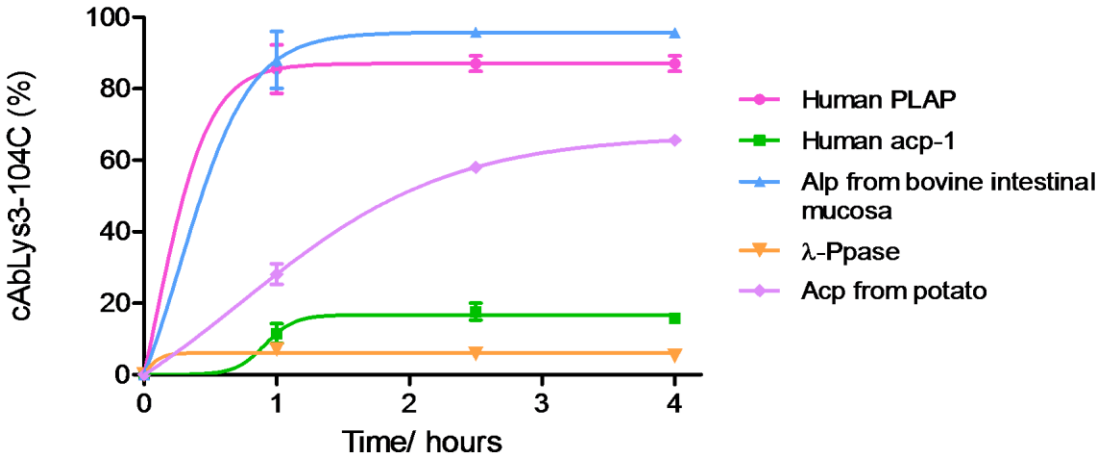

Figure 4.25. MS Monitoring of the formation of regenerated cAb-Lys3-Cys104 by treatment of cAb-Lys3-pCys104 with different phosphatases.

4.2.5 Creation of an antibody following Boolean AND logic and application *in vitro*

The introduction of pCys at position 104 generated a multi input antibody. cAb-Lys3-pCys104, in a temporary inhibitory state would require two inputs (antigen and phosphatase) in order to regain function of binding. The system could therefore be considered an AND logic gate.[11] AND logic gate conditions were tested by ELISA, where cAb-Lys3-pCys104 was treated with the varying combinations of inputs as shown in **Figure 4.26**. Gratifyingly, only in the case where both antigen and phosphatase were present, was binding to lysozyme observed. In the absence of one or both inputs, binding of cAb-Lys3-pCys104 was not possible (**Figure 4.26**).

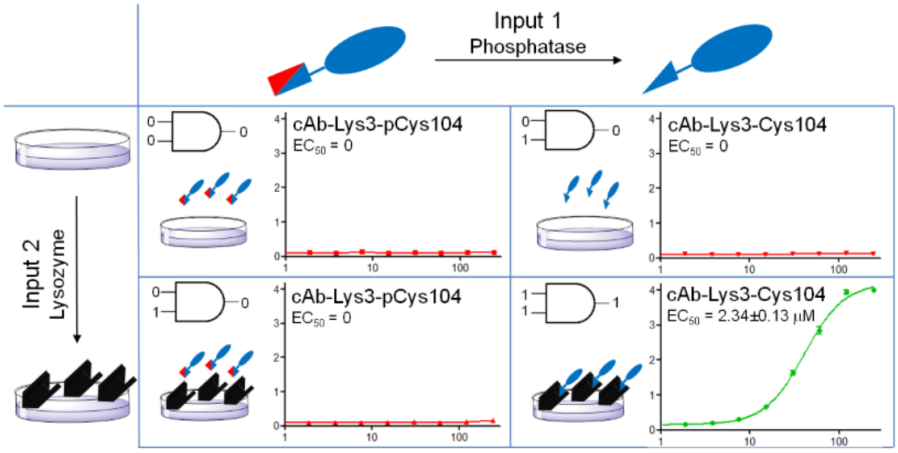

Figure 4.26. Testing AND logic gate conditions by ELISA.

In order to obtain functional antibody *in vitro*, the presentation of both inputs was required. Despite reports that their small size renders some camelid antibodies cell permeable,[74] this was not found to be the case with cAb-Lys3 and Human Embryonic Kidney cells (HEK293T). We therefore designed experiments where the binding of antibody could be controlled extracellularly, by the cell surface presentation of antigen and the exogenous addition or secretion of phosphatase (**Figure 4.27**).

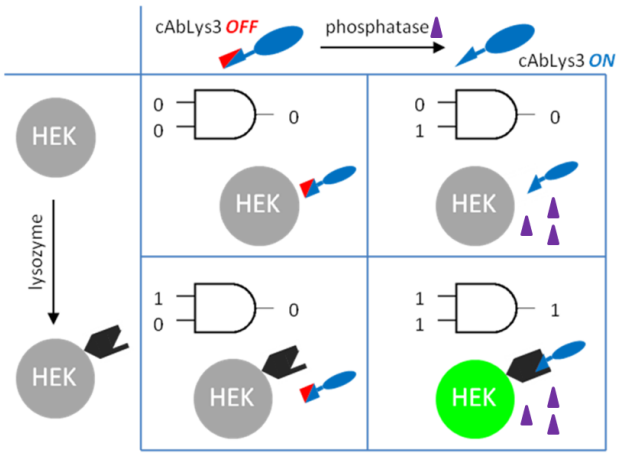

Figure 4.27. AND logic gate conditions for directing cAb-Lys3 to bind to a cell surface under the control of inputs antigen and phosphatase. Black shape: lysozyme, purple triangle: phosphatase.

Presentation of input 1: the antigen lysozyme

Extracellular presentation of antigen was achieved by the transfection of HEK293T cells with DNA encoding for lysozyme (D52S) in pIMMS2011 (pIMMS2011:lysozyme). pIMMS2011

is a plasmid containing a signal sequence for cell surface localisation of the desired protein under the control of the cytomegalovirus (CMV) promoter. The transfection of lysozyme in HEK293T cells was tested with a number of reagents. Following transfection attempts, cells were treated with WT-cAb-Lys3 and then a fluorophore-antiHis conjugate, specific for WT-cAb-Lys3. Subsequently samples were analysed using Fluorescence Activated Cell Sorting (FACS). Lyovec, a cationic phosphonolipid[75] showed quite low transfection efficiencies with HEK293T and HEK-Blue cells, as did transfection via the calcium phosphate method[76] (**Figure 4.28**). However, transfection with Xtreme HP DNA reagent gave rise to approximately 50% fluorescent cells, whilst Xfect reagent, a cationic biodegradable polymeric reagent forming nanoparticle complexes with DNA, showed the highest level of transfection efficiency (**Figure 4.28**). Transfection of cells using Xfect was subsequently tested further by screening DNA quantities (**Figure 4.29**), and the amount of WT-cAb-Lys3 attached to cells was also checked by addition of the antibody at various concentrations to ensure antibody was not sticking to cells in a non-specific fashion (**Figure 4.30**). The percentages of labelled cells were in the same region for a range of WT-cAb-Lys3 concentrations.

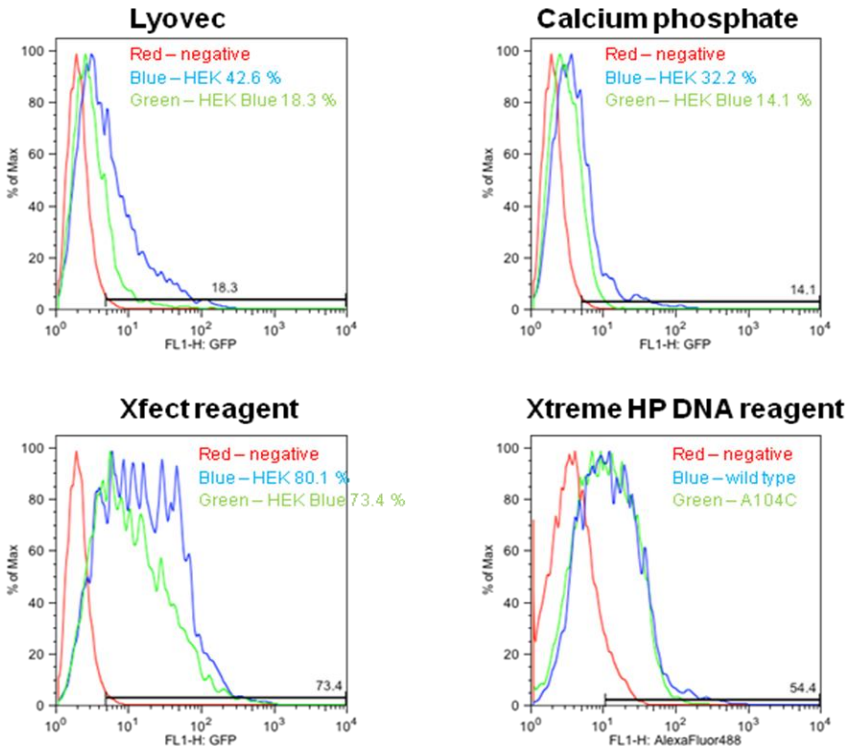

Figure 4.28. FACS traces for various transfection reagents with HEK and HEK Blue cells. Transfection efficiency was tested by adding WT-cAb-Lys3, followed by fluorophore-AntiHis conjugate to transfected cells for Lyovec, calcium phosphate and Xfect. For Xtreme HP DNA reagent, either WT-cAb-Lys3 or cAb-Lys3-Cys104 was added to HEK Blue cells, followed by the same fluorophore.

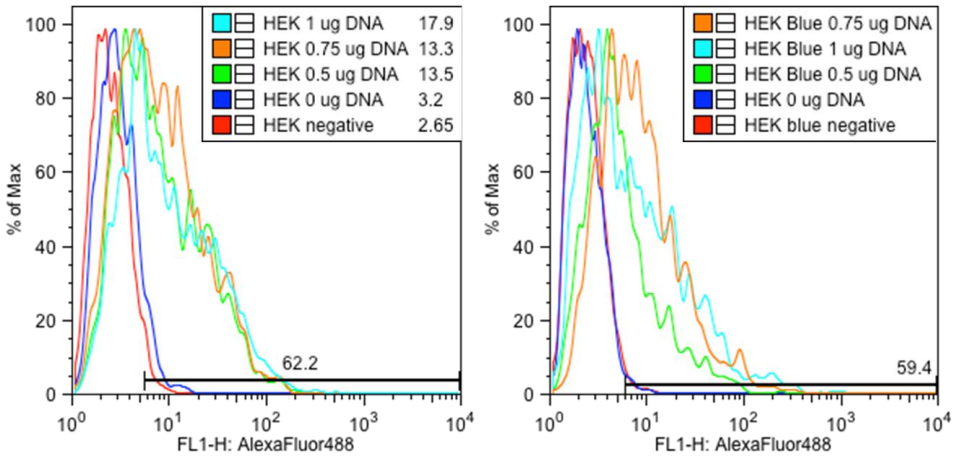

Figure 4.29. Transfection optimisation with Xfect and HEK cells (left) and HEK Blue cells (right).

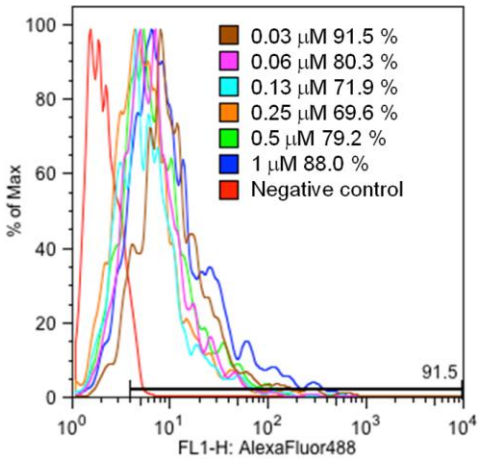

Figure 4.30. Determination of cell surface lysozyme expression by FACS. WT-cAb-Lys3 was added in varying concentrations to HEK293T cells transfected with lysozyme followed by fluorophore-AntiHis conjugate.

Presentation of Input 2: Phosphatase

cAb-Lys3-pCys104 requires both antigen and phosphatase to regain function. Initially, λ-ppase (previously shown to efficiently dephosphorylate cAb-Lys3, **Figure 4.21**) was added as an exogenous phosphatase source to HEK293T cells expressing cell surface lysozyme in the presence of inhibited antibody cAb-Lys3-pCys104. Unfortunately, on the addition of λ-ppase as well as Mn^{2+}, internalisation of fluorescence was observed by microscopy, probably due to cell death (**Figure 4.31**). Manganese, although essential as a cofactor in many enzymatic reactions, is known to be cytotoxic to humans in excessive quantities.[77]

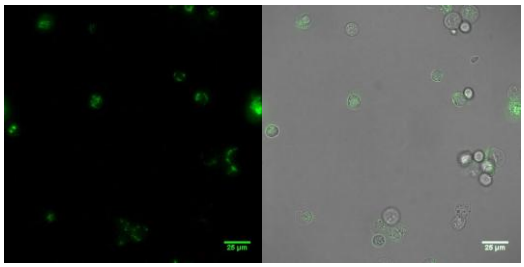

Figure 4.31. Mn^{2+}, λ-ppase and cAb-Lys3-pCys104 added to HEK293T cells expressing cell surface lysozyme. Scale bar reads 25 μm.

It was thought that the endogenous production of the phosphatase input would be more desirable, allowing external control at a cellular level. In the interests of controlling antibody

function extracellularly, a secreted phosphatase was required. Previously, human PLAP was found to efficiently desphosphorylate cAb-Lys3-pCys104 at physiological pH. PLAP is a membrane protein, and a truncated form (Secreted Embryonic Alkaline Phosphatase, SEAP) lacking the 24 amino acids which comprise the membrane-anchoring domain is a widely used extracellular reporter for the study of promoter activity or gene expression.[78] As the phosphatase input source, SEAP was expressed in two ways. Firstly, SEAP expression was induced by the addition of a cytokine to HEK-Blue Null1 cells. HEK-Blue Null1 cells are engineered to express the SEAP reporter gene under the control of the IFN-β minimal promoter fused to five NF-κB and AP-1 binding sites. For these cells, SEAP expression by two different cytokines were tested. HEK-Blue Null1 cells stably express endogenous levels of both the poly(I:C) receptor TLR3 (TLR – Toll Like Receptor) and the TNF-α receptors, TNFR1 and TNFR2 (TNF – Tumour Necrosis Factor). TNF-α is a mammalian messenger protein with widespread signalling function in disease states.[79] Treatment with the appropriate cytokines should activate NF-kB and AP-1, inducing the expression of SEAP. Detection of SEAP was measured by the addition of the chromophoric substrate, QUANTI-Blue™, to the cell culture medium. The substrate produces a colorimetric change upon hydrolysis, which is visible to the naked eye and can also be accurately quantified by a shift in OD between 620 – 655 nm. For poly(I:C), no evidence of SEAP expression was detected, whilst for the inflammatory cytokine TNF-α, an increase in OD was observed for increasing concentrations of the cytokine (**Figure 4.32**), indicating successful expression and secretion of phosphatase.

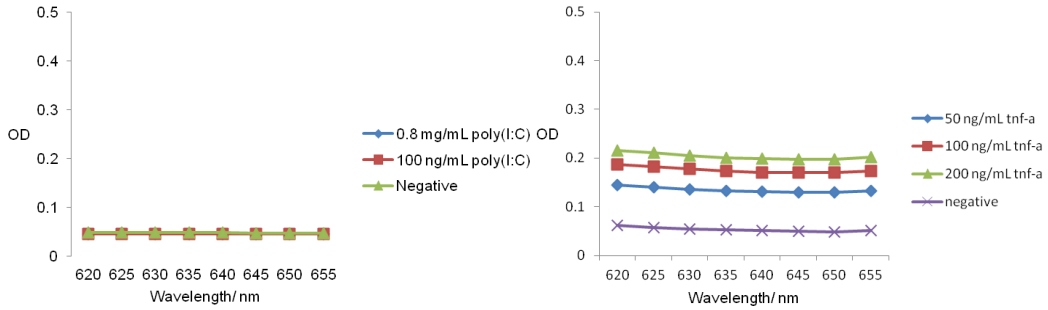

Figure 4.32. a) Addition of poly(I:C) to HEK-Blue Null1 cells, b) addition of TNF-α to HEK-Blue Null1 cells.

The expression of SEAP was also tested using a gene encoding for SEAP under the CMV promoter in pBluescript (pBluescript:SEAP). HEK293T cells were transfected with the plasmid using Xfect, under the same conditions as described for the transfection of cell surface lysozyme. Following transfection, addition of the chromophoric substrate to the cell culture medium led to an increase in OD in SEAP-positive cells (**Figure 4.33**).

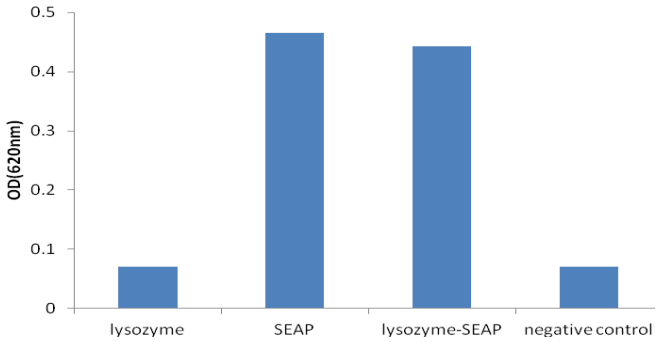

Figure 4.33. Testing SEAP expression with pBluescript:SEAP in singly and co-transfected HEK293T cells.

Generation of an antibody following AND logic

Following the efficient and reproducible development of transfection methods for expression of the two inputs required for activity of cAb-Lys3-pCys104, conditions to dephosphorylate the antibody in the presence of HEK293T cells expressing cell surface lysozyme and secreted phosphatase were sought. The aim of this work was to direct the antibody specifically to the cell surface where the antigen for the antibody is expressed.

HEK-Blue Null1 AND antibody gate

Four sets of HEK-Blue Null1 cells were cultured and transfected according to the conditions depicted in **Figure 4.27**. Cells were transfected with pIMMs2011:lysozyme-D52S, and TNF-α was added to induce SEAP expression. The inhibited phosphorylated antibody cAb-Lys3-pCys104 was added from a stock solution of 0.1 mg/mL (6.3 μM) to give reaction mixtures with a final antibody concentration of 1 and 10 μM respectively. After addition of the fluorophore-AntiHis conjugate, selective targeting of the antibody to the cell surface was tested by FACS. When 1 μM inhibited antibody and the two required inputs were added, no shift was observed by FACS, indicating that antibody had not bound to the cell surface (**Figure 4.34**). Initial analysis of the same reaction with 10 μM inhibited antibody suggested that again the antibody had not bound to the cell surface. However, closer analysis indicated that the trace for cells expressing both inputs was slightly shifted relative to the other traces (where one or both inputs are missing) (**Figure 4.34**).

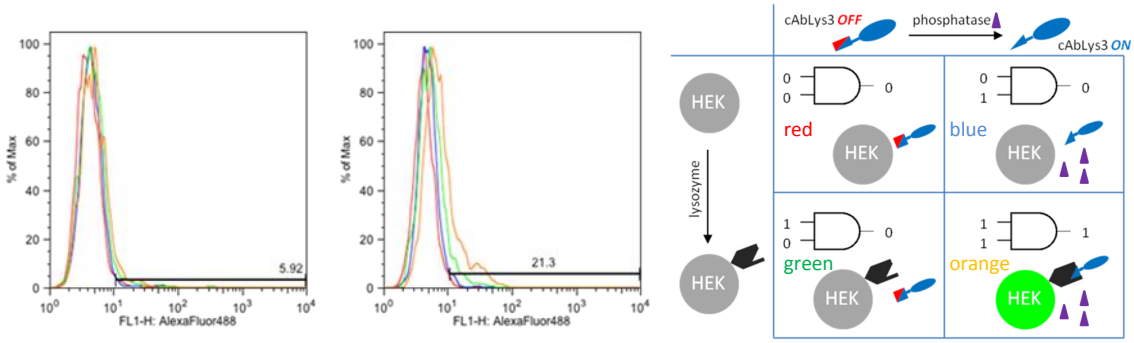

Figure 4.34. AND antibody conditions using 1 (left) and 10 (middle) μM inhibited antibody.

The stock solution of inhibited antibody was concentrated to 1.8 mg/mL (113 μM) so that a lower volume could be added to the cell culture medium, diluting it less. Inhibited antibody at 1 μM was therefore added to the 4 cell sets expressing varying combinations of inputs. Following the addition of the fluorophore, FACS analysis showed that a significant shift

corresponding to fluorescent cells could only be seen when inhibited antibody was added to cells expressing both inputs (**Figure 4.35a**). Expression of only one input was not sufficient to effect a shift. In this case, the cells used were at a passage number of 16, and HEK-Blue cells are not recommended for use beyond passage 20 due to potential genomic changes. To check that the results obtained were down to the controlled expression of inputs, a frozen cell stock at passage 4 was thawed, and the experiment repeated with cells at passage 5. Gratifyingly, similar results were obtained (**Figure 4.35b**).

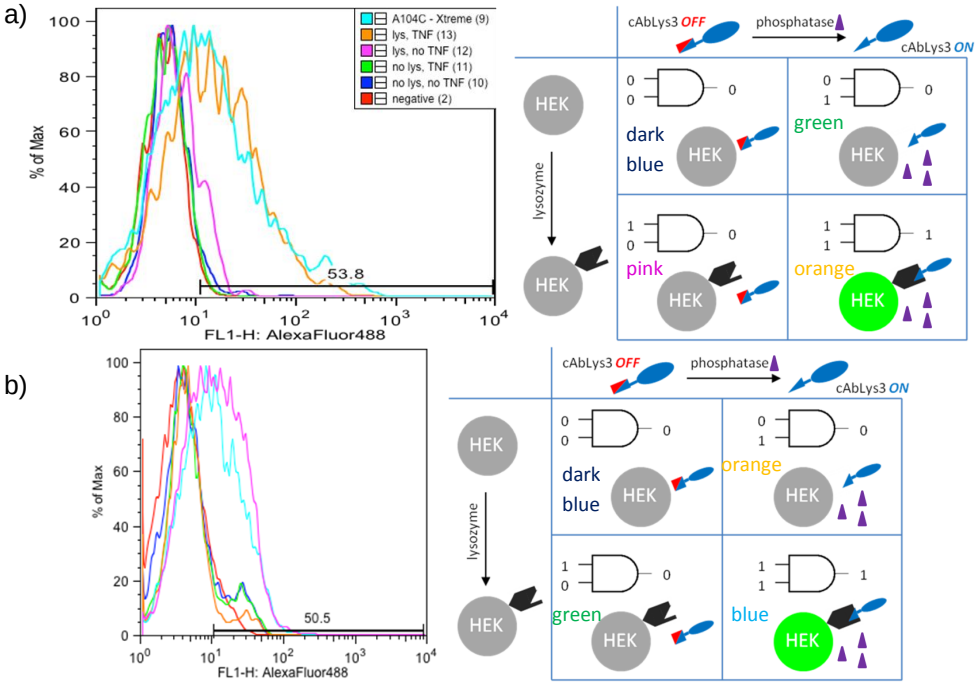

Figure 4.35. a) HEK-Blue Null1 AND antibody gate using cells at passage 16 (positive control is blue), b) HEK-Blue Null1 AND antibody gate using cells at passage 5 (positive control is pink).

Finally, the same experiment was repeated using fresh transfection reagent. The same result was observed, i.e. the FACS trace only showed a shift for the cell set where both inputs were present (**Figure 4.36**). Positive SEAP expression was tested by the addition of a chromophoric substrate to the cell culture medium (**Experimental Figure 4.16**). Conditional cell surface labelling was also observed by fluorescence microscopy (**Experimental Figure 4.17**). These results clearly demonstrate that cAb-Lys3-pCys104 displays the required

characteristics of an AND antibody: conditional directing of the antibody to a cell surface was only observed under the influence of two inputs.

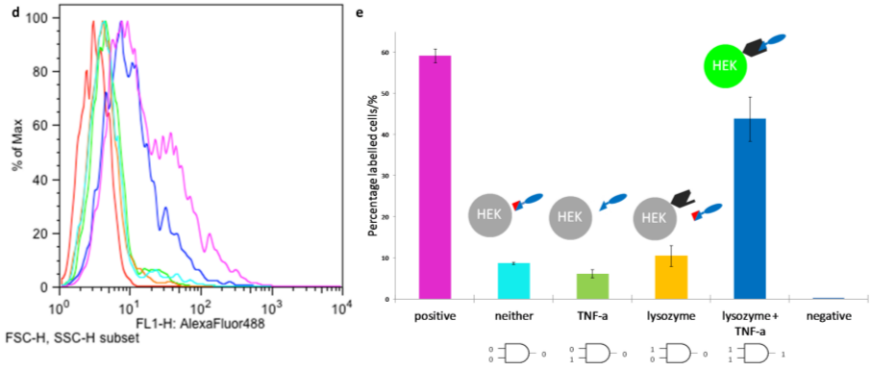

Figure 4.36. a) FACS analysis and b) corresponding percentage labelled cells for HEK Blue Null1 cells expressing varying combinations of inputs. Colours in the bar chart correspond to colours in FACS.

HEK293T cell line AND antibody gate

As mentioned previously, a second method for the expression of SEAP was possible by transfection of HEK cells with pBluescript:SEAP. AND antibody gate conditions were set up using similar conditions to those for the HEK-Blue Null1 AND antibody gate (*vide supra*), with the difference that, where required, cells were transfected with pBluescript:SEAP instead of the addition of TNF-α to promote SEAP production (**Figure 4.27**). Positive SEAP expression was tested by the addition of a chromophoric substrate to the cell culture medium (**Experimental Figure 4.18**). Following addition of the inhibited antibody at 1 μM and staining with the fluorophore-AntiHis conjugate, a clear shift was observed for cells expressing both inputs (**Figure 4.37**). This approach therefore demonstrates an alternative method for controlling antibody function *in vitro*. Again, conditional cellular detection was also observed by fluorescence microscopy (**Experimental Figure 4.19**).

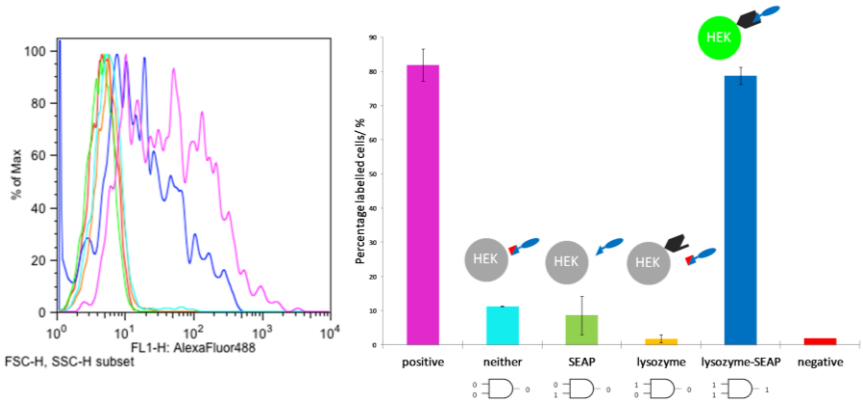

Figure 4.37. a) FACS analysis and b) corresponding percentage labelled cells for HEK293T cells expressing varying combinations of inputs. Colours in the bar chart correspond to colours in FACS.

4.2.6 Demonstrating the *in vitro* AND antibody logic gate in mammalian tissue

Two *in vitro* logic gates following Boolean AND behaviour were synthesised, whereby antibody in a chemically-induced inhibitory state could bind to selected cell surfaces only in the presence of two inputs. This type of system may have application in a therapeutic setting, for example to minimise the binding of an antibody therapeutic to antigen in non-desired sites.[8] In order to further test the specificity of the *in vitro* AND antibody gate, experiments in mammalian tissue were devised, with the aim of seeing if the same level of specificity could be obtained in a more complex environment. Experiments with both the HEK-Blue Null1 AND antibody gate, and HEK293T AND antibody gate were attempted.

HEK-Blue Null1 cell line AND antibody gate in mammalian tissue

In the HEK-Blue Null1 AND antibody gate system, cell surface antigen is presented via transfection, whilst the expression of secreted phosphatase is induced by the addition of the cytokine, TNF-α. It was hypothesised that *in vivo*, the injection of HEK-Blue Null1 cells (expressing cell surface lysozyme) into a mouse brain may trigger an inflammatory response such that the amount of TNF- α would be raised. It was hoped that the presence of increased cytokine would induce the expression of SEAP in the cells. Following sacrifice of the mouse

and slicing of the brain, inhibited antibody could be added. The antibody could diffuse into the tissue section, become dephosphorylated and would therefore be able to bind to cell surface antigen.

Before carrying out experiments in mammalian tissue, the ability of mouse TNF-α to induce SEAP expression in HEK-Blue Null1 cells was tested. Thus far, recombinant human TNF-α had been used. Human and mouse TNF-α are known to have 79% homology, and although mouse-TNF-α is glycosylated where human TNF-α is not, cross-species reactivity has been reported.[80,81] HEK-Blue Null1 cells were incubated with varying concentrations of mouse TNF-α overnight (0.5 – 100 ng/mL), and the presence of SEAP was then detected and monitored by the addition of the chromophoric alkaline phosphatase substrate, QUANTI-Blue over time. Gratifyingly, an increase in OD at 620 nm was observed, implying successful expression of SEAP by mouse TNF-α (**Figure 4.38**).

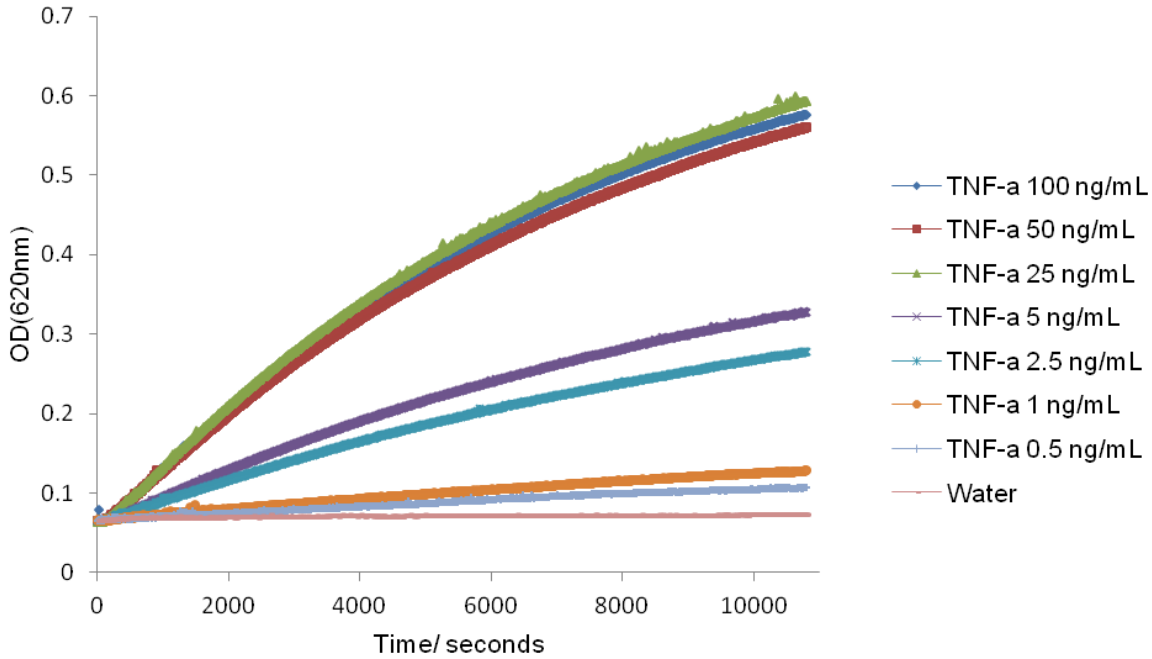

Figure 4.38. HEK Blue Null1 Cells were incubated with varying concentrations of mouse TNF-α overnight, then cell supernatant was treated with QUANTI-Blue to release a product detectable at 620 nm.

Following confirmation that mouse TNF-α was able to induce SEAP expression in HEK-Blue Null1 cells, 10^4 cells (transfected or not transfected with cell surface lysozyme in 1 μL cell culture medium) were unilaterally injected into the left striatum of the brain.[6] Following overnight incubation, mice were sacrificed, and the brains sliced into 10 μm thick tissue sections. Tissue sections were treated with inhibited antibody, then fluorophore-AntiHis conjugate (analogous to *in vitro* method). Analysis of sections by fluorescence microscopy revealed that no slices exhibited fluorescence, even where WT-cAb-Lys3 was added to tissue sections injected with lysozyme-expressing cells (positive control used for *in vitro* methods). It was thought that the concentration of cells may have been too low, and it is problematic to both control and predict the distribution of cells post-injection.

HEK293T AND antibody gate in mammalian tissue

Instead of relying upon a sufficient inflammatory response producing TNF-α to induce SEAP expression, it was decided to try to apply the HEK293T AND antibody gate in mammalian tissue using cells which had been transfected with plasmids expressing both cell surface lysozyme and secreted phosphatase. Mammalian tissue experiments were carried out in two ways, by biolistic transfection, and by injection into mice brains.

Biolistic transfection

Organotypic cultures are widely used as suitable systems for modelling *in vivo* environments.[82] We therefore sought to determine whether neurons within rat hippocampal slices could be transfected biolistically with cell surface antigen and secreted phosphate using a gene gun.[83] DNA 'bullets' were prepared by adhering plasmid DNA for cell surface lysozyme and SEAP onto gold using spermidine in small plastic inserts. These were loaded

[6] Procedures involving live animals were performed by Dr. Daniel C. Anthony.

into a gene gun, and fired onto organotypic rat hippocampal slices under helium pressure (1200 psi). Successful delivery of the bullets into the slice was confirmed by the observation of gold in slices under a microscope. Transfection was allowed to occur for two days, after which time antibody (both WT-cAb-Lys3 and inhibited antibody cAb-Lys3-pCys104) was added to the slices. Incubation with antibody, then with the fluorophore-AntiHis conjugate was carried out as described previously, and fluorescence was detected by microscopy. Unfortunately, in all 24 slices with added WT-cAb-Lys3, no fluorescence was observed (**Experimental Figure 4.20**). Biolistic transfection is associated with extremely low transfection efficiencies, where as little as 5 neurons out of hundreds of thousands may be transfected. As the success of the demonstration of the HEK293T AND antibody gate in mammalian tissue was highly dependent on expression of sufficient levels of SEAP for dephosphorylation of the inhibited antibody, it was decided to proceed with the injection of transfected cells.

Injection of HEK293T cells into mice

Based on the previous observation that 10^4 HEK-Blue Null1 cells may have been too low an amount for sufficient distribution, 10^6 cells which had been transfected with none, 1 or both inputs, were unilaterally injected into the left striatum of the brain. Cells were tested for positive transfection prior to injection (**Experimental Figure 4.21**). On this occasion the cells were injected in 2 μL of cell culture medium, where previously we had used 1 μL of medium. It was hoped that the higher volume of the injection would aid cell distribution. Following overnight incubation, mice were sacrificed, and the brains sliced into 10 μm thick tissue sections. These were mounted onto slides for antibody treatment and imaging. Tissue sections were treated as described previously with inhibited antibody cAb-Lys3-pCys104 and fluorophore-AntiHis conjugate. After the tissue sections were fixed with formaldehyde, they

were covered with mounting medium containing 4',6-diaminidino-2-phenylindole (DAPI, for nuclei visualisation). Again, fluorescence in tissue sections was tested by microscopy. No fluorescence was observed in any sections under the initial visualisation conditions. We investigated the effect of varying many conditions including adding the detergent Tween to buffers, the use of Tris buffer instead of PBS, blocking of the slices before the addition of cAb-Lys3, the use of mouse serum in line with the fluorophore species and incubation times. Gratifyingly, after significant optimisation, fluorescence was observed in tissue sections injected with cells which were co-transfected with both inputs and had cAb-Lys3-pCys104 added (**Figure 4.39**), and also tissue sections injected with lysozyme-transfected cells and WT-cAb-Lys3 added as a positive control (**Experimental Figure 4.22**). Crucially, no fluorescence was observed when one or both of the inputs were absent (**Figure 4.39**). Results were found to be reproducible, thus demonstrating the potential of the system for targeted drug delivery *in vivo*.

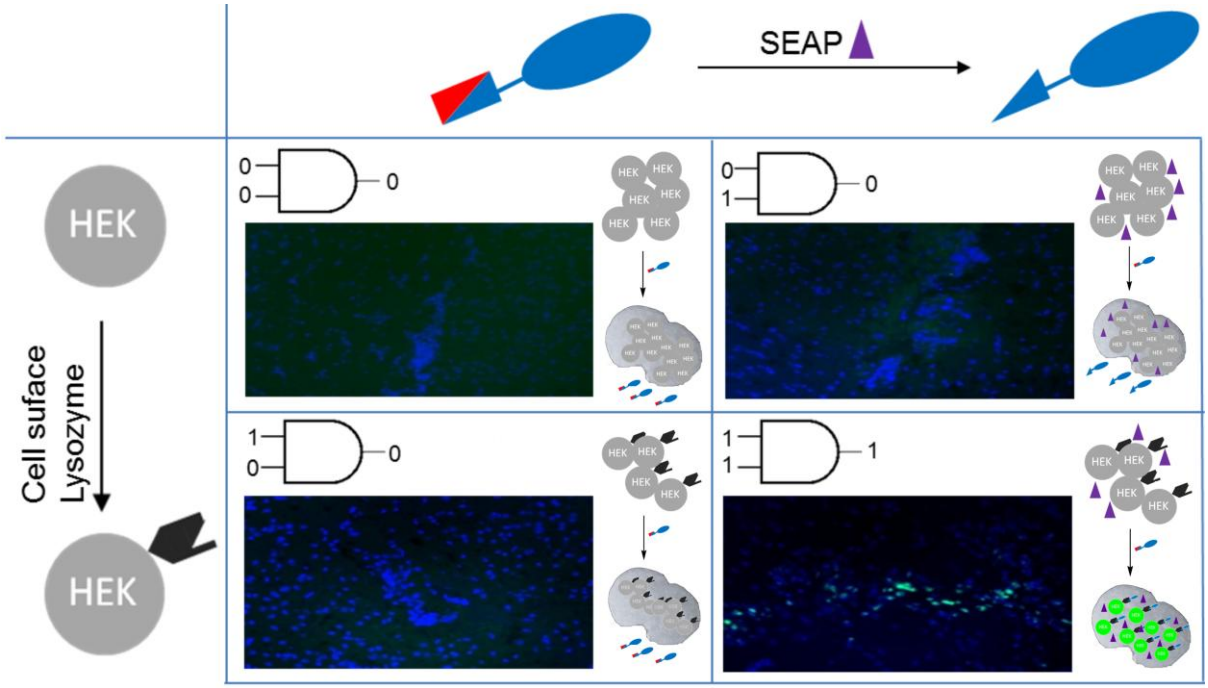

Figure 4.39. Demonstration of the HEK293T AND antibody gate in mammalian tissue.

4.3 Discussion

In this chapter, the generation of an antibody following Boolean AND logic has been described. The AND antibody was synthesised using a combination of site-specific chemical methods to turn antigen binding off and site-specific enzymatic methods to turn antigen binding back on. Initially, turning binding off by the chemical installation of glycosyl groups was described. Chemical modifications with GlcNAc, glucose and galactose thiol were successful within cAb-Lys3, but subsequent attempts to cleave thioglycosides with glycosidases did not work, indicating the generation of hydrolytically stable *O*-glycosyl analogues. In general, thioglycosides are known to be stable to a multitude of glycosidases,[38] however reports describing their cleavage by *O*-specific glycosidases have been previously described .[39,40] The substrates reported previously contain efficient leaving groups, and it is thought the pKa of the sulfide in the glycosylated antibodies may not have been sufficient to cleave the free sugar. Notably the cleavage of thioglycosides on proteins using *O*-glycosidases has not been described before. Alternatively, it may be possible to introduce a natural *O*-glycoside linkage into cAb-Lys3 by mutating a glycosylation motif into the CDR3 loop, which may be processed by a glycosidase specific for the glycoside. This may have application in the targeted delivery of antibody therapeutics to tumour environments overexpressing elevated levels of certain glycosidases.[41,44]

Next, the installation of pCys at position 104 of cAb-Lys3 was described. As expected, the introduction of a large and polar group at a pivotal residue in the antibody binding region inhibited binding to lysozyme,[23] and investigations into its removal were carried out. Phosphatases are reported to be somewhat more promiscuous than glycosidases,[49,50] and the chemical similarity between pCys and pSer encouraged us to test pCys as an efficient PTM mimic. Although pCys chemically installed via Dha has been shown by others to be an

efficient PTM mimic,[27,64] processing of this analogue by phosphatases has not previously been described. Gratifyingly, efficient phosphate removal was observed with a range of phosphatases, and activity at physiological conditions allowed the design of *in vitro* experiments, where multi input antibody function could be controlled by the transfection of cells with both inputs. As well as observing conditional function *in vitro,* further specificity was achieved in mammalian tissue, demonstrating the potential of the AND antibody system in a therapeutic context. This AND antibody system is a rare and novel example of a protein-based gated logic. Previous protein 'devices' are based on using codified functional inputs to gene networks,[11] whereas in the AND system described here, both input and output states are co-localised in the CDR3 of the antibody, which allows direct synchronisation of recognition function.[21] Essentially, the use of a single molecule (cAb-Lys3) as the computational element rather than gene networks generates enhanced function. The methods used here should be transferable to other antibodies without the need to design individual genetic networks for each system. This is a significant advantage over the previous approach which would require significant genetic manipulation and translation for each device. The use of a synthetic PTM mimics also implies that the AND system could be considered an artificial recapitulation of a dynamic PTM, but with a designed rather than an evolved goal. To the best of our knowledge, this is the first example of the use of chemical modification to temporarily inhibit an antibody's binding ability, and then restore it using an endogenous enzyme. Such systems may have application in a therapeutic setting where 'inhibited' antibody therapeutics could target cell surface antigen specifically where an overexpression of a relevant enzyme is known, minimising binding to cell surface receptors in healthy tissues.[42,43]

4.4 Conclusions

The synthesis of a range of thio-linked glycosylated antibodies was described, inhibiting binding of cAb-Lys3 to lysozyme. Each glycosylated antibody was found to be stable to hydrolytic cleavage, rendering the 'turning off' of binding permanent. Therefore, glycosylation at other sites away from the binding region using the same methodology may be used to form stable and robust immunoconjugates.[5] The concept of an AND antibody, where function of binding is dependent on two inputs rather than one could be demonstrated using a chemically installed pCys residue, which was able to act as an efficient pSer mimic, with a range of phosphatases able to process it. The use of a natural process to regain binding allowed the AND antibody system to be applied *in vitro* and in more complex mammalian tissue, with the specific and efficient directing of antibody to bind to cell surfaces by introducing inputs by transfection. In the future, the application of this methodology to more relevant therapeutic antibodies should be attempted, as well as investigations into the use of other cleavable groups such as sequences recognised by proteases[9] and *O*-linked glycosides.[41]

4.5 Experimental

General considerations

Proton nuclear magnetic resonance (^{1}H NMR) spectra were recorded on a Bruker AV400 (400 MHz) spectrometer. Carbon nuclear magnetic resonance (^{13}C NMR) spectra were recorded on a Bruker AV400 (101 MHz) spectrometer. NMR spectra were assigned using COSY and HSQC. All chemical shifts are quoted on the δ scale in ppm using residual solvent as the internal standard (^{1}H NMR: $CDCl_3$ = 7.26, D_2O = 4.65; ^{13}C NMR: $CDCl_3$ = 77.0). Coupling constants (*J*) are reported in Hz with the following splitting abbreviations: s = singlet, d = doublet, t = triplet, q = quartet and a = apparent.

Infrared (IR) spectra were recorded on a Bruker Tensor 27 Fourier Transform spectrophotometer using KBr discs for solids. Absorption maxima (υ_{max}) are reported in wavenumbers (cm^{-1}).

Low resolution mass spectra (LRMS) were recorded on a Waters Micromass LCT Premier TOF spectrometer using electrospray ionization (ESI). Nominal and exact m/z values are reported in Daltons.

Optical rotations were measured on a Perkin-Elmer 241 polarimeter with a path length of 1.0 dm and are reported with implied units of 10^{-1} deg cm^2 g^{-1}. Concentrations (c) are given in g/100 ml.

Thin layer chromatography (TLC) was carried out using Merck aluminium backed sheets coated with $60F_{254}$ silica gel. Visualization of the silica plates was achieved using a UV lamp (λ_{max} = 254 nm), and/or ammonium molybdate (5% in 2M H_2SO_4), and/or potassium permanganate (5% $KMnO_4$ in 1M NaOH with 5% potassium carbonate). Flash column chromatography was carried out using BDH PROLAB® 40-63 mm silica gel (VWR). Mobile

phases are reported in % volume of more polar solvent in less polar solvent for binary systems (e.g. 20% EtOAc in petrol = 1:4 ethyl acetate:petrol) and in relative composition for ternary systems (e.g. 1:2:4 H_2O:^{i}PrOH:EtOAc).

Anhydrous solvents were purchased from Fluka or Acros with the exception of dichloromethane and THF, which were dried on an alumina column under nitrogen. All other solvents were used as supplied (Analytical or HPLC grade), without prior purification. Deionized water was used for chemical reactions and Milli-Q purified water for protein manipulations. Protein concentrations were determined by bicinchoninic acid (BCA) assay (Pierce) and/or Nanodrop. Reagents were purchased from Sigma-Aldrich and used as supplied, unless otherwise indicated. 'Petrol' refers to the fraction of light petroleum ether boiling in the range 40-60 ºC. All reactions using anhydrous conditions were performed using flame-dried apparatus under an atmosphere of argon or nitrogen. Brine refers to a saturated solution of sodium chloride. Anhydrous magnesium sulfate ($MgSO_4$) or sodium sulfate (Na_2SO_4) were used as drying agents after reaction workup, as indicated.

DOWEX-50WX8 (H^+ form) was conditioned as follows: 100 g of the commercial resin was placed in a 500 mL sintered filter funnel and allowed to swell with 200 mL of acetone for 5 minutes. The solvent was removed by suction filtration and the resin was washed successively with 800 mL of acetone, 500 mL methanol, 500 mL 5M HCl, and then 1 L of water or until the pH of the filtrate was ~ 7, as indicated by pH paper. The resin was partially dried on the filter and then stored and used as needed.

Procedures

cAb-Lys3-Dha104 was synthesised as described in chapter 3.

Synthesis of cAb-Lys3-GlcNAcCys104.[65] GlcNAc thiol (15 mg, 63 μmol) was added as a solid to cAb-Lys3-Dha104 (1 mL, c = 0.5 mg/mL in PBS, pH 8.0) and the reaction was incubated at 37 °C. Additional GlcNAc thiol was added every 15 minutes until a total of 150 mg had been added. The reaction was monitored directly by LC-MS. Full conversion to the glycosylated antibody fragment was observed after 10 hours at 37 ºC (calculated mass = 16000; observed mass = 15994).

Chemical corroboration. To cAb-Lys3-GlcNAcCys104 (100 μL, c = 0.5 mg/mL in PBS, pH 8.0) was added DTT (1 mg), the solution shaken (600 rpm) at room temperature, and then desalted through a Micro BioSpin6 (BioRad). Antibody was analysed by LC-MS (**Experimental Figure 4.1**). β-Mercaptoethanol (2 μL) was added to the glycosylated antibody, and the resulting solution shaken (600 rpm) at 37 ºC for 1 hour, after which time analysis by LC-MS revealed no change in mass (**Experimental Figure 4.2**).

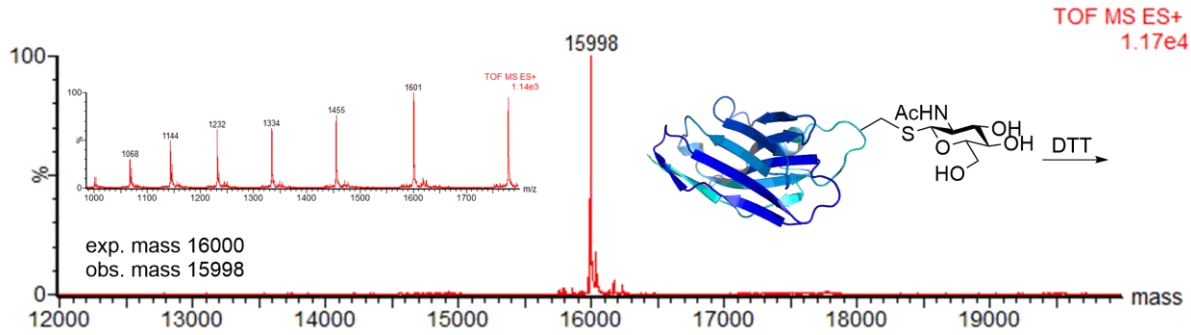

Experimental Figure 4.1. No reaction was observed when cAb-Lys3-GlcNAcCys104 was treated with DTT.

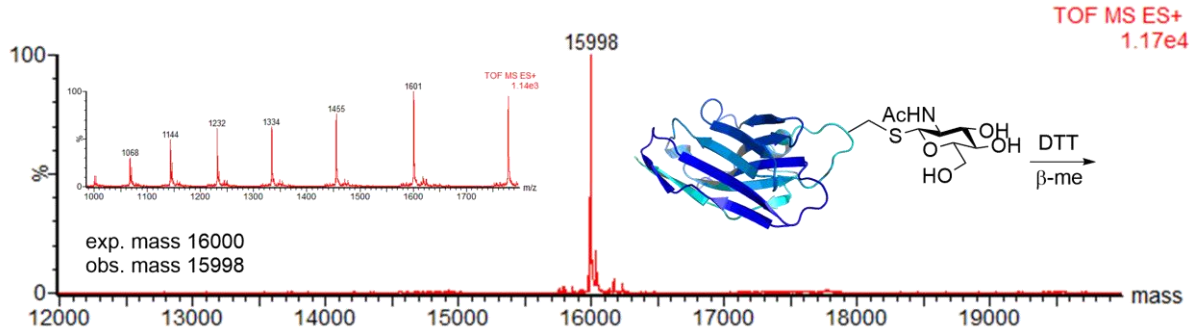

Experimental Figure 4.2. No reaction was observed when cAb-Lys3-GlcNAcCys104 was treated with DTT then β-mercaptoethanol.

Expression and purification of family 84 human OGA[39]

Sequence. DNA encoding human OGA (GenBank identifier NM_012215) was ordered from Genscript in pET-28a(+).

```
TCTAGAATATTTTGTTTAACTTTAAGAAGGAGATATACCATGGGCAGCAGCCATCATCATCATCATCACAGCAGC
GGCCTGGTGCCGCGCGGCAGCCATATGGTGCAGAAGGAGAGTCAAGCGACGTTGGAGGAGCGGGAGAGCGAGCTC
AGCTCCAACCCTGCCGCCTCTGCGGGGGCATCGCTGGAGCCGCCGGCAGCTCCGGCACCCGGAGAAGACAACCCC
GCCGGGGCTGGGGGAGCGGCGGTGGCCGGGGCTGCAGGAGGGGCTCGGCGGTTCCTCTGCGGTGTGGTGGAAGGA
TTTTATGGAAGACCTTGGGTTATGGAACAGAGAAAAGAACTCTTTAGAAGGCTCCAGAAATGGGAATTAAATACA
TACTTGTATGCCCCAAAAGATGACTACAAACATAGGATGTTTTGGCGAGAGATGTATTCAGTGGAGGAAGCTGAG
CAACTTATGACTCTCATCTCTGCTGCACGAGAATATGAGATAGAGTTCATCTATGCGATCTCACCTGGATTGGAT
ATCACTTTTTCTAACCCCAAGGAAGTATCCACATTGAAACGTAAATTGGACCAGGTTTCTCAGTTTGGGTGCAGA
TCATTTGCTTTGCTTTTTGATGATATAGACCATAATATGTGTGCAGCAGACAAAGAGGTATTCAGTTCTTTTGCT
CATGCCCAAGTCTCCATCACAAATGAAATCTATCAGTACCTAGGAGAGCCAGAAACTTTCCTCTTCTGTCCCACA
GAATACTGTGGCACTTTCTGTTATCCAAATGTGTCTCAGTCTCCATATTTAAGGACTGTGGGTGAAAAGCTTCTA
CCTGGAATTGAAGTGCTTTGGACAGGTCCCAAAGTTGTTTCTAAAGAAATTCCAGTAGAGTCCATCGAAGAGGTT
TCTAAGATTATTAAGAGAGCTCCAGTAATCTGGGATAACATTCATGCTAATGATTATGATCAGAAGAGACTGTTT
CTGGGCCCCGTACAAAGGAAGATCCACAGAACTCATCCCACGGTTAAAAGGAGTCCTCACTAATCCAAATTGTGA
ATTTGAAGCCAACTACGTTGCTATCCACACCCTTGCCACCTGGTACAAATCAAACATGAATGGANTGAGAAAGAT
GTANNGATGACTGACAGTGAA
```

DNA was used to transform Tuner (λ DE3) cells (Novagen). A colony was selected and cultured to exponential phase in LB media (5 mL) containing 50 μg/ml of kanamycin. This culture was used to inoculate 2 x 500 mL cultures that were grown to an $OD_{600} \approx$ 0.8 at 37 °C. At this point protein expression was induced using 1 mM IPTG for 16 h at 30 °C. Post-induction, cells were harvested by centrifugation (15 min, 5000 rpm, 4 °C), frozen in liquid nitrogen and stored at -80 °C. Thawed cell pellets were resuspended in 25 mL of nickel-column binding buffer (50 mM Na_2PO_4, 500 mM NaCl, 5 mM imidazole; pH 7.4) per 1 L of

cell culture. The resuspended cells were incubated on ice for 30 min with 1 mg/ml of lysozyme and 1 mM PMSF followed by sonication (3 x 20 s at 60% power with a 20 s break in between). The cell debris was then removed by centrifugation (45 min, 15000 rpm, 4 °C) and the supernatant was loaded onto 5 mL Ni-NTA resin and incubated for 5 mins to ensure binding of the His_6 tag. Flow-through was collected, and then the column was washed with 100 mL of wash buffer (same as binding buffer but containing 60 mM imidazole) and eluted with 30 mL of elution buffer (same as binding buffer but containing 250 mM imidazole). Fractions containing purified enzyme (identified by SDS-PAGE) were subsequently dialysed overnight against 4 L of PBS (pH 7.4) in a membrane with a 12 – 14 kDa MWCO. Next, dialysed protein solution was concentrated using a VivaSpin with a 10 kDa MWCO (45 mins, 3750 rpm, 4 °C) to 1 mL, and then to 0.5 mL (MWCO 3 kDa). Protein solution (0.5 mL) was then desalted using a PD10 desalting column, and the protein concentration determined by BCA assay to be 0.39 mg/mL (1 mL), i.e. 0.39 mg/L.

Activity assay. A 1 mM solution of 4-nitrophenyl-*N*-acetyl-β-D-glucosaminide (Sigma) was prepared in PBS, pH 7.4. The wells of a 96-well plate were filled as follows: a) 100 μL no substrate (negative control) + OGA (3.9 μg, 10 μL, c = 0.39 mg/mL); b) 100 μL 1 mM substrate + OGA (3.9 μg, 10 μL, c = 0.39 mg/mL); c) 100 μL 0.5 mM substrate + OGA (3.9 μg, 10 μL, c = 0.39 mg/mL); d) 100 μL 0.25 mM substrate + OGA (3.9 μg, 10 μL, c = 0.39 mg/mL). The absorbance at 400 nm was measured every 4 seconds for 10 minutes at 37 °C, with an increase in OD observed upon release of *para*-nitrophenol (pNP). Initial velocity kinetic data was fitted using Excel and Prism.

Attempted reaction between cAb-Lys3-GlcNAcCys104 and OGA

SPy1600 (OGA from *Streptococcus pyogenes*) + cAb-Lys3-GlcNAcCys104. cAb-Lys3-GlcNAcCys104 was buffer exchanged into 10 mM HEPES, pH 7.6, and then SPy1600 (Prozomix) added, and the reaction shaken (600 rpm) at 37 °C (various conditions described in **Table 4.2**). Enzyme activity was tested by LC-MS.

hOGA + cAb-Lys3-GlcNAcCys104. cAb-Lys3-GlcNAcCys104 was buffer exchanged into PBS, pH 7.4, and then human OGA added, and the reaction shaken (600 rpm) at 37 °C (various conditions described in **Table 4.3**). Enzyme activity was tested by LC-MS.

1-Thio-β-D-glucopyranose (glucose thiol)

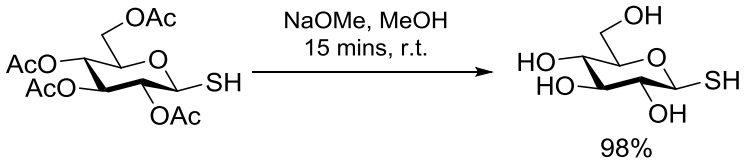

2,3,4,6-Tetra-*O*-acetyl-1-thio-β-D-glucopyranose (200 mg, 0.55 mmol) in a 10 mL round-bottomed flask was placed under argon and dissolved in MeOH (5 mL). NaOMe (143 μL, 25 % wt. soln in methanol) was added dropwise to the stirring solution. After 1 hour of stirring at room temperature, TLC (water:isopropanol:EtOAc 2:2:1) indicated complete consumption of starting material. The reaction mixture was neutralised using DOWEX 50WX8-200, filtered and concentrated *in vacuo*. The crude product was dissolved in water (5 mL) and lyophilised overnight to yield yellow crystals (108 mg, 98%).

TLC R_f = 0.57 (water:isopropanol:EtOAc 2:2:1); **$[\alpha]_D^{23}$** = +31.5 (c. 1.0, H_2O) [Lit. $[\alpha]_D^{23}$ = +35.7 (c. 1.0, H_2O)][26]; **IR** (neat): υ_{max} 2970, 1739, 1366, 1229, 1217 cm^{-1}; **^{1}H NMR** (400 MHz, D_2O): δ ppm 4.44 (d, 1H, $J_{1,2}$ = 9.1 Hz, H-1), 3.76 (d, 1H, $J_{4,5}$ = 12.2 Hz, H-4), 3.56

(dd, 1H, $J_{4,5}$ = 12.4 Hz, $J_{5,6}$ = 5.5 Hz, H-5), 3.36 – 3.27 (m, 3H, H-3, H-6a/6b), 2.92 (t, 1H, $J_{1,2}$ = 9.0 Hz, H-2); **^{13}C NMR** (101 MHz, D_2O): δ ppm 84.3 (C-1), 79.6 (C-3), 78.6 (C-2), 76.8 (C-6), 70.4 (C-4), 61.2 (C-5); **ESI-MS** cald. for $C_6H_{12}O_5S$ 196.2 found 219.0 ($M+Na^+$).

cAb-Lys3-GluCys104

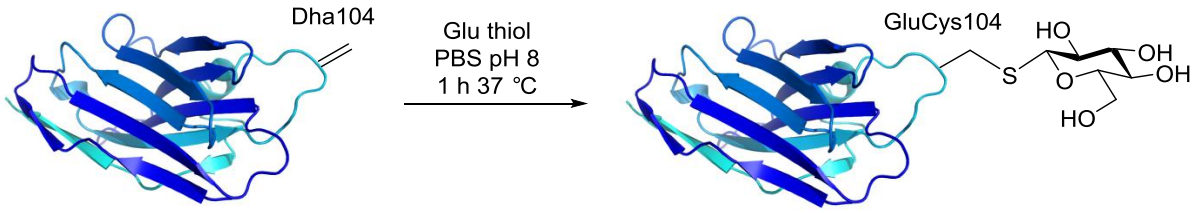

To cAb-Lys3-Dha104 (150 μL, 4.8 nmol, c = 0.5 mg/mL in PBS, pH 8) was added 1-thio-β-D-glucopyranose (0.74 mg, 3.8 μmol, 800 eq.). The reaction was shaken at 37 °C for 1 hour, after which time LC-MS analysis showed complete consumption of the starting material, and a mass corresponding to the formation of the glucosylated antibody.

1-Thio-β-D-galactopyranose (galactose thiol)

2,3,4,6-Tetra-*O*-acetyl-α-D-galactopyranosyl bromide[26]

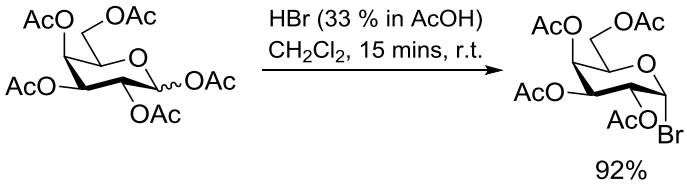

1,2,3,4,6-Penta-*O*-acetyl-β-D-galactopyranose (5.0 g, 12.8 mmol) in a 250 mL round-bottomed flask was placed under nitrogen and dissolved in CH_2Cl_2 (30 mL). HBr (37.5 mL, 33 % wt. soln in AcOH) was added dropwise to the stirred solution, which turned from colourless to yellow. After 15 minutes at room temperature, TLC (50% EtOAc in petrol) indicated complete consumption of starting material. The reaction mixture was partitioned

between CH_2Cl_2 (50 mL) and H_2O (50 mL), and the aqueous phase re-extracted with CH_2Cl_2 (2 x 40 mL). The combined organics were washed with sat. aq. $NaHCO_3$ until ~ pH 8 was reached, brine (50 mL) and then dried over $MgSO_4$, filtered and concentrated *in vacuo*. The resulting light yellow oil was dried under a high vacuum pump to give a yellow/white waxy solid (4.82 g, 92%).

TLC R_f = 0.62 (50% EtOAc in petrol); **$[\alpha]_D^{23}$** = +215.6 (c. 1.0, $CHCl_3$) [Lit. $[\alpha]_D^{23}$ = +210 (c. 1.0, $CHCl_3$)][84]; **IR** (neat): υ_{max} 1745, 1371, 1216, 1078 cm^{-1}; **^{1}H NMR** (400 MHz, $CDCl_3$): δ ppm 2.02, 2.07, 2.12, 2.16 (4s, 4 x COC*H*$_3$), 4.11 (dd, $J_{6a,6b}$ = 11.5 Hz, $J_{5,6b}$ = 6.8 Hz, 1H, CH_2, H-6b), 4.19 (dd, $J_{6a,6b}$ = 11.7 Hz, $J_{5,6a}$ = 6.6 Hz, 1H, CH_2, H-6a), 4.49 (dd, $J_{5,6}$ = 6.4 Hz, 1H, CH, H-5), 5.05 (dd, $J_{1,2}$ = 3.9 Hz, $J_{2,3}$ = 10.7 Hz, 1H, CH, H-2), 5.41 (dd, $J_{2,3}$ = 10.7 Hz, 1H, CH, H-3), 5.52 (dd, $J_{3,4}$ = 2.3 Hz, $J_{4,5}$ = 1.2 Hz, 1H, CH, H-4), 6.70 (d, $J_{1,2}$= 4.1 Hz, 1H, CH, H-1); **^{13}C NMR** (101 Mhz, $CDCl_3$): δ ppm 20.6, 20.6, 20.7, 20.8 (4s, 4 x CO*C*H$_3$), 60.8 (s, 1C, CH_2, C-6), 67.0 (s, 1C, CH, C4), 67.8 (s, 1C, CH, C-2), 68.0 (s, 1C, CH, C-3), 71.1 (s, 1C, CH, C-5), 88.1 (s, 1C, CH, C-1), 169.8, 170.0, 170.1, 170.4 (4s, 4 x *C*OCH$_3$); **ESI-MS** cald. for $C_{14}H_{19}BrO_9$ 411.2 found 433.0 ($M+Na^+$).

2,3,4,6-Tetra-*O*-acetyl-*S*-acetyl-1-thio-β-D-galactopyranose

2,3,4,6-Tetra-*O*-acetyl-α-D-galactopyranosyl bromide (2.04 g, 4.96 mmol) in a 100 mL round-bottomed flask was placed under argon and dissolved in DMF (20 mL). KSAc (2.73 g, 24.8 mmol, 5 eq.) was added in a single portion to the stirring solution, causing it to turn black. After 15 minutes of stirring at room temperature, TLC (50% EtOAc in petrol)

indicated complete consumption of starting material. The reaction mixture was diluted with EtOAc (250 mL), and then washed with sat. aq. $NaHCO_3$ (4 x 50 mL), H_2O (4 x 50 mL) and brine (4 x 50 mL). The combined organics were dried over $MgSO_4$, filtered and concentrated *in vacuo*. The resulting brown solid was dissolved in EtOH (3 mL) and incubated at 4 °C overnight after which brown crystals were seen. 2 spots were observed by TLC (0.11 and 0.41 in 50% EtOAc in petrol). The crude mixture was purified by column chromatography (30 - 70% EtOAc in petrol). The fractions containing the single top spot were concentrated and dried under high vacuum to give a white foamy solid (1.26 g, 62 %).

TLC R_f = 0.41 (50% EtOAc in petrol); $\mathbf{[\alpha]_D^{23}}$ = + 30.3 (c. 1.0, $CHCl_3$) [Lit. $[\alpha]_D^{23}$ = +29.0 (c. 1.0, $CHCl_3$)][85]; **IR** (neat): υ_{max} 2970, 1743, 1367, 1217, 1057 cm^{-1}; **^{1}H NMR** (400 MHz, $CDCl_3$): δ ppm 1.99, 2.03, 2.04, 2.16, (4s, 4 x OCOC*H*3), 2.40 (s, SCOC*H*$_3$), 4.04 – 4.16 (m, 3H, CH/CH_2, H-5/H-6), 5.11 (dd, $J_{2,3}$ =9.5 Hz, $J_{3,4}$=3.5 Hz, CH, H3), 5.25 (d, $J_{1,2}$ = 10.4 Hz, 1H, CH, H-1), 5.32 (t, $J_{2,3}$ = 10.0 Hz, 1H, CH, H2), 5.46 (d, $J_{4,5}$ = 3.1 Hz, 1 H, CH, H-4); **^{13}C NMR** (101 Mhz, $CDCl_3$): δ ppm 20.6, 20.7, 20.7, 20.7 (4s, 4C, OCO*C*H_3), 30.9 (s, 1C, SCO*C*H_3), 61.3 (s, 1C, CH_2, C-6), 66.4 (s, 1C, CH, C-4), 67.2 (s, 1C, CH, C-2), 71.9 (s, 1C, CH, C-3), 75.0 (s, 1C, CH, C-5), 80.6 (s, 1C, CH, C-1), 169.9, 170.0, 170.2, 170.4 (4s, 4C, O*C*OCH$_3$), 192.1 (s, 1C, S*C*OCH$_3$); **ESI-MS** cald. For $C_{16}H_{22}O_{10}S$ 406.4 found 429.1 ($M+Na^+$).

1-Thio-β-D-galactopyranose

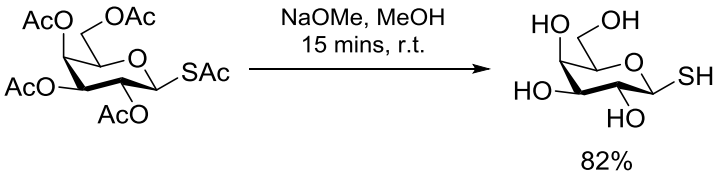

2,3,4,6-Tetra-*O*-acetyl-*S*-acetyl-1-thio-D-galactopyranose (0.50 g, 1.23 mmol) in a 100 mL round-bottomed flask was placed under argon and dissolved in MeOH (20 mL). NaOMe (290

μL, 25% wt. soln in methanol, 1.1 eq.) was added dropwise to the stirring solution. After 15 minutes of stirring at room temperature, TLC (10% MeOH in CH_2Cl_2) indicated complete consumption of starting material. The reaction mixture was neutralised using DOWEX 50WX8-200, filtered and concentrated *in vacuo*. The product was dissolved in water (5 mL) and lyophilised overnight to yield a pink powder (197 mg, 82%).

TLC R_f = 0.01 (100% EtOAc); $\mathbf{[\alpha]_D^{23}}$ = +49.2 (c. 1.0, H_2O) [Lit. $[\alpha]_D^{23}$ = +47.6 (c. 1.0, H_2O)][86]; **IR** (neat): υ_{max} 3358, 2885, 1634, 1311, 1083 cm^{-1}; **^{1}H NMR** (400 MHz, D_2O): δ ppm 3.23 (t, $J_{1,2}$ = 9.3 Hz, 1H, CH, H-2), 3.51 (dd, $J_{2,3}$ = 3.4 Hz, $J_{3,4}$ = 3.7 Hz, 1H, CH, H-3), 3.54 – 3.69 (m, 3H, CH/CH_2, H-5/H-6), 3.86 (d, $J_{3,4}$= 3.4 Hz, 1H, CH, H-4), 4.42 (d, J= 9.1 Hz, 1H, CH, H-1); **^{13}C NMR** (101 Mhz, D_2O): δ ppm 61.4 (s, 1C, CH_2, C-6), 69.6 (s, 1C, CH, C-4), 73.6 (s, 1C, CH, C-2), 76.2 (s, 1C, CH, C-3), 78.7 (s, 1C, CH, C-5), 84.7 (s, 1C, CH, C-1); **ESI-MS** cald. for $C_6H_{12}O_5S$ 196.2 found 219.1 ($M+Na^+$).

cAb-Lys3-GalCys104

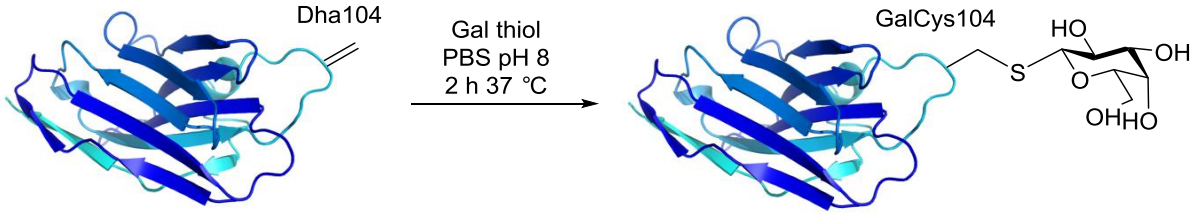

To cAb-Lys3-Dha104 (150 μL, 4.8 nmol, c = 0.5 mg/mL in PBS, pH 8) was added 1-thio-β-D-galactopyranose (0.74 mg, 3.8 μmol, 800 eq.). The reaction was shaken at 37 °C for 1 hour, after which LC-MS analysis showed complete consumption of the starting material, and a mass corresponding to the formation of the galactosylated antibody.

CD. Spectra were obtained under the same parameters and conditions as described in chapter 2.

ELISA. ELISA was carried out according to the protocol described in chapter 2.

Test with Ellman's reagent. The same protocol as described in chapter 2 was used.

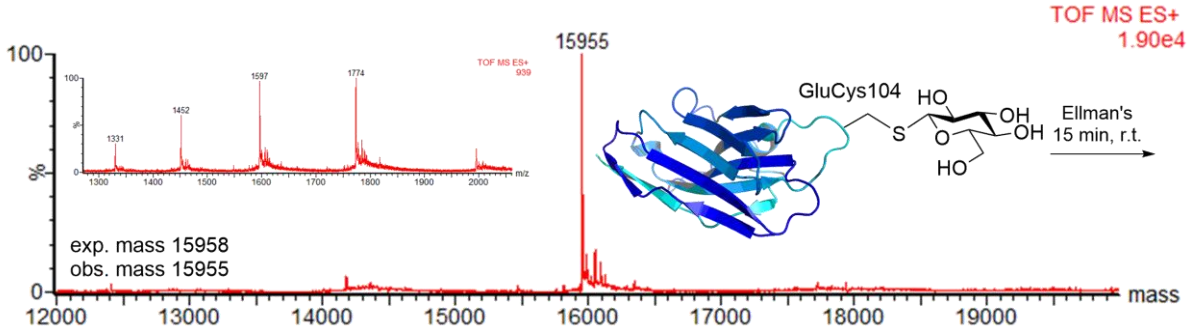

Figure 4.3. No reaction was observed for cAb-Lys3-GluCys104 with Ellman's reagent.

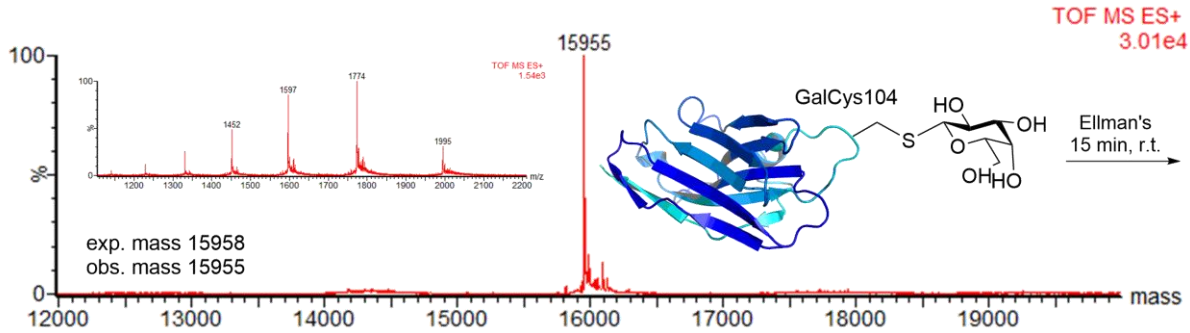

Figure 4.4. No reaction was observed for cAb-Lys3-GalCys104 with Ellman's reagent.

Testing β-thioglucosidase activity on sinigrin. (-)-Sinigrin hydrate (Sigma) was dissolved in MES, pH 6.0 (1 mg, 2.5 μmol in 100 μL buffer) and added to a solution of β-thioglucosidase from *Sinapis alba* (white mustard) seed (Sigma) in MES, pH 6.0 (9 mg, 2.5 U in 100 μL buffer). The reaction was shaken at room temperature for 10 minutes, and then enzymatic activity tested by the detection of glucose by ESI-MS. **ESI-MS** cald. for $C_{10}H_{18}KNO_8S_2 \cdot xH_2O$ (sinigrin) 397.5 found 436.0 (M+Na). **ESI-MS** cald. for $C_6H_{12}O_6$ (glucose) 180.2 found 383.1 ($2M+Na^+$).

General procedure for enzymatic reactions on cAb-Lys3-GluCys104. β-Thioglucosidase from *Sinapis alba* (white mustard) seed was prepared as a solution of 0.6 U/mL in either

MES, pH 6.0 or PBS, pH 7.4. The desired quantities (according to **Table 4.4**) were added to cAb-Lys3-GluCys104 (1.1 nmol, 135 μL, c = 0.13 mg/mL in MES, pH 6.0 or PBS, pH 7.4), and shaken (600 rpm) at room temperature for 10 mins. Where protease inhibitor was used, the desired quantity (according to **Table 4.5**) was added to antibody from a solution (1 Roche cOmplete protease inhibitor cocktail tablet in 5 mL H_2O) before the addition of enzyme. Reactions were analysed by LC-MS.

Testing β-galactose activity on β-lactose. β-Lactose (Sigma) was dissolved in MES, pH 4.5 (1 mg, 3.3 μmol in 100 μL buffer) and added to a solution of β-galactosidase from *Aspergillus oryzae* (Sigma) in MES, pH 4.5 (0.3 mg, 3.3 U in 100 μL buffer). The reaction was shaken at room temperature for 10 minutes, and then enzymatic activity tested by the detection of glucose by ESI-MS. **ESI-MS** cald. for $C_{12}H_{22}O_{11}$ (β-lactose) 342.3 found 365.0 (M+Na). **ESI-MS** cald. for $C_6H_{12}O_6$ (glucose) 180.2 found 203.1 ($M+Na^+$).

General procedure for enzymatic reactions on cAb-Lys3-GalCys104. β-Galactosidase from *Aspergillus oryzae* (Sigma) was prepared as a solution of 4.5 U/mL in either MES, pH 4.5 or PBS, pH 7.4. The desired quantities (according to **Table 4.6**) were added to cAb-Lys3-GalCys104 (1.1 nmol, 100 μL, c = 0.18 mg/mL in MES, pH 4.5 or PBS, pH 7.4), and shaken (600 rpm) at room temperature for 10 mins. Where protease inhibitor was used, the desired quantity (according to **Table 4.7**) was added to antibody from a solution (1 Roche cOmplete protease inhibitor cocktail tablet in 5 mL H_2O) before the addition of enzyme. Reactions were analysed by LC-MS.

Microscopy. HEK293T cells were visualised on a Leica Microsystems SP5 Inverted Confocal Microscope. All experiments were performed with the pinhole set at 1 Airy diameter. All images were captured at 512 x 512 pixels at 400 Hz or 1400 Hz capture rates. Z stacks of cell samples were obtained with the 63 x oil objective with further magnification being achieved with the optical zoom. PentaHis™ Alexa Fluor® 488 was excited at 488 nm (Ar laser) and emission collected between 500-640 nm. Images were processed using Image J. Gains were kept constant throughout measurements, at a point where saturation was not reached in the most fluorescent sample.

Immunostained sections were examined with a Leica CM5000B fluorescent microscope and images were captured with a Hamamatsu Orca-ER B/W CCD digital camera.

Flow Cytometry. Flow cytometry was performed on a BD FACSCalibur flow cytometer with excitation at 488 nm (Ar-laser) and fluorescence detected in the FL-1 channel. 10,000 events were collected for each experiment, with live cells being detected with an FL-1 intensity of 10^0-10^3. Data was collected in CellQuest Pro and processed in FlowJo.

cAb-Lys3-pCys104. cAb-Lys3-Dha104 (980 μL, c = 0.5 mg/mL in PBS pH 8) was concentrated down to 500 μL (Vivaspin, 5 kDa MWCO, Sartorius Stedim) and then split into 5 aliquots of 100 μL each. A solution of Na_3SPO_3 (59 mg, 328 μmol) was made in 18.6 μL MQ H_2O and 20 μL 5 M HCl. Four aliquots of 2.5 μL of the Na_3SPO_3 solution (84.9 μmol, ~ 2700 eq.) were added to each aliquot over 30 minutes whilst shaking (600 rpm) at 37 °C. The reactions were continued for 7 hours in total, after which analysis by LC-MS revealed full conversion to cAb-Lys3-pCys104 (calc. mass 15874; obs. mass 15875). The reaction solution was buffer exchanged and desalted using a PD10 minitrap.

Proteolytic digest and LC-MS/MS. cAb-Lys3-pCys104 was proteolytically digested following the procedure described in chapter 2. LC-MS/MS analysis of the digest fragments is shown below.

Residue at position 104 (X)	Calculated monoisotopic mass of neutral peptide
Phosphocysteine	2530.92

Experimental Table 5.1. Calculated monoisotopic masses of neutral peptides with specified modification at position 104.

a

Associated Datafile: SG_cAb-104SPO3 1 (50 - 1990 amu)
AspN:-/D

Frag#	Res#	Sequence	Theor (Bo)	[M+H]	[M+2H]	[M+3H]
D4	90-98	(E)DTAIYYBAA(D)	1046.44	1047.45	524.23	349.82
D2	62-72	(A)DSVKGRFTISQ(D)	1236.65	1237.65	619.33	413.22
D3	73-89	(Q)DNAKNTVYLLMNSLEPE(D)	1949.94	1950.95	975.98	650.99
■D5	99-120	(A)DSTIYXSYYEBGHGLSTGGYGY(D)	2530.92	2531.93	1266.47	844.65
D6	121-146	(Y)DSWGQGTQVTVSRENLYFQGHHHHHH(-)	3093.41	3094.42	1547.71	1032.14
D1	1-61	(-)DVQLVESGGGSVQAGGSLRLSBAASGYTIGPYBMGWFRQAPGKEREGVAAINMGGGITYYA(D)	6331.12	6332.13	3166.57	2111.38

b

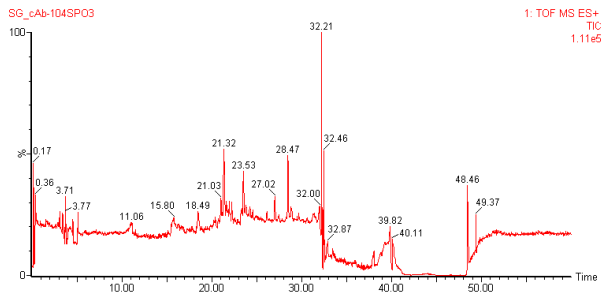

c

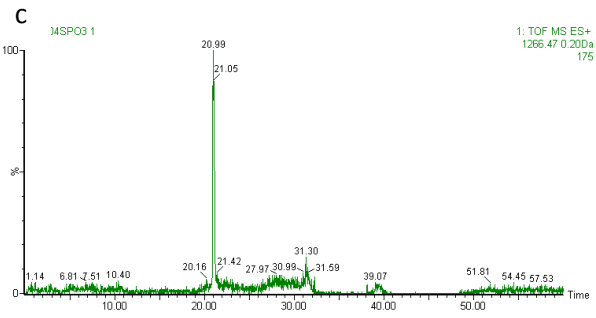

d

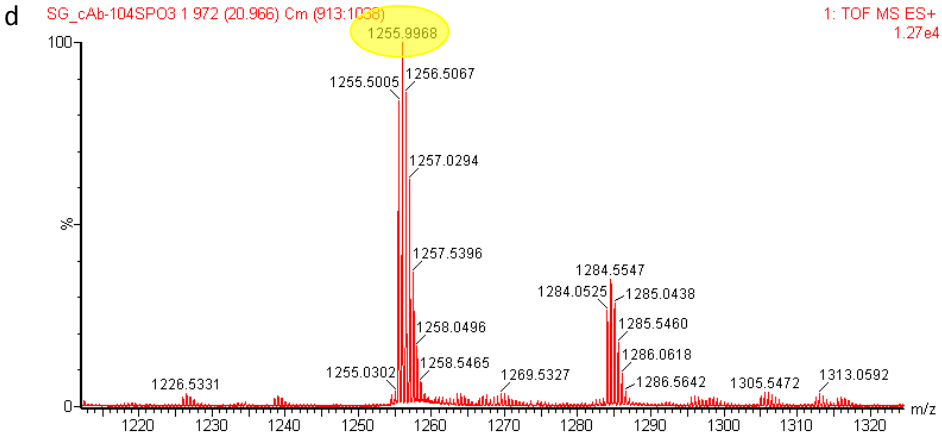

e

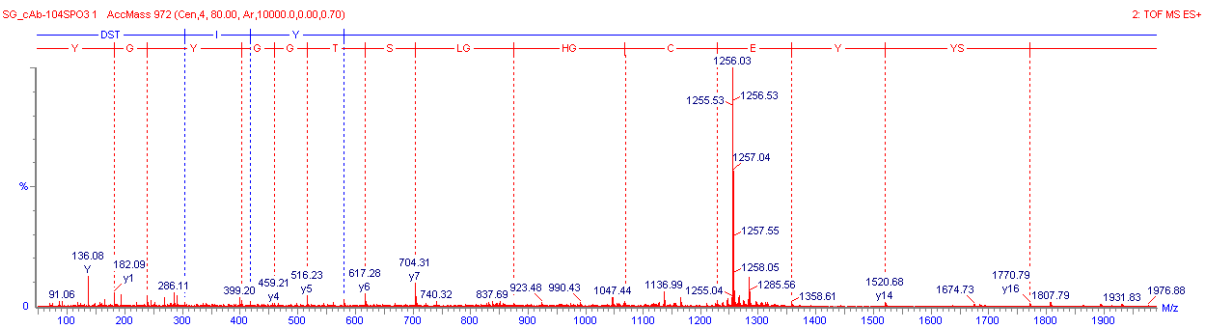

f

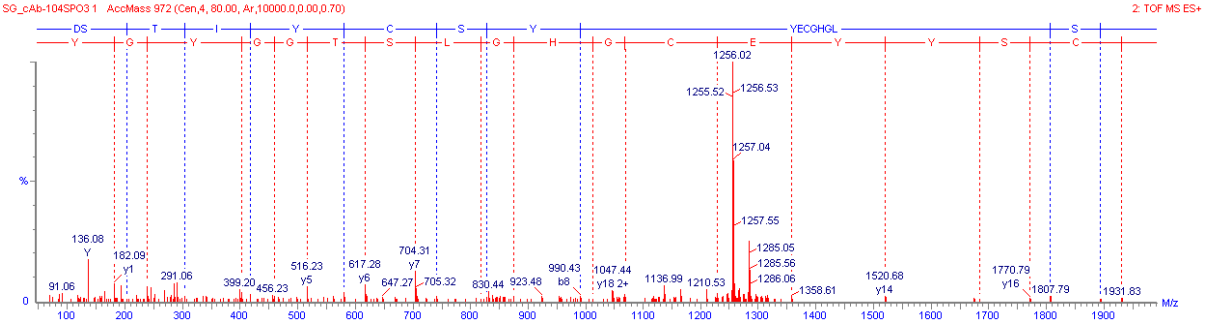

Experimental Figure 4.5. Enzymatic digest of cAb-Lys3-pCys104 and sequencing. a) Expected sequences and theoretical masses of the peptides resulting from digestion of cAb-Lys3-pCys104 with Asp-N. Masses identified in the mass spectrum integrated over the whole LC-MS chromatogram are highlighted in black (ΔDa = 0.1). B corresponds to carboxymethylamide cysteine, X is phosphocysteine. b) LC-MS chromatogram. c) Extracted mass chromatogram for the theoretical mass $[D5+2H]^{2+}$: M = 1266.47. d) MS of peak at 20.99 minutes. e) MS/MS of peptide D5, phosphocysteine is not observed at position 104, even though the mass was detected. f) MS/MS of peptide D5, where Cys is observed at position 104. No Dha is detected over the chromatogram, indicating the phosphate group is labile during data acquisition.[87]

Phosphatase activity on cAb-Lys3-pCys104

Human acid phosphatase-1 (Human acp-1, Source BioScience). To a solution of cAb-Lys3-pCys104 (140 μL, 4.4 nmol, c = 0.48 mg/mL in 20 mM MES pH 6.0) was added human acp-1 (1 μL, 80 U). After 2.5 hours at 37 °C (600 rpm), LC-MS analysis revealed full conversion to regenerated cAb-Lys3-Cys104 (calc. mass 15797; obs. mass 15798).

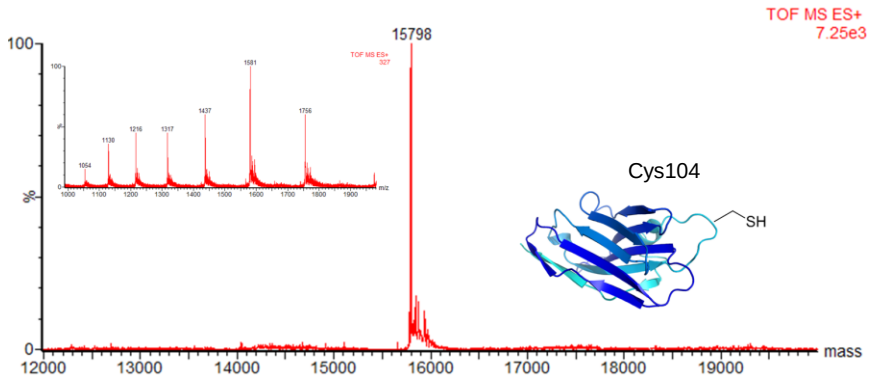

Experimental Figure 4.6. cAb-Lys3-Cys104 can be regenerated by reaction with human acp-1. Calculated mass 15797, observed mass 15798.

Alkaline phosphatase (alp) - bovine intestinal mucosa phosphatase (bIMP, Sigma). To a solution of cAb-Lys3-pCys104 (140 µL, 4.4 nmol, c = 0.48 mg/mL in 10 mM PBS pH 9.8) was added bIMP (1.5 µL, 209 U). After 20 minutes at 37 °C (600 rpm), LC-MS analysis revealed full conversion to regenerated cAb-Lys3-Cys104 (calc. mass 15797; obs. mass 15796).

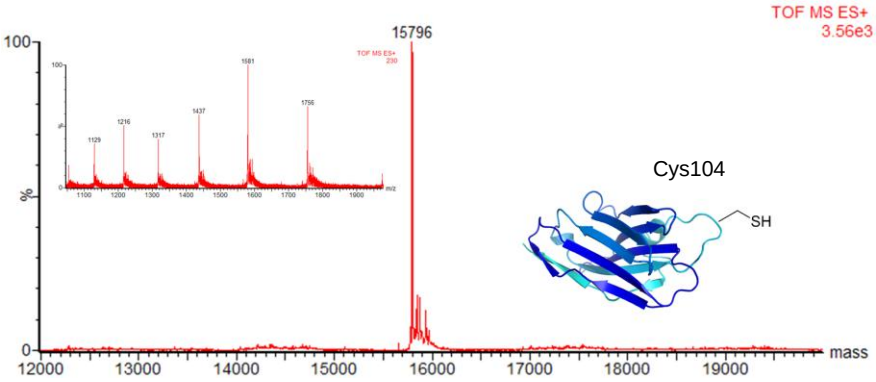

Experimental Figure 4.7. Regeneration of cAb-Lys3-Cys104 by reaction with alp from bovine intestinal mucosa. Calculated mass 15797, observed mass 15796.

λ-Protein Phosphatase (λ-ppase, New England Biolabs). cAb-Lys3-pCys104 (150 µL, 4.6 nmol, c = 0.48 mg/mL in 50 mM Tris-HCl pH 7.4) was concentrated to 40 µL (Vivaspin, 5 kDa MWCO, Sartorius Stedim), and then desalted into 50 mM Tris-HCl pH 7.4 using a Micro Bio-Spin 6 column (Bio-Rad Laboratories). To the protein solution was added λ-ppase (1 µL, 400 U, Sigma), 10x λ-ppase buffer (5 µL) and 2 mM $MnCl_2$ (5 µL, 20 mM). After 10

minutes at 30 °C (600 rpm), the reaction was analysed by LC-MS, and revealed full conversion to regenerated cAb-Lys3-Cys104 (calc. mass 15797; obs. mass 15801).

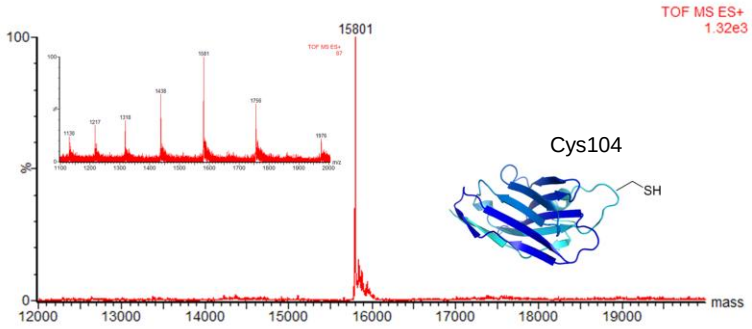

Experimental Figure 4.8. Regeneration of cAb-Lys3-Cys104 reaction with λ-ppase. Calculated mass 15797, observed mass 15801.

Acid phosphatase (acp) from potato (Sigma). A solution of acp from potato (1 mg, 3 U) in 50 μL 10 mM MES pH 4.8 was prepared. 5 μL of the enzyme solution (0.3 U) was added to cAb-Lys3-pCys104 (150 μL, 4.6 nmol, c = 0.45 mg/mL in 10 mM MES pH 4.8), and the reaction shaken at 37 °C (600 rpm). After 2 hours, LC-MS analysis revealed full conversion to regenerated cAb-Lys3-Cys104 (calc. mass 15797; obs. mass 15793).

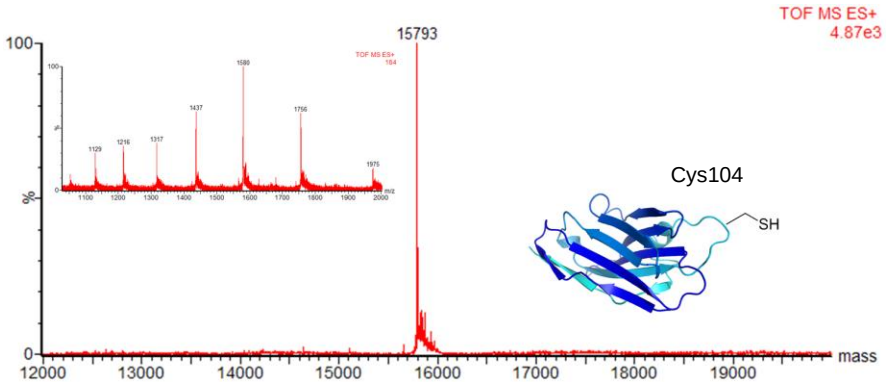

Experimental Figure 4.9. Regeneration of cAb-Lys3-Cys104 by reaction with acp from potato. Calculated mass 15797, observed mass 15793.

Human Placental Alkaline Phosphatase (PLAP, Sigma). A solution of PLAP (1 mg, 1.3 U) in 50 μL 50 mM Tris-HCl pH 7.4 was prepared. 17 μL of the enzyme solution (0.44 U) was added to cAb-Lys3-pCys104 (150 μL, 4.6 nmol, c = 0.45 mg/mL in 50 mM Tris-HCl pH

7.4), and the reaction shaken at 37 °C (600 rpm). After 2 hours, LC-MS analysis revealed full conversion to regenerate cAb-Lys3-Cys104 (calc. mass 15797; obs. mass 15800).

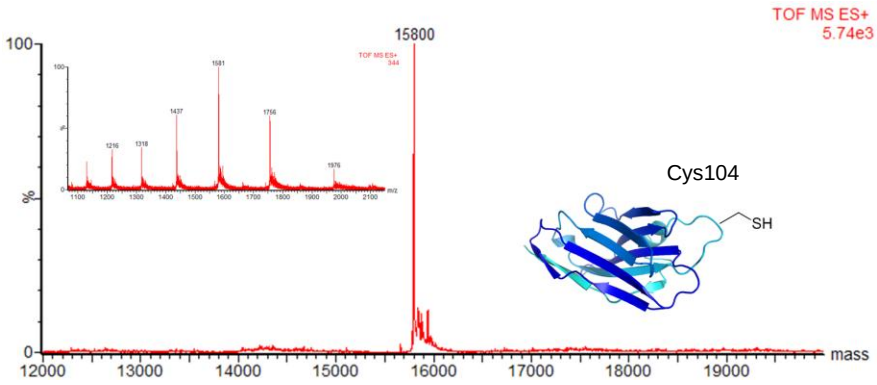

Experimental Figure 4.10. Regeneration of cAb-Lys3-Cys104 by reaction with PLAP. Calculated mass 15797, observed mass 15800.

Comparative phosphatase activity. Each of the phosphatases' ability to cleave the thiophosphate group from cAb-Lys3 were compared directly by conducting reactions under identical conditions with a low amount of enzyme equivalents. Physiological pH was used. Accordingly, enzyme solutions were prepared (2.5 – 13.9 U in 50 μL 50 mM Tris-HCl pH 7.4) and the volume corresponding to 0.17 U added to cAb-Lys3-pCys104 (64 μL, 1.7 nmol, c = 0.42 mg/mL in 50 mM Tris-HCl pH 7.4). Reactions were shaken at 37 °C (600 rpm), and monitored over 4 hours. Conversion to product was extrapolated by measuring the relative intensities of peaks obtained in the MS.

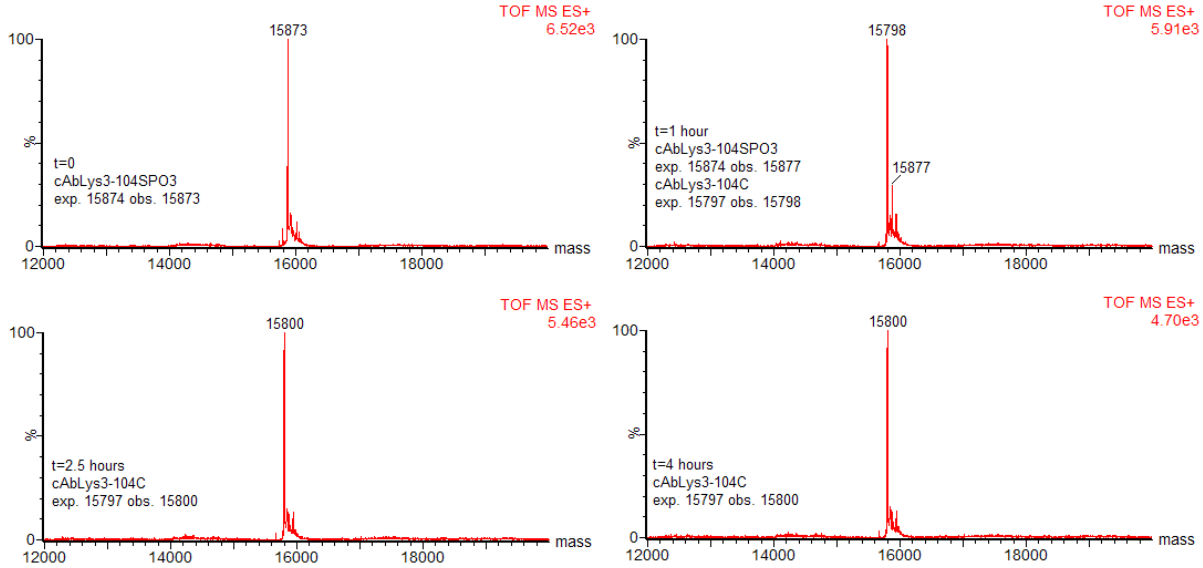

Experimental Figure 4.11. MS data for cAb-Lys3-pCys104 treated with PLAP in 50 mM Tris-HCl (pH 7.4) over 4 hours.

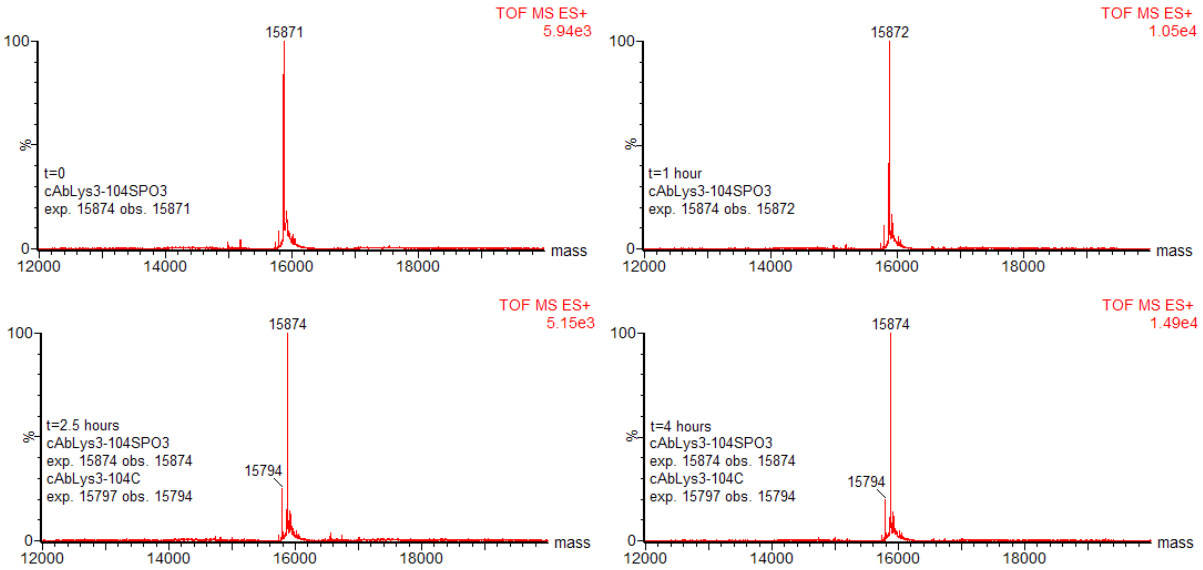

Experimental Figure 4.12. MS data for cAb-Lys3-pCys104 treated with human acp-1 in 50 mM Tris-HCl (pH 7.4) over 4 hours.

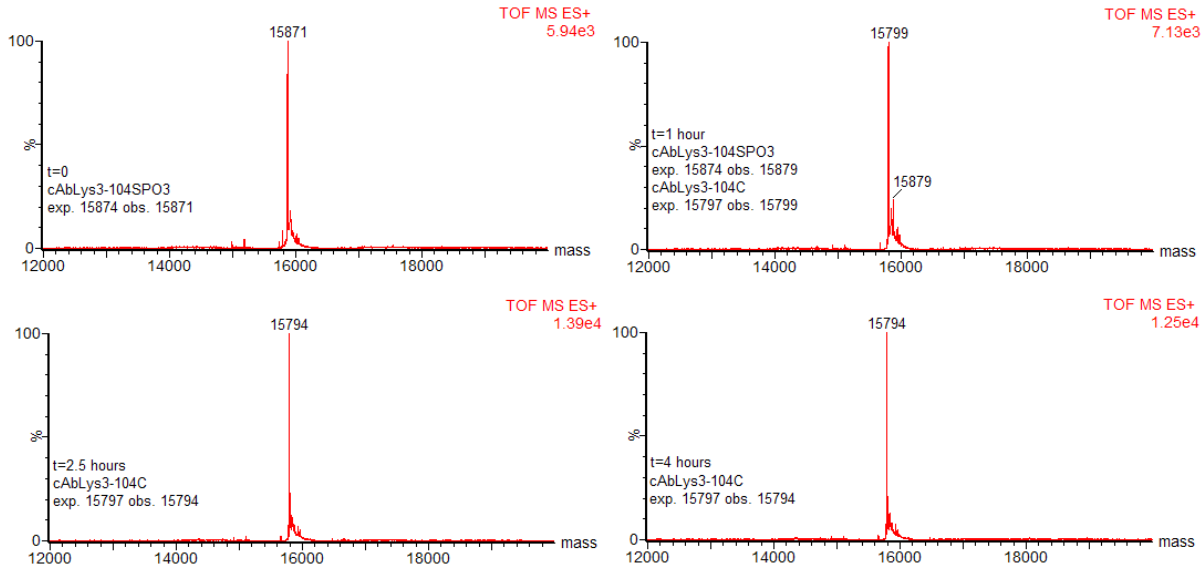

Experimental Figure 4.13. MS data for cAb-Lys3-pCys104 treated with bIMP in 50 mM Tris-HCl (pH 7.4) over 4 hours.

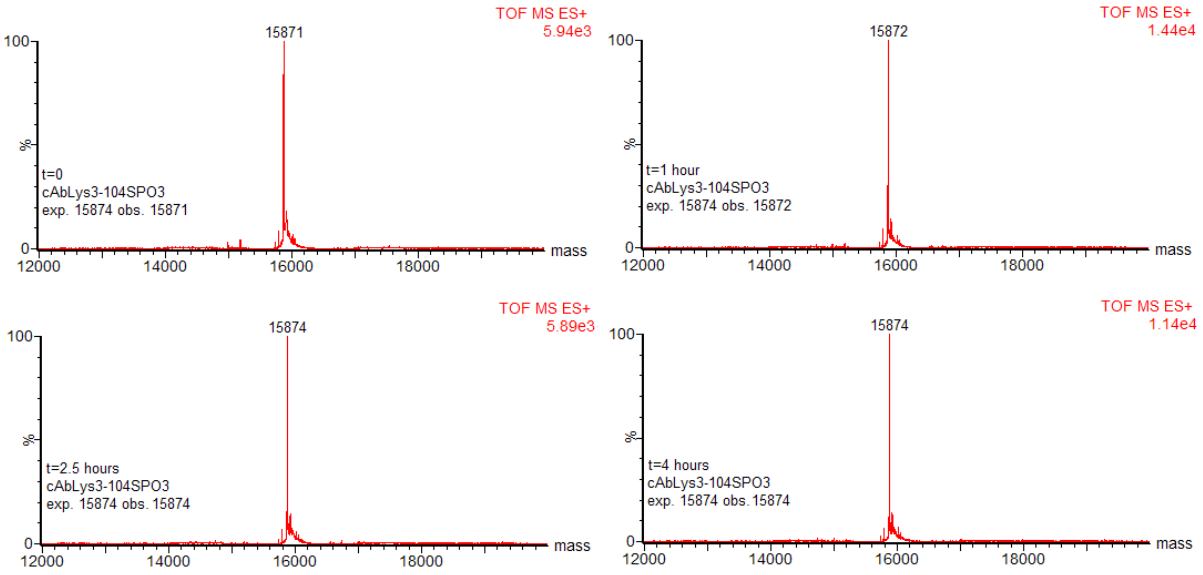

Experimental Figure 4.14. MS data for cAb-Lys3-pCys104 treated with λ-ppase in 50 mM Tris-HCl (pH 7.4) over 4 hours.

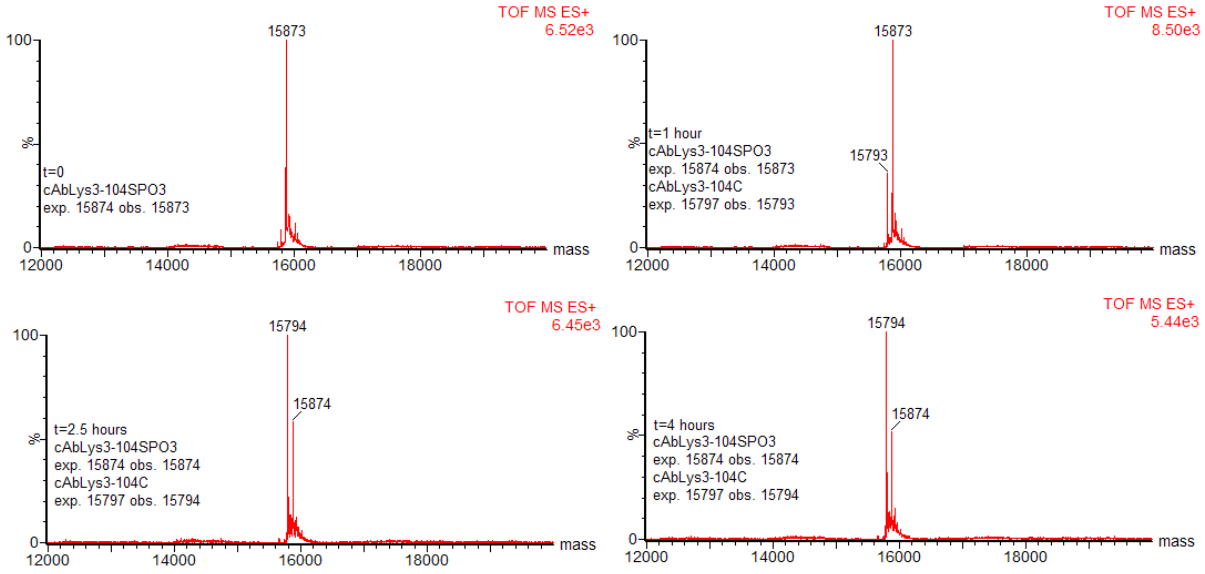

Experimental Figure 4.15. MS data for cAb-Lys3-pCys104 treated with acp from potato in 50 mM Tris-HCl (pH 7.4) over 4 hours.

Cell Culture. Lysozyme (pIMMs2011:LysD52S) under the CMV promoter was obtained from H. Finney (UCB). CMV-SEAP in pBluescript was obtained from Addgene (plasmid 24595). Human Embryonic Kidney (HEK293T) cells were cultured in Dulbecco's modified Eagle Medium (DMEM, Life Technologies) supplemented with 10% (v/v) FBS (Sigma), 50 U/mL penicillin, 50 μg/mL streptomycin (Sigma) and 100 μg/mL Normocin™ (Invivogen) in a T25 flask (Greiner Bio-One). HEK-Blue™ Null1 cells (HEK-Blue Null1 (NF-κB-*seap*+), Invivogen) were cultured in DMEM supplemented with 10% (v/v) FBS, 50 U/mL penicillin, 50 μg/mL streptomycin, 100 μg/mL Normocin™ and 100 μg/mL Zeocin™ (Invivogen) in a T25 flask. All cells were maintained at 37 °C under 5% CO_2 with passaging every 3 – 4 days. Xfect™ transfection reagent was purchased from Clontech and PentaHis™ Alexa Fluor® 488 from Qiagen. Recombinant human TNF-α was purchased from Invivogen, and recombinant mouse TNF-α from E-Bioscience.

Transfection. Xfect-mediated transfection of HEK293T cells with lysozyme and SEAP were carried out according to the manufacturers' protocol. Accordingly, one day prior to

transfection, cells were plated in 500 μL complete growth medium (in each well of a 12-well plate) to reach 50 – 70% confluency. After 24 hours, plasmid (2.5 μg lysozyme or SEAP, in the case of co-transfections, 1.2 μg of each plasmid was used) was diluted with Xfect reaction buffer to a final volume of 50 μL and vortexed. Xfect Polymer was added to the diluted plasmid DNA (0.3 μL for every 1 μg plasmid) and vortexed. The polymer-plasmid solutions were incubated at room temperature for 10 minutes to allow nanoparticle complexes to form. 50 μL of the nanoparticle complex solution was added dropwise to the cell culture medium of each well. Plates were rocked gently back and forth, and then incubated at 37 °C for 4 hours. After this time, cell culture medium was replaced with 1 mL of fresh complete growth medium, and returned to 37 °C for approximately 40 hours. For the induction of SEAP expression in HEK293T cells, TNF-α was added to relevant wells at 100 ng/mL after approximately 24 hours expression time. Antibody (WT-cAb-Lys3 or cAb-Lys3-pCys104) was added to relevant wells at 1 μM after approximately 28 hours expression time. For SEAP detection, 18 μL test medium (containing 10 % (v/v) heat-inactivated FBS) was added to wells of a 96-well plate, with 2 μL cell supernatant. 180 μL QUANTI-Blue™ (chromophoric phosphatase substrate) was added, and the plate incubated at 37 °C for 1 – 3 hours, after which SEAP activity could be observed by the naked eye (pink – purple), and quantitatively determined using a spectrophotometer at 620 nm. After expression (~ 44 hours), cells were washed three times with 500 μL of washing buffer (PBS + 2% FBS) and incubated at room temperature with PentaHis™ Alexa Fluor® 488 (0.5 μg/mL) for 30 minutes. Cells were washed three more times with washing buffer, and then analysed by flow cytometry and microscopy.

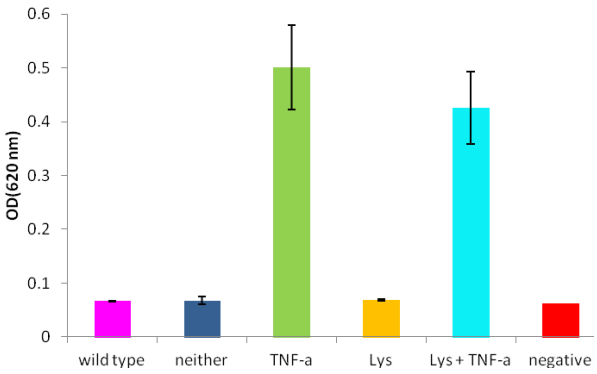

Experimental Figure 4.16. Testing SEAP expression in HEK-Blue Null1 cell AND gate by QUANTI-Blue addition to cell culture medium.

Lysozyme	-	-	-	+	+
TNF-α	-	-	+	-	+
Inihibited	-	+	+	+	+
Antibody (1 μM)					
Fluorescence					
Brightfield	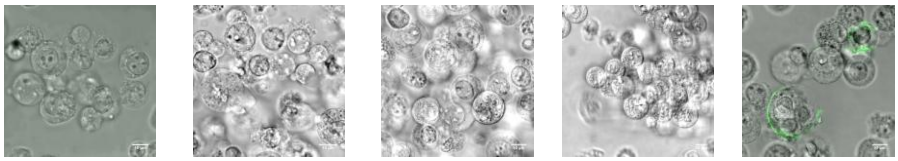				
merge					

Experimental Figure 4.17. Displaying cell surface labelling of the HEK-Blue Null1 cell AND gate. Scale bar reads 10 μm.

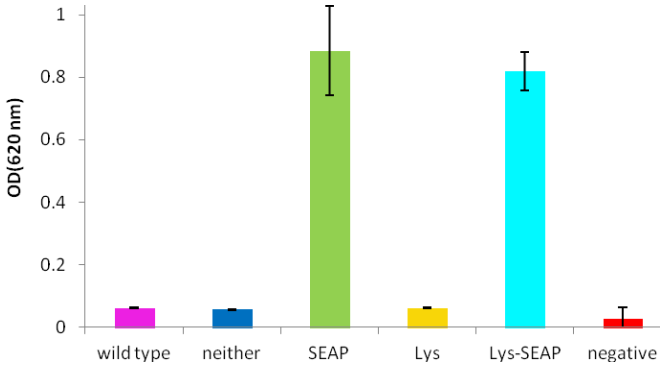

Experimental Figure 4.18. Testing SEAP expression in HEK293T cell AND gate by QUANTI-Blue addition to cell culture medium.

Lysozyme	-	-	-	+	+
SEAP	-	-	+	-	+
Inhibited	-	+	+	+	+
Antibody (1 μM)					
Fluorescence					
Brightfield	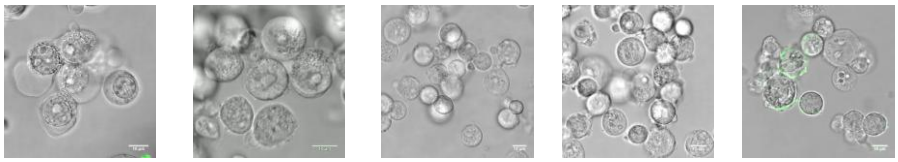				
merge					

Experimental Figure 4.19. Displaying cell surface labelling of the HEK293T cell AND gate. Scale bar reads 10 μM.

Biolistic transfection of rat hippocampal slices.[7] pIMMs2011:lysozyme-D52S and pBluescript:SEAP stocks were prepared at 1.6 and 1.2 μg/μL respectively. A length of tubing was slid into the tubing station and dried under nitrogen for 1 hour. In the meantime, DNA was precipitated onto gold beads. DNA was diluted to 30 μg in 50 μL. Gold (12 mg) was weighed into a plastic tube, and spermidine (100 μL, 0.05 M stock) added. The plastic tube was vortexed then sonicated for 20 seconds to break up the suspension. DNA (50 μL of diluted stock) was added to the gold/spermidine suspension, and then vortexed with the cap closed, then open. $CaCl_2$ (100 μL, 1 M stock) was added dropwise, and then the plastic tube flicked. Precipitation was allowed to occur for 10 minutes at room temperature, and then the suspension sonicated briefly. Sonication was brief to prevent shearing of DNA. Gold beads were sonicated (13.2 krpm, 10 sec). The supernatant was discarded, and a small amount of liquid was kept above the gold beads. Gold beads were washed with EtOH (3 x 1 mL), with brief sonication (1 s) each time. Gold beads were resuspended in EtOH (200 μL), and transferred to a 15 mL falcon tube. Remaining gold was transferred by sequentially washing

[7] A slightly modified protocol by Bio-Rad laboratories was followed.

the tube with 200 μL EtOH portions until the total volume in the falcon tube was 15 mL. Next, the tubing was coated with the gold/DNA beads. The nitrogen supply was switched off, and the dried tubing removed and attached to a 10 mL syringe. The 15 mL falcon tube was shaken vigorously, then placed at the end of the tubing and the gold/DNA beads removed very slowly via syringe. Approximately 4 cm of tubing was kept dry at either end. The tubing was carefully slid back into the tubing station, and the gold was allowed to settle for 5 minutes with the syringe attached. The ends of the solution were marked on the tubing. The solution was removed very slowly via syringe by pulling the syringe so the settled gold was left behind, and then the syringe disconnected. The tubing was rotated 90° and left for 10 seconds, 180° and left for 10 seconds, and then rotated for 5 seconds. Nitrogen was passed through the tubing (at 0.4 pressure), and it spun whilst drying for 5 minutes. A labelled scintillation vial was placed under a tubing chopper and cut with a clean razor into 1 cm wide sections. The cut tubing sections (gold/DNA bullets in plastic cartridges) were stored at 4 °C in the scintillation vial with dessication pellets.

Cultured rat hippocampal slices at passage 7 were co-transfected by means of shooting with a Helios Gene Gun. 2 12-well plates with each well containing 2 slices were shot with the DNA/gold bullets. The gene gun was prepared as follows. Sterile forceps were used to place the gold/DNA bullets in plastic cartridges into the cartridge holder. The cartridge holder was secured with a lock, and the barrel-line secured into the gene gun. For shooting, a hose connected to a helium gas tank was plugged into the gene gun. The pressure on the tank was turned up to 120 PSI, and a blank was shot into the air to remove any dust or debris from the diffuser screen and to equilibrate the pressure. After checking the pressure was still at 120 PSI, the safety interlock button was depressed until the gun beeped, then another blank shot. Slices were shot by holding the gun directly over each well (0.5 – 1 inch over the slice) and pulling the trigger, advancing the cartridge holder each time. After shooting, plates were

incubated at 37 °C (5% CO_2) for 48 hours. WT-cAb-Lys3 or cAb-Lys3-pCys104 was prepared as a 1 μM solution in media. The plates were removed from the incubator, and the media from each well aspirated. Ab solution (200 μL) was added to each well (WT-cAb-Lys3 in one plate, and cAb-Lys3-pCys104 in the other) and the plates were incubated at 37 °C for 3 hours. Slices were then washed three times (50 mM Tris-HCl), fixed in 4% FA for 5 minutes, washed three times (50 mM Tris-HCl), blocked with Tris-HCl + 5% FBS, washed three times again (50 mM Tris-HCl), incubated with PentaHis™ Alexa Fluor® 488 (0.5 μg/mL) for 1 hour and then washed 3 times with 50 mM Tris-HCl. Slices were analysed by brightfield and fluorescence microscopy. No fluorescence were observed in any slices (even for the WT-cAb-Lys3 positive control), and brightfield images are shown below (**Experimental Figure 4.20**)

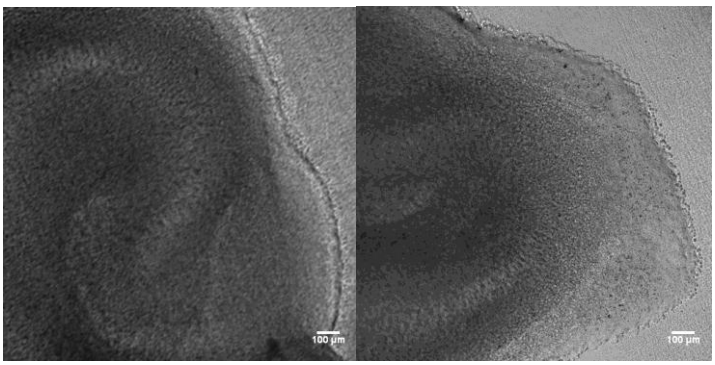

Experimental Figure 4.20. Brightfield images of rat hippocampal slices transfected with lysozyme and SEAP using a gene gun. No fluorescence was observed in corresponding fluorescence images. Scale bar reads 100 μm.

Mammalian tissue experiments. Mouse serum, TWEEN® 20, a PAP pen for immunostaining and formalin solution were purchased from Sigma. Vectashield HardSet mounting medium with DAPI was obtained from Vector Laboratories.

HEK293T cells were transfected in a 12-well plate with varying combinations of inputs as described above (using pIMMs2011:LysD52S and pBluescript:SEAP. 48 hours after transfection, media was removed. A sample was taken for confirmation of SEAP expression.

Cells were washed three times with DMEM (no additives) and lifted with 500 μL DMEM and counted. An aliquot of 10^4 cells was taken to test for lysozyme expression, and a sample containing 10^6 cells was centrifuged (5 mins, 1.2 krpm). Supernatant was removed, and the cell pellet resuspended in 2 μL DMEM.

Stereotaxic Surgery. Eight-week-old male C57BL/6 mice (Harlan, UK) were allowed to acclimatize for 7 days prior to injection. All surgical procedures were performed under an operating microscope (Wild M650, Leica, Milton Keynes, UK) with UK Home Office and local ethical approval. Animals were anaesthetised with isoflurane (Rhodia Organique Fine Ltd, Bristol, UK) for induction and maintenance at 2.5–3% in oxygen. Stereotaxic surgery was performed as described previously[88] using a Hamilton syringe with a 30FG needle for the injection of the cells. Briefly, anaesthetised mice were held in a stereotaxic frame, a burr hole was drilled in the skull and a 2 μl volume of the cell suspension (see above) was unilaterally microinjected into the left striatum through a glass microcapillary needle over a period of 5 minutes. The stereotaxic co-ordinates were: bregma +0.5 mm, lateral 1.8 mm, and the cells were injected from a rising depth of 2.5-1.5 mm. During the surgical procedures, body temperature was maintained on a heated blanket throughout the period of anaesthesia, and the animals were allowed to recover in a heated chamber. Mice were killed after 24h by deep anaesthetic with sodium pentobarbitone and transcardial perfusion with cold saline (4 °C). Brains were frontally cut into 10 μm thick cryostat sections through the injection site onto RNAse free Super Frost Plus slides (Thermo Scientific, Germany). Tissue sections on slides were removed from -20 °C and 50 μL blocking buffer (50 mM Tris-HCl pH 7.4, 2% mouse serum, 0.01% TWEEN® 20) was added to immerse each tissue slice in a well constructed with a PAP pen for immunostaining. Blocking was allowed to occur for 10 minutes at room temperature after which it was replaced with antibody solution (1 μM in blocking buffer).

Slide-mounted tissue was incubated at 37 °C 5% CO_2 in a humidity chamber for 2 hours. As a positive control, WT-cAb-Lys3 was added to a single tissue section injected with HEK293T-*lys*+ cells. Slides were washed to remove excess antibody by dipping in a beaker of 50 mM Tris-HCl pH 7.4 ten times and then each tissue slice fixed with 50 µL 4% formaldehyde for 5 minutes at room temperature, and then washed three times. Blocking was repeated for 10 minutes at room temperature. PentaHis™ Alexa Fluor® 488 in blocking buffer (0.5 µg/mL) was added to each slice in the humidity chamber and staining was allowed to occur for 1 hour at room temperature. Again, slides were dipped ten times into 50 mM Tris-HCl pH 7.4 to remove excess antibody. Excess liquid was removed from the slides with a medical wipe, each slice was covered with a coverslip containing one drop of mounting medium (with DAPI) and allowed to harden overnight at 4 °C. Immunostained sections were tested for fluorescence by microscopy.

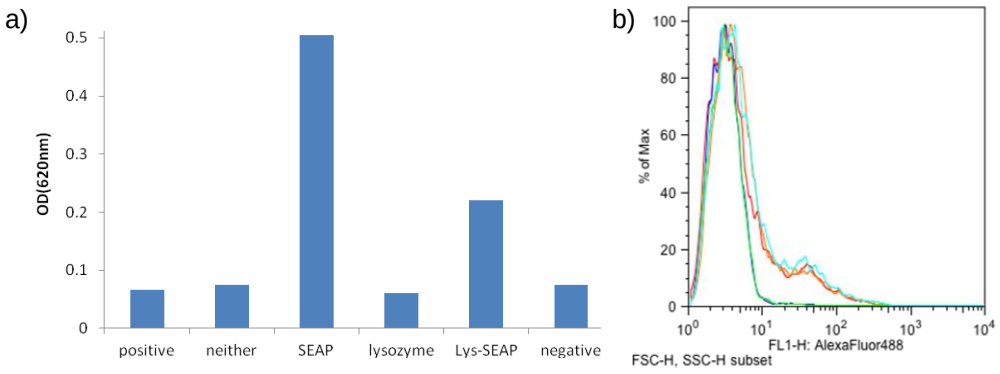

Experimental Figure 4.21. Testing SEAP and lysozyme expression in HEK293T cells before injection into mice. a) OD values following addition of chromophoric substrate to cell culture medium, b) FACS following WT-cAb-Lys3 and PentaHis™ Alexa Fluor® 488 addition to cells corresponding to each input transfection combination. Red – positive control, dark blue – no inputs, green – SEAP input, turquoise – lysozyme input, orange – lysozyme-SEAP inputs.

a)

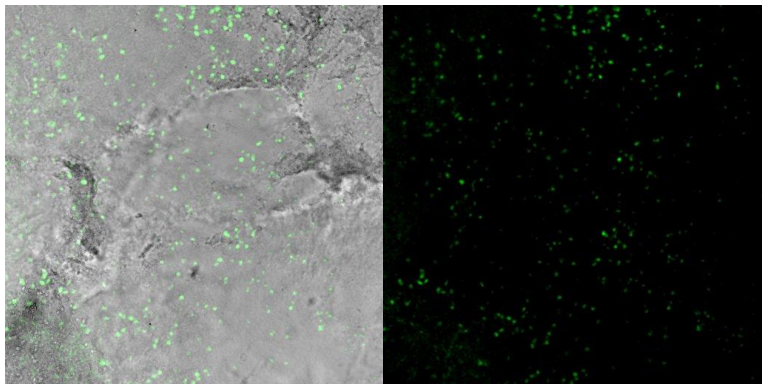

b)

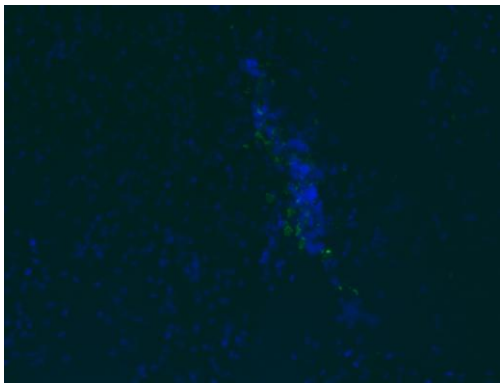

Experimental Figure 4.22. Positive controls testing for antibody binding. WT-cAb-Lys3 added to tissue sections previously injected with HEK293T cells transfected with pIMMs2011:lysozyme-D52S. a) fluorescence (488 nm) and brightfield-fluorescence merge, b) showing nuclei staining by DAPI.

4.6 Chapter 4 References

1. Weiner, L. M., Dhodapkar, M. V., Ferrone, S. Monoclonal antibodies for cancer immunotherapy. *Lancet* **373,** 1033–1040 (2009).

2. Rodeck, U. Skin toxicity caused by EGFR antagonists-an autoinflammatory condition triggered by deregulated IL-1 signaling? *J. Cell. Physiol.* **218,** 32–34 (2009).

3. Strebhardt, K., Ullrich, A. Paul Ehrlich's magic bullet concept: 100 years of progress. *Nat. Rev. Cancer* **8,** 473–480 (2008).

4. Köhler, G., Milstein, C. Continuous cultures of fused cells secreting antibody of predefined specificity. *Nature* **256,** 495–497 (1975).

5. Wu, A. M., Senter, P. D. Arming antibodies: prospects and challenges for immunoconjugates. *Nat. Biotechnol.* **23,** 1137–1146 (2005).

6. Webb, S. Pharma interest surges in antibody drug conjugates. *Nat. Biotechnol.* **29,** 297–298 (2011).

7. Koshkaryev, A., Sawant, R., Deshpande, M., Torchilin, V. Immunoconjugates and long circulating systems: origins, current state of the art and future directions. *Adv. Drug Deliv. Rev.* **65,** 24–35 (2013).

8. Donaldson, J. M., Kari, C., Fragoso, R. C., Rodeck, U., Williams, J. C. Design and development of masked therapeutic antibodies to limit off-target effects: application to anti-EGFR antibodies. *Cancer Biol. Ther.* **8,** 2147–2152 (2009).

9. Cox, G., Jones, J., O'Byrne, K. Matrix metalloproteinase 9 and the epidermal growth factor signal pathway in operable non-small cell lung cancer. *Clin. Cancer Res.* **6,** 2349–2355 (2000).

10. Janssen, B. M. G., Lempens, E. H. M., Olijve, L. L. C., Voets, I. K., van Dongen, J. L. J., de Greef, T. F. A., Merkx, M. Reversible blocking of antibodies using bivalent peptide–DNA conjugates allows protease-activatable targeting. *Chem. Sci.* **4,** 1442–1450 (2013).

11. Salis, H., Kaznessis, Y. N. Computer-aided design of modular protein devices: Boolean AND gene activation. *Phys. Biol.* **3,** 295-310 (2006).

12. Siuti, P., Yazbek, J., Lu, T. K. Synthetic circuits integrating logic and memory in living cells. *Nat. Biotechnol.* **31,** 448–452 (2013).

13. Gardner, T. S., Cantor, C. R., Collins, J. J. Construction of a genetic toggle switch in Escherichia coli. *Nature* **403,** 339–342 (2000).

14. Lu, T. K., Khalil, A. S., Collins, J. J. Next-generation synthetic gene networks. *Nat. Biotechnol.* **27,** 1139–1150 (2009).

15. Wang, B., Kitney, R. I., Joly, N., Buck, M. Engineering modular and orthogonal genetic logic gates for robust digital-like synthetic biology. *Nat. Commun.* **2,** 508 (2011).

16. Bonnet, J., Yin, P., Ortiz, M. E., Subsoontorn, P., Endy, D. Amplifying genetic logic gates. *Science* **340,** 599–603 (2013).

17. Mahdavi, A., Segall-Shapiro, T. H., Kou, S., Jindal, G. A., Hoff, K. G., Liu, S., Chitsaz, M., Ismagilov, R. F., Silberg, J. J., Tirrell, D. A. A genetically encoded and gate for cell-targeted metabolic labeling of proteins. *J. Am. Chem. Soc.* **135,** 2979–2982 (2013).

18. Ding, M., Zhang, E., He, R., Wang, X., Li, R., Wang, W., Yi, Q., The radiation dose-regulated AND gate genetic circuit, a novel targeted and real-time monitoring strategy for cancer gene therapy. *Cancer Gene Ther.* **19,** 382–392 (2012).

19. Douglas, S. M., Bachelet, I., Church, G. M. A logic-gated nanorobot for targeted transport of molecular payloads. *Science* **335,** 831–834 (2012).

20. Bray, D. Protein molecules as computational elements in living cells. *Nature* **376,** 307–312 (1995).

21. Unger, R., Moult, J. Towards computing with proteins. *Proteins* **63,** 53–64 (2006).

22. Van Kasteren, S. Synthesis of post-translationally modified proteins. *Biochem. Soc. Trans.* **40,** 929–944 (2012).

23. Desmyter, A., Transue, T. R., Ghahroudi, M. A., Ti, M-H, D., Poortmans, F., Hamers, R., Muyldermans, S., Wyns, L. Crystal structure of a camel single-domain V_H antibody fragment in complex with lysozyme. *Nat. Struct. Biol.* **3,** 803–811 (1996).

24. Transue, T. R., De Genst, E., Ghahroudi, M. A., Wyns, L., Muyldermans, S. Camel single-domain antibody inhibits enzyme by mimicking carbohydrate substrate. *Proteins* **32,** 515–522 (1998).

25. Lin, Y. A., Chalker, J. M., Floyd, N., Bernardes, G. J. L., Davis, B. G. Allyl sulfides are privileged substrates in aqueous cross-metathesis: application to site-selective protein modification. *J. Am. Chem. Soc.* **130,** 9642–9643 (2008).

26. Floyd, N., Vijayakrishnan, B., Koeppe, J. R., Davis, B. G. Thiyl glycosylation of olefinic proteins: *S*-linked glycoconjugate synthesis. *Angew. Chem. Int. Ed. Engl.* **48,** 7798–7802 (2009).

27. Chalker, J. M., Lercher, L., Rose, N. R., Schofield, C. J., Davis, B. G. Conversion of cysteine into dehydroalanine enables access to synthetic histones bearing diverse post-translational modifications. *Angew. Chem. Int. Ed. Engl.* **51,** 1835–1839 (2012).

28. Spicer, C. D., Davis, B. G. Rewriting the bacterial glycocalyx via Suzuki-Miyaura cross-coupling. *Chem. Commun. (Camb).* **49,** 2747–2749 (2013).

29. Lote, C., Weiss, J. Identification of digalactosylcysteine in a glycopeptide isolated from urine by a new preparative technique. *FEBS Lett.* **16,** 81–85 (1971).

30. Sardzík, R., Both, P., Flitsch, S. L. Post-translational modifications: *S*-linked sugars lost and found. *Nat. Chem. Biol.* **7,** 69–70 (2011).

31. Lafite, P., Daniellou, R. Rare and unusual glycosylation of peptides and proteins. *Nat. Prod. Rep.* **29,** 729–738 (2012).

32. Oman, T. J., Boettcher, J. M., Wang, H., Okalibe, X. N., van der Donk, W. A. Sublancin is not a lantibiotic but an *S*-linked glycopeptide. *Nat. Chem. Biol.* **7,** 78–80 (2011).

33. Wang, H., van der Donk, W. A. Substrate selectivity of the sublancin S-glycosyltransferase. *J. Am. Chem. Soc.* **133,** 16394–16397 (2011).

34. Stepper, J., Shastri, S., Loo, T. S., Preston, J. C., Novak, P., Man, P., Moore, C. H., Havlíček, V., Patchett, M. L., Norris, G. E. Cysteine *S*-glycosylation, a new post-translational modification found in glycopeptide bacteriocins. *FEBS Lett.* **585,** 645–650 (2011).

35. Venugopal, H., Edwards, P. J. B., Schwalbe, M., Claridge, J. K., Libich, D. S., Stepper, J., Loo, T., Patchett, M. L., Norris, G. E., Pascal, S. M. Structural, dynamic, and chemical characterization of a novel *S*-glycosylated bacteriocin. *Biochemistry* **50,** 2748–2755 (2011).

36. Pachamuthu, K., Schmidt, R. R. Synthetic routes to thiooligosaccharides and thioglycopeptides. *Chem. Rev.* **106,** 160–187 (2006).

37. Asano, N. Glycosidase inhibitors: update and perspectives on practical use. *Glycobiology* **13,** 93R–104R (2003).

38. Witczak, Z. J., Culhane, J. M. Thiosugars: new perspectives regarding availability and potential biochemical and medicinal applications. *Appl. Microbiol. Biotechnol.* **69,** 237–244 (2005).

39. Macauley, M. S., Stubbs, K. A., Vocadlo, D. J. *O*-GlcNAcase catalyzes cleavage of thioglycosides without general acid catalysis. *J. Am. Chem. Soc.* **127,** 17202–17203 (2005).

40. Yip, V. L. Y., Withers, S. G. Family 4 glycosidases carry out efficient hydrolysis of thioglycosides by an alpha,beta-elimination mechanism. *Angew. Chem. Int. Ed. Engl.* **45,** 6179–6182 (2006).

41. Bernacki, R. J., Niedbala, M. J., Korytnyk, W. Glycosidases in cancer and invasion. *Cancer Metastasis Rev.* **4,** 81–101 (1985).

42. Lin, M., Garciaarenas, R., Chao, Y. Regulation of prostatic acid phosphatase expression and secretion by androgen in LNCaP human prostate carcinoma cells. *Arch. Biochem. Biophys.* **300,** 384–390 (1993).

43. Adams, L. M., Warburton, M. J., Hayman, A. R. Human breast cancer cell lines and tissues express tartrate-resistant acid phosphatase (TRAP). *Cell Biol. Int.* **31,** 191–195 (2007).

44. Thompson, J., Gruber, M., Kruuv, J. Changes in glycosidase enzyme activity during growth of normal and transformed cells. *Exp. Cell Res.* **111,** 47–53 (1978).

45. Wielgat, P., Walczuk, U., Szajda, S., Bień, M., Zimnoch, L., Mariak, Z., Zwierz, K. Activity of lysosomal exoglycosidases in human gliomas. *J. Neurooncol.* **80,** 243–249 (2006).

46. Rubin, D., Rubin, E. A minimal toxicity approach to cancer therapy: possible role of beta-glucuronidase. *Med. Hypotheses* 85–92 (1980).

47. Björkman, R., Janson, J. Studies on myrosinases: I. Purification and characterization of a myrosinase from white mustard seed (Sinapis alba, L.). *Biochim. Biophys. Acta (BBA)-Enzymology* **276,** 508–518 (1972).

48. Meulenbeld, G. H., Hartmans, S. Thioglucosidase activity from *Sphingobacterium* sp. strain OTG1. *Appl. Microbiol. Biotechnol.* **56,** 700–706 (2001).

49. Gallego, M., Virshup, D. M. Protein serine/threonine phosphatases: life, death, and sleeping. *Curr. Opin. Cell Biol.* **17,** 197–202 (2005).

50. Tarrant, M. K., Cole, P. A. The chemical biology of protein phosphorylation. *Annu. Rev. Biochem.* **78,** 797–825 (2009).

51. Kee, J.-M., Muir, T. W. Chasing phosphohistidine, an elusive sibling in the phosphoamino acid family. *ACS Chem. Biol.* **7,** 44–51 (2012).

52. Elsholz, A. K. W., Turgay, K., Michalik, S., Hessling, B., Gronau, K., Oertel, D., Mäder, U., Bernhardt, J., Becher, D., Hecker, M., Gerth, U. Global impact of protein arginine phosphorylation on the physiology of *Bacillus subtilis*. *Proc. Natl. Acad. Sci. U. S. A.* **109,** 7451–7456 (2012).

53. Binkley, F. Preparation and properties of *S*-phosphocysteine. *J. Biol. Chem.* **195,** 283–285 (1952).

54. Signarvic, R. S., DeGrado, W. F. *De Novo* Design of a molecular switch: phosphorylation-dependent association of designed peptides. *J. Mol. Biol.* **334,** 1–12 (2003).

55. Riemen, A. J., Waters, M. L. Controlling peptide folding with repulsive interactions between phosphorylated amino acids and tryptophan. *J. Am. Chem. Soc.* **131,** 14081–14087 (2009).

56. Broncel, M., Wagner, S. C., Hackenberger, C. P. R., Koksch, B. Enzymatically triggered amyloid formation: an approach for studying peptide aggregation. *Chem. Commun. (Camb).* **46,** 3080–3082 (2010).

57. Riemen, A. J., Waters, M. L. Positional effects of phosphoserine on β-hairpin stability. *Org. Biomol. Chem.* **8,** 5411–5417 (2010).

58. Valette, N. M., Radford, S. E., Harris, S. A., Warriner, S. L. Phosphorylation as a tool to modulate aggregation propensity and to predict fibril architecture. *Chembiochem* **13,** 271–281 (2012).

59. Yang, Z., Liang, G., Wang, L., Xu, B. Using a kinase/phosphatase switch to regulate a supramolecular hydrogel and forming the supramolecular hydrogel *in vivo*. *J. Am. Chem. Soc.* **128,** 3038–3043 (2006).

60. Kühnle, H., Börner, H. G. Biotransformation on polymer-peptide conjugates: a versatile tool to trigger microstructure formation. *Angew. Chem. Int. Ed. Engl.* **48,** 6431–6434 (2009).

61. Caponi, P.-F., Qiu, X.-P., Vilela, F., Winnik, F. M., Ulijn, R. V. Phosphatase/temperature responsive poly(2-isopropyl-2-oxazoline). *Polym. Chem.* **2,** 306-308 (2011).

62. Shannon, D. A., Weerapana, E. Orphan PTMs: Rare, yet functionally important modifications of cysteine. *Biopolymers* (2013). 'Accepted Article' doi:10.1002/bip.22252

63. Sun, F., Ding, Y., Ji, Q., Liang, Z., Deng, X., Wong, C. C. L., Yi, C., Zhang, L., Xie, S., Alvarez, S., Hicks, L. M., Luo, C., Jiang, H., Lan, L., He, C. Protein cysteine phosphorylation of SarA/MgrA family transcriptional regulators mediates bacterial virulence and antibiotic resistance. *Proc. Natl. Acad. Sci. U. S. A.* **109,** 15461–15466 (2012).

64. Rowan, F., Richards, M., Bibby, R. A., Thompson, A., Bayliss, R. Blagg, J. Insights into Aurora-A kinase activation using unnatural amino acids incorporated by chemical modification. *ACS Chem. Biol.* (2013) ASAP

65. Chalker, J. M., Gunnoo, S. B., Boutureira, O., Gerstberger, S. C., Fernandez-Gonzalez, M., Bernades, G. J. L., Griffin, L., Hailu, H., Schofield, C. J., Davis, B. G.Methods for converting cysteine to dehydroalanine on peptides and proteins. *Chem. Sci.* **2,** 1666-1676 (2011).

66. Macauley, M. S., Whitworth, G. E., Debowski, A. W., Chin, D., Vocadlo, D. J. *O*-GlcNAcase uses substrate-assisted catalysis: kinetic analysis and development of highly selective mechanism-inspired inhibitors. *J. Biol. Chem.* **280,** 25313–25322 (2005).

67. Sheldon, W. L., Macauley, M. S., Taylor, E. J., Robinson, C. E., Charnock, S. J., Davies, G. J., Vocadlo, D. J., Black, G. W. Functional analysis of a group A

streptococcal glycoside hydrolase Spy1600 from family 84 reveals it is a beta-N-acetylglucosaminidase and not a hyaluronidase. *Biochem. J.* **399,** 241–247 (2006).

68. Riemen, A. J., Waters, M. L. Dueling post-translational modifications trigger folding and unfolding of a beta-hairpin peptide. *J. Am. Chem. Soc.* **132,** 9007–9013 (2010).

69. Cohen, P. T. W., Cohen, P. Discovery of a protein phosphatase activity encoded in the genome of bacteriophage A. *Biochem. J.* **260,** 931–934 (1989).

70. Hopkinson, D., Spencer, N., Harris, H. Genetical studies on human red cell acid phosphatase. *Human Genetics* **16,** 141–154 (1964).

71. Bingham, E. W., Farrell, H. M. Removal of phosphate groups from casein with potato acid phosphatase. *Biochim. Biophys. Acta* **429,** 448–460 (1976).

72. Besman, M., Coleman, J. E. Isozymes of bovine intestinal alkaline phosphatase. *J. Biol. Chem.* **260,** 11190–11193 (1985).

73. Chang, T. C., Huang, S. M., Huang, T. M., Chang, G. G. Human placental alkaline phosphatase. An improved purification procedure and kinetic studies. *Eur. J. Biochem.* **209,** 241–247 (1992).

74. Harmsen, M. M., De Haard, H. J. Properties, production, and applications of camelid single-domain antibody fragments. *Appl. Microbiol. Biotechnol.* **77,** 13–22 (2007).

75. Floch, V., Le Bolc'h, G., Audrézet, M., Yaouanc, J., Clément, J., des Abbayes, H., Mercier, B., Abgrall, J., Férec, C. Cationic phosphonolipids as non viral vectors for DNA transfection in hematopoietic cell lines and CD34+ cells. *Blood Cells. Mol. Dis.* **23,** 69–87 (1997).

76. Jordan, M., Schallhorn, A., Wurm, F. M. Transfecting mammalian cells: optimization of critical parameters affecting calcium-phosphate precipitate formation. *Nucleic Acids Res.* **24,** 596–601 (1996).

77. Aschner, M., Guilarte, T. R., Schneider, J. S., Zheng, W. Manganese: recent advances in understanding its transport and neurotoxicity. *Toxicol. Appl. Pharmacol.* **221,** 131–147 (2007).

78. Berger, J., Hauber, J., Hauber, R., Geiger, R., Cullen, B. R. Secreted placental alkaline phosphatase: a powerful new quantitative indicator of gene expression in eukaryotic cells. *Gene* **66,** 1–10 (1988).

79. Balkwill, F. Tumour necrosis factor and cancer. *Nat. Rev. Cancer* **9,** 361–371 (2009).

80. Bossen, C., Ingold, K., Tordivel, A., Bodmer, J., Gaide, O., Hertig, S., Ambrose, C., Tschopp, J., Schneider, P. Interactions of tumor necrosis factor (TNF) and TNF receptor family members in the mouse and human. *J. Biol. Chem.* **281,** 13964–13971 (2006).

81. Young, A. M. H., Campbell, E. C., Lynch, S., Dunn, M. H., Powis, S. J., Suckling, J. Regional susceptibility to TNF-α induction of murine brain inflammation via classical IKK/NF-κB signalling. *PLoS One* **7,** e39049 (2012).

82. Sundstrom, L., Pringle, A., Morrison, B., Bradley, M. Organotypic cultures as tools for functional screening in the CNS. *Drug Discov. Today* **10,** 993–1000 (2005).

83. O'Brien, J. A., Lummis, S. C. R. Biolistic transfection of neuronal cultures using a hand-held gene gun. *Nat. Protoc.* **1,** 977–981 (2006).

84. Zhang, Z., Magnusson, G. Conversion of p-methoxyphenyl glycosides into the corresponding glycosyl chlorides and bromides, and into thiophenyl glycosides. *Carbohydr. Res.* **925,** 41–55 (1996).

85. Lopez, M., Drillaud, N., Bornaghi, L. F., Poulsen, S. Synthesis of *S*-Glycosyl Primary Sulfonamides. *J. Org. Chem.* **2009,** 2811–2816 (2009).

86. Gamblin, D. P., Garnier, P., van Kasteren, S., Oldham, N. J., Fairbanks, A. J., Davis, B. G. Glyco-SeS: Selenenylsulfide-Mediated Protein Glycoconjugation—A new strategy in post-translational modification. *Angew. Chemie. Int. Ed. Engl.* **116,** 846–851 (2004).

87. Boersema, P. J., Mohammed, S., Heck, A. J. R. Phosphopeptide fragmentation and analysis by mass spectrometry. *J. Mass Spectrom.* **44,** 861–878 (2009).

88. Anthony, D. C., Miller, K. M., Fearn, S., Townsend, M. J., Opdenakker, G., Wells, G. M. A., Clements, J. M., Chandler, S., Gearing, A. J. H., Perry, V. H. Matrix metalloproteinase expression in an experimentally-induced DTH model of multiple sclerosis in the rat CNS. *J. Neuroimmunol.* **87,** 62–72 (1998).

Post-submission update

Prior to submission of this thesis, a publication was submitted covering the work carried out with the phosphorylated antibody. After submission, this was received with a number of revisions, which have since been carried out prior to the viva. These revisions are summarised below.

a) Improved microscope images of HEK293T and HEK-Blue Null1 cells

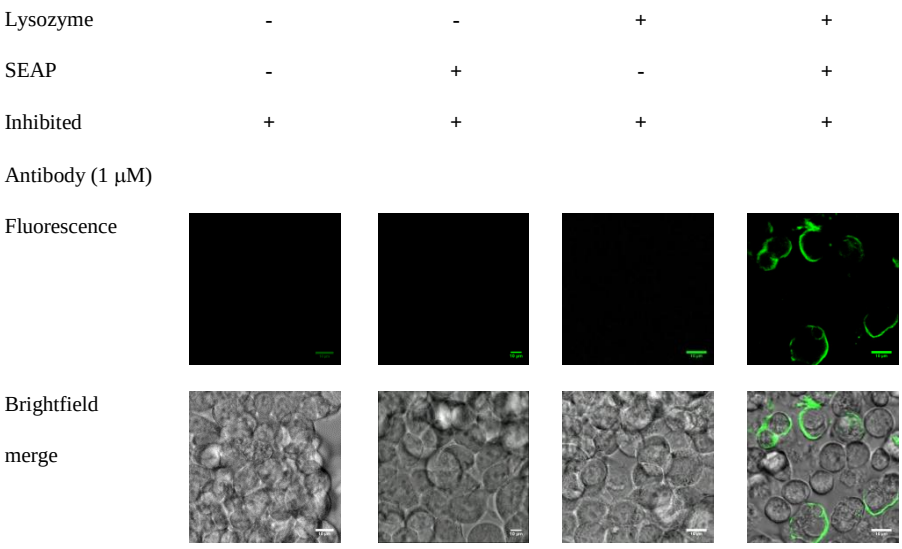

Displaying cell surface labelling of the HEK cell AND gate. Cells transfected with the varying combinations of inputs are stained with PentaHis™ Alexa Fluor® 488 after the addition of cAb-Lys3-104SPO$_3$ (inhibited antibody). Scale bars read 10 μm.

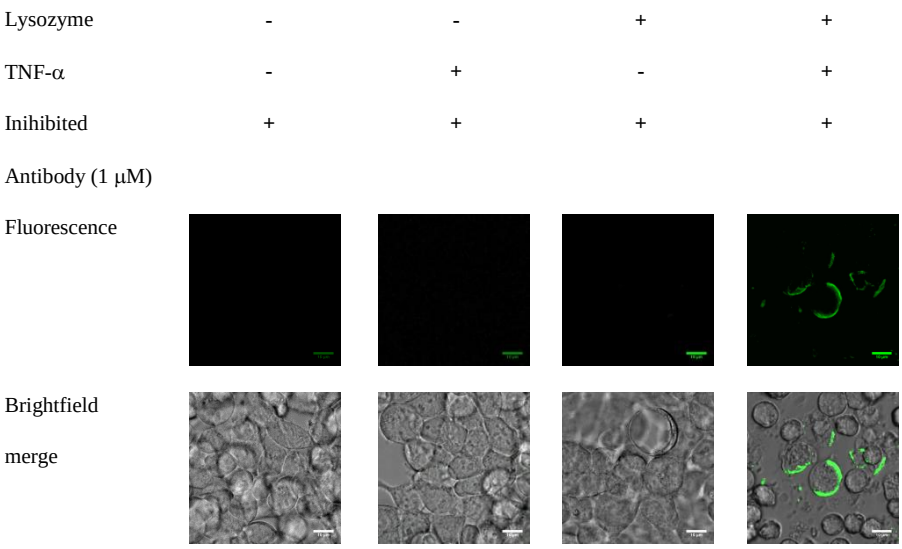

Displaying cell surface labelling of the HEK-Blue™ Null1 cell AND gate. Cells with the varying combinations of inputs are stained with PentaHis™ Alexa Fluor® 488 after the addition of cAb-Lys3-104SPO_3 (inhibited antibody). Scale bars read 10 μm.

b) Stability of cAb-Lys3-pCys104 in plasma

The potential of the phosphorylated antibody to be used in *in vivo* applications was tested by incubation in plasma to test if the thiophosphate group would be susceptible to dephosphorylation by circulating phosphatases. At 5 μM antibody in mouse plasma, no dephosphorylation was observed over 24 hours.

Blood was withdrawn from adult C57BL/6 mice by cardiac puncture under terminal anaesthesia with isoflurane and collected in heparin-containing paediatric blood tubes. The blood was centrifuged at 13 krpm for 5 minutes to generate plasma. cAb-Lys3-pCys104 (6.3 μL, stock 1.28 mg/mL) was added to plasma (93.7 μL, 5 μM final antibody concentration) and the solution incubated at 37 °C. Samples were taken at 15 minutes, 2 hours and 24 hours. Samples were diluted with binding buffer (50 mM KH_2PO_4, 300 mM NaCl, 10 mM imidazole, pH 8), and then added to HIS-Select® Cobalt Affinity Gel in a 1.5 mL plastic tube. The gel-plasma solutions were incubated at 4 °C for 1 hour, and then washed with 2 x 200 μL binding buffer by centrifugation (10 mins, 14 kprm), and eluted with 3 x 200 μL elution buffer (50 mM KH_2PO_4, 300 mM NaCl, 250 mM imidazole, pH 8) by centrifugation. Samples from washes and elutions were analysed by SDS-PAGE and LC-MS. Trace amounts of cAb-Lys3-pCys104 were found in eluted samples, but no dephosphorylated cAb-Lys3-Cys104.

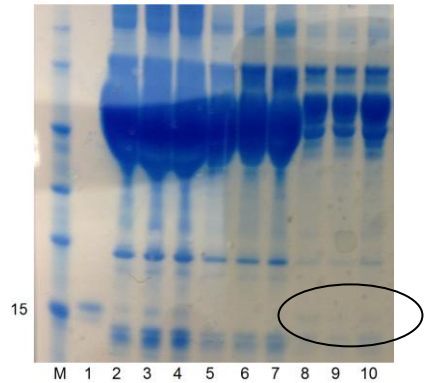

SDS-PAGE of cAb-Lys3-pCys104 and plasma. 1 – cAb-Lys3-pCys104, 2 – 4 – first wash with binding buffer for samples taken at 15 minutes, 2 hours and 24 hours, 5 – 7 – second wash with binding buffer for samples taken at 15 minutes, 2 hours and 24 hours, 8 – 10 – elution fractions for samples taken at 15 minutes, 2 hours and 24 hours.

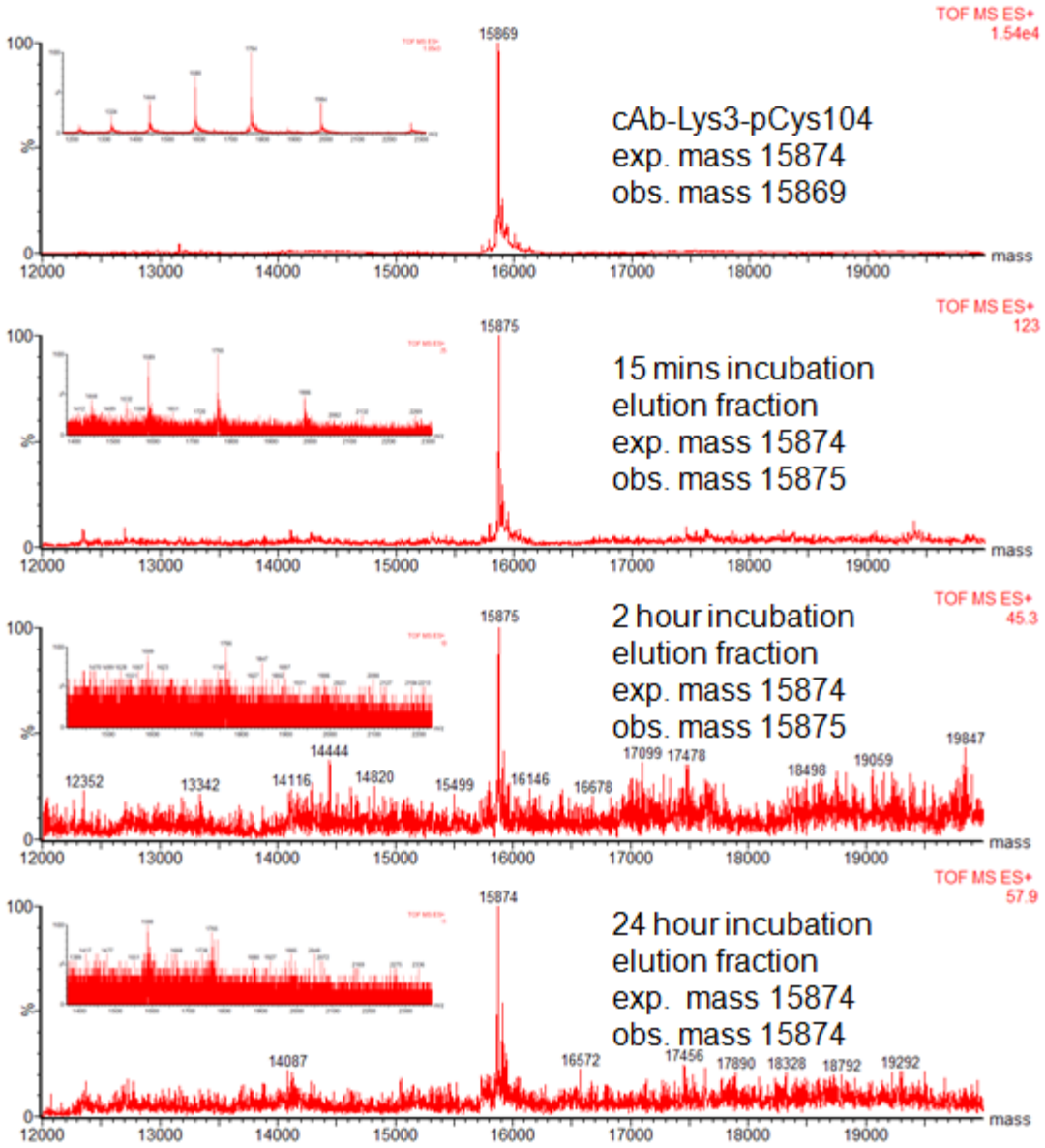

MS for cAb-Lys3-pCys104 incubated with plasma (5 μM antibody) at various time points.

Plasma (3 μL, 10 % of total volume) was added to cAb-Lys3-pCys104 (27 μL, 1.28 mg/ml), and the solution incubated at 37 °C. Samples were taken at 15 minutes, 2 hours and 24 hours, and analysed by LC-MS. No evidence of dephosphorylation or degradation of the antibody was detected at all time points.

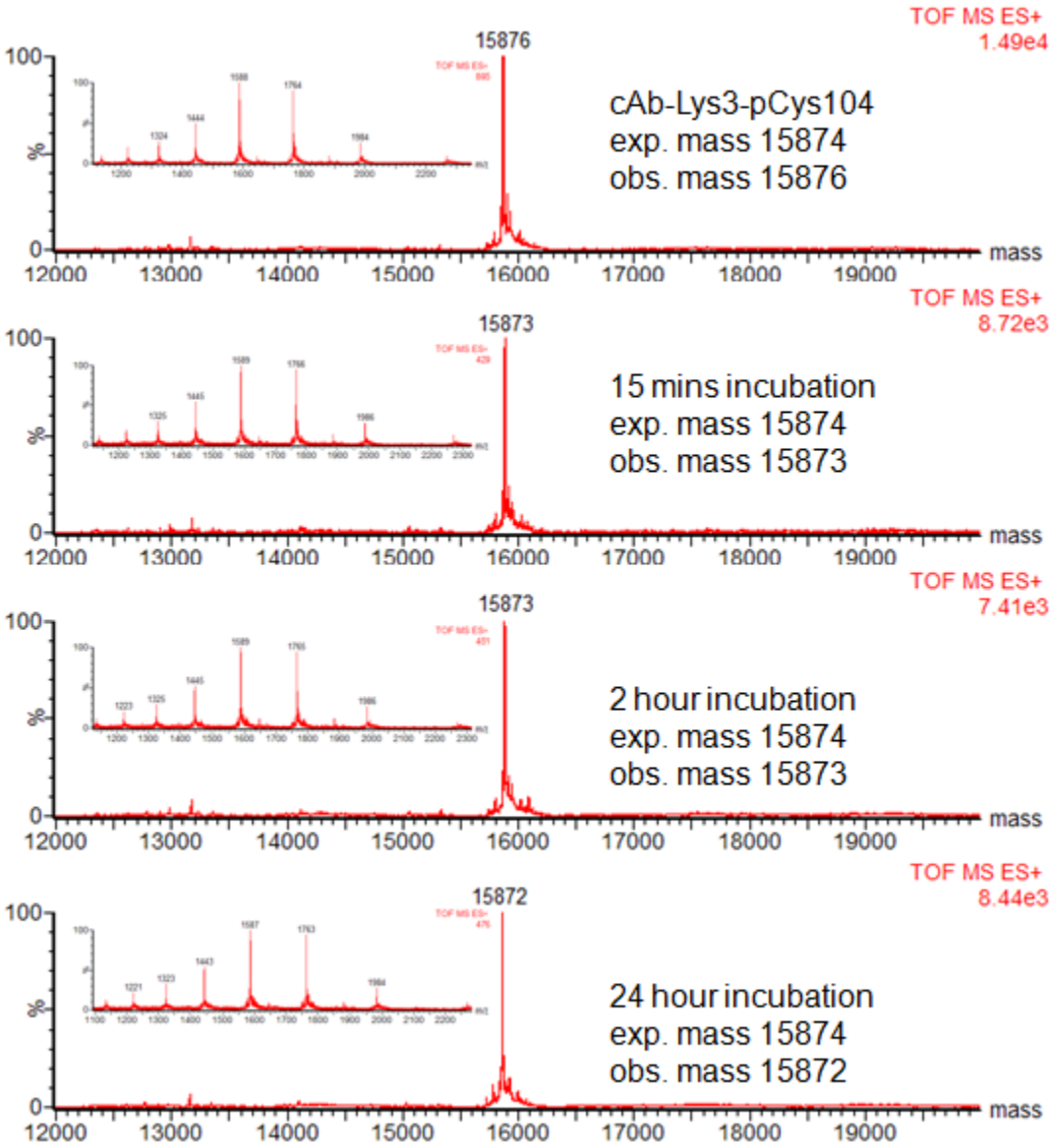

MS for cAb-Lys3-pCys104 incubated with plasma (10 %) at various time points.

c) Directing of antibody to bind to HEK-Blue Null1 cells in mouse brain tissue

In an analogous fashion to the mammalian tissue experiments described previously with HEK293T cells, phosphorylated antibody was directed to HEK-Blue Null1 cells (*lys*+) injected into the brains of mice, along with LPS. The injection of LPS induced an inflammatory response, thereby inducing the expression of SEAP by the engineered HEK-Blue Null1 cells. This set of experiments demonstrates the AND antibody concept, where one of the inputs is induced by an endogenous source (TNF-α).

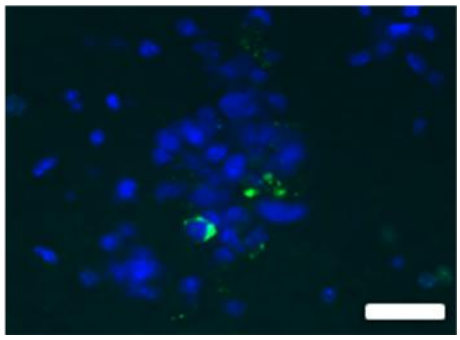

Testing presence of HEK-Blue Null1-*lys*+ cells in tissue section. WT-cAb-Lys3 was added to a tissue section injected with HEK-Blue Null1-*lys*+. Subsequent addition of PentaHis™ Alexa Fluor® 488 allowed visualisation of fluorescent cells by microscopy. Scale bar reads 50 μm.